

PHARMACOGNOSTIC SPECIFICATION, MANGIFERIN CONTENT,  
BIOLOGICAL ACTIVITIES OF *AQUILARIA CRASSNA* LEAVES  
AND DNA BARCODES OF SELECTED PLANTS IN GENUS *AQUILARIA*



Mr. Woratouch Thitikornpong

จุฬาลงกรณ์มหาวิทยาลัย

บทคัดย่อและแฟ้มข้อมูลฉบับเต็มของวิทยานิพนธ์ตั้งแต่ปีการศึกษา 2554 ที่ให้บริการในคลังปัญญาจุฬาฯ (CUIR)  
เป็นแฟ้มข้อมูลของนิสิตเจ้าของวิทยานิพนธ์ ที่ส่งผ่านทางบัณฑิตวิทยาลัย

The abstract and full text of theses from the academic year 2011 in Chulalongkorn University Intellectual Repository (CUIR)  
are the thesis authors' files submitted through the University Graduate School.

A Dissertation Submitted in Partial Fulfillment of the Requirements  
for the Degree of Doctor of Philosophy Program in Public Health Sciences

College of Public Health Sciences

Chulalongkorn University

Academic Year 2017

Copyright of Chulalongkorn University

ข้อกำหนดทางเภสัชเวช ปริมาณสารแมงกานีส ปริมาณสารแมงกานีส ฤทธิ์ทางชีวภาพของใบกฤษณา  
และดีเอ็นเอบาร์โค้ดของพืชบางชนิดในสกุลกฤษณา



วิทยานิพนธ์นี้เป็นส่วนหนึ่งของการศึกษาตามหลักสูตรปริญญาวิทยาศาสตรดุษฎีบัณฑิต  
สาขาวิชาวิทยาศาสตร์สาธารณสุข  
วิทยาลัยวิทยาศาสตร์สาธารณสุข จุฬาลงกรณ์มหาวิทยาลัย  
ปีการศึกษา 2560  
ลิขสิทธิ์ของจุฬาลงกรณ์มหาวิทยาลัย

Thesis Title PHARMACOGNOSTIC SPECIFICATION, MANGIFERIN  
CONTENT, BIOLOGICAL ACTIVITIES OF *AQUILARIA*  
*CRASSNA* LEAVES AND DNA BARCODES OF SELECTED  
PLANTS IN GENUS *AQUILARIA*  
By Mr. Woratouch Thitikornpong  
Field of Study Public Health Sciences  
Thesis Advisor Associate Professor Nijisiri Ruangrunsi, Ph.D.  
Thesis Co-Advisor Assistant Professor Chanida Palanuvej, Ph.D.

---

Accepted by the College of Public Health Sciences, Chulalongkorn University in  
Partial Fulfillment of the Requirements for the Doctoral Degree

..... Dean of the College of Public Health Sciences  
(Professor Sathirakorn Pongpanich, Ph.D.)

THESIS COMMITTEE

..... Chairman  
(Assistant Professor Naowarat Kanchanakhan, Ph.D.)

..... Thesis Advisor  
(Associate Professor Nijisiri Ruangrunsi, Ph.D.)

..... Thesis Co-Advisor  
(Assistant Professor Chanida Palanuvej, Ph.D.)

..... Examiner  
(Assistant Professor Boonsri Ongpipattanakul, Ph.D.)

..... Examiner  
(Associate Professor Kanchana Rungsahirunrat, Ph.D.)

..... Examiner  
(Tepanata Pumpaibool, Ph.D.)

..... External Examiner  
(Assistant Professor Piyanut Thongphasuk, Ph.D.)

วรัชช วิฑิตกรพงศ์ : ข้อกำหนดทางเภสัชเวท ปริมาณสารเมงกิเฟอร์ินฤทธิ์ทางชีวภาพของใบกฤษณาและดีเอ็นเอบาร์โค้ดของพืชบางชนิดในสกุลกฤษณา (PHARMACOGNOSTIC SPECIFICATION, MANGIFERIN CONTENT, BIOLOGICAL ACTIVITIES OF *AQUILARIA CRASSNA* LEAVES AND DNA BARCODES OF SELECTED PLANTS IN GENUS *AQUILARIA*) อ.ที่ปริกษาวิทยานิพนธ์หลัก: รศ. ภก. ดร. นิจศิริ เรืองรังษี, อ.ที่ปริกษาวิทยานิพนธ์ร่วม: ผศ. ดร. ชนิตา พลาอนุเวช, 214 หน้า.

กฤษณา (*Aquilaria crassna* Pierre ex Lecomte) (วงศ์ Thymelaeaceae) มีการนำมาใช้ประโยชน์เพื่อการบำบัดรักษาโรคต่างๆ โดยงานวิจัยก่อนหน้านี้ได้พบว่าสารเมงกิเฟอร์ินเป็นองค์ประกอบสำคัญในใบกฤษณา แม้ว่ามีการค้นพบสารดังกล่าวแล้ว แต่การศึกษาคุณลักษณะทางเภสัชเวทและการวิเคราะห์ปริมาณสารเมงกิเฟอร์ินในใบกฤษณายังไม่เคยมีการศึกษาวิจัยมาก่อน นอกจากนี้ยังพบข้อมูลการศึกษาที่ไม่มากนักเกี่ยวกับฤทธิ์ทางชีวภาพของสารสกัดใบกฤษณาและเมงกิเฟอร์ินที่เป็นเมตาบอไลต์ที่สำคัญ รวมถึงการวิเคราะห์ทางชีวโมเลกุลของพืชในสกุล *Aquilaria* ในการศึกษาวิจัยนี้มีจุดมุ่งหมายเพื่อกำหนดและพัฒนามาตรฐานสมุนไพรตามข้อกำหนดขององค์การอนามัยโลกและวิธีการวิเคราะห์ที่ถูกต้องเพื่อหาปริมาณสารเมงกิเฟอร์ินในใบกฤษณา และยังคงตรวจสอบฤทธิ์ทางชีวภาพบางอย่าง เช่น ฤทธิ์ยับยั้งเอนไซม์แอลฟาไกลูโคซิเดส ฤทธิ์ต้านปฏิกิริยาออกซิเดชัน ฤทธิ์ความเป็นพิษต่อเซลล์ และคุณสมบัติการปกป้องเซลล์ นอกจากนี้ยังตรวจสอบถึงตำแหน่งของยีนที่มีคุณสมบัติเป็นดีเอ็นเอบาร์โค้ดและเสนออย่างน้อยหนึ่งตำแหน่งที่เหมาะสมสำหรับการพิสูจน์ชนิดของพืชในสกุล *Aquilaria* การศึกษาลักษณะทางเภสัชเวทและการวิเคราะห์หาปริมาณสารเมงกิเฟอร์ินในใบกฤษณาด้วยวิธีทีนเลเยอร์โครมาโทกราฟี-เดินซีโธเมทรีโดยใช้โปรแกรม winCATS และวิธีการวิเคราะห์ทีนเลเยอร์โครมาโทกราฟีโดยวิเคราะห์ภาพถ่ายนั้นได้นำตัวอย่างใบกฤษณาจำนวน 15 แห่งทั่วประเทศมาใช้เป็นตัวอย่างในการศึกษา โดยได้ศึกษาลักษณะทางมหัพภศาสตร์ ลักษณะทางจุลทรรศน์ การศึกษาลายพิมพ์ทางเคมีด้วยเทคนิคทีนเลเยอร์โครมาโทกราฟีตลอดจนคุณสมบัติทางกายภาพเคมีด้วย ค่าเฉลี่ยของปริมาณน้ำหนักที่หายไปเมื่อทำให้แห้ง ปริมาณความชื้น ปริมาณเถ้ารวมและปริมาณเถ้าที่ละลายในกรด มีค่าร้อยละ  $8.62 \pm 0.13$ ,  $8.16 \pm 0.14$ ,  $6.82 \pm 0.09$  และ  $1.49 \pm 0.03$  โดยน้ำหนักแห้งตามลำดับ ขณะที่ค่าปริมาณสิ่งสกปรกในเอทานอลและสิ่งสกปรกในน้ำมีค่าอยู่ที่ร้อยละ  $9.05 \pm 0.39$  และ  $16.94 \pm 0.22$  โดยน้ำหนักแห้งตามลำดับ ทั้งนี้การศึกษานี้ยังได้พัฒนาวิธีการวิเคราะห์ที่ถูกต้องขึ้นเพื่อใช้วิเคราะห์ปริมาณสารเมงกิเฟอร์ิน สารเมงกิเฟอร์ินในใบกฤษณาที่วิเคราะห์ทีนเลเยอร์โครมาโทกราฟี-เดินซีโธเมทรีและวิธีการวิเคราะห์ทีนเลเยอร์โครมาโทกราฟีโดยวิเคราะห์ภาพถ่ายมีปริมาณร้อยละ  $1.2992 \pm 0.5980$  และ  $1.3036 \pm 0.5874$  ตามลำดับ การเปรียบเทียบปริมาณสารเมงกิเฟอร์ินระหว่างวิธีทั้งสองพบว่าไม่มีความแตกต่างกันอย่างมีนัยสำคัญทางสถิติ การศึกษาฤทธิ์ยับยั้งเอนไซม์แอลฟาไกลูโคซิเดสจากเชื้อยีสต์พบว่ามีฤทธิ์ในการยับยั้งเอนไซม์ดังกล่าวโดยมีค่า  $IC_{50}$  ของสิ่งสกัดใบกฤษณาและเมงกิเฟอร์ินอยู่ที่  $0.1840 \pm 0.0032$  และ  $0.5714 \pm 0.0044$  มิลลิกรัมต่อมิลลิลิตรตามลำดับ และได้ศึกษาฤทธิ์ต้านออกซิเดชันในหลอดทดลองโดยใช้วิธีการทดสอบมาตรฐานซึ่งผลการทดสอบแสดงให้เห็นว่าสิ่งสกัดใบกฤษณาและสารเมงกิเฟอร์ินมีคุณสมบัติต้านออกซิเดชันได้ นอกจากนี้การศึกษานี้ยังได้ทดสอบความเป็นพิษของสิ่งสกัดใบกฤษณาและสารเมงกิเฟอร์ินต่อเซลล์มะเร็งของมนุษย์จำนวน 3 ชนิด ซึ่งพบว่าสิ่งสกัดใบกฤษณา มีฤทธิ์ในการยับยั้งการเพิ่มจำนวนของเซลล์ MDA-MB-321 (เซลล์มะเร็งเต้านม) โดยมีค่า  $IC_{50}$  อยู่ที่  $33.89 \pm 0.50$  ไมโครกรัมต่อมิลลิลิตร ซึ่งมีประสิทธิภาพในการยับยั้งมากกว่าเซลล์ HT-29 (เซลล์มะเร็งลำไส้ใหญ่ส่วนปลาย) และเซลล์ HepG2 (เซลล์มะเร็งตับ) โดยมีค่า  $IC_{50}$  อยู่ที่  $51.74 \pm 1.42$  และ  $53.63 \pm 1.54$  ไมโครกรัมต่อมิลลิลิตรตามลำดับ ส่วนเมงกิเฟอร์ินแสดงความเป็นพิษต่อเซลล์มะเร็งทั้งสามชนิดแต่ที่ความเข้มข้นสูงสุด (100 ไมโครกรัมต่อมิลลิลิตร) มีความเป็นพิษต่อเซลล์ประมาณร้อยละ 33 - 38 นอกจากนี้การพิจารณาคุณสมบัติการปกป้องเซลล์ EA.hy926 นั้นพิจารณาถึงการอยู่รอดของเซลล์ด้วยวิธี MTT และการตรวจสอบปริมาณอนุมูลอิสระภายในเซลล์ด้วยวิธี DCFH-DA ซึ่งพบว่า เมงกิเฟอร์ินเท่านั้นที่มีคุณสมบัติปกป้องเซลล์โดยลดการสร้างอนุมูลอิสระในเซลล์ที่ถูกเหนี่ยวนำด้วยไฮโดรเจนเปอร์ออกไซด์และที่ความเข้มข้นน้อยกว่า 200 ไมโครกรัมต่อมิลลิลิตรไม่พบพิษต่อเซลล์ การศึกษาการปกป้องเซลล์โดยใช้การวิเคราะห์ western blot พบว่าการบ่มสารเมงกิเฟอร์ินก่อนการกระตุ้นด้วยไฮโดรเจนเปอร์ออกไซด์ที่ความเข้มข้น 0.25 มิลลิโมลาร์นาน 6 ชั่วโมงนั้นสามารถเพิ่มการแสดงออกของเอนไซม์ SOD-1 แต่ลดการแสดงออกของเอนไซม์ HO-1 และการศึกษาโปรตีนที่เกี่ยวข้องกับการตายแบบอะพอพโทซิส พบว่าการบ่มด้วยสารเมงกิเฟอร์ินก่อนการกระตุ้นด้วยไฮโดรเจนเปอร์ออกไซด์ที่ความเข้มข้น 0.25 มิลลิโมลาร์นาน 6 ชั่วโมงนั้น ทำให้เกิดการเพิ่มการแสดงออกขององค์ประกอบที่ด้านการเกิดการตายแบบอะพอพโทซิส (Bcl-2) และลดการแสดงออกขององค์ประกอบที่สนับสนุนให้ตายแบบอะพอพโทซิส (Bax) เมื่อเปรียบเทียบกับกลุ่มควบคุมที่ได้รับการกระตุ้นด้วยไฮโดรเจนเปอร์ออกไซด์ สำหรับการศึกษาดีเอ็นเอบาร์โค้ดนั้นได้เก็บรวบรวมพืชในสกุล *Aquilaria* จำนวน 3 สปีชีส์ ได้แก่ *A. crassna*, *A. malaccensis* Lam. และ *A. subintegra* Ding Hou และใช้ *Enkleia siamensis* (Kurz) Nervling เป็นพืชเปรียบเทียบนอกกลุ่ม และพิจารณาลำดับเบสในตำแหน่งต่าง ๆ ของดีเอ็นเอจำนวน 6 ตำแหน่ง ได้แก่ ITS, *matK*, *rbcL*, *rpoC1*, *psbA-trnH* intergenic spacer และ *ycf1* แล้วสร้างแผนภูมิวิวัฒนาการของพืชที่ศึกษาจากดีเอ็นเอแต่ละตำแหน่งและศึกษาระยะห่างทางพันธุกรรมโดยใช้วิธีการ Maximum Likelihood บริเวณส่วน ITS สามารถใช้เป็นเครื่องหมายที่เหมาะสมในการระบุชนิดของพืชสกุล *Aquilaria* โดยพิจารณาจากแผนภูมิวิวัฒนาการและความยาวที่เหมาะสมของระยะห่างทางพันธุกรรม ข้อมูลทั้งหมดจากงานวิจัยนี้สามารถนำไปใช้พิสูจน์เอกลักษณ์สมุนไพรกฤษณา และก่อให้เกิดประสิทธิผลในการรักษาและความปลอดภัยต่อผู้ใช้สมุนไพร

สาขาวิชา วิทยาศาสตร์สาธารณสุข

ปีการศึกษา 2560

ลายมือชื่อ นิสิต .....

ลายมือชื่อ อ.ที่ปริกษาหลัก .....

ลายมือชื่อ อ.ที่ปริกษาร่วม .....

# # 5779053453 : MAJOR PUBLIC HEALTH SCIENCES

KEYWORDS: AQUILARIA CRASSNA / MANGIFERIN / IN VITRO BIOLOGICAL ACTIVITY / PHARMACOGNOSTIC SPECIFICATION / DNA BARCODE

WORATOUCH THITIKORNONG: PHARMACOGNOSTIC SPECIFICATION, MANGIFERIN CONTENT, BIOLOGICAL ACTIVITIES OF *AQUILARIA CRASSNA* LEAVES AND DNA BARCODES OF SELECTED PLANTS IN GENUS *AQUILARIA*. ADVISOR: ASSOC. PROF. NIJSIRI RUANGRUNGSI, Ph.D., CO-ADVISOR: ASST. PROF. CHANIDA PALANUVEJ, Ph.D., 214 pp.

*Aquilaria crassna* Pierre ex Lecomte (Thymelaeaceae) has been used as a medicinal plant in many aspects. Previous research has revealed that *A. crassna* leaves contain mangiferin as an active compound. Although the active component has been investigated, the pharmacognostic specification and quantification of mangiferin from *A. crassna* leaves have never been established. There still have little findings about biological activities of *A. crassna* leaves extract and its metabolite, mangiferin as well as the molecular evaluation of plant in genus *Aquilaria*. The study aimed to conduct and develop a pharmacognostic standard according to WHO guidance as well as the validated method for quantifying mangiferin content, and also investigated some biological activities such as alpha-glucosidase inhibitory activity, antioxidation activity, cytotoxic activity, and cytoprotective property; in addition, it also investigated the efficient DNA barcoding loci and suggested the most suitable one for *Aquilaria* species identification. The dried *A. crassna* leaves from 15 separated locations throughout Thailand were investigated for pharmacognostic specification and their mangiferin contents were quantitatively analysed by TLC densitometry with winCATS software and TLC image analysis. Macroscopic-, microscopic- characteristics, TLC fingerprinting, and physicochemical parameters were reported in this study. The loss on drying, moisture content, and total ash content as well as acid-insoluble ash content were determined to be  $8.62 \pm 0.13$ ,  $8.16 \pm 0.14$ ,  $6.82 \pm 0.09$  and  $1.49 \pm 0.03\%$ , respectively. Ethanol- and water-extractable values were found to be  $9.05 \pm 0.39$  and  $16.94 \pm 0.22\%$ , respectively. In addition, the validation method for quantifying the mangiferin content was developed. The contents of mangiferin in *A. crassna* leaf extract determined by TLC-densitometry and TLC-image analysis were found to be  $1.2992 \pm 0.5980$  and  $1.3036 \pm 0.5874\%$  by dried weight, respectively. The results between these two analytical methods were shown to have an insignificant difference. The yeast alpha-glucosidase inhibitory assay was performed, and the  $IC_{50}$  of *A. crassna* leaf extract and mangiferin were found to be  $0.1840 \pm 0.0032$ ,  $0.5714 \pm 0.0044$  mg/ml, respectively. In addition, these samples were analyzed in term of the *in vitro* antioxidant activities using standard antioxidant assays. The results showed that *A. crassna* leaf extract and mangiferin possessed antioxidant properties. Moreover, the cytotoxicity of *A. crassna* leaf extract and mangiferin was also evaluated against three human cancer cell lines using MTT assay. *A. crassna* leaf extract could inhibit cell proliferation of MDA-MB-231; breast cancer cells ( $IC_{50} = 33.89 \pm 0.50$   $\mu$ g/ml) greater than HT-29; colorectal cancer cells ( $IC_{50} = 51.74 \pm 1.42$   $\mu$ g/ml) and HepG2; hepatic cancer cells ( $IC_{50} = 53.63 \pm 1.54$   $\mu$ g/ml). Mangiferin showed the toxicity against these cancer cell lines but the inhibition was around 33-38% at the highest concentration (100  $\mu$ g/ml). In addition, the cytoprotective properties of EA.hy926 cell was determined via cell viability testing by MTT assay and intracellular reactive oxygen species (ROS) investigation by DCFH-DA assay. Only mangiferin performed cellular protective attribute from the reduction of H<sub>2</sub>O<sub>2</sub>-induced ROS generation, and no cytotoxic effect on EA.hy926 cells at the concentration not more than 200  $\mu$ g/ml. Western blotting analysis revealed that the mangiferin incubation before exposure to 0.25 mM of H<sub>2</sub>O<sub>2</sub> for 6 h could increase the SOD-1 expression, whereas the HO-1 expression was down-regulated. For determination of apoptosis proteins, mangiferin treatment prior exposure to 0.25 mM H<sub>2</sub>O<sub>2</sub> for 6 h resulted in augmentation of the expression level of anti-apoptotic factor (Bcl-2), decline the level of proapoptotic factor (Bax) compared to H<sub>2</sub>O<sub>2</sub>-induced injury control. For DNA barcoding study, three *Aquilaria* species; *A. crassna*, *A. malaccensis* Lam., and *A. subintegra* Ding Hou, and *Enkleia siamensis* (Kurz) Nervling were investigated. The DNA barcoding sequences from six candidate of barcoding loci (ITS, *matK*, *rbcl*, *rpoC1*, *psbA-trnH* intergenic spacer, and *ycf1*) were established. The phylogenetic tree of each locus was reconstructed and the genetic distances were also determined using a maximum likelihood method. According to ML phylogenetic tree reconstruction and the optimum length of genetic distance, only ITS was suitable marker for *Aquilaria* species identification. All of these results provide highly useful information for the authentication of *A. crassna* leaves, and also the contribution to the effectiveness and safety of *A. crassna* uses.

Field of Study: Public Health Sciences

Academic Year: 2017

Student's Signature .....

Advisor's Signature .....

Co-Advisor's Signature .....

## ACKNOWLEDGEMENTS

The author truly wishes to express his appreciation to his dissertation advisor, Associate Professor Nijsiri Ruangrunsi Ph.D. and his dissertation co-advisor, Associate Professor Chanida Palanuvej Ph. D. for their advice, valuable suggestion, and encouragements throughout this research study. The author is grateful to the dissertation committees, Assistant Professor Naowarat Kanchanakhan Ph. D. , Associate Professor Kanchana Rungsihirunrat Ph. D. , Assistant Professor Boonsri Ongpipattanakul Ph. D. , Lecturer Tepanata Pumpaibool Ph.D., and Assistant Professor Piyanuch Thongphasuk Ph.D., for their critical consideration and valuable suggestion to improve this dissertation.

The author also acknowledges the cell culture techniques advice and expert opinion by Mr. Nonthaneth Nalinratana, Ph.D. candidate from Faculty of Pharmaceutical Sciences, Chulalongkorn University. The acknowledgement also extends to Chulalongkorn Drug and Health Products Innovation Promotion Center (CUDHIP), Faculty of Pharmaceutical Sciences, Chulalongkorn University and College of Public Health Sciences, Chulalongkorn University for providing equipment, and chemical throughout this study. Their kindly assistance will be always kept in his mind.

The author also would like to thanks the 100th Anniversary Chulalongkorn University Fund for Doctoral Scholarships and the 90th Anniversary of Chulalongkorn University, Rachadapiseksomphot Endowment Fund from Graduate School for funding and sponsoring this dissertation.

The author is thankful to Mr. Watchara Damjuti, Miss Naruemon Witheethummasak and Miss Yamon Pitakpawasutthi, Mr. Bhattacharit Pinthakup, Miss Aphiradee Panya-ngam, and staff members, friends and other person who is not mentioned from College of Public Health Sciences and Faculty of Pharmaceutical Sciences, Chulalongkorn University for having friendship and helping the researcher through the difficult time.

Finally, the author owes a great debt of gratitude to his family, especially his parents for their love, understanding, encouragement, and support. The author dedicates this degree to them.

## CONTENTS

	Page
THAI ABSTRACT .....	iv
ENGLISH ABSTRACT .....	v
ACKNOWLEDGEMENTS .....	vi
CONTENTS .....	vii
LIST OF TABLES .....	xv
LIST OF FIGURES .....	xix
LIST OF ABBREVIATIONS .....	xxiv
CHAPTER I INTRODUCTION .....	1
1.1 Background and rationale.....	1
1.2 Objectives of the study.....	3
CHAPTER II LITERATURE REVIEWS .....	5
2.1 Description of plant in genus <i>Aquilaria</i> .....	5
2.2 Chemical constituents of <i>Aquilaria</i> spp. leaves .....	10
2.3 Pharmacological activities of agarwood leaves.....	17
2.3.1 Antihyperglycemic activity .....	17
2.3.2 Anti-inflammatory, anti-nociceptive/analgesic/antipyretic.....	17
2.3.3 Anti-microbial activity .....	18
2.3.4 Anti-oxidation activity .....	19
2.3.5 Effect on central nervous system (CNS).....	19
2.3.6 Hepatoprotective .....	19
2.3.7 Laxative activity .....	19
2.4 Mangiferin.....	20

	Page
2.5 Pharmacological activities of mangiferin .....	21
2.6 Quality control method for herbal material .....	22
2.6.1 Macroscopic and microscopic examination .....	22
2.6.2 Chemical fingerprinting .....	22
2.6.3 Physico-chemical parameter .....	22
2.6.3.1 Determination of loss on drying .....	22
2.6.3.2 Determination of water content .....	22
2.6.3.3 Determination of total ash and acid insoluble ash.....	23
2.6.3.4 Determination of extractable matter .....	23
2.6.4 TLC-densitometry and TLC image analysis.....	23
2.6.4.1 Thin layer chromatography .....	23
2.6.4.2 TLC- densitometry.....	24
2.6.4.3 TLC-image analysis .....	25
2.7 Biological activities .....	25
2.7.1 Anti-oxidant activities.....	25
2.7.1.1 DPPH radical scavenging assay.....	28
2.7.1.2 Ferric reducing antioxidant power assay .....	28
2.7.1.3 Nitric oxide (NO) scavenging activity .....	29
2.7.1.4 Total phenolic content .....	30
2.7.2 <i>In vitro</i> $\alpha$ -glucosidase inhibitory activity.....	30
2.7.3 Cell viability or cytotoxicity testing (MTT tetrazolium reduction assay) ...	32
2.8 Cellular model for determination of endothelial dysfunction under oxidative stress.....	33



	Page
2.9 Protein involved in cytoprotection of endothelial cells.....	35
2.9.1 SOD1 .....	35
2.9.2 Heme oxygenase 1 (HO-1) .....	36
2.9.3 BAX and Bcl-2 .....	38
2.10 DNA barcoding .....	42
2.10.1 Internal transcribe spacer (ITS).....	43
2.10.2 <i>matK</i> gene.....	44
2.10.3 The <i>trnH-psbA</i> intergenic spacer region.....	46
2.10.4 <i>rpoC</i> gene .....	46
2.10.5 <i>ycf1</i> gene .....	47
2.11 The polymerase chain reaction (PCR) and sequencing technique .....	48
2.11.1 The polymerase chain reaction (PCR) .....	48
2.11.2 Sequencing technique.....	49
2.12 Sequence alignment .....	52
2.13 Phylogenetic analysis .....	52
2.13.1 Distance-based method .....	53
2.13.2 Character-based method .....	53
2.13.2.1 Maximum Likelihood method .....	53
2.13.2.2 Bayesian Analysis method .....	54
2.13.2.3 Maximum Parsimony methods.....	55
2.13.3 Bootstrap analysis.....	56
CHAPTER III MATERIALS AND METHODS .....	57

3.1 PHARMACOGNOSTIC EVALUATIONS AND MANGIFERIN CONTENTS OF <i>AQUILARIA CRASSNA</i> LEAVES .....	57
3.1.1 Chemicals .....	58
3.1.2 Materials.....	58
3.1.3 Instruments .....	59
3.1.4 Plant materials .....	60
3.1.5 Macroscopic and microscopic determination of <i>Aquilaria crassna</i> leaves.....	60
3.1.5.1 Macroscopic evaluation .....	60
3.1.5.2 Microscopic evaluation.....	60
3.1.6 TLC examination of ethanolic extracts of <i>Aquilaria crassna</i> leaves.....	62
3.1.7 Quality control of herbal materials using physicochemical method .....	63
3.1.7.1 Loss on drying.....	63
3.1.7.2 Total ash.....	63
3.1.7.3 Acid insoluble ash.....	64
3.1.7.4 Ethanol-soluble extractive value .....	64
3.1.7.5 Water-soluble extractive value.....	64
3.1.7.6 Determination of water content (Azeotropic distillation method) .....	65
3.1.8 Quantitative analysis of mangiferin content in <i>Aquilaria crassna</i> leaves by TLC-densitometry compared with image analysis method.....	65
3.1.8.1 Preparation of mangiferin standard solution .....	65
3.1.8.2 Preparation of ethanolic extract of <i>A. crassna</i> leaves .....	65
3.1.8.3 Chromatographic conditions .....	66

	Page
3.1.8.4 TLC-densitometry and TLC image analysis studies.....	66
3.1.8.5 Method validation.....	67
3.1.9 Data analysis.....	68
3.2 Biological assessment of ethanolic extract of <i>Aquilaria crassna</i> leaves.....	69
3.2.1 Chemical and reagents.....	69
3.2.2 Equipment.....	71
3.2.3 Plant materials.....	71
3.2.4 Preparation of Ac14 ethanolic extract.....	72
3.2.5 Free radical scavenging activities in a cell-free system.....	72
3.2.5.1 DPPH free radical scavenging assay.....	72
3.2.5.2 Scavenging of NO <sup>•</sup> .....	72
3.2.5.3 Superoxide radical scavenging activity.....	73
3.2.5.4 Ferric reducing antioxidant power (FRAP) assay.....	73
3.2.5.4 Total phenolic contents.....	74
3.2.6 Antidiabetic activity.....	74
3.2.6.1 Inhibition of yeast alpha-glucosinase activity.....	74
3.2.7 Cytotoxicity activity on cancer cell.....	75
3.2.7.1 Cell culture.....	75
3.2.7.2 Determination of cytotoxicity activity of Ac14 extract and mangiferin using MTT assay.....	75
3.2.8 Cytoprotective effect of mangiferin and Ac14 extract.....	76
3.2.8.1 Cell culture.....	76
3.2.8.2 Determination of the effect of Ac14 extract, mangiferin or H <sub>2</sub> O <sub>2</sub> on cell viability.....	76

	Page
3.2.8.3 Measurement of Ac14 extract, mangiferin or H <sub>2</sub> O <sub>2</sub> on intracellular ROS.....	77
3.2.8.4 Western blotting analysis.....	78
3.2.9 Statistical analysis .....	79
3.3 DNA Barcoding of selected species in genus <i>Aquilaria</i> .....	80
3.3.1 Chemicals and reagents .....	80
3.3.2 Instruments .....	80
3.3.3 Plant materials .....	81
3.3.4 Genomic DNA extraction.....	82
3.3.5 PCR amplification.....	82
3.3.6 Data analysis .....	83
CHAPTER IV RESULTS .....	84
4.1 Pharmacognostic specifications of <i>A. crassna</i> leaves.....	84
4.1.1 Plant materials .....	84
4.1.2 Macroscopic and microscopic characteristics of <i>A. crassna</i> leaves .....	86
4.1.3 TLC fingerprinting.....	90
4.1.4 Physico-chemical parameter .....	93
4.1.5 Mangiferin content in ethanolic extract of <i>A. crassna</i> leaves.....	93
4.1.5.1 Method validation for quantified mangiferin.....	93
4.1.5.2 Quantitative analysis of mangiferin.....	102
4.2 Biological activities of <i>A. crassna</i> leaf extract and its metabolite, mangiferin .	106
4.2.1 Alpha-glucosidase inhibitory activity.....	106
4.2.2.1 DPPH scavenging activity.....	107

	Page
4.2.2.2 Nitric oxide radical (NO <sup>•</sup> ) scavenging activity.....	108
4.2.2.3 Superoxide radical scavenging activity.....	109
4.2.2.4 Ferric reducing antioxidant power (FRAP).....	111
4.2.2.5 Total phenolic content (TPC) .....	112
4.2.3 Cytotoxic activity against cancer cell lines.....	113
4.2.4 Cytotoxic effect on a EA.hy926 cells line and intracellular ROS determination.....	115
4.2.4.1 Effect of ethanolic extract of <i>Aquilaria crassna</i> leaves and its metabolite, mangiferin on cell viability and intracellular ROS....	115
4.2.4.2 Effect of H <sub>2</sub> O <sub>2</sub> on cell viability and intracellular ROS .....	118
4.2.4.3 Effect of ethanolic extract of <i>Aquilaria crassna</i> leaves and its metabolite, mangiferin on the viability and intracellular ROS of H <sub>2</sub> O <sub>2</sub> -injured cells .....	120
4.2.5 Effect of ethanolic extract of <i>A. crassna</i> leaves and its metabolite; mangiferin on protein expression in EA.hy926 cells .....	124
4.2.5.1 Effect of ethanolic extract of <i>A. crassna</i> leaves and its metabolite; mangiferin on protein expression levels of Cu/Zn- SOD in EA.hy926 cells .....	124
4.2.5.2 Effect of ethanolic extract of <i>A. crassna</i> leaves and its metabolite; mangiferin on protein expression levels of HO-1 in EA.hy926 cells.....	127
4.2.5.3 Effect of ethanolic extract of <i>A. crassna</i> leaves and its metabolite; mangiferin on protein expression levels of Bcl-2 and Bax in EA.hy926 cells .....	130
4.3 DNA barcoding of selected species in genus <i>Aquilaria</i> .....	133
4.3.1 PCR amplification and DNA sequencing.....	133

	Page
4.3.2 Phylogenetic analysis of selected plant in genus <i>Aquilaria</i> based on each locus.....	145
4.3.2.1 Phylogenetic tree of ITS region .....	145
4.3.2.2 Phylogenetic tree of rbcL gene .....	146
4.3.2.3 Phylogenetic tree of matK gene.....	147
4.3.2.4 Phylogenetic tree of psbA-trnH intergenic spacer.....	148
4.3.2.5 Phylogenetic tree of rpoC1 gene .....	149
4.3.2.6 Phylogenetic tree of ycf1 gene.....	150
4.3.2.6 Phylogenetic tree of combination sequence of chloroplast genome .....	151
CHAPTER V DISCUSSION .....	152
REFERENCES .....	166
APPENDICES.....	187
Appendix A Physicochemical parameters.....	188
Appendix B Alpha-glucosidase inhibitory activities.....	191
Appendix C Antioxidation activities.....	194
Appendix D Cytotoxic activities.....	198
Appendix E Intracellular ROS and cell viability on EA.hy926 cell .....	202
Appendix F Protein expression SOD-1, HO-1, Bcl-2, Bax, and $\beta$ -actin on EA.hy926 cell .....	209
Appendix G The accession number of submitted DNA sequences of <i>Aquilaria</i> species and outgroup ( <i>E.siamensis</i> ) of six barcoding locus .....	212
VITA.....	214

## LIST OF TABLES

<b>Table 1</b>	The species of plant in genus <i>Aquilaria</i> .....	7
<b>Table 2</b>	The phenolic acid compounds found in <i>Aquilaria</i> spp. leaves.....	11
<b>Table 3</b>	The benzophenones compounds found in <i>Aquilaria</i> spp. leaves.....	11
<b>Table 4</b>	The xanthonoids compounds found in <i>Aquilaria</i> spp. leaves.....	13
<b>Table 5</b>	The flavonoids compounds found in <i>Aquilaria</i> spp. leaves .....	13
<b>Table 6</b>	The terpenoids compounds found in <i>Aquilaria</i> spp. leaves.....	15
<b>Table 7</b>	Chemical description of mangiferin .....	20
<b>Table 8</b>	Plant materials and place of collection .....	81
<b>Table 9</b>	Sequence of each primer .....	83
<b>Table 10</b>	The samples of <i>A. crassna</i> leaves used in this study.....	85
<b>Table 11</b>	The microscopic leaf measurement values of <i>A. crassna</i> leaves.....	90
<b>Table 12</b>	$R_f$ values of components in the ethanolic extract of <i>A. crassna</i> leaves.....	92
<b>Table 13</b>	Physicochemical values (% w/w) of <i>A. crassna</i> leaves .....	93
<b>Table 14</b>	The validity parameter of TLC-densitometry and image analysis method..	94
<b>Table 15</b>	Recovery of mangiferin by TLC-densitometry .....	96
<b>Table 16</b>	Intra-day and inter-day precision of mangiferin by TLC-densitometry .....	97
<b>Table 17</b>	Robustness of mangiferin quantitative analysis by TLC-densitometry method.....	98
<b>Table 18</b>	Recovery of mangiferin by TLC image analysis .....	99
<b>Table 19</b>	Intra-day precision of mangiferin by TLC image analysis .....	100
<b>Table 20</b>	Robustness of mangiferin quantitative analysis by TLC image analysis method.....	101

<b>Table 21</b> Extraction yield of <i>A. crassna</i> leaves and the amount of mangiferin in ethanolic extract of <i>A. crassna</i> leaves by TLC-densitometry and TLC image analysis method.....	105
<b>Table 22</b> The antioxidant activities of Ac14 ethanolic extract and mangiferin. Quercetin was used as a positive control .....	110
<b>Table 23</b> Cytotoxic activities of Ac14 ethanolic extract, mangiferin, and doxorubicin against cancer cell lines.....	113
<b>Table 24</b> Evaluation of the six DNA barcode loci.....	134
<b>Table 25</b> Estimates of evolutionary divergence between sequences of ITS region..	136
<b>Table 26</b> Estimates of evolutionary divergence between sequences of <i>rbcl</i> gene .	136
<b>Table 27</b> Estimates of evolutionary divergence between sequences of <i>matK</i> gene	140
<b>Table 28</b> Estimates of evolutionary divergence between sequences of <i>psbA-trnH</i> intergenic spacer .....	140
<b>Table 29</b> Estimates of evolutionary divergence between sequences of <i>rpoC1</i> gene .....	143
<b>Table 30</b> Estimates of evolutionary divergence between sequences of <i>ycf1</i> gene..	143
<b>Table 31</b> Estimates of evolutionary divergence between combination sequence of chloroplast genome .....	151
<b>Table 32</b> Physiocochemical values of <i>A. crassna</i> leaves from 15 different sources.	189
<b>Table 33</b> The percentage of yeast alpha-glucosidase inhibition of Ac14 extract.....	192
<b>Table 34</b> The percentage of yeast alpha-glucosidase inhibition of mangiferin.....	192
<b>Table 35</b> The percentage of yeast alpha-glucosidase inhibition of acarbose .....	193
<b>Table 36</b> The percentage of DPPH scavenging activity of Ac14 extract.....	195
<b>Table 37</b> The percentage of DPPH scavenging activity of mangiferin .....	195
<b>Table 38</b> The percentage of DPPH scavenging activity of quercetin .....	195



<b>Table 39</b>	The percentage of $\text{NO}^\bullet$ scavenging activity of Ac14 extract.....	196
<b>Table 40</b>	The percentage of $\text{NO}^\bullet$ scavenging activity of mangiferin .....	196
<b>Table 41</b>	The percentage of $\text{NO}^\bullet$ scavenging activity of quercetin.....	196
<b>Table 42</b>	The percentage of $\text{O}_2^{\bullet-}$ scavenging activity of Ac14 extract.....	197
<b>Table 43</b>	The percentage of $\text{O}_2^{\bullet-}$ scavenging activity of mangiferin.....	197
<b>Table 44</b>	The percentage of $\text{O}_2^{\bullet-}$ scavenging activity of quercetin .....	197
<b>Table 45</b>	Cytotoxic activity of Ac14 extract against MDA-231 cell line.....	199
<b>Table 46</b>	Cytotoxic activity of mangiferin against MDA-231 cell line.....	199
<b>Table 47</b>	Cytotoxic activity of doxorubicin against MDA-231 cell line .....	199
<b>Table 48</b>	Cytotoxic activity of Ac14 extract against HepG2 cell line .....	200
<b>Table 49</b>	Cytotoxic activity of mangiferin against HepG2 cell line.....	200
<b>Table 50</b>	Cytotoxic activity of doxorubicin against HepG2 cell line .....	200
<b>Table 51</b>	Cytotoxic activity of Ac14 extract against HT-29 cell line .....	201
<b>Table 52</b>	Cytotoxic activity of mangiferin against HT-29 cell line .....	201
<b>Table 53</b>	Cytotoxic activity of doxorubicin against HT-29 cell line.....	201
<b>Table 54</b>	The percentage of cell viability of Ac14 extract at various concentrations for 24 h measured by MTT assay.....	203
<b>Table 55</b>	The percentage of DCF fluorescence of Ac14 extract at various concentrations for 24 h measured by DCFH-DA assay. ....	203
<b>Table 56</b>	The percentage of cell viability of mangiferin at various concentrations for 24 h measured by MTT assay .....	204
<b>Table 57</b>	The percentage of DCF fluorescence of mangiferin at various concentrations for 24 h measured by DCFH-DA assay .....	204
<b>Table 58</b>	The percentage of cell viability of $\text{H}_2\text{O}_2$ at various concentrations for 0.5 h measured by MTT assay. ....	205

<b>Table 59</b>	The percentage of DCF fluorescence of H <sub>2</sub> O <sub>2</sub> at various concentrations for 0.5 h measured by DCFH-DA assay.....	206
<b>Table 60</b>	The percentage of cell viability of pretreatment with Ac14 extract for 24 h prior to 0.25 mM H <sub>2</sub> O <sub>2</sub> for 0.5 h measured by MTT assay.....	207
<b>Table 61</b>	The percentage of DCF fluorescence of pretreatment with Ac14 extract for 24 h prior to 0.25 mM H <sub>2</sub> O <sub>2</sub> for 0.5 h by DCFH-DA assay.....	207
<b>Table 62</b>	The percentage of cell viability of pretreatment with mangiferin for 24 h prior to 0.25 mM H <sub>2</sub> O <sub>2</sub> for 0.5 h measured by MTT assay.....	208
<b>Table 63</b>	The percentage of DCF fluorescence of pretreatment with mangiferin for 24 h prior to 0.25 mM H <sub>2</sub> O <sub>2</sub> for 0.5 h measured by DCFH-DA assay. ...	208
<b>Table 64</b>	The relative ratio of Ac14 extract on the protein expressions of SOD-1, HO-1, and Bcl-2/Bax ratio in EA.hy926 cells normalized by β-actin and quantitated by Western blot analysis .....	210
<b>Table 65</b>	The relative ratio of Ac14 extract on the protein expressions of SOD-1, HO-1 in H <sub>2</sub> O <sub>2</sub> -treated EA.hy926 cells normalized by β-actin and quantitated by Western blot analysis .....	210
<b>Table 66</b>	The relative ratio of mangiferin on the protein expressions of SOD-1, HO-1, and Bcl-2/Bax ratio in EA.hy926 cells normalized by β-actin and quantitated by Western blot analysis .....	211
<b>Table 67</b>	The relative ratio of mangiferin on the protein expressions of SOD-1, HO-1 in H <sub>2</sub> O <sub>2</sub> -treated EA.hy926 cells normalized by β-actin and quantitated by Western blot analysis .....	211
<b>Table 68</b>	Plant materials and their respective accession numbers .....	213

## LIST OF FIGURES

<b>Figure 1</b> Conceptual framework .....	4
<b>Figure 2</b> The morphological characters of plant in genus <i>Aquilaria</i> .....	8
<b>Figure 3</b> Chemical structure of mangiferin .....	20
<b>Figure 4</b> Formation of free radicals .....	26
<b>Figure 5</b> The biological effect of NO .....	27
<b>Figure 6</b> DPPH and antioxidant reaction .....	28
<b>Figure 7</b> mechanism reaction of FRAP assay .....	28
<b>Figure 8</b> The Griess test reaction .....	29
<b>Figure 9</b> Mechanism of action of $\alpha$ -glucosidase inhibitors .....	31
<b>Figure 10</b> The chemical reaction of MTT assay .....	32
<b>Figure 11</b> EA.hy926 morphology after freshly isolated in culture .....	34
<b>Figure 12</b> Common mechanism of scavenging $O_2^{\cdot-}$ by SOD .....	36
<b>Figure 13</b> Degradative reaction of heme via heme oxygenase .....	37
<b>Figure 14</b> The cytoprotective mechanism of HO-1 .....	38
<b>Figure 15</b> The process of apoptosis .....	39
<b>Figure 16</b> Extrinsic and intrinsic pathways of apoptosis .....	41
<b>Figure 17</b> Schematic diagram of the rDNA cluster .....	43
<b>Figure 18</b> General map of <i>matK</i> gene .....	45
<b>Figure 19</b> Gene map of tobacco ( <i>Nicotiana tabacum</i> ) chloroplast genome .....	45
<b>Figure 20</b> General map of <i>trnH-psbA</i> region .....	46
<b>Figure 21</b> General map of <i>rpoC</i> gene .....	47
<b>Figure 22</b> General map of <i>ycf1</i> gene .....	47

<b>Figure 23</b> The polymerase chain reaction (PCR) .....	49
<b>Figure 24</b> Maxam-Gilbert sequencing techniques .....	50
<b>Figure 25</b> Sanger sequencing techniques.....	51
<b>Figure 26</b> Macroscopic characteristics of <i>A. crassna</i> .....	86
<b>Figure 27</b> Transverse section of midrib and lamina of <i>A. crassna</i> leaves .....	87
<b>Figure 28</b> Microscopic characteristics of the surface views of <i>A. crassna</i> lamina. ....	88
<b>Figure 29</b> Microscopic characteristics of powdered <i>A. crassna</i> .....	89
<b>Figure 30</b> Thin layer chromatographic fingerprinting of a ethanolic extract of dried <i>A. crassna</i> leaves (E) and mangiferin at concentration 0.4 mg/ml (M).....	91
<b>Figure 31</b> Absorbance spectra of mangiferin among standard and the <i>A. crassna</i> leaf extracts .....	95
<b>Figure 32</b> Calibration curve of mangiferin standard by TLC-densitometry .....	96
<b>Figure 33</b> Calibration curve of mangiferin standard by TLC image analysis method ..	99
<b>Figure 34</b> 3D-TLC densitometric chromatogram of mangiferin standard and the ethanolic extracts of <i>A. crassna</i> leaves .....	102
<b>Figure 35</b> The developed siliga gel-TLC plate .....	103
<b>Figure 36</b> The TLC image subtract background from UV 254 nm picture using imageJ software.....	104
<b>Figure 37</b> TLC image analysis chromatogram by imageJ software .....	104
<b>Figure 38</b> Dose-response curve of yeast alpha glucosidase inhibitions .....	106
<b>Figure 39</b> Dose-response curve of DPPH scavenging activity.....	107
<b>Figure 40</b> Dose-response curve of nitric oxide radical scavenging activity .....	108
<b>Figure 41</b> Dose-response curve of superoxide radical scavenging activity .....	109
<b>Figure 42</b> Standard curve of ferrous sulfate for determining the ferric reducing antioxidant power.....	111

<b>Figure 43</b> Standard curve of gallic acid for determining the total phenolic content	112
<b>Figure 44</b> Cytotoxic activity of mangiferin (A), Ac14 ethanolic extract (B), and doxorubicin (C)	114
<b>Figure 45</b> The viability testing of Ac14 ethanolic extract (A) and mangiferin (B) on EA.hy926 cell	115
<b>Figure 46</b> Effect of ethanolic extract of Ac14 on intracellular ROS generation and cell viability in EA.hy926 cell	116
<b>Figure 47</b> Effect of mangiferin on intracellular ROS generation and cell viability in EA.hy926 cell	117
<b>Figure 48</b> The viability testing of hydrogen peroxide (H <sub>2</sub> O <sub>2</sub> ) on EA.hy926 cell	118
<b>Figure 49</b> Effect of H <sub>2</sub> O <sub>2</sub> on intracellular ROS generation and cell viability in EA.hy926 cell	119
<b>Figure 50</b> Effect of ethanolic extract of Ac14 on intracellular ROS generation and cell viability of H <sub>2</sub> O <sub>2</sub> -injured EA.hy926 cell	121
<b>Figure 51</b> Effect of mangiferin on intracellular ROS generation and cell viability of H <sub>2</sub> O <sub>2</sub> -injured EA.hy926 cell	123
<b>Figure 52</b> Effect of mangiferin and ethanolic extract of Ac14 on protein expression of Cu/Zn-SOD in EA.hy926 cell	125
<b>Figure 53</b> Effect of mangiferin and ethanolic extract of Ac14 on protein expression of Cu/Zn-SOD in H <sub>2</sub> O <sub>2</sub> -treated EA.hy926 cell	126
<b>Figure 54</b> Effect of mangiferin and ethanolic extract of Ac14 on protein expression of HO-1 in EA.hy926 cell	128
<b>Figure 55</b> Effect of mangiferin and ethanolic extract of Ac14 on protein expression of HO-1 in H <sub>2</sub> O <sub>2</sub> -treated EA.hy926 cell	129
<b>Figure 56</b> Effect of mangiferin and ethanolic extract of Ac14 on protein expression of Bcl-2 and Bax in EA.hy926 cell	131

<b>Figure 57</b> Effect of mangiferin and ethanolic extract of Ac14 on protein expression of Bcl-2 and Bax in EA.hy926 cell.....	132
<b>Figure 58</b> Alignment of partial sequence ITS region of three <i>Aquilaria</i> plants and outgroup ( <i>E. siamensis</i> ).....	135
<b>Figure 59</b> Alignment of partial sequence <i>rbcL</i> gene of three <i>Aquilaria</i> plants and outgroup ( <i>E. siamensis</i> ).....	137
<b>Figure 60</b> Alignment of partial sequence <i>matK</i> gene of three <i>Aquilaria</i> plants and outgroup ( <i>E. siamensis</i> ).....	139
<b>Figure 61</b> Alignment of partial sequence <i>psbA-trnH</i> intergenic spacer of three <i>Aquilaria</i> plants and outgroup ( <i>E. siamensis</i> ).....	141
<b>Figure 62</b> Alignment of partial sequence <i>rpoC1</i> gene of three <i>Aquilaria</i> plants and outgroup ( <i>E. siamensis</i> ).....	142
<b>Figure 63</b> Alignment of partial sequence <i>ycf1</i> of three <i>Aquilaria</i> plants and outgroup ( <i>E. siamensis</i> ).....	144
<b>Figure 64</b> Molecular phylogenetic analysis by ML method of ITS region.....	145
<b>Figure 65</b> Molecular phylogenetic analysis by ML method of <i>rbcL</i> gene partial sequences.....	146
<b>Figure 66</b> Molecular phylogenetic analysis by ML method of <i>matK</i> gene partial sequences.....	147
<b>Figure 67</b> Molecular phylogenetic analysis by ML method of <i>psbA-trnH</i> intergenic spacer sequences.....	148
<b>Figure 68</b> Molecular phylogenetic analysis by ML method of <i>rpoC1</i> gene partial sequences.....	149
<b>Figure 69</b> Molecular phylogenetic analysis by ML method of <i>ycf1</i> gene partial sequences.....	150
<b>Figure 70</b> Molecular phylogenetic analysis by ML method of combination sequence of chloroplast genome.....	151

**Figure 71** The nonactive site binding nodes in  $\alpha$ -glucosidase. .... 156

**Figure 72** The generation of ROS and endogenous antioxidant mechanism ..... 159

**Figure 73** The effect of mangiferin on Nrf2/ARE detoxification pathway ..... 160



## LIST OF ABBREVIATIONS

°C	Celsius degree
μg	microgram
μM	micromolar
A	adenine
BAX	Bcl-2 associated X protein
Bcl-2	B cell lymphoma-2
bp	base pairs
C	cytosine
CAT	catalase
cm	centimetre
CO1	cytochrome oxidase 1
cpDNA	chloroplast DNA
DNA	deoxyribonucleic acid
dNTPs	deoxyribonucleotide triphosphates
FDA	Food and Drug Administration
G	guanine
GPx	glutathione peroxidases
H <sub>2</sub> O <sub>2</sub>	hydrogen peroxide
HO-1	heme oxygenase 1
HUVECs	human umbilical vein endothelial cells
Kbp	Kilo base pairs
KCl	potassium chloride
KDa	Kilodalton
LOD	limit of detection
LOQ	limit of quantitation



m	meter
mg	milligram
MgCl <sub>2</sub>	magnesium chloride
ml	milliliter
ML	Maximum Likelihood
mm	millimeter
mm <sup>2</sup>	square millimeter
nDNA	nuclear DNA
nm	nanometer
NO	nitric oxide
NOS	nitric oxide synthase
PCR	polymerase chain reaction
R <sub>f</sub>	retention factor
ROS	reactive oxygen species
RSD	relative standard deviation
SOD	superoxide dismutase
T	thymine
TLC	thin layer chromatography
UV	ultraviolet
VIS	visible light
WHO	World Health Organization



## CHAPTER I

### INTRODUCTION

#### 1.1 Background and rationale

Nowadays, traditional medicine dispensing is internationally recognized as an effective treatment. Thailand is a country which has a medical civilization from prehistory indigenous regional practices until modern medicine in present. This year (2017), Thai food and drug administration (Thai FDA) announced the National List of Essential Medicines [1], which comprised of chemicals, biologics drug and drug derived from medicinal plants. As a result, herbal products have been promoted in term of dispensing in the health care system. There are 50 traditional recipes and 24 drugs derived from medicinal plants in the National List of Essential Medicines; however, the specification of medicinal plant raw materials in the Thai Herbal Pharmacopoeia [2] cannot be included all plants in those lists. Nonetheless, the quality control of drugs is an essential process to guarantee their efficacy as well as safety.

From the National List of Essential Medicines, Agarwood (*Aquilaria crassna* Pierre ex Lecomte, Thymelaeaceae) has been used in many recipes, such as Yahom-Teppajit, Yahom-Navakot, Yahom-Intajak. *A. crassna* is a medium-sized evergreen tree found throughout Southeast Asia and China. Agarwood has been a part of Ayurvedic, Traditional Chinese Medicine and Traditional Thai Medicine for centuries. This plant is not only well known in aromatherapy uses, but also recognized as herbal medicine for the treatment of various diseases such as sedative, analgesic, and digestive [3]. Previous studies on the leaves of *A. crassna* revealed that it contained various potential activities including anti-diabetic [4], antipyretic, analgesic [5], antioxidant [6], and laxative [7, 8]. Recently, mangiferin was identified as an active component in *A. crassna* leaves [9]. Mangiferin is a potent antioxidant from various natural sources [10-13] and

has been reported for the treatment of diabetes [14-18], cancer [19], rheumatoid arthritis [20], hypolipidemic [16], oxidative stress [21-23], and inflammation [24].

As aforementioned, the standardization of herbal raw materials is a crucial process for quality assurance and therapeutic efficacy. The method for authentication, quality control and the validation process is still preferred for standardization of herbal materials. Macroscopic, microscopic, and chemical fingerprinting are the routine procedures for medicinal plant materials identification, while physicochemical parameters and the content of active substances are used to ensure the quality [25-27]. Polymerase chain reaction (PCR)-based molecular markers, which have been widely applied to authentication of species, these markers are forceful process to provide the genetic relationship of the species, and also appraise the genetic evolution [28]. Interestingly, molecular markers has an advantage above macro-, microscopic determination, chemical fingerprinting because the age of the plant, environmental and physiological conditions have less influenced on the investigation process [29-31]. DNA barcoding has been procuring widespread acceptance as a rapidity, reproducibility, and simple method for species identification [32, 33]. DNA barcode is a short DNA sequence that amplified using specific primers in interesting region [34]. The mitochondrial gene cytochrome c oxidase I (CO1) is broadly agreed as a universal DNA barcode for animal species [35]. However, CO1 gene was informed improper for flowering plants because the mutation rate of mitochondrial DNA was low [36]. Thus, the using chloroplast genome (cpDNA) and nuclear DNA (nDNA) region was proposed as another option. The Consortium for the Barcode of Life (CBOL) suggested a combination of both the cpDNA maturase K (*matK*) gene and the ribulose-bisphosphate carboxylase (*rbcL*) gene as the core of DNA barcode for plants, and further combined them with the non-coding *psbA-trnH* intergenic spacer and the nuclear ribosomal internal transcribed spacer (ITS) or ITS2 regions to attain high

differentiation at the species level [37-41]. Currently, DNA barcoding is acknowledged as an efficient tool for species-level identification in plants, and has contributed in the resolution of relationships among taxa, forensic identification, and species authentication [42, 43].

However, the scientific report on pharmacognostic parameters and simultaneous quantification of mangiferin using TLC method for standardization of *A. crassna* leaves have never been established. Moreover, natural products which prefer to be used as food supplement, cosmetic products, drink, and herbal medicine, the utility of medicinal plants should be considered to document its side effects, toxicity, and therapeutic levels. Even though, agarwood leaves herbal tea was claimed by vendor as anticancer and anti-hyperglycemic, but the scientific experiments are still needed to proof the biological activity and mechanism of action of the herbal product claim.

## 1.2 Objectives of the study

- (1) To develop the pharmacognostic specification of *Aquilaria crassna* leaves
- (2) To evaluate the mangiferin content of *Aquilaria crassna* leaves using thin layer chromatography technique combined with image analysis (Image J software) compare to TLC densitometry
- (3) To investigate the genetic relationships of selected *Aquilaria* species by determination of the DNA barcoding
- (4) To investigate biological activities consisted of anti-hyperglycemia, anti-oxidant, anticancer and cytoprotective activity from the ethanolic extract of *Aquilaria crassna* leaves and mangiferin compound

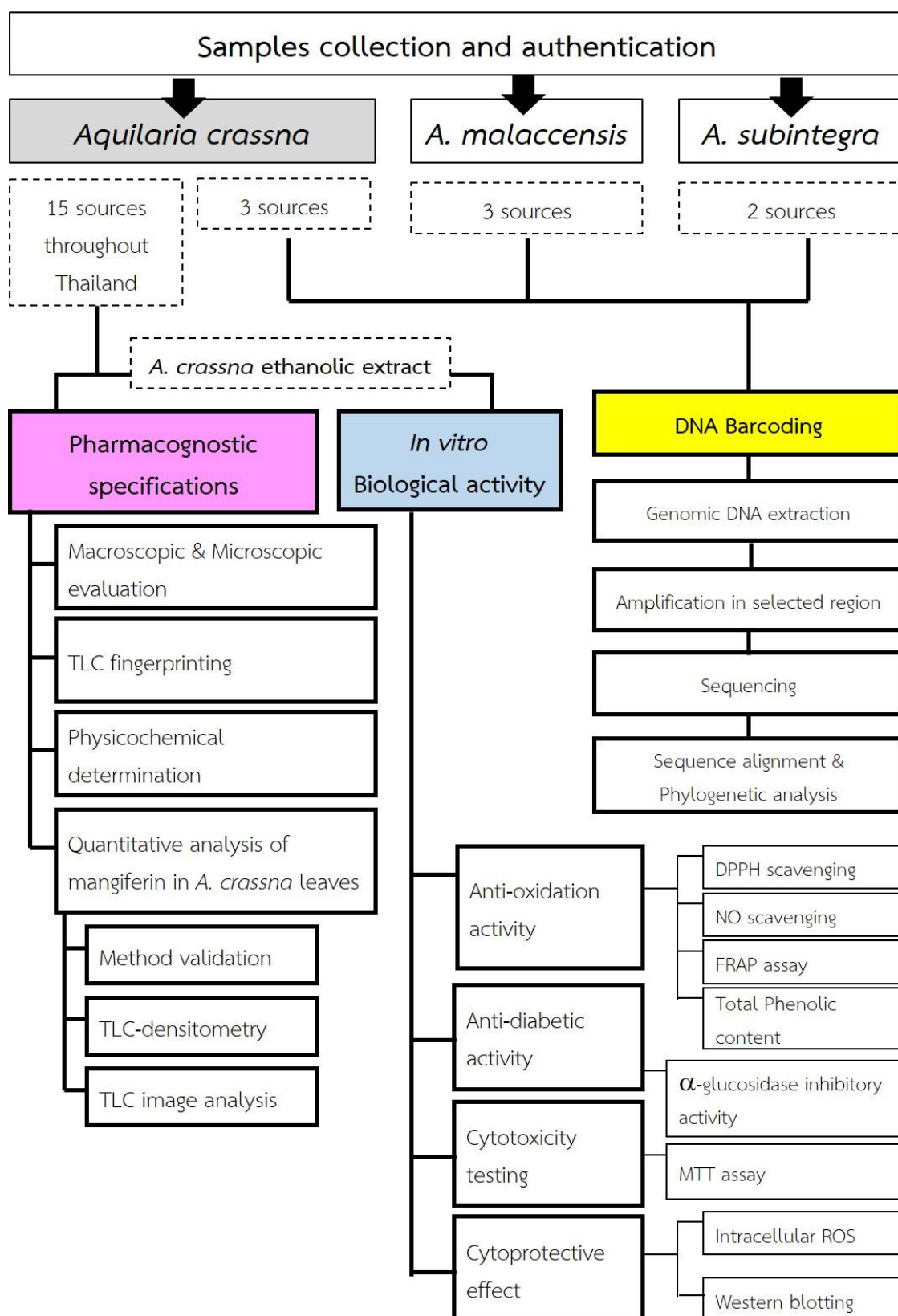


Figure 1 Conceptual framework

## CHAPTER II

### LITERATURE REVIEWS

#### 2.1 Description of plant in genus *Aquilaria*

*Aquilaria* spp. (agarwood) is valuable and well-known medicinal plant for aromatherapy. Plants in this genus belong to Thymelaeaceae family which accounted for 21 species in the world (Table 1). *Aquilaria* spp. only distributed in South and Southeast Asian country, such as China, Vietnam, Laos, Cambodia, Malaysia, Singapore, Pakistan, India and Thailand [44]. However, only four species including *Aquilaria crassna*, *Aquilaria malaccensis*, *Aquilaria subintegra*, and *Aquilaria hirta* can be found in Thailand [45].

#### Taxonomic Hierarchy:

**Kingdom:** Plantae – Plants  
**Phylum:** Tracheophyta  
**Class:** Magnoliopsida  
**Order:** Myrtales  
**Family:** Thymelaeaceae  
**Genus:** *Aquilaria*

According to Flora of Thailand, Peterson has described the character of plant in this genus that “*the type of tree are shrubs or trees, branches pubescent, and later glabrescent. The characteristic of leaves is alternate, simple, entire, elliptic to slightly ovate, penninerved, nerves sometimes branched, margins undulate, often slightly recurved, thickened. Inflorescence axillary, terminal, umbelliform, rarely with small bracts. Flowers 5-merous, articulated, pedicelled. Calyx-tube campanulate or tubular, persistent, often splitting on one side in fruit; calyx-lobes reflexed or erect, puberulous outside and often inside. Petals 10, free or connate at the base, elliptic or ovate,*

*pilose or villous, inserted in the throat of the tube opposite the calyx-lobes. Stamens 10, at the same level as the petals or attached slightly below them, sessile or filamentous, those alternating with the sepals sometimes slightly longer than the episepalous ones; anthers linear, dorsifixed. Ovary subsessile, elliptic or ovate, puberulous, 2-loculed; style obscure or distinct; stigma globose or oblong; disc none. Fruit a loculicidal capsule, elliptic to suborbicular, compressed contrary to the dissepiment, puberulous. Seeds elliptic to ovoid, testa crustaceous, with a caruncle-like appendage at the base; endosperm very thin or none; cotyledons thick, planoconvex.”*



**Table 1** The species of plant in genus *Aquilaria*

Species	Authorship
<i>Aquilaria apiculata</i>	Merr.
<i>Aquilaria baillonii</i>	Pierre ex Lecomte
<i>Aquilaria banaensis</i>	P.H.Hô
<i>Aquilaria beccariana</i>	Tiegh.
<i>Aquilaria brachyantha</i>	(Merr.) Hallier f.
<i>Aquilaria citrinicarpa</i>	(Elmer) Hallier f.
<i>Aquilaria crassna</i>	Pierre ex Lecomte
<i>Aquilaria cumingiana</i>	(Decne.) Ridl.
<i>Aquilaria decemcosta</i>	Hallier f.
<i>Aquilaria filarial</i>	(Oken) Merr.
<i>Aquilaria hirta</i>	Ridl.
<i>Aquilaria khasiana</i>	Hallier f.
<i>Aquilaria malaccensis</i>	Lam.
<i>Aquilaria microcarpa</i>	Baill.
<i>Aquilaria parvifolia</i>	(Quisumb.) Ding Hou
<i>Aquilaria rostrate</i>	Ridl.
<i>Aquilaria rugosa</i>	K. Le-Cong and Kessler
<i>Aquilaria sinensis</i>	(Lour.) Spreng.
<i>Aquilaria subintegra</i>	Ding Hou
<i>Aquilaria urdanetensis</i>	(Elmer) Hallier f.
<i>Aquilaria yunnanensis</i>	S.C. Huang



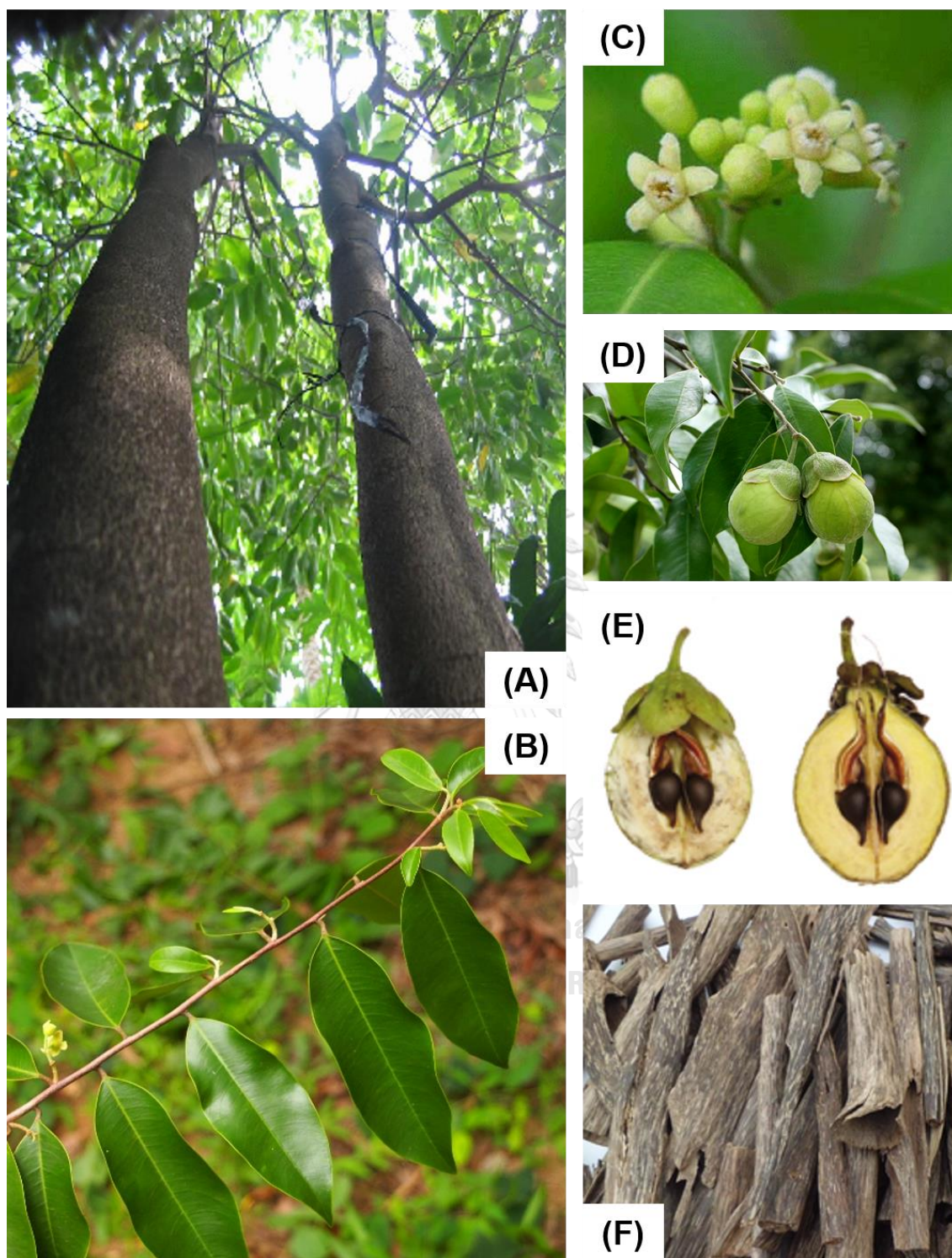


**Figure 2** The morphological characters of plant in genus *Aquilaria*  
(A) trees; (B) branch with leaves; (C) flowers; (D) fruits; (E) fruit and seed; (F) bark

However, Peterson also explained the characteristic of *A. crassna*, *A. subintegra*, and *A. malaccensis* in the Flora of Thailand [45] as “*A. crassna*, tree 10-30 m high, bark grey or whitish, smooth or rugose. Pulp spongy, white. Branchlets pubescent to glabrescent. Leaves acute to acuminate, usually with a pronounced tip, 6-10 cm long, base cuneate to acute, 7-11.5 by 2.5-5 cm, coriaceous, green, shining, glabrous above, glabrous below or with scattered hair along the margin and midrib; secondary nerves 12-18 pairs, prominent on both sides, petiole pubescent, 3-7 mm long. Inflorescence in fascicles, 4-6-flowered; peduncle pubescent, 3-5 mm long. Flowers greenish; pedicel pubescent, 5-10 mm long. Calyx-tube puberulous outside and inside, 3-4 mm long; calyx lobes 3-4 by 2-3.5 mm, puberulous on both sides (calyx much enlarge after flowering). Petals densely pilose, 1-1.5 mm long. Stamens with filaments 1-1.5 mm long; anthers 1 mm long. Fruit suborbicular, puberulous, 2.5-3.5 by 2-2.5 cm, at the base surrounded by the persistent calyx, increasing in size after flowering; seeds 10 by 5 mm.”

“*A. malaccensis*, tree up to 40 m tall, bark whitish to greyish, smooth; branchlets slender, pubescent glabrescent. Leaves acuminate, sometimes with a rather pronounced tip, 0.5-1 cm long, 5-15 cm by 2-5.2 cm, base cuneate, chartaceous, glabrous or with scattered hairs along the midrib beneath; secondary nerves 12-16 pairs, elevated beneath, obscure above; petiole pubescent or glabrous, 3-6 mm long. Inflorescence terminal or axillary, 8-10-flowered; peduncle pubescent to slightly hairy, 4-10 mm long. Flowers green or yellowish; pedicel slightly hairy, 2-5 mm long. Calyx-tube 3-5 mm long puberulous outside, almost glabrous inside; calyx-lobes 2-3 by 1.5-2 mm, puberulous on both sides. Petals pilose, 1-1.45 mm long. Stamens with filaments 1-2 mm long; anthers 1-1.5 mm long. Ovary pubescent, 1-2 mm long; style not distinct; stigma globose, 1 mm. Fruit oblong, 2.5-4 by 1.5-2.5 cm (unripe), pubescent. Seed ovoid, 10 by 6 cm, covered with red hairs, beak ca 4 mm long, appendage twisted, as long as the seed.”

“*A. subintegra*. Shrubs or small trees up to 2 m tall. Leaves acuminate, base cuneate to obtuse, (14-)19-27.5 by (5-)7-10.5 cm, chartaceous, lower surface slightly pubescent to glabrescent; petiole pubescent or glabrous, 5-10 mm long. Inflorescence axillary, 8-20-flowered; peduncle puberulous, 1-3 cm long. Flowers white; pedicel puberulous, 6-13 mm long. Calyx-tube 5-12 mm long, outside slightly puberulous or glabrous, inside hairy towards base; calyx-lobes 3-5 by 1.2-2.5 mm, ± puberulous on the upper half inside, sparsely hairy or glabrous outside, ciliated. Petals united at the base, erose, villous, 1-1.5 mm long. Stamen sessile; anthers 1.5-2 mm long. Ovary sessile, puberulous, 2-3 mm long; style 0.5-1 mm long; stigma globose, 1 mm. Fruit elliptic; seed narrowly elliptic, sparsely puberulous, the glabrous appendage attached along one side of the elongate part.”

## 2.2 Chemical constituents of *Aquilaria* spp. leaves

Phytochemical screening of ethanolic, methanolic, and water extracts of agarwood leaves illustrated the presence of tannins, flavonoids, terpenoids, saponin, and alkaloids [46-50]. The phytochemical studies of *Aquilaria* spp. leaves and their chemical structure are summarized in Table 2 – 6.

**Table 2** The phenolic acid compounds found in *Aquilaria* spp. leaves

Chemical compound	species	Reference
4-hydroxybenzoic acid	<i>A. sinensis</i> (Lour.) Gilg	[51-54]
	<i>A. agallocha</i> Roxb.	[55]
Isovanillic acid	<i>A. sinensis</i> (Lour.) Gilg	[53]
	<i>A. agallocha</i> Roxb.	[55]
Protocatechuic acid	<i>A. sinensis</i> (Lour.) Gilg	[4]
Syringic acid	<i>A. sinensis</i> (Lour.) Gilg	[53]
	<i>A. agallocha</i> Roxb.	[55]
Vanillic acid	<i>A. sinensis</i> (Lour.) Gilg	[53]
	<i>A. agallocha</i> Roxb.	[55]

**Table 3** The benzophenones compounds found in *Aquilaria* spp. leaves

Chemical compound	species	Reference
Benzophenones aglycones		
Aglycone of aquilarisinin (iriflophenone)	<i>A. sinensis</i> (Lour.) Gilg	[54]
Mono-glycosides		
Aquilarinoside A	<i>A. sinensis</i> (Lour.) Gilg	[56, 57]
Iriflophenone 2-O- $\alpha$ -L-rhamnopyranoside	<i>A. sinensis</i> (Lour.) Gilg	[54, 57-59]
	<i>A. crassna</i> Pierre ex Lecomte	[60-62]
Iriflophenone 3-C- $\beta$ -D-rhamnopyranoside	<i>A. sinensis</i> (Lour.) Gilg	[54, 60, 63]
	<i>A. crassna</i> Pierre ex Lecomte	[57, 64]

Table 3 The benzophenones compounds found in *Aquilaria* spp. leaves (Cont.)

Chemical compound	species	Reference
Iriflophenone, [2-(2-O-acetyl- $\alpha$ -L-rhamnopyranosyl)oxy]	<i>A. crassna</i> Pierre ex Lecomte	[57]
Iriflophenone, [2-(3-O-acetyl- $\alpha$ -L-rhamnopyranosyl)oxy]	<i>A. crassna</i> Pierre ex Lecomte	[57]
Iriflophenone, [2-(4-O-acetyl- $\alpha$ -L-rhamnopyranosyl)oxy]	<i>A. crassna</i> Pierre ex Lecomte	[57]
Di-glycosides		
Aquilarineside A	<i>A. sinensis</i> (Lour.) Gilg	[65]
Aquilarineside B	<i>A. sinensis</i> (Lour.) Gilg	[65]
Aquilarineside C	<i>A. sinensis</i> (Lour.) Gilg	[65]
Aquilarineside D	<i>A. sinensis</i> (Lour.) Gilg	[65]
Aquilarineside E	<i>A. sinensis</i> (Lour.) Gilg	[65]
Aquilarisinin	<i>A. sinensis</i> (Lour.) Gilg	[54]
Iriflophenone 3,5-C- $\beta$ -D-diglucoyranoside	<i>A. sinensis</i> (Lour.) Gilg	[54, 59, 60, 62]
Iriflophenone 3-C- $\beta$ -glucoside	<i>A. crassna</i> Pierre ex Lecomte	[57]
	<i>A. sinensis</i> (Lour.) Gilg	[62]

**Table 4** The xanthonoids compounds found in *Aquilaria* spp. leaves

Chemical compound	species	Reference
Aglycones		
1,2,3,6,7-pentahydroxy-9H-xanthen-9-one	<i>A. sinensis</i> (Lour.) Gilg	[62]
Mono-glycosides		
Aquilarixanthone	<i>A. crassna</i> Pierre ex Lecomte	[57]
Homomangiferin	<i>A. crassna</i> Pierre ex Lecomte	[57]
Isomangiferin	<i>A. crassna</i> Pierre ex Lecomte	[57]
Mangiferin	<i>A. crassna</i> Pierre ex Lecomte	[57, 66]
	<i>A. sinensis</i> (Lour.) Gilg	[7, 54, 59, 60, 62, 63, 67]
Di-glycosides		
Neomangiferin	<i>A. crassna</i> Pierre ex Lecomte	[57]

**Table 5** The flavonoids compounds found in *Aquilaria* spp. leaves

Chemical compound	species	Reference
Flavanols		
Epicatechin gallate	<i>A. crassna</i> Pierre ex Lecomte	[64]
Epigallocatechin gallate	<i>A. crassna</i> Pierre ex Lecomte	[64]
Tri-oxygenated flavones		
Apigenin-7,4'-dimethylether	<i>A. sinensis</i> (Lour.) Gilg	[51-54, 63, 68]
	<i>A. agallocha</i> Roxb.	[55]
7-hydroxy-5,4'-dimethoxyflavone	<i>A. sinensis</i> (Lour.) Gilg	[51]

**Table 5** The flavonoids compounds found in *Aquilaria* spp. leaves (Cont.)

Chemical compound	species	Reference
Genkwanin	<i>A. sinensis</i> (Lour.) Gilg	[51, 52, 54, 57, 59, 60, 62, 63, 67, 68]
	<i>A. crassna</i> Pierre ex Lecomte	[66]
Tetra-oxygenated flavones		
Luteolin	<i>A. sinensis</i> (Lour.) Gilg	[52, 67-69]
Hydroxygenkwanin	<i>A. sinensis</i> (Lour.) Gilg	[57, 67, 68]
Luteolin-7,4'-dimethylether	<i>A. sinensis</i> (Lour.) Gilg	[53, 68]
	<i>A. agallocha</i> Roxb.	[55]
Luteolin-7,3',4'-trimethylether	<i>A. sinensis</i> (Lour.) Gilg	[51-53, 57, 68]
	<i>A. agallocha</i> Roxb.	[55]
5,4'-dihydroxy-7,3'-dimethoxyflavone	<i>A. sinensis</i> (Lour.) Gilg	[51]
Penta-oxygenated flavones		
7,3',5'-tri-O-methyltricerin	<i>A. sinensis</i> (Lour.) Gilg	[58]
Mono-glycosides		
Delphinidin-3-glucoside	<i>A. sinensis</i> (Lour.) Gilg	[54, 57]
7-O- $\beta$ -D-glucopyranoside of 5-O-methylapigenin	<i>A. sinensis</i> (Lour.) Gilg	[58, 67]
Hypolaetin 5-O- $\beta$ -D-glucuronopyranoside	<i>A. sinensis</i> (Lour.) Gilg	[54, 57]
Genkwanin-5-O- $\beta$ -D-glucopyranoside	<i>A. sinensis</i> (Lour.) Gilg	[59, 60, 69]
Di-glycosides		
4'-hydroxy-5-methoxyflavone-7-O-glucoxyloside	<i>A. sinensis</i> (Lour.) Gilg	[69]
7,4'-di-O-methylapigenin-5-O-xylosy;glucoside	<i>A. sinensis</i> (Lour.) Gilg	[57]

**Table 5** The flavonoids compounds found in *Aquilaria* spp. leaves (Cont.)

Chemical compound	species	Reference
5- <i>O</i> -xylosylglucoside of 7- <i>O</i> -methylapigenin	<i>A. sinensis</i> (Lour.) Gilg	[67]
5- <i>O</i> -xylosylglucoside of 7,4'-di- <i>O</i> -methylapigenin	<i>A. sinensis</i> (Lour.) Gilg	[67]
Aquisiflavoside	<i>A. sinensis</i> (Lour.) Gilg	[70]
Genkwanin-4'-methyl ether 5- <i>O</i> - $\beta$ -primeveroside	<i>A. sinensis</i> (Lour.) Gilg	[59]
	<i>A. crassna</i> Pierre ex Lecomte	[60]
Genkwanin-5- <i>O</i> - $\beta$ -D-primeveroside (yuankanin)	<i>A. sinensis</i> (Lour.) Gilg	[7, 59, 69]
	<i>A. crassna</i> Pierre ex Lecomte	[60, 62]

**Table 6** The terpenoids compounds found in *Aquilaria* spp. leaves

Chemical compound	species	Reference
Diterpenoids		
Cryptotanshinone	<i>A. sinensis</i> (Lour.) Gilg	[71]
Dihydotanshinone I	<i>A. sinensis</i> (Lour.) Gilg	[54]
Tanshinone I	<i>A. sinensis</i> (Lour.) Gilg	[54]
Tanshinone IIA	<i>A. sinensis</i> (Lour.) Gilg	[54]
3,7,11,15-tetramethyl-2-hexadecan-1-ol (phytol)	<i>A. malaccensis</i> Lam.	[72]
Triterpenoids		
2- $\alpha$ -hydroxyursane	<i>A. sinensis</i> (Lour.) Gilg	[71]
2- $\alpha$ -hydroxyursolic acid	<i>A. sinensis</i> (Lour.) Gilg	[54]
Epifriedelanol	<i>A. sinensis</i> (Lour.) Gilg	[51]
Friedelan	<i>A. sinensis</i> (Lour.) Gilg	[51]



**Table 6** The terpenoids compounds found in *Aquilaria* spp. leaves (Cont.)

Chemical compound	species	Reference
Friedelin	<i>A. sinensis</i> (Lour.) Gilg	[51]
Squalene	<i>A. malaccensis</i> Lam.	[72]
Phytosterols/steroids		
Stigmasterol	<i>A. sinensis</i> (Lour.) Gilg	[53]
	<i>A. agallocha</i> Roxb.	[55]
(3 $\beta$ ,7 $\alpha$ )-stigmast-5-ene-3,7-diol	<i>A. sinensis</i> (Lour.) Gilg	[58]
Stigmasta-4,22-dien-3-one	<i>A. sinensis</i> (Lour.) Gilg	[53]
$\beta$ -sitostenone	<i>A. sinensis</i> (Lour.) Gilg	[53]
	<i>A. agallocha</i> Roxb.	[55]
$\beta$ -sitosterol	<i>A. sinensis</i> (Lour.) Gilg	[53, 71]
	<i>A. agallocha</i> Roxb.	[55]
Daucosterol	<i>A. sinensis</i> (Lour.) Gilg	[71]

## 2.3 Pharmacological activities of agarwood leaves

There are various pharmacological studies on agarwood leaf extracts, such as anti-diabetic activity, anti-inflammatory activity, antipyretic activity, analgesic activity, antimicrobial activity, antioxidant activity, and laxative activity.

### 2.3.1 Antihyperglycemic activity

Medicinal plants in genus *Aquilaria* were extracted for *in vitro* and *in vivo* anti-diabetic researches. There are various targets for reducing the blood sugar level. The inhibition of  $\alpha$ -glucosidase is the popular target because this enzyme takes a response on starch and glycogen digestion. The methanolic extracts of *A. malaccensis* and *A. hirta* showed lower value of  $IC_{50}$  than acarbose (positive control) in *in vitro* testing, 375.50  $\mu\text{g/mL}$ , 452.82  $\mu\text{g/mL}$ , and 823.94  $\mu\text{g/mL}$ , respectively [73]. In contrast, Feng *et al.* (2011) found that the *A. sinensis* leaf had potential as alpha-glucosidase inhibitory activity with the  $IC_{50}$  of ethyl acetate fraction ( $336.0 \pm 45.1 \mu\text{g/mL}$ ), butanol fraction ( $990.1 \pm 59.1 \mu\text{g/mL}$ ), water soluble fraction ( $993.2 \pm 68.2 \mu\text{g/mL}$ ), petroleum ether fraction ( $1046.0 \pm 42.1 \mu\text{g/mL}$ ), and ethanol fraction ( $1056.0 \pm 28.6 \mu\text{g/mL}$ ), had lower potency than acarbose ( $372.0 \pm 37.8 \mu\text{g/mL}$ ) [54]. However, the *in vivo* experiments displayed the potential of agarwood leaf extract for reduced blood glucose level in mice [4, 63, 74].

### 2.3.2 Anti-inflammatory, anti-nociceptive/analgesic/antipyretic

Various *in vivo* researches focus on determination of anti-inflammation, anti-nociceptive, analgesia, and antipyretic activity using agarwood leaf extract. Sattayasai *et al.* (2012) determined the antipyretic, analgesic and anti-inflammatory activity of methanolic extract of *Aquilaria crassna* [5]. Researchers used baker's yeast-induced fever Sprague Dawley rats for determining the antipyretic effect and carrageenan-

induced paw edema rats for ascertaining the inflammatory response, whereas mice were used to investigate analgesia activity using the hot plate test. The results of fever reduction found that *A. crassna* leaf extract decreased the rectal temperature in experimental group when compared to control, and this extract can be increased the thermal threshold in *in vivo* hot plate assay. While, this leaf extract did not respond to anti-inflammatory activity. However, the results of *in vitro* anti-inflammatory response are not consistent to *in vivo* study. Zhou *et al.* (2008) summarized that *A. sinensis* extracts showed anti-inflammatory effects through the inhibition of CMC-NA-induced leukocyte emigration and decrease the release of nitric oxide from lipopolysaccharide-stimulated macrophages [75].

### 2.3.3 Anti-microbial activity

The extracts of *Aquilaria* spp. had been tested for screening the potential as bactericidal activity. The aqueous extract of *Aquilaria crassna* leaves caused swelling and distortion of *Staphylococcus epidermidis* cell wall and inhibited biofilm formation [46]. In addition, Kakino *et al.* (2012) mentioned that aqueous and ethanolic extract of *A. crassna* leaves could inhibit the growth of *Staphylococcus aureus*, *Clostridium difficile*, *Peptostreptococcus anaerobius*, whereas neither aqueous nor ethanol displayed antimicrobial activity against *Escherichia coli*, *Enterococcus faecalis*, *Bifidobacterium longum*, and *Bifidobacterium adolescentis* [8]. Additionally, this study found that the dichloromethane extract of *A. crassna* leaves gave the highest inhibition zone compared to another solvent when tested against *S. aureus*. For another *Aquilaria* species, *A. subintegra*, its leaf extracts possessed antimicrobial activity. The acetone extract showed inhibition against *Bacillus subtilis*, while hexane extract could inhibit *Staphylococcus aureus* [76].

#### 2.3.4 Anti-oxidation activity

The plants in genus *Aquilaria* had highly potential on anti-oxidant activity. There are assorted publication revealed this activity *via* DPPH scavenging activity assay, total oxidation capacity (TAC) assay, cupric reducing antioxidant capacity (CUPRAC) assay, ABTS assay, ferric reducing antioxidant power (FRAP) assay, xanthine oxidase assay. The IC<sub>50</sub> of *A. crassna* extract on DPPH was reported at ranged from 24.6 – 32.25 µg/mL [5, 46, 64, 66].

#### 2.3.5 Effect on central nervous system (CNS)

The chloroform extract of *A. subintegra* leaves was able to reduce the number of repeated entries to arms of the maze but increased number of entry to arms of the maze until the first error occurs in mice with valium-impaired memory [77].

#### 2.3.6 Hepatoprotective

The ethanolic extract of *A. agallocha* leaves was able to decrease the hepatic enzyme levels, which comprised of alanine aminotransferase (ALT), aspartate aminotransferase (AST), and alkaline phosphatase (ALP), in carbon tetrachloride-induced hepatic damage in rats [78].

#### 2.3.7 Laxative activity

The leaves of *A. crassna* and *A. sinensis* exhibited the laxative effect in *in vivo* study. Kakino *et al.* (2012) administrated the water extract of *A. crassna* leaves in single dose and multiple doses, resulting in the decline of the amount of intestinal toxins (indoles and ammonium) in feces [8]. In addition, the ethanolic extract from the leaves of *A. crassna* and *A. sinensis* were augmented the weight and times of stool, and gastrointestinal transit in mouse model [7, 59, 62, 79].

## 2.4 Mangiferin

Mangiferin (1,3,6,7-tetrahydroxyxanthone-C2- $\beta$ -D glucoside) is a natural compound with polyphenol of C-glycosylxanthone structure (Figure 3). The chemical description was mentioned in Table 7.

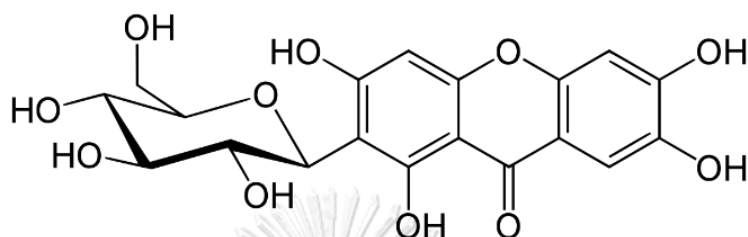


Figure 3 Chemical structure of mangiferin

Table 7 Chemical description of mangiferin [80]

Chemical name	Mangiferin
Molecular formula	C <sub>19</sub> H <sub>18</sub> O <sub>11</sub>
IUPAC name	1,3,6,7-tetrahydroxy-2-[(2S,3R,4R,5S,6R)-3,4,5-trihydroxy-6-(hydroxymethyl)oxan-2-yl]xanthen-9-one
Molecular weight	422.342 g/mol
CAS number	4773-96-0
Synonym	2- $\beta$ -D-glucopyranosyl-1,3,6,7-tetrahydroxy-9H-xanthen-9-one 9H-xanthen-9-one, 2- $\beta$ -D-glucopyranosyl-1,3,6,7-tetrahydroxy- alpizarin chinonin 1,3,6,7-Tetrahydroxyxanthone C2- $\beta$ -D-glucoside
Appearance	Light yellow

## 2.5 Pharmacological activities of mangiferin

Mangiferin showed various pharmacological effects; eventually it could be separated from many plant species in cashew family [10-13]. In addition, the mango tree (*Mangifera indica*) was not only a common source of mangiferin, but other medicinal plants also contain mangiferin such as leaves from plant in genus *Aquilaria* [66, 81, 82]. Mangiferin, a xanthonoid with norathyriol glucoside molecule, possesses four aromatic hydroxyl groups which acts as a powerful antiradical and antioxidant activities. Mangiferin can prevent the generation of hydroxyl radical in Fenton's reaction, and also tends to be a powerful iron chelator. Many researchers conducted experiments both *in vitro* and *in vivo* to explore pharmacological activities of mangiferin and found its effective potency in anti-diabetic, antimicrobial and antiviral, analgesic, anti-inflammatory, anti-allergic, MAO inhibiting, memory enhancement, cardioprotective, hepatoprotective, neuroprotective and radioprotective activities. Furthermore, mangiferin is also scientifically documented that they can inhibit the growth of cancer cell and carcinogenesis by *in vitro* and *in vivo* apoptosis induction [14-24, 83-86].

## 2.6 Quality control method for herbal material

### 2.6.1 Macroscopic and microscopic examination

An examination of macroscopic is the first approach to ascertain the characteristics, identity and degree of purity of medicinal plant materials, and should be carried out before any further tests were undertaken. Macroscopic identity of herbal materials is found on shape, size, color, texture, surface characteristics, fracture characteristics and appearance of the cut surface. Microscopic inspection of herbal materials is investigation for the identification of broken or powdered materials [87].

### 2.6.2 Chemical fingerprinting

Chemical fingerprints of plants could be constructed for evaluation of the distribution patterns of substances in the plant materials. These fingerprinting can be used for assessment the structure of substance in different sources or ecosystems [88].

### 2.6.3 Physico-chemical parameter

#### 2.6.3.1 *Determination of loss on drying*

The test for loss on drying find out both water and volatile matters. Drying process can be completed by heating in oven at 100-105 °C and cooling in desiccator [87].

#### 2.6.3.2 *Determination of water content*

Azeotropic method is specifically used for measurement of water content in plant material specification. An excess of water in herbal materials encouraged microbial growth, the presence of insects or fungi, and deterioration following hydrolysis. The azeotropic distillation method gives a direct measurement of the water

present in the material being examined. The plant material is distilled together with a water immiscible solvent such as saturated toluene or xylene. Solvent should be saturated with water before use to avoid water absorption in solvent for accurate result [87].

#### *2.6.3.3 Determination of total ash and acid insoluble ash*

Ash values are helpful in determination of the purity and quality which indicate the inorganic substances in plant materials. Total ash method determines the total amount of non-volatile inorganic matters remaining in herbal materials after complete incineration at 500°C. Silicon dioxide which is mainly found in the remaining insoluble matter of acid insoluble ash might be obtained after boiling the total ash with 70 g/l hydrochloric acid and incinerating [87].

#### *2.6.3.4 Determination of extractable matter*

Extractable matters represented the amount of active constituents from plant materials. The plant material is extracted with specified solvents such as water and ethanol. Ethanol is used for the slightly non-polar substances whereas water was used for the polar substances [87].

### 2.6.4 TLC-densitometry and TLC image analysis

#### *2.6.4.1 Thin layer chromatography*

Thin layer chromatography (TLC) is a planar chromatographic technique that is a simple, easy to use, inexpensive, short time for analysis and convenient method to separate and to identify the substances. Since the advantages of this technique, TLC is commonly used to check the purity of compounds as well as used for quantitative analysis after spotting, development and visualization. TLC system consists of mobile



phase and stationary phase. During the procedure, a mobile phase (eluent) distributes the compounds present in a mixture over a stationary phase (adsorbent). The result of TLC can be detected when the spots are visualized under UV light or sprayed with suitable detection reagents [89].

The retention factor ( $R_f$ ) is a calculated value for the distance of the spots from compound appear from origin in TLC plates and the distance moved of the solvent from origin. The  $R_f$  value can be used for identify the compounds under the same conditions. The  $R_f$  values can be calculated using the following formula:

$$R_f = \frac{\text{distance of compound from origin}}{\text{distance of solvent front from origin}}$$

#### 2.6.4.2 TLC- densitometry

TLC-densitometric method is a procedure for the separation and identification of organic compound. The compound which has been separated by TLC are quantified using TLC densitometer. Densitometry is the quantitative and qualitative measurement of absorbed visible, UV light or emitted fluorescence upon excitation with UV light [90]. The TLC densitometer (CAMAG TLC scanner 3) contains a single wavelength, multiple wavelengths up to 31 selected wavelengths or a combination of measurements in absorption and fluorescence detection mode. It transforms the selected compound on TLC plate into digital computer data using winCATS software. It can evaluate a reflection in absorbance or fluorescence mode with the spectrums range from 190-900 nm. There is three light sources including of deuterium lamp (190-450 nm), halogen-tungsten lamp in the visible region (350-900 nm) and high pressure mercury lamp (254-578 nm) [91].

### 2.6.4.3 TLC-image analysis

ImageJ is a public domain Java image processing and analysis program developed at the National Institutes of Health (USA). ImageJ is a freeware, which can quantitate and calculate the pixel intensity in digital image of TLC spot and transform to chromatographic peak. It can be used as a tool for calculation of an area and the pixel value statistics to define the selections by user [92].

## 2.7 Biological activities

### 2.7.1 Anti-oxidant activities

The free radicals mean to be atoms or molecules that carry unpaired electron in its structure, which are displayed unstable and highly reactive properties. The free radicals are divided into two types. First of all, the type of free radicals which has unpaired electron on oxygen element is called the reactive oxygen species (ROS); for example, superoxide radical ( $O_2^{\cdot-}$ ), hydrogen peroxide ( $H_2O_2$ ), and hydroxyl radical ( $OH^{\cdot}$ ). Another one is named as reactive nitrogen species (RNS) which contained radical on nitrogen species; for example, nitric oxide radical ( $NO^{\cdot}$ ), and peroxy nitrite ( $OONO^{\cdot}$ ). Free radicals can be generated from various factors, such as ultraviolet light, pollutions, inflammation as well as cellular metabolism (Figure 4). The proper amount of ROS results in cells' injury because it can be reacted with biomolecules, lipids, nucleic acid, and proteins [93-95]. However, some of free radical at optimum concentration have necessary function to the cells, such as intracellular killing of bacteria, and cell signaling pathway [96-98]. An enormous ROS production has been associated with the endothelial dysfunction, vascular diseases, atherosclerosis, stroke, and hemorrhoid [97, 99]. The free radical scavengers can eliminate or react with the unpaired electrons, and stop the chain reaction.

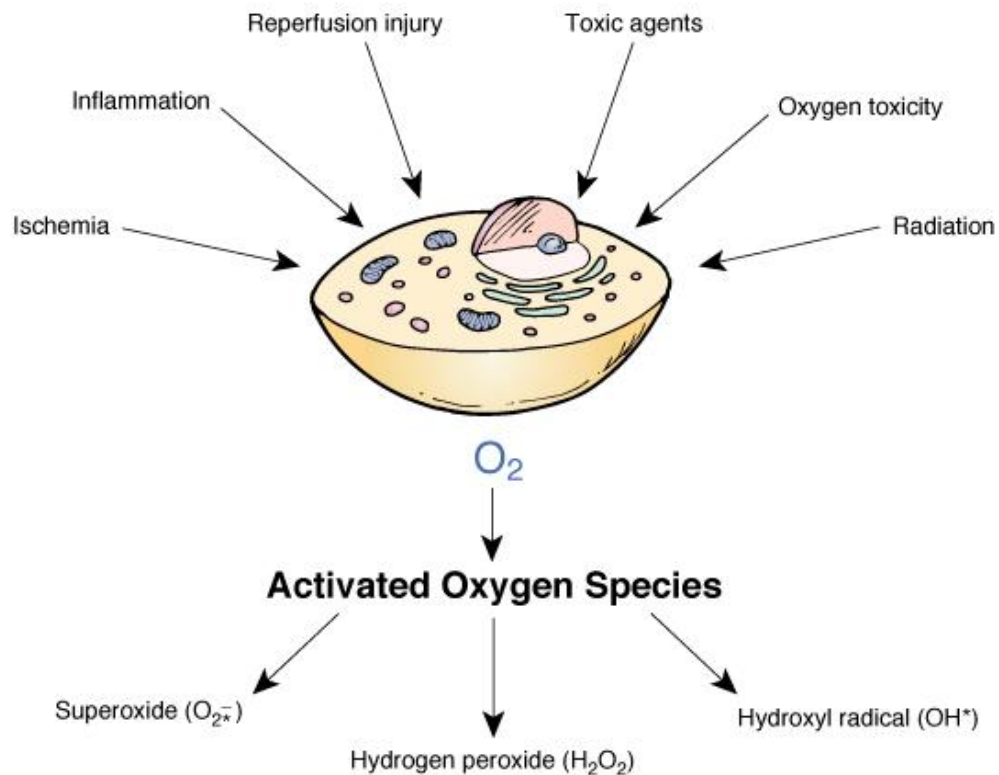


Figure 4 Formation of free radicals [100]

Nitric oxide (NO) is an enzymatically formed from L-arginine in the presence of nitric oxide synthase (NOS), which there are three isoforms of NOS: constitutively expressed endothelial NOS (eNOS), inducible NOS (iNOS), and neuronal NOS (nNOS) [101]. NO are originated from eNOS, which involved in a vasodilation and antiplatelet aggregation in blood vessel [102]. The inflammation-mediating cytokines are stimulated the iNOS, and it can be contributed to the production of  $NO^*$  in higher level and longer duration than constitutive eNOS or nNOS. In addition, the major factor influenced on cytotoxicity and endothelial dysfunction is triggered from high level of inducible  $NO^*$ . Moreover, the excessive  $NO^*$  can interact with  $O_2^-$  by a reaction that have more speedily rate than dismutation by superoxide dismutase enzyme (SOD) and forms potent oxidants, which are ability of toxic nitrosylation or nitration of some amino acid residues such as tyrosine and cysteine [99, 103]. In addition, the study of the lactate

dehydrogenase levels on cerebral endothelial cell of Sprague-Dawley rat of sodium nitroprusside (SNP) and/or paraquat was increased the enzyme level. Gobbel *et al.* (1997) suggested that the toxicity of the cooperation of  $\text{NO}^*$  and  $\text{O}_2^*$  had synergistic effect [104], which was an enlargement of nitrotyrosine formation by peroxynitrite [105]. Therefore, Wink and Mitchell (1998) summarized that  $\text{NO}^*$  associated with pathophysiological conditions, and inflammatory illness that bring about tissue injury [106]. (Figure 5)

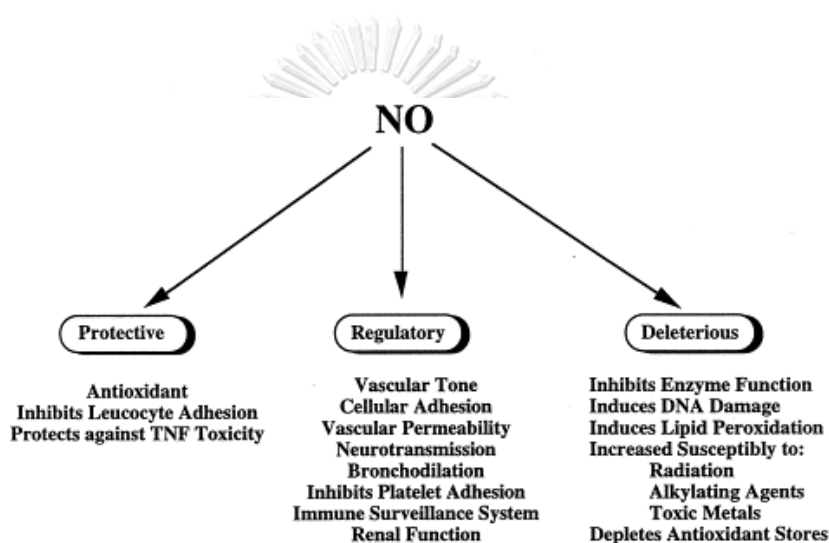
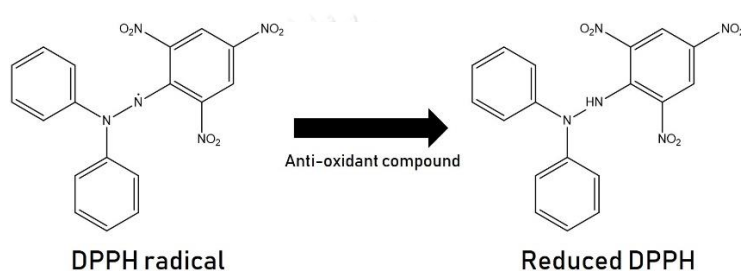


Figure 5 The biological effect of NO [106]

There are various methods which used to examine the *in vitro* anti-oxidant capacity of samples, such as DPPH radical scavenging assay, hydrogen peroxide scavenging ( $\text{H}_2\text{O}_2$ ) assay, nitric oxide scavenging activity, peroxynitrite radical scavenging activity, trolox equivalent antioxidant capacity (TEAC) method/ABTS radical cation decolorization assay, total radical-trapping antioxidant parameter (TRAP) method, ferric reducing-antioxidant power (FRAP) assay, superoxide radical scavenging activity (SOD), hydroxyl radical scavenging activity, hydroxyl radical averting capacity (HORAC) method,  $\beta$ -carotene linoleic acid method/conjugated diene assay, *etc* [107, 108].

### 2.7.1.1 DPPH radical scavenging assay

DPPH (2, 2-diphenyl-1-picrylhydrazyl) is a stable free radical form which gives characteristics of deep purple color with a maximum absorbance of 517 nm. This method evaluates the ability to scavenge DPPH radical by antioxidant compounds. The delocalization of DPPH molecule due to the donation of hydrogen or electron to quench the DPPH radical. The color turns from purple to yellow when receives hydrogen atom from antioxidant (Figure 6) [109].



**Figure 6** DPPH and antioxidant reaction [108]

### 2.7.1.2 Ferric reducing antioxidant power assay

Ferric reducing antioxidant power (FRAP) assay is a method to measure the ability of an antioxidant compound to reduce ferric ions into ferrous complex. This method uses ferric tripyridyltriazine, complex compound of iron as the tested compounds. Iron atom of ferric ion ( $\text{Fe}^{3+}$ -TPTZ) is reduced by the antioxidant and produces a complex compound of ferrous ion ( $\text{Fe}^{2+}$ -TPTZ) that gives the blue color at the maximum absorbance of 593 nm (Figure 7) [110].

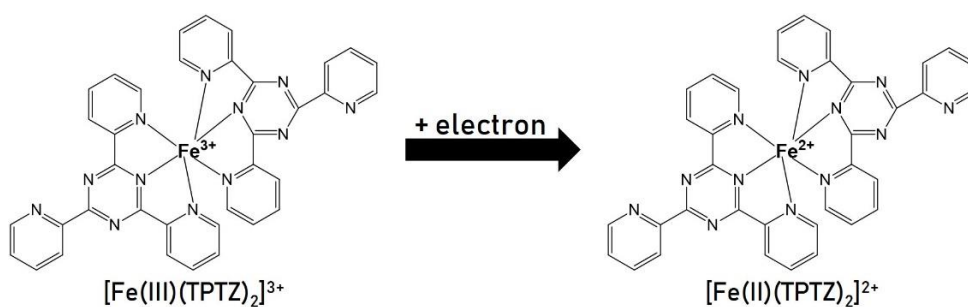


**Figure 7** mechanism reaction of FRAP assay [109]

### 2.7.1.3 Nitric oxide (NO) scavenging activity

The nitric oxide scavenging activity are determined in indirect spectrophotometric method using the stable decomposed products. The sodium nitroprusside is used as NO producer in aqueous solution at physiological pH (pH7.2). After that, NO reacts with oxygen to generate the stable NO-derived nitrosating agent. Finally, the Griess reaction are used to quantified the scavenging activity. The Griess reaction is a two steps diazotization reaction (Figure 8). The stable product react with sulfanilic acid to produce a diazonium ion, and then coupled to N-1-naphthylethylenediamine to form a chromophoric azo product that strongly absorbs at 540 nm [111].

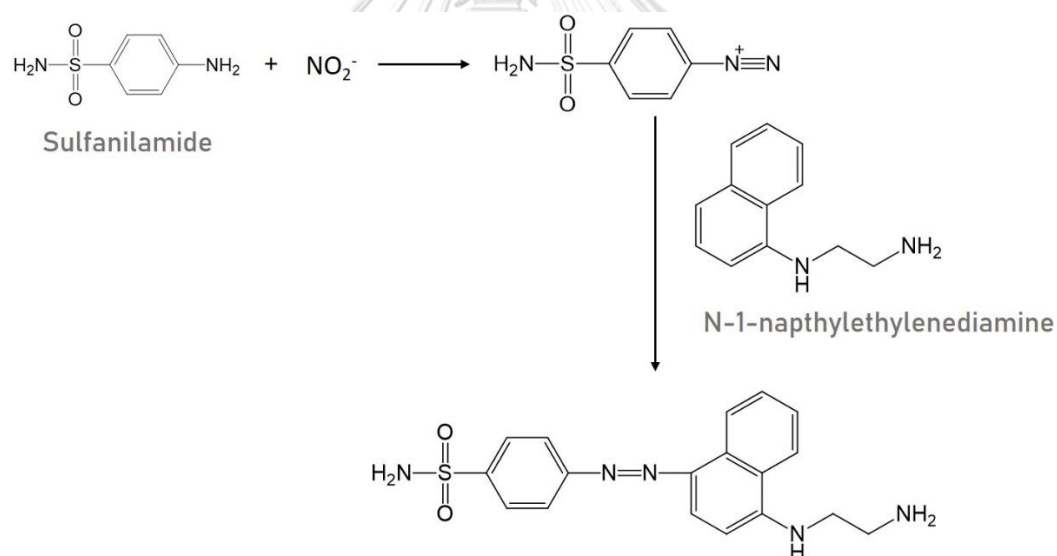


**Figure 8** The Griess test reaction [110]

#### 2.7.1.4 Total phenolic content

Colorimetric reactions are widely used in the UV/VIS spectrophotometric method, which is easy to perform, rapid and applicable in routine laboratory use, and low-cost. However, it is important that colorimetric assay need to use a reference substance. Then, this method measures the total concentration of phenolic hydroxyl groups in the plant extract using the Folin-Ciocalteu assay and a gallic acid used for setting up a calibration curve. This assay is based on the oxidation of a phenolate ion from the sample and the reduction of the phosphotungstic-phosphomolybdic reagent (Folin-Ciocalteu reagent) to form a blue complex of phosphotungstic-phosphomolybdenum in the alkaline solution that can be quantified by visible-light spectrophotometry [112, 113].

#### 2.7.2 *In vitro* $\alpha$ -glucosidase inhibitory activity

Diabetes is described as a metabolic disease in a person which has high blood sugar, either because the body does not produce enough insulin or cells do not respond to the insulin that is produced. This high blood sugar produced the classical symptoms of polyuria, polydipsia and polyphagia. There are two major types of diabetes.

Type 1 diabetes used to be known as insulin-dependent diabetes, or juvenile-onset diabetes as it often begins in childhood. Type 1 diabetes is an autoimmune condition where the immune system wrongly identifies and subsequently attacks the pancreatic cells that produce insulin, leading to little or no insulin production.

Type 2 diabetes used to be known as non-insulin dependent diabetes and adult onset diabetes, but it is commonly increase in children, mostly due to children being more likely to be overweight or obese. In this condition, the body usually still produces some insulin, but this is not enough to meet demand and the body's cells do not properly respond to the insulin. The latter effect is called insulin resistance,

where consistently elevated blood glucose has caused cells to be overexposed to insulin, making them less responsive or unresponsive to the hormonal messenger [114].

Alpha-glucosidases is a complex enzymes located in the brush border of the small intestine that acts upon alpha 1,4-glycosidic linkages. Inhibition of this enzyme system reduces the rate of digestion of starch. Less glucose is absorbed because the starch is not broken down into glucose molecules. Starch is digested by salivary and pancreatic  $\alpha$ -amylase to form oligosaccharide-dextrins. Alpha-glucosidases cleave dextrins to absorbable glucose in small intestine. The synthetic or natural  $\alpha$ -glucosidase inhibitors are interested as therapeutics to delay postprandial hyperglycemia in Type 2 diabetes [115]. Anti-diabetic drugs orally used for diabetes mellitus type 2 such as acarbose, miglitol, nojirimycin and 1-deoxynojirimycin act as competitive inhibitors of  $\alpha$ -glucosidase (Figure 9) [116].

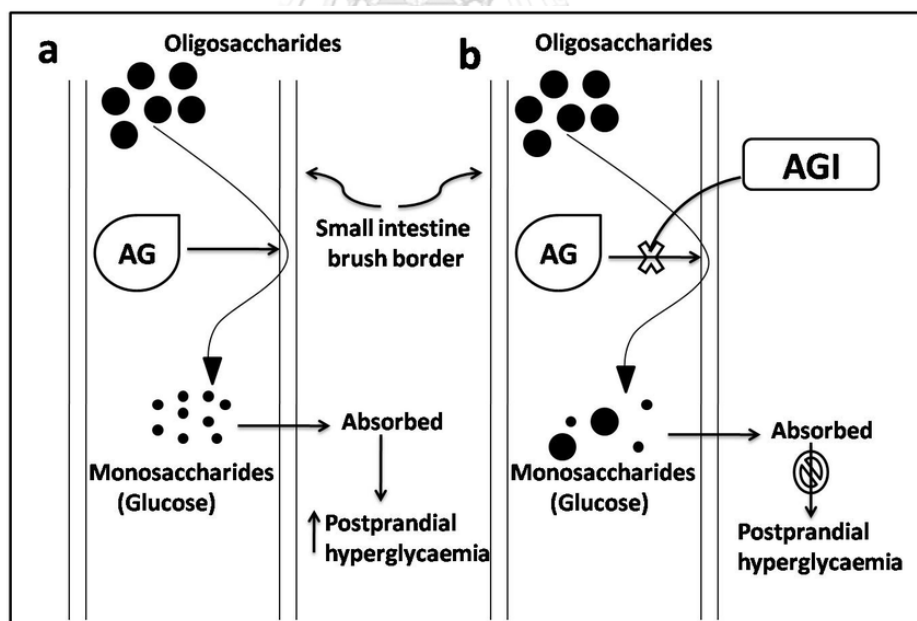


**Figure 9** Mechanism of action of  $\alpha$ -glucosidase inhibitors [117]

- a) action of  $\alpha$ -glucosidase on carbohydrate in absence of  $\alpha$ -glucosidase inhibitor,
- b) action of  $\alpha$ -glucosidase on carbohydrate in presence of  $\alpha$ -glucosidase inhibitor.

AG means to  $\alpha$ -glucosidase, AGI means to  $\alpha$ -glucosidase inhibitors



### 2.7.3 Cell viability or cytotoxicity testing (MTT tetrazolium reduction assay)

The MTT (or 3-(4,5-dimethylthiazol-2-yl)-2,5-diphenyltetrazolium bromide) is the chemical compound that can be used for determined the proliferation or cytotoxicity activity of cells. The MTT assay is a precise method for indicated the cellular metabolic activity. In addition, this method is favorable test over the other end-point measuring tests (the ATP and  $^3\text{H}$ -thymidine incorporation assay). The principle of this method utilizes the reduction of MTT by mitochondrial dehydrogenases that change a yellow water-soluble tetrazolium dye to purple colored formazan crystals (Figure 10). After that, the formazan crystal in cells is solubilized using DMSO or organic solvent, and then spectrophotometrically analyzed at 570 nm [118-122].

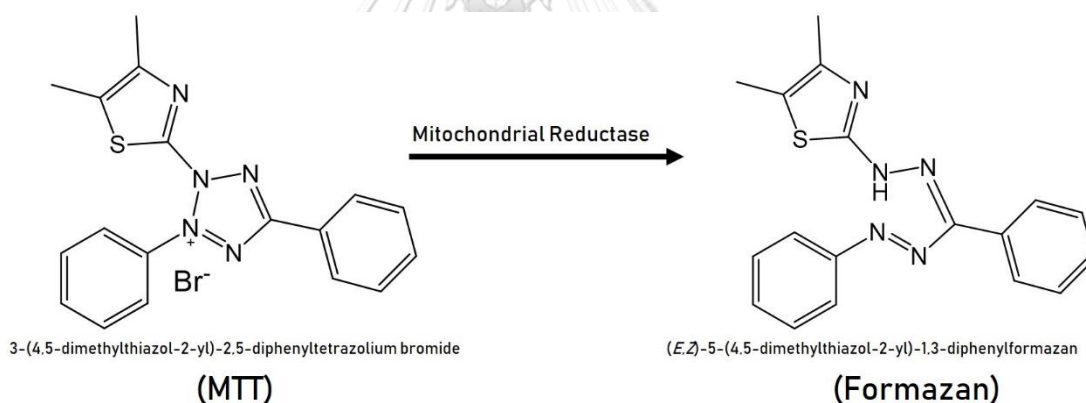


**Figure 10** The chemical reaction of MTT assay [117]

For interpretation of MTT assay, the result of test samples is compared to the control cells. When the absorbance of test sample is less than the control, it means to be toxic to the cell. In contrast, the cell proliferation effect shows higher absorbance value of treatment sample than control.

## 2.8 Cellular model for determination of endothelial dysfunction under oxidative stress

Human umbilical vein endothelial cells (HUVECs) are presently used as *in vitro* model for diverse physiological and pathological research. In addition, Chen *et al.* (2010), and Gong *et al.* (2012) reported that  $H_2O_2$  could be influence the oxidative stress and cellular dysfunction on HUVECs [123, 124]. Therefore, the compound that have antioxidant properties may prevent the damage to the endothelial cells. Ophiopogonin D, which was isolated from *Ophiopogon japonicas*, decreased  $H_2O_2$ -induced lipid peroxidation, protein carbonylation, and attenuated mitochondrial ROS generation and cell apoptosis in HUVECs [125]. In addition, Kuo *et al.* (2009) used HUVECs for determined the cellular protection by investigating the expression of antioxidant enzymes [126]. The oxidized low-density lipoprotein induced oxidative stress in HUVECs via the unbalance among intracellular ROS and antioxidant enzymes. ROS was inactivated by down regulated the copper/zinc superoxide dismutase (Cu/Zn SOD) and eNOS. However, the pretreatment with *Solanum lyratum* extract, which comprised of various antioxidant components, founded to be reversed effect.

EA.hy926 cells (Figure 11), which is an immortalized human umbilical vein endothelial cell (HUVEC) line, derived from the fusion of HUVECs and lung adenocarcinoma cell line A549 [127]. This cell line was used to applied *in vitro* treatment with  $H_2O_2$  to cause cellular injury, imitating *in vivo* status of oxidative stress and inflammation [128-130]. Moreover, EA.hy926 cells have been broadly used in the study of leukocyte adhesion to endothelial cells, oxidative stress and protein expression. Endothelial cell can expressed the antioxidant enzymes such as superoxide dismutase (SOD), glutathione peroxidase (GPX), catalase (CAT), including endothelial nitric oxide synthase (eNOS) and inducible nitric oxide synthase (iNOS) [128, 131-134]. These enzymes play a crucial role to protect cells from excessive ROS formation and

vasodilation. The protection of EA.hy926 cells from H<sub>2</sub>O<sub>2</sub>-induced cell injury was attenuated by Sailuotong (SLT), which was a standardised three-herb formulation consisting of *Panax ginseng*, *Ginkgo biloba*, and *Crocus sativus*, via the direct reduction of intracellular ROS generation and increase of SOD activity. Furthermore, numerous researches were used EA.hy 926 for determination of cellular protection from oxidative stress as well as inflammation. So, EA.hy926 cells are considerable model for detect the cytoprotective property [135].

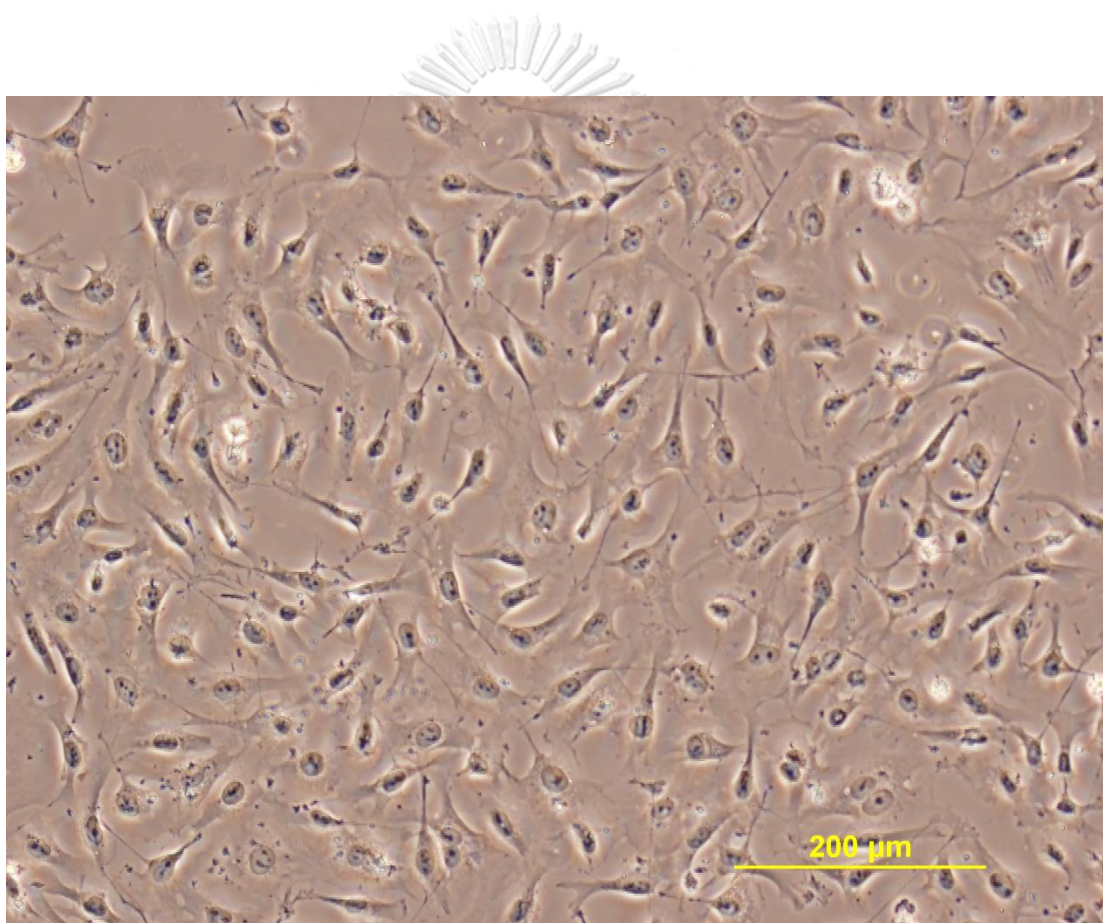


**Figure 11** EA.hy926 morphology after freshly isolated in culture

## 2.9 Protein involved in cytoprotection of endothelial cells

There are various pathways to determine the cytoprotective properties of candidate compounds. The decrease of oxidative stress in the cell is the favorite mechanism that detected the protective activity. The degradation of heme by heme oxygenase 1 can also be used for detected the cellular stress. Furthermore, the balance of anti-apoptotic and pro-apoptotic in apoptosis pathway is used for investigate the cellular protection property.

### 2.9.1 SOD1

SOD1 is abbreviated from the Copper/Zinc superoxide dismutase. SOD1 is the crucial cytosolic superoxide dismutase. This enzyme contains 32 kDa homodimer and is largely founded in the cytosol with a tiny portion in the intermembranes spacer of mitochondria [137]. Moreover, Chang *et al.* (1988) reported that SOD1 existence in lysosomes, nuclei, and peroxisomes is discovered using immuno-cytochemical methods [138]. Crapo *et al.* (1992) concluded that SOD1 was commonly found in various cell lines [139], whereas the location of SOD1 gene in human was placed at the 21q22.1 region of chromosome 21 [140]. The presence of copper and zinc has impact on the enzymatic activity of SOD1. Zinc partakes in the suitable folding and stability of protein. The SOD effect is equivalent to the amount of copper bound in the native site. Another metal cannot replace to copper, while zinc can be substitute with cobalt and copper [141, 142]. The mechanism of SOD acts as scavenging the superoxide radical, and implicates alternate reduction and re-oxidation of the copper at the active site of the enzyme (Figure 12). Hence, McCord and Fridovich (1969) concluded that catalytic copper to scavenge superoxide radical was required for SOD1 activity [141].

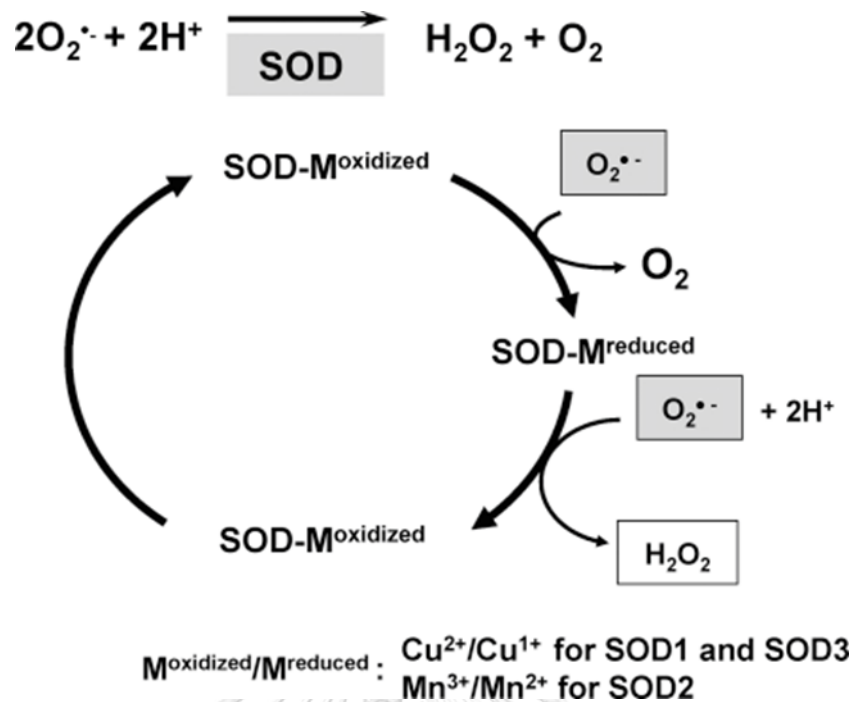


**Figure 12** Common mechanism of scavenging  $\text{O}_2^{\bullet-}$  by SOD [137]

### 2.9.2 Heme oxygenase 1 (HO-1)

Heme oxygenases (HOs) are omnipresent and crucial enzymes in eukaryotic creatures that based on the aerobic oxidation and electron transport through heme-containing proteins [143, 144]. Heme Oxygenases are known as a booster in the rate-limiting step of the degradative mechanism of iron protoporphyrin IX catabolism. There are two isoforms of heme oxygenase; HO-1 and HO-2. HO-1 is a transmembrane inducible protein which can be found in endoplasmic reticulum, nucleus and mitochondria, whereas HO-2 is localized to the mitochondria and has 40% amino acid homology to HO-1 which provided a further activity against pro-oxidant heme at heme binding site. HO-1 is an inducible enzyme which deals with anti-inflammatory, antioxidant, and anti-apoptotic attributes to the cells [145-147]. The degradation of heme using heme oxygenase can be generate carbon monoxide (CO), ferrous ion and biliverdin. After that, biliverdin is catalyzed by biliverdin reductase to formed bilirubin (Figure 13) [148]. There are various stimuli that can be made HO-1 over-expression,

such as heavy metal, hydrogen peroxide, hypoxia, endotoxins, oxidized low-density lipoproteins, nitric oxide, stress, and ultraviolet radiation [149].

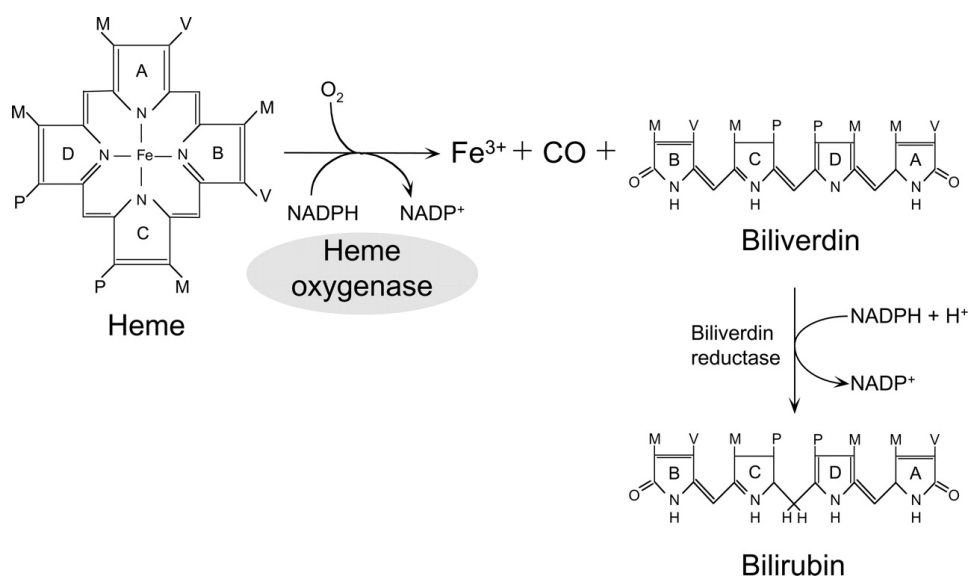


**Figure 13** Degradative reaction of heme via heme oxygenase [143]

The firstly research about cytoprotection activity of HO-1 was reported by Vile in 1994 [150], and found that the HO-1 over-expression triggers the protective response from oxidative stress in cultured human fibroblasts. In addition, Balla (1992) used the endothelial cells for ascertaining cytoprotective response against oxidative injury [151]. Soares (1998) mentioned about the protective effect of HO-1 on endothelial cells that the mechanism of cytoprotection undergoes TNF-mediated apoptosis [152]. Furthermore, carbon monoxide can imitate the protection activity of endothelial cell (Figure 14) [153]. However, the degradation products from heme catalytic reaction are contributed to protect the cells against a various immune-mediated inflammatory diseases. For example, the cytoprotective effect of carbon monoxide depend seemingly on the ability of interaction between divalent metals in the prosthetic heme groups of hemoproteins [154].

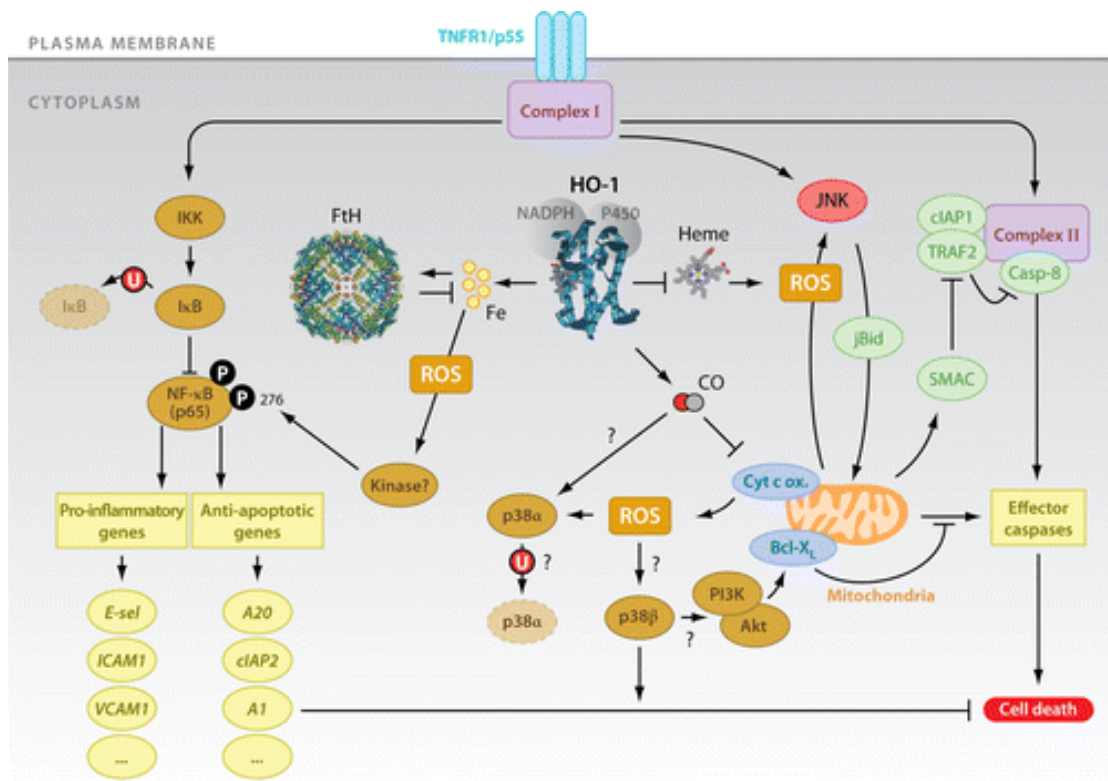


Figure 14 The cytoprotective mechanism of HO-1 [154]

### 2.9.3 BAX and Bcl-2

Bax (Bcl-2-associated X protein) and Bcl-2 (B-cell lymphoma 2) are crucial proteins in apoptosis pathway. Apoptosis is a form of programmed cell death in which energy requirement, and spontaneous death with definite morphological and biochemical characters. The morphological characters of cell during apoptosis are shrinkage, the cytoplasm and the organelles is tightly packed, and the chromatin is condensed. After that, the cell membrane blebs are occurred and generated the cell fragments into apoptotic bodies. Finally, the apoptotic bodies are accordingly phagocytosed by macrophages, and do not have any inflammation [155]. The process of apoptosis is shown in Figure 15.

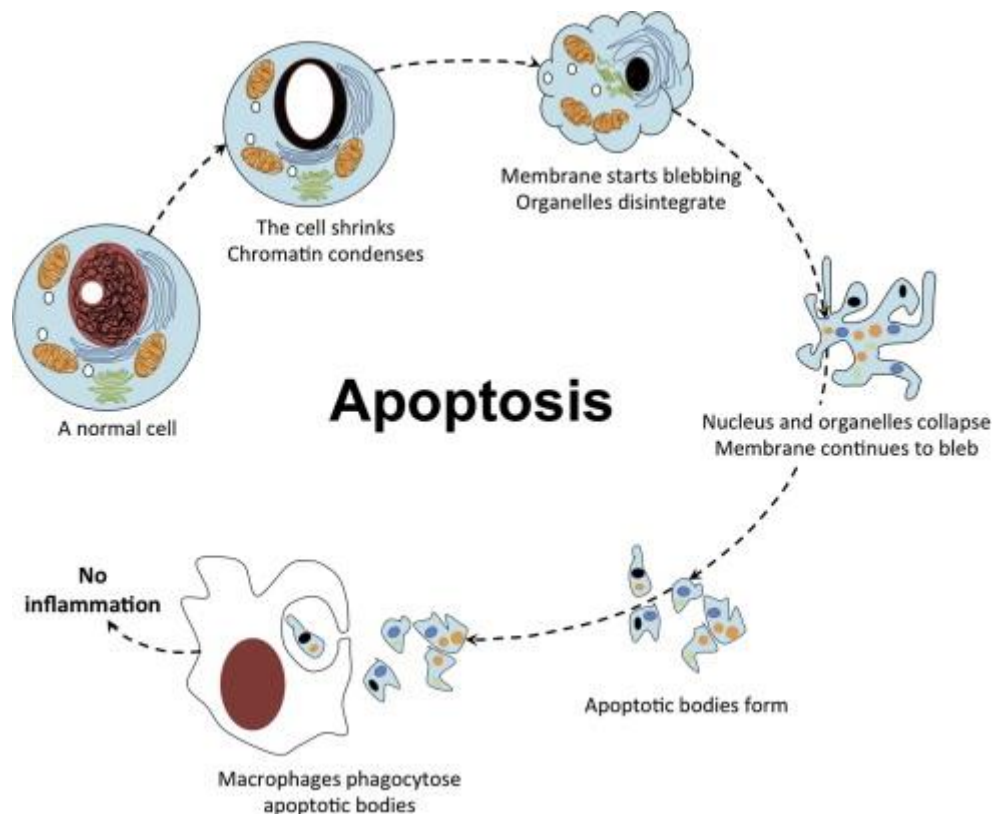
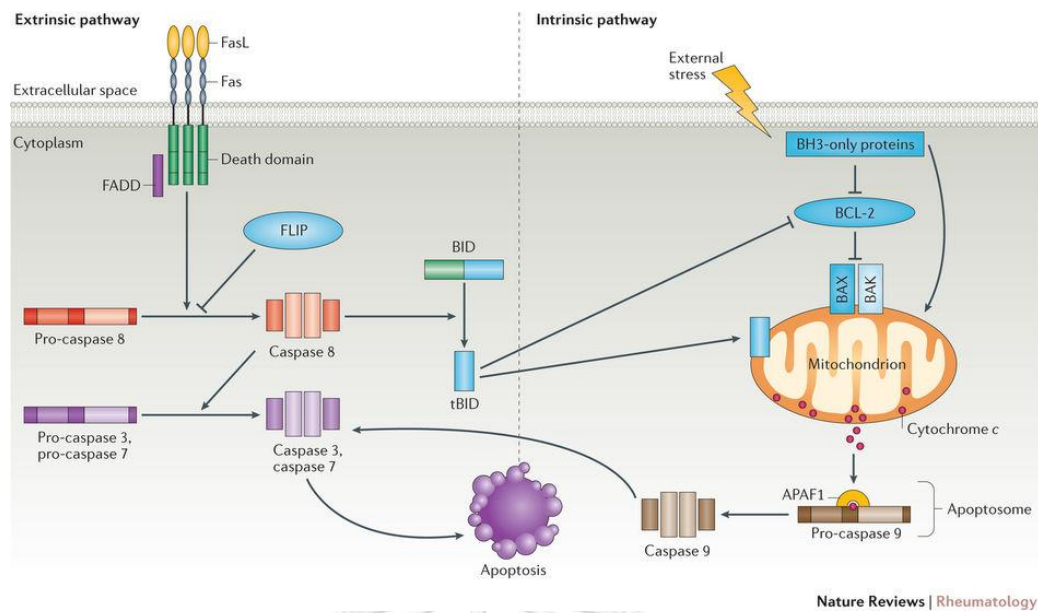


Figure 15 The process of apoptosis [156]

Apoptosis can be triggered through two pathways; Intrinsic or mitochondrial pathway, and extrinsic or death receptor pathway (Figure 16). The extrinsic signaling pathway is associated with transmembrane receptor-mediated interaction. These receptors are members of the tumor necrosis factor (TNF) receptor. The dominant death receptors which deals with extrinsic pathway are fatty acid synthase ligand/fatty acid synthase receptor (FasL/FasR), and tumor necrosis factor alpha/tumor necrosis factor receptor 1 (TNF- $\alpha$ /TNFR1). The binding of FasL to FasR induces the recruitment of the Fas-associated protein with death domain (FADD) adaptive protein, while the binding of TNF ligand to TNF receptor leads to the binding of the TNFR1-associated death domain (TRADD) protein with recruitment of FADD and Receptor-interacting protein (RIP) kinase. FADD are contained procaspase-8 dimerization, the cleavage of procaspase-8 is activated when the death-inducing signaling complexed (DISC) is



organized. Later, the caspase 8 splits and can be activated the caspase-3 and caspase-7, which induce the degradative stage of apoptosis. In addition, the caspase-8 can cleave BH3 interacting-domain death agonist (Bid), and generates truncated Bid (tBid) which has its properties as Bcl-2 inhibition in mitochondria membrane. The intrinsic signaling pathway originate the apoptosis by non-receptor-mediated stimuli, it can produce intracellular signals that act directly on targets in the mitochondria. Stimuli change the inner mitochondrial membrane that lead to an opening of the mitochondrial permeability transition (MPT) pore, loss of the mitochondrial transmembrane potential and release of two main groups of pro-apoptotic proteins from the intermembrane space into the cytosol. The first group comprises of cytochrome c, Smac/DIABLO, and the serine protease HtrA2/Omi. These proteins activate the caspase-dependent mitochondrial pathway. Cytochrome c binds and activates Apaf-1 and procaspase-9, forming an “apoptosome”. The second group of pro-apoptotic proteins, AIF, endonuclease G and CAD, are released from the mitochondria during apoptosis, but this is a late event that occurs after the cell has committed to die. In addition, the control and regulation of these apoptotic mitochondrial events occurs through members of the Bcl-2 family of proteins. The Bcl-2 family of proteins governs mitochondrial membrane permeability and can be either pro-apoptotic or anti-apoptotic [157-168].



**Figure 16** Extrinsic and intrinsic pathways of apoptosis [155]

The balance between the pro- and anti-apoptotic members of the Bcl-2 family is critical for determining cell fate. Bcl-2, Bcl-XL and A1 are localized in mitochondria and although predominantly anti-apoptotic, they also exert anti-inflammatory and cytoprotective effects. However, their protective actions may be overcome if pro-apoptotic Bim, Bid and Bad are present in sufficient amounts. They bind to Bcl-2 and Bcl-XL and result in the release of sequestered Bax and Bak, and the escape of mitochondrial cytochrome c. The resultant apoptosome cleaves and activates apoptosis effector caspases 3, 6 and 7. Bax is a pro-apoptotic Bcl-2-family protein that resides in the cytosol and translocates to mitochondria upon induction of apoptosis. Recently, Bax has been shown to induce cytochrome C release and caspase activation *in vivo* and *in vitro*. This release was reportedly dependent upon induction of the mitochondrial permeability transition, an event that is associated with disruption of the mitochondrial inner transmembrane potential and has been implicated in a variety of apoptotic phenomena. The Bcl-2 has neutralizing properties by their protective effect and promoting cell death. Reports indicate that Bcl-2 and Bcl-XL inhibit apoptotic death primarily by controlling the activation of caspase proteases [169-172].

## 2.10 DNA barcoding

DNA barcoding is the method for detection of nucleotide variation to discriminate and identify the species using short nucleotide sequences and agree-upon position in the genome. The DNA barcoding is depended on the principle that the inter-specific sequence divergence is commonly much more than the intra-specific sequence divergence. The barcoding technique has been prosperously used to various animal groups as the competent species authentication tool. In 2003, Hebert's work is the first publication that proposed "DNA barcoding" as a way to identify species using cytochrome oxidase 1 (*CO1*) mitochondrial gene [34]. DNA barcoding can also be utilize in various purposes: for example, to reveal obscure species [173], to sustain intellectual property rights [174], to conjoin the biological samples to violation scenes [175-177], to assist food authenticity and safety of labelling by proving their identity or purity [178, 179], and in ecological and environmental genomic studies.

The *CO1* sequences has been utilized as the universal barcode in animals. The discrimination in plants using DNA barcode is more difficult than animal domain because of the species hybridization and slower mutation rate [36, 180]. There were various researches which have been studied on the universal barcode in plant system, but there was unsuitable locus for identify all plant species. In recently, the Consortium for the Barcode of Life-Plant Working Group (CBOL) proposed the combination of *matK* and *rbcl* loci as the efficient barcode for plant discrimination. Nowadays, the multi-locus gene determination may be appropriated method for discrimination of plant species. The widely used regions are described below.

### 2.10.1 Internal transcribe spacer (ITS)

The internal transcribe spacer (ITS) is the part of the ribosomal DNA (rDNA) and located between the small subunit rDNA and the large subunit rDNA coding regions. The eukaryotic rRNA encoding cluster comprises of the 18S, 5.8S, and 26S rRNA genes which transcribed as a unit by RNA polymerase [181]. ITS regions have two types; ITS1 located between 18S and 5.8S rRNA genes, while ITS2 is between 5.8S and 26S (Figure 17).

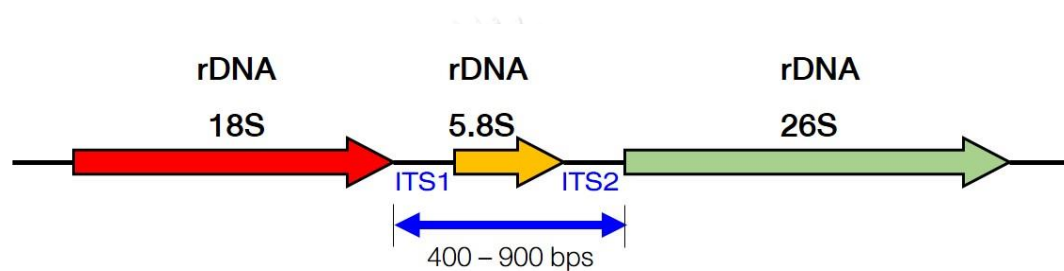


**Figure 17** Schematic diagram of the rDNA cluster

Ribosomal DNA (rDNA) has benefit in phylogenetic investigation because it contains regions with different rates of evolution, from extremely conserved (18S, 5.8S, and 26S) to extremely variable (non-transcribed or intergenic spacer regions). The 18S rDNA (or small subunit ribosomal DNA gene) and 26s rDNA (or large subunit ribosomal DNA gene) were found in living organism and could be used to determine the genetic relationship among ancient ancestry [182, 183]. The internal transcribed spacer region (ITS region) of the nuclear ribosomal DNA (Figure 17) has been used as the significant gene barcode for discrimination of species at the interspecific and intraspecific levels or phylogeny construction because their sequences mainly displayed variation. Currently, the ITS region of rDNA has been approved to be used for identify plant species of medicinal materials. ITS rDNA cluster have been applied for differentiate *Plantago* species [184], *Dendrobium* species [185], and *Mitragyna* species [186].

Sahin and their researchers described that the ITS region is an interesting barcode for molecular analysis because there are a great number of gene copies in plant genome which comprised of the highly conserved encoding regions (18S-, 5.8S, and 26S rDNA) and variable non-encoding region (ITS1 and ITS2). So, internal transcribed spacers can be used as a probably sources of polymorphisms for plant identification.

#### 2.10.2 *matK* gene

The *matK* gene, previously recognized as open reading frame K (ORF-K), has high potential gene for determining molecular systematics and evolution study in plant [187-189]. The *matK* gene is tentatively 1.5 Kbps in length (Figure 18) which located in the Large Single-Copy Region (LSC) of the chloroplast genome (Figure 19). In addition, *matK* gene is located in an intron of approximately 2.6 Kbps and positioned between the 5' and 3' exons of the transfer RNA gene of lysine (*trnK*). This gene is transcribed and translated to the maturase K protein that deals with the splicing type II introns from RNA transcription [190, 191].

This *matK* gene is convenient to multiplied because it has a highly conserved flanking coding region including the *trnK* exons. The evolutionary rate of *matK* gene is suitable for determining the intergeneric or interspecific association among seed plants. The data of Saxifragaceae [187], Cornaceae [192] and Taxodiaceae/Cupressaceae [187] showed that the average numbers of the different nucleotide per site of *matK* gene in pairwise alignment found to be 3.2, 2.4, and 3.4 times, respectively, greater than *rbcl* gene.

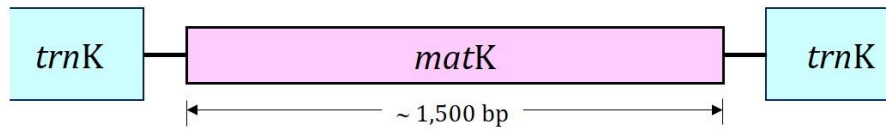


Figure 18 General map of *matK* gene  
(Boxed areas represent coding regions and connecting lines represent spacer regions.)

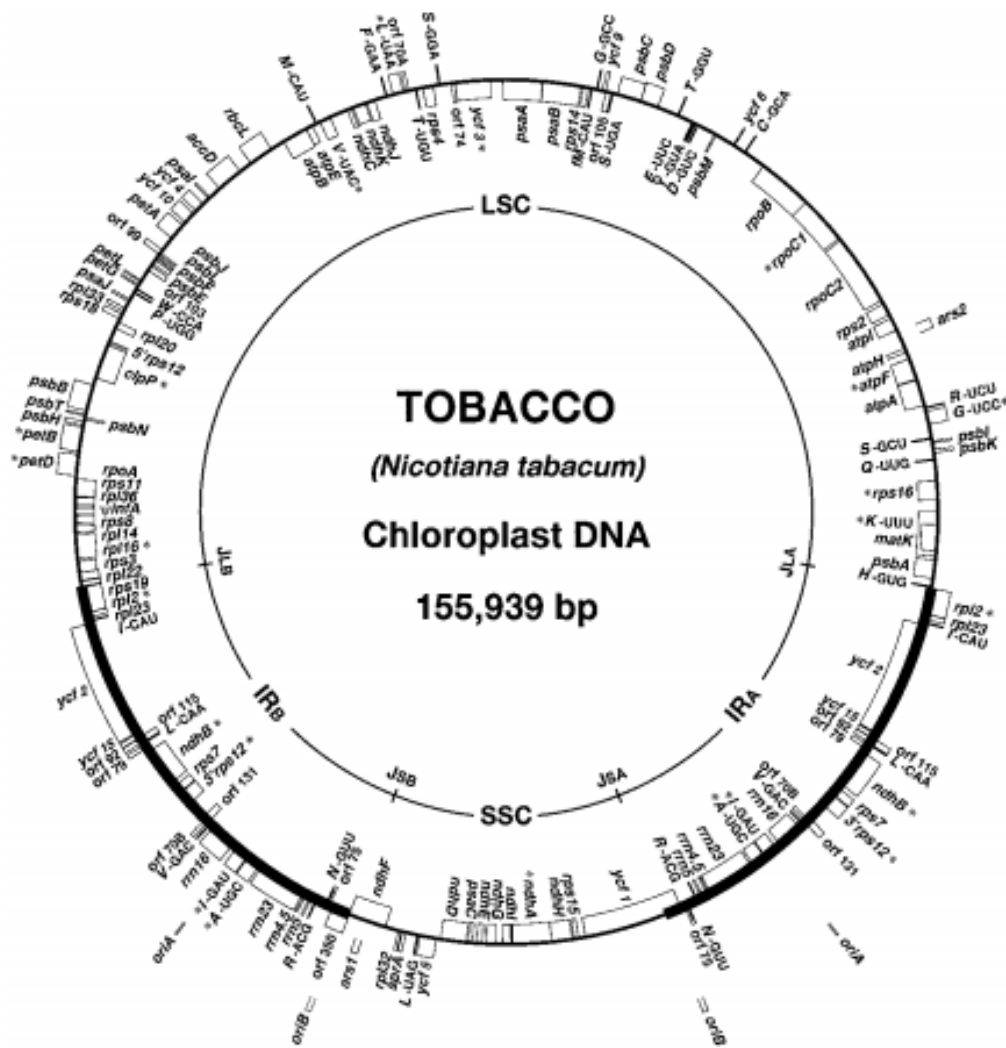


Figure 19 Gene map of tobacco (*Nicotiana tabacum*) chloroplast genome that illustrate location of many of the chloroplast regions [193]

### 2.10.3 The *trnH-psbA* intergenic spacer region

The sequence of chloroplast *trnH* gene has been determined in various plant species, and showed the conserved structure during cpDNA evolution. The *trnH* gene is commonly located near the LSC/IRA junction in higher plant chloroplast genomes (Figure 19, and 20), such as common bean, soybean, and spinach. The region of *trnH-psbA* gene was founded in variable area. The *trnH-psbA* gene of rice is located in the inverted repeated region of cpDNA, but this gene of liverwort is placed at the center of the LSC of cpDNA. Nevertheless, Carelse *et al.* (1994) stated that the *trnH* gene is discovered downstream of the *psbA* gene in pea and broad bean [194]. In addition, Kress *et al.* (2005) mentioned that the length of the intergenic spacer between the *psbA* gene and *trnH* gene varies from one plant to the other [36].

The *trnH-psbA* intergenic spacer was tested on 99 species in 80 genera from 53 plant families, and the results exhibited the high divergence levels and easily amplified [36, 195]. This spacer can be applied to test *Ephedra* in dietary supplements, which sold in commercial markets [42]. In addition, this gene can also been used to authenticate the *Stemona* species [196].

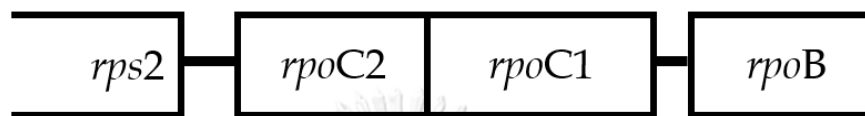


Figure 20 General map of *trnH-psbA* region

### 2.10.4 *rpoC* gene

RNA polymerase gene (*rpo* gene) is the functional gene that can encode the RNA polymerase. Open reading frames (ORF) with partial homology to the genes for the  $\alpha$ -subunit (*rpoA*),  $\beta$  subunit (*rpoB*), and  $\beta'$  subunit (*rpoC*) (Figure 21) of *E.coli* RNA

polymerase were also discovered in cpDNA from higher plants [197-199]. In addition, Watson and Surzyeki (1983) stated that the DNA fragments which carried the *rpoB* and *rpoC* genes of *E. coli* has low stringency to cpDNA as well as nuclear DNA of *Chlamydomonas* [200]. Nevertheless, Lerbs *et al.* (1985) could not find out the difference between bacterial *rpoC* gene and spinach chloroplast [201].



**Figure 21** General map of *rpoC* gene

#### 2.10.5 *ycf1* gene

The *ycf1* plastid gene is the crucial gene of plant viability and encodes Tic214, which is an essential element of the *Arabidopsis* TIC complex [202]. The *ycf1* located between the small single copy (SSC) region and the inverted repeated (IR) regions in the plastid genome (Figure 22). The section of *ycf1* gene in IR region is too short and acts as conserved region, whereas the remaining part of *ycf1* gene in SSC region has high sequence variability in flowering plants. Neubig *et al.* (2009) suggested that the *ycf1* region has genetic alteration more than *matK* gene in determination species [203]. In addition, Drew and Sytsma (2013) summarized that *ycf1* gene can be used in molecular systematics at low taxonomic level [204]. Because of the high variability of *ycf1* gene, the sequence of this gene has high potential for construct the DNA barcoding of the plants [205].

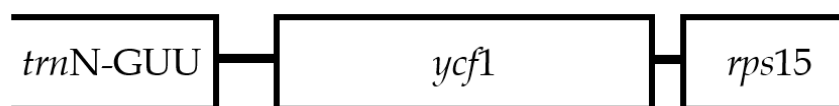


**Figure 22** General map of *ycf1* gene



## 2.11 The polymerase chain reaction (PCR) and sequencing technique

### 2.11.1 The polymerase chain reaction (PCR)

PCR is the *in vitro* enzymatic amplification of DNA [206]. The use of PCR in researches and clinical laboratories was extremely increased since the introduction of thermostable DNA polymerases in 1988. There are numerous publications and books mentioned about this technique, so it shows the success of this technique. In the typical PCR, there are three temperature-controlled steps (denaturation step, annealing step, and extension step) which are repeated in a series of 25 to 40 cycles. A reaction consists of:

- A buffer usually containing Tris-HCl, KCl, and MgCl<sub>2</sub>.
- A thermostable DNA polymerase acts as addition of nucleotides to the 3'-end of a primer annealed to single-stranded DNA; such as *Taq* DNA polymerase (from *Thermus aquaticus*), *Pfu* DNA polymerase (from *Pyrococcus furiosus*).
- Four deoxyribonucleotide triphosphates (dNTPs) comprises of dATP, dCTP, dGTP, and dTTP, which are crucial for elongation of new DNA strands.
- Oligonucleotide primers are the 10-25 nucleotide sequences that are complementary on the target sequence. In addition, the synthesizing step begins from the end of the primer.
- DNA template contains the target sequence for amplification.

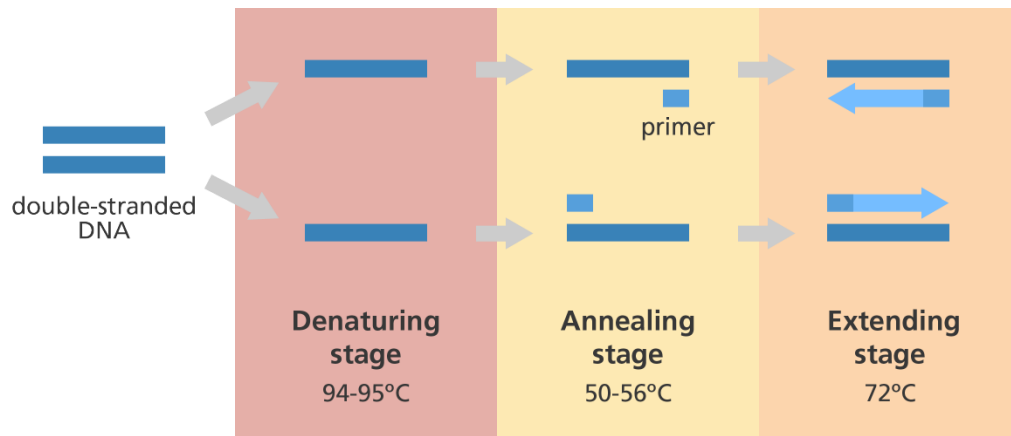


**Figure 23** The polymerase chain reaction (PCR)

The principle of the cycling reaction is shown in Figure 23. In the reaction cycle, the DNA template is denatured to single-stranded by raising the temperature to 94 – 95°C (denaturation step). Next, lowering the temperature to about 35 to 65°C (depending on primer sequence and experimental design) results in primer annealing to the target sequences on the DNA template (annealing step). The primers hybridized to binding site that are identical or highly homologous to their nucleotide sequence, though some mismatch at 5'-end are allowed. Finally, the temperature is increased to 65 – 72°C depend on activity of the thermostable polymerase (extension step). The polymerase extends the 3'-ends of the primer hybrids toward the other primer binding site. These three steps are repeated for 25 – 50 cycles leads to the exponential amplification of the target amplicon between 5'-end of the two primer binding site.

### 2.11.2 Sequencing technique

Two fundamental techniques of DNA sequencing have been developed since the mid-1970s. First, the chemical degradation method was originated by Maxam and Gilbert in 1977 [207], which methodized using chemicals to cleave the specific bases in an end-labeled molecule of DNA. This manner used four nested groups of labeled

cleavage products, each terminating at a specific base. After that, the sets of labeled fragment were separated on highly denaturing polyacrylamide gels electrophoresis, and visualized by autoradiography. Finally, the resulting sequence can be directly interpreted from the autoradiogram (Figure 24).

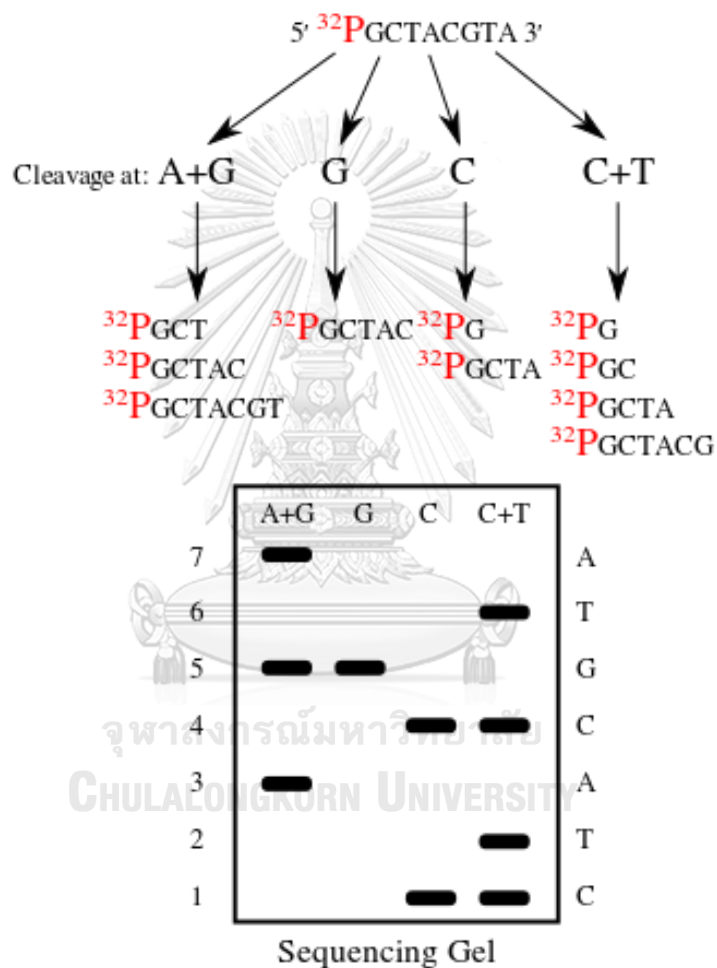


Figure 24 Maxam-Gilbert sequencing techniques

Second, Sanger *et al.* developed another sequencing technique in 1977, which called as chain termination method [208]. The principle of this technique used dideoxynucleotides (ddNTPs) to discontinuing the extension activity of the DNA polymerase. Practically, Sanger sequencing reaction is contained the component of

PCR amplification mixture, but reaction is added four 2',3'-dideoxynucleotides (ddATP, ddGTP, ddCTP, ddTTP). These nucleotide analogs are suitably recognized by the polymerase enzyme and fused into the extended chain. From the properties of ddNTPs, there are not 3'-hydroxyl group in its structure, so the elongation process is stopped at the position which ddNTP is incorporated. Lastly, a numerous band are produced and separated on highly denaturing polyacrylamide gels electrophoresis. Nowadays, the detection of these technique was used dye-labeled dideoxynucleotides instead of silver staining. Each fragments were run through capillary gel electrophoresis, and illuminated by a laser light, allowing the attached dye to be detected. The data reported from the detector comprised of sets of fluorescence-intensity peaks or called chromatogram (Figure 25). Finally, the DNA sequence was interpreted from the chromatogram.

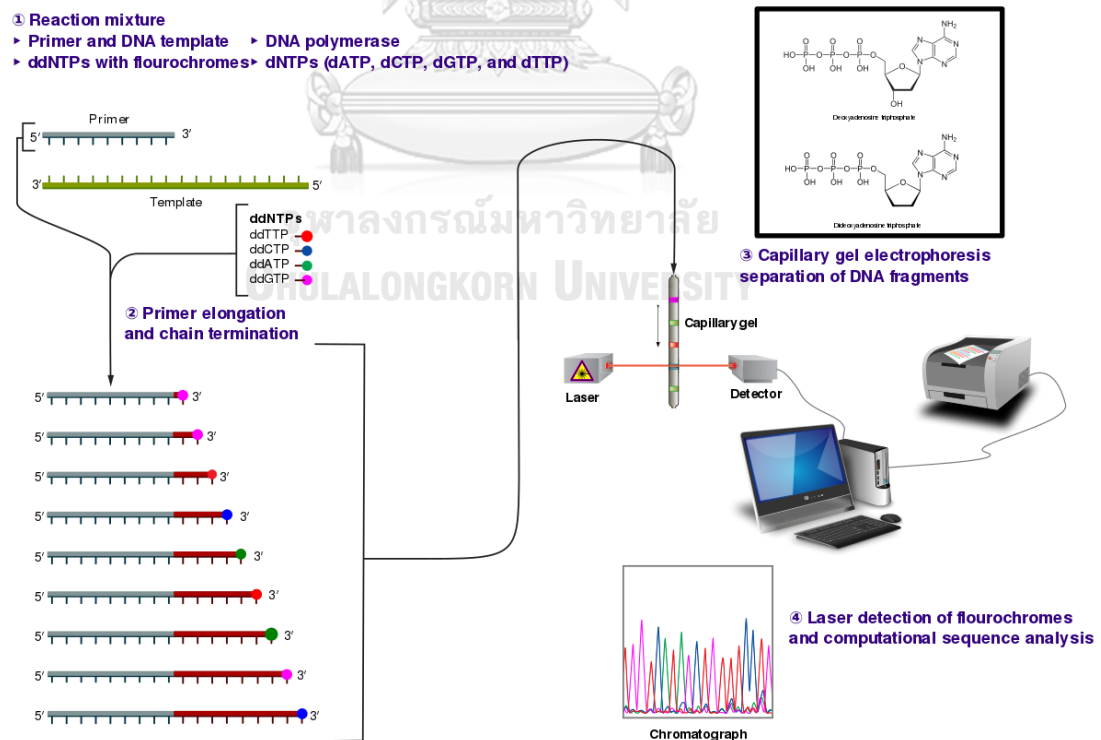


Figure 25 Sanger sequencing techniques

## 2.12 Sequence alignment

A sequence alignment in bioinformatics is a process of arranging the DNA, RNA, or protein sequences to identify regions of similarity that might be determined the functional, structural, or evolutionary relationships between the sequences. Aligned nucleotide or amino acid sequences are essentially expressed as rows within a matrix. Alignments are generally described as pictorial and in text format. For presentation of sequence alignment, sequences are arranged in rows and aligned remaining sequences in successive columns. On the other hands, the identical or similar characters of text format alignment are used a systems of conservation symbol. In addition, various sequences alignment software also utilized the color to represent each nucleotides [209].

Multiple Sequence Alignment (MSA) is the alignment of three or more biological sequences. Homology can be assumed from the output and the evolutionary relationships between the sequences studied. There are various free online MSA program, for example: Clustal Omega, Muscle, MAFFT, T-Coffee [210].

## 2.13 Phylogenetic analysis

Phylogenetic analysis of DNA sequences has become a crucial tool for evolutionary investigation of organisms. Since the rate of evolutionary sequences is widely different in gene or DNA segment, one can examine the evolutionary relationships of virtually all levels of classification of creature; for example, kingdom, phyla, families, genera, and intraspecific populations, using various genes or DNA segment. So, phylogenetic analysis is an important tool for clarifying the evolutionary model of multigene families and for conceiving the process of adaptive evolution at the molecular level.

There are many statistical methods which can be utilized for reconstructed cladogram from molecular data. The generally used methods are classified into two groups; (1) distance-based methods, and (2) character-based methods [211].

#### 2.13.1 Distance-based method

Distance methods or distance matrix methods are computed the evolutionary distances by all pairs of taxa. Therefore, the phylogenetic tree is constructed by determining the relationship between these distance values. There are various methods of constructing cladogram from distance data. The distances method, such as Unweighted Pair-Group Method Using Arithmetic Averages (UPGMA), Weighted Pair-Group Method Using Arithmetic Averages (WPGMA), Neighbor-Joining (NJ) method, Least Squares (LS) method, Minimum Evolution (ME) method, have been used for data determination.

#### 2.13.2 Character-based method

Character-based methods use the aligned sequences directly during tree construction. There are various methods for tree building; for example, Maximum Likelihood (ML) method, Bayesian Analysis method, and Maximum Parsimony (MP) method.

##### 2.13.2.1 *Maximum Likelihood method*

Maximum likelihood (ML) is a statistical method for evaluating unknown parameters of a probability model. ML method was primarily proposed by an English statistician R.A. Fisher in 1922. Likelihood is defined to be a proportional amount to the probability of observing the given set of sequence data for a specific substitution model. The likelihood value of each topology is calculated, and then the greatest ML

value is chosen as the parameter of the tree and/or branch lengths at that point is the maximum likelihood estimate of the parameter [212].

In maximum likelihood methods, there are two assumptions;

Assumption 1: Different sites can evolve independently.

Assumption 2: Diverge sequences (or species) evolve independently after diverge.

The calculation formula for ML method followed this equation;

$$L = \prod_{i=1}^n P(D_i | T) = \prod_{i=1}^n \prod_{j=1}^m P(D_{ij} | T_j)$$

$$\ln L = \sum_{i=1}^n \ln \prod_{j=1}^m P(D_{ij} | T_j)$$

Where, L = likelihood value, D = data, T= hypothesis, Pr = probability

The cladogram from ML method represent the best justified method from a theoretical aspect because ML evaluate all possible trees and sampling error have least effect on the model. In addition, the sequence simulation experiments have exhibit that this method performs more accurate than other method. However, ML method is not practical for analyzing the large data set and the operations by this method are extremely slow.

จุฬาลงกรณ์มหาวิทยาลัย  
CHULALONGKORN UNIVERSITY

#### 2.13.2.2 Bayesian Analysis method

Bayesian Equation was proposed by Thomas Bayes, an English mathematician. Bayesian analysis, a method of statistical inference that combine prior data about a parameter with evidence to guide the statistical inference process. The evidence is obtained and combined through an application of Bayes's theorem to provide a posterior probability distribution for the parameter [213].

The calculation formula for Bayesian analysis method followed this equation;

$$\text{Posterior probability} = \frac{\text{prior probability} \times \text{data fit tree probability}}{\text{data probability}}$$

$$\text{Pr(Tree|Data)} = \frac{\text{Pr(Tree)} \times \text{Pr(Data|Tree)}}{\text{Pr(Data)}}$$

### 2.13.2.3 Maximum Parsimony methods

Maximum parsimony (MP) method is the first phylogenetic method which developed by Willi Hennig in 1966. MP methods were developed to analyze the data contained in at least four aligned nucleotide sequences. The nucleotides of ancestral taxa are inferred separately at each site for a given topology under the assumption that mutational changes occur in all directions among the four nucleotides. The smallest number of nucleotide substitutions that explain the entire evolutionary process for the topology is computed. This computation is done for all potentially correct topologies, and the topology that requires the smallest number of substitutions is chosen to be the best cladogram.

MP principle mentioned that a tree that does not fit the data well will require many changes to explain the data, and thus shorter trees are better than longer trees. Finally, the tree with the smallest tree score is the estimate of the true tree. It is called “the Maximum Parsimony Tree” or the most parsimonious tree [214].



### 2.13.3 Bootstrap analysis

Bradley Efron (1986) gave the definition of bootstrap is “a computational technique for estimating a statistic for which the underlying distribution is unknown or difficult to derive analytically” [215]. After that, Joseph Felsenstein applied the bootstrap analysis into phylogenetics fields in 1985. Bootstrap are used to estimate the confidence level of phylogenetic hypothesis. Bootstrap was implemented into cladogram construction in the step of resampling because it estimates the sampling distribution by repeatedly resampling data from the original sample data set. This process is repeated many times, and then the reliability of the cladogram is calculated by the percentage of times in which each branching pattern is found among all the replicate bootstrap trees.



## CHAPTER III

### MATERIALS AND METHODS

#### 3.1 PHARMACOGNOSTIC EVALUATIONS AND MANGIFERIN CONTENTS OF *AQUILARIA CRASSNA* LEAVES

Pharmacognostic evaluations are the methodology associated with the identification and quality control of the medicinal plants. This study is not only necessary for authentication but it also put the acceptance criteria for standardization and authentication of herbal materials. In addition, this study can prevent the adulteration and substitution of the crude drug. The pharmacognostic evaluations consist of the investigation of macroscopic and microscopic characteristics, the chemical profiling and physicochemical parameters. The macroscopic characters are determined using organoleptic sensation in terms of size, shape, color, odor, taste. The microscopic method is described about plant histology. The thin layer chromatography technique is used for showing chemical profiles of each plant. The physicochemical studies are following in WHO guidance [87] and Thai Herbal Pharmacopoeia [2]. In addition, the quantitative analysis of mangiferin content using TLC-densitometry compared with image analysis method was also performed.

The scope of this investigation;

- Macroscopic and microscopic determination of *Aquilaria crassna* leaves
- TLC examination of ethanolic extracts of *Aquilaria crassna* leaves
- Quality control of herbal materials using physicochemical method
- Quantitative analysis of mangiferin content in *Aquilaria crassna* leaves by TLC-densitometry compared with image analysis method

## 3.1.1 Chemicals

p-Anisaldehyde	Merck, Germany
Chloral hydrate	Ajax Finechem Pty. Ltd., New Zealand
Ethanol	BDH ProLabo. France
Ethyl acetate	Burdick & Jackson, USA
Formic acid	Merck, Germany
Haiter <sup>®</sup> solution (6% sodium hypochlorite)	Kao Corp., Japan
Hydrochloric acid	Merck, Germany
Mangiferin	MIRA Biotechnologies, China
Methanol	Burdick & Jackson, USA
Phloroglucinol	Merck, Germany
Toluene	Burdick & Jackson, USA
Ultrapure water	



จุฬาลงกรณ์มหาวิทยาลัย

CHULALONGKORN UNIVERSITY

## 3.1.2 Materials

Beaker	Pyrex, Germany
Filter paper No. 40 ashless	Whatman <sup>TM</sup> paper, UK
Filter paper No.1	Whatman <sup>TM</sup> paper, UK
Glass slide and coverglass	HDA, China
TLC silica 60 F254	Merck, Germany

## 3.1.3 Instruments

Ash furnace	Corbolite, United Kingdom
Balance, readability 0.01 g	Sartorius, Germany
Balance, readability 0.0001 g	Mettler Toledo, USA
Clevenger apparatus	
Desiccator	
Hot air oven	Binder, Germany
ImageJ software	The National Institute of Mental Health, USA
Incubator shaker	GFL, Germany
Light microscope with digital camera	Carl Zeiss model Axio Lab, Germany
Rotary evaporator	Buchi, Switzerland
Soxhlet apparatus	
Syringe (100 $\mu$ L)	Hamilton, USA
TLC-densitometry	CAMAG, Switzerland
<input type="checkbox"/> CAMAG Linomat 5 <input type="checkbox"/> CAMAG Automatic Developing Chamber 2 (ADC 2) <input type="checkbox"/> CAMAG TLC Scanner 3 <input type="checkbox"/> CAMAG TLC Visualizer 2 <input type="checkbox"/> CAMAG TLC plate heater	
Ultrasonic bath	Elma, Germany
Water bath	GFL, Germany



### 3.1.4 Plant materials

*Aquilaria crassna* leaves were collected from fifteen sources throughout Thailand. The plant samples were identified by Associate Professor Dr. Nijisiri Ruangrunsi and the voucher specimens were deposited at College of Public Health Sciences, Chulalongkorn University, Thailand. The leaves were dried in a hot air oven at 60 °C until dried, then the dried materials were ground and stored at room temperature protected from light prior to use.

### 3.1.5 Macroscopic and microscopic determination of *Aquilaria crassna* leaves

#### 3.1.5.1 Macroscopic evaluation

The fresh leaves were collected and determined the morphological characters of leaves. In addition, *A. crassna* dried leaves characters were determined using organoleptic sensation in term of shape, size, color, odor, and taste of powdered drug.

#### 3.1.5.2 Microscopic evaluation

Microscopic method determined the characteristics of cells and tissues using light microscope. Furthermore, the constant number of leaves was used as character for identification concerning their constant value in each species.

##### ○ *Histological character investigation*

Transverse section of midrib and surface view of laminar of leaves was determined for plant histological structure.

##### ○ *Determination of powdered drug*

The dried leaves were ground and passed through the sieve mesh number 60. The powdered drug was get onto the glass-slide and then mounted with water to investigate the cell and tissue characters. Chloral hydrate reagent was added onto the

powder for the transparency improvement of the plant tissue. The cell and tissue were photographed using photo-micrographic equipment.

#### ○ Determination of leaf constant values

The leaf constant values; such as stomatal index, stomatal number, palisade ratio, are used as one of the characteristics for medicinal plant identification.

#### *Preparation of leaves*

The fresh mature leaves were collected from Faculty of Pharmaceutical Sciences, Chulalongkorn University, Bangkok and 2 samples from Princess Maha Chakri Sirindhorn Herbal Garden, Rayong. The leaves were cut and removed chlorophyll using HAITER® solution and then soaked in warmed chloral hydrate 4 g/ml in water until clear. When the leaf fragments were cleared, it was rinsed with ultrapure water at least 2 times and kept in glycerin to maintain the structure and moisture of the cells.

#### *Determination of the stomatal number*

The number of stomata was counted in the area of view and incomplete part of cell in one semi-square. Thirty fields were counted. Finally, this constant value calculated by this formula:

$$\text{Stamatal number} = \text{Number of stomata} / \text{Area of epidermal cell (mm}^2\text{)}$$

#### *Determination of the stomatal index*

The percentage proportion of stomata index was calculated from this formula:

$$\text{Stomatal index} = [ S / (S + E) ] \times 100$$

Where S = number of stomata per unit area, E = number of ordinary epidermal cells in the same unit area.

### *Determination of the palisade ratio*

The palisade cell beneath four epidermal cell were counted. The palisade ratio is obtained from the number of palisade cell divided by four.

### *Determination of the epidermal cell area*

The number of epidermal cell were counted in the area of view and incomplete part of cell in one semi-square. Thirty field were counted. Then, the epidermal cell area can be calculated by this formula:

$$\text{Epidermal cell area} = \text{Number of epidermal cell} / \text{Area of view (mm}^2\text{)}$$

### 3.1.6 TLC examination of ethanolic extracts of *Aquilaria crassna* leaves

The dried leaves were ground and passed through a sieve with mesh number 20. Three grams of dried leaf powder were macerated in 100 ml of ethanol for 24 hours, after that filtrate was filtered through filter paper and evaporated to dryness. The crude extracts were accurately weighted then the concentration was adjusted to 1 mg/ml. Three microliters were applied on silica gel TLC plate using CAMAG Linomat 5 which operated by WinCAT software. The chemical profile was done as these following;

Technique	:	One-dimensional thin layer chromatography
Stationary phase	:	Silica gel 60 GF254 (Merck) pre-coated plate
Mobile phase	:	Ethyl acetate: Water: Formic acid, 34:6:4 v/v/v
Distance	:	8.0 centimeters
Temperature	:	Room temperature (25 – 30 °C)
Detection	:	Visible daylight, UV 254 nm, UV 365 nm and Anisaldehyde-sulfuric acid TS with heat

Finally, the locations and colors of the spots were recorded using CAMAG TLC Visualizer 2. The  $R_f$  values were determined.

### 3.1.7 Quality control of herbal materials using physicochemical method

The constant values owing to the quality of *A. crassna* leaves were determined following standard procedure of WHO guidance [87] and Thai Herbal Pharmacopoeia [2]. Each sample was performed in triplicate. The procedures are described as following;

#### 3.1.7.1 Loss on drying

The leaf powders was accurately weighed in pre-weighed crucible, and then dried at 105°C until obtained constant weight. After that, the percentage of loss on drying was calculated using this formula;

$$\% \text{ Loss on drying} = \frac{\text{Weight before drying} - \text{Weight after drying}}{\text{Weight before drying}} \times 100$$

#### 3.1.7.2 Total ash

The leaf powders was accurately weighed in pre-weighed crucible, and then gradually incinerated to 500 – 600 °C until white ash obtained. The ash was cooled in desiccator and weighed without delay. The percentage of total ash was calculated using this formula;

$$\% \text{ Total ash} = \frac{\text{Weight of ash}}{\text{Weight of leaf powders}} \times 100$$



### 3.1.7.3 Acid insoluble ash

The ash in crucible was added with 25.0 ml of 2N hydrochloric acid. Next, the crucible was covered with a watch-glass, and the mixture was gently boiled for 5 minutes. The watch-glass was rinsed with hot water, and this liquid was added into the crucible. This suspension was filtered using ashless filter paper. The insoluble matter was collected on ashless filter paper and washed with hot water until the filtrate pH is neutral. Then, the filter paper containing the insoluble matter was transferred to the original crucible, dried on a hot plate and incinerated to constant weight. The residue was cooled in a desiccator and weighed without delay. The percentage of acid-insoluble ash was calculated using this formula;

$$\% \text{ Acid-insoluble ash} = \frac{\text{Weight of acid-insoluble ash}}{\text{Weight of leaf powders}} \times 100$$

### 3.1.7.4 Ethanol-soluble extractive value

The ground herbal material was macerated with 70 mL absolute ethanol in a glass stoppered conical flask under shaking for 6 hours and standing for 18 hours. After that, the extract was rapidly filtered to avoid loss of ethanol, the marc was rinsed with ethanol and the volume was adjusted to 100 mL. Twenty milliliters of filtrate were transfer to evaporating disc and evaporated to dryness. The evaporating disc with dried extract was dried in hot air oven at 105 °C to receiving the constant weight. Then, the content of ethanol extractable value was calculated in a percentage of weight.

### 3.1.7.5 Water-soluble extractive value

The process of water-soluble extraction was performed as directed for ethanol-soluble extractive, but using water in place of ethanol.

### 3.1.7.6 Determination of water content (Azeotropic distillation method)

The ground herbal material in 200 mL water-saturated toluene was subjected to azeotropic distillation. When the water is completely distilled, the inside of condenser tube was rinsed with toluene. The heat was removed, and the receiving tube was allowed to cool to room temperature. The water and toluene layer were separated, and then volume of water was read and percentage of water content was calculated.

### 3.1.8 Quantitative analysis of mangiferin content in *Aquilaria crassna* leaves by TLC-densitometry compared with image analysis method

#### 3.1.8.1 Preparation of mangiferin standard solution

Stock solution of mangiferin was prepared by dissolving in 85% ethanol in a volumetric flask at a concentration of 1 mg/ml. The six working standard solutions (concentrations of 0.15, 0.25, 0.35, 0.45, 0.55 and 0.65 mg/ml) were diluted from standard stock solution using ethanol as a diluent.

#### 3.1.8.2 Preparation of ethanolic extract of *A. crassna* leaves

Each sample of *A. crassna* leaves were accurately weighed (3.00 g) and extracted by soxhlet extraction with 95% ethanol until exhaustion. The extracts were filtered, evaporated using rotary evaporator equipped with vacuum pump and dried using freeze-dryer techniques. The dried extracts were weighed and calculated for percentage yield. Each ethanolic extract was dissolved in absolute ethanol in volumetric flask to obtain concentration of 5 mg/mL, and the extract was diluted with absolute ethanol to provide the test extract at a concentration 1 mg/ml. The solution

was filtered using 0.22  $\mu\text{M}$  nylon membrane filter before application onto the TLC plate. Each sample were carried out in triplicate.

### 3.1.8.3 Chromatographic conditions

The TLC pre-treatment process was performed prior to use by washing the TLC plate with methanol and activating at 105°C for 15 minutes. Three microliters of each sample were spotted with 5-mm. bands width using a 100  $\mu\text{L}$ -syringe. The solutions of mangiferin standard and ethanolic *A. crassna* extract were spotted at 10 mm from the bottom edge of TLC plate using a CAMAG Linomat-5 automatic sample spotter under a flow of  $\text{N}_2$  gas. Each sample solution was done in triplicate. The mobile phase comprises of ethyl acetate: water: formic acid, 17:3:2 v/v/v respectively. The TLC plate was developed in CAMAG Automatic Developing Chamber after pre-saturated chamber with the mobile phase for 1 hours at room temperature. The mobile phase was run to 80 mm.

### 3.1.8.4 TLC-densitometry and TLC image analysis studies

The developed TLC plates were scanned densitometrically using a CAMAG TLC 3 Scanner in the absorbance mode at 254 nm, which is operated by WinCATs software. While TLC image analysis was done using Image analysis software, the developed TLC plate was photographed under short wave (254 nm) ultraviolet light. The photo was taken using CAMAG TLC Visualizer and saved as TIFF file. The color intensity of mangiferin band was transformed to chromatographic peak by ImageJ software. Six-point calibration of two methods was done and each sample were quantified the amount of mangiferin by peak area. Each sample were carried out triplicate.

### 3.1.8.5 Method validation

The analytical method was validated for linearity, precision, accuracy, limit of detection (LOD), limit of quantitation (LOQ) and robustness according to International Conference on Harmonization (ICH) guideline (Q2R1).

#### ○ Linearity

Linearity was determined using the working standard solution. Three microliters of six concentrations of standard (0.15, 0.25, 0.35, 0.45, 0.55 and 0.65 mg/mL) were spotted on TLC plate to obtain the calibration range of 0.45-1.95  $\mu\text{g}/\text{spot}$ . The calibration curve was obtained by plotting the data of peak area *versus* the amount of mangiferin.

#### ○ Accuracy

The accuracy of this analytical method was performed by recovery studies of three levels of standard added to the sample solution. The sample solutions were spotted onto a TLC plate and analyzed by the proposed method. Three concentration levels of standard addition were analyzed. The average recoveries were calculated.

#### ○ Precision

The precision was performed by three levels of standard solution added to the sample solution. After that, applications onto the TLC plate on the same day for intra-day precision and on three consecutive days for inter-day precision were analyzed. The precision was expressed as percent relative standard deviation (RSD).

#### ○ Limit of Detection and Limit of Quantitation (LOD and LOQ)

LOD and LOQ were found out by preparing six concentrations (0.15, 0.25, 0.35, 0.45, 0.55 and 0.65 mg/mL) of standard stock solution. LOD and LOQ were calculated from corresponding average calibration curve using formula  $\text{LOD} = 3.3 \cdot (\text{S.D.}/S)$  and  $\text{LOQ} = 10 \cdot (\text{S.D.}/S)$  where, S.D. is the standard deviation of y-intercept of regression line, and

S is the slope of respective calibration curve. The signal to noise ratio 3:1 and 10:1 for LOD and LOQ, respectively were considered.

#### ○ Robustness

The robustness of the method was experimentally evaluated by setting little changes in certain chromatographic conditions and parameters. The ratio of mobile phase composition was slightly changed as 33.9:6.1:4, 34.1:5.9:4, 34.1:6:3.9, 33.9:6:4.1, 34:5.9:4.1 and 34:6.1:3.9, v/v/v, for ethyl acetate: water: formic acid, respectively. The RSD values of the peak areas of standard and selected sample were calculated for all variations.

#### 3.1.9 Data analysis

The content of physicochemical parameters was calculated using grand mean and pooled standard deviation. Mangiferin contents in each sample were calculated based on each extract yield. The contents between TLC-densitometry method and TLC image analysis method were compared statistically using paired student t-test ( $P \leq 0.05$ ).

### 3.2 Biological assessment of ethanolic extract of *Aquilaria crassna* leaves

#### 3.2.1 Chemical and reagents

30% Acrylamide/bisacrylamide (29:1)	Bio-Rad Laboratories, USA
Albumin from bovine serum (BSA)	Sigma-Aldrich, USA
2-Amino-2-(hydroxymethyl)-1,3-propanediol (Tris base)	Sigma, USA
Ammonium persulfate (APS)	Bio-Rad Laboratories, USA
Anti-rabbit IgG, HRP-linked Antibody	Cell Signaling Technology, USA
Ascorbic acid	Fluka Chemicals, Germany
Bax antibody	Cell Signaling Technology, USA
Bcl-2 Antibody (Human Specific)	Cell Signaling Technology, USA
Beta-actin mouse mAb antibody (HRP conjugate)	Cell Signaling Technology, USA
Beta-mercaptoethanol	Sigma, USA
Bovine serum albumin	Merck, USA
Bromophenol blue	Sigma, USA
Coomassie Brilliant Blue G-250	Thermo Fisher Scientific, USA
2', 7'-Dichlorodihydrofluorescein diacetate (DCFH-DA)	Sigma, USA
Dimethyl sulfoxide (DMSO)	Merck, USA
3-(4,5-Dimethylthiazol-2-yl)-2,5-diphenyltetrazolium bromide (MTT)	Sigma, USA
Disodium hydrogenphosphate	Sigma, USA
2,2-Diphenyl-1-picrylhydrazyl (DPPH)	Fluka Chemicals, Germany
Enhanced chemiluminescence (ECL) prime Western blotting - detection reagent	Amersham, UK
Ethylenediaminetetraacetic acid (EDTA)	Univar, Australia
Fetal bovine serum (FBS)	Hyclone, UK
Glycerol	Merck, Germany
Glycine	Sigma, USA

Griess reagent (modified)	Sigma, USA
Hydrochloric acid	Merck, Germany
Hydrogen peroxide	Fisher Scientific, USA
Mangiferin	MIRA Biotechnologies, China
Medium (DMEM)	Gibco, New Zealand
Methanol (AR grade)	Burdick & Jackson, USA
Mouse monoclonal to $\beta$ -actin, horseradish peroxidase conjugated	Abcam, England
N-1-naphthylethylenediamine dihydrochloride	
N, N, N', N'-tetramethylethylenediamine (TEMED)	Bio-Rad Laboratories, USA
PageRuler™ prestain protein ladder	Fermentas, USA
Penicillin streptomycin	Gibco, New Zealand
Phosphoric acid	Merck, Germany
Potassium chloride	Merck, Germany
Potassium dihydrogen phosphate	Merck, Germany
Protease inhibitor	Amersham Biosciences, USA
Quercetin	Sigma, USA
Rabbit polyclonal to Cu/Zn-SOD	Abcam, England
Sodium chloride	Merck, USA
Sodium deoxycholate	Sigma-Aldrich, USA
Sodium dodecyl sulfate (SDS)	Bio-Rad Laboratories, USA
Sodium hydroxide	Merck, Germany
Sodium nitroprusside (SNP)	Fluka Chemical, Germany
Tris-(hydroxymethyl)aminomethane	Sigma-Aldrich, USA
Triton X-100	Fluka, Switzerland
Trypsin solution (0.5%)	Gibco, New Zealand
Tween 20	Fisher Biotech, USA

### 3.2.2 Equipment

Autoclave	HVP-50, Hirayama, USA
Centrifuge	Hettich Lab Technology, Germany
Centrifugal evaporator	MaxiVac Evaporators, Scanvac, Denmark
Chemiluminescence document	GE Healthcare, UK
5% CO <sub>2</sub> incubator	3111, Thermo Fisher Scientific, USA
Chemi-luminescence Documentation	Image Quant LAS4010, GE Healthcare, USA
Electrophoresis apparatus	
- Mini-PROTEAN® Tetra Cell Systems	Bio-Rad, USA
- PowerPac™ Basic Power Supply	Bio-Rad, USA
Hemocytometer	Bright-line, Hausser, USA
Microplate reader	Spectramax M5, Molecular device, USA
Phase contrast inverted microscope	Primo Vest, Carl Zeiss, Germany
Rotary evaporator	R210-Rotavapor, Buchi, Switzerland
Shaker	GFL, Germany

### 3.2.3 Plant materials

The leaves of *Aquilaria crassna* was collected from Nan Province, Thailand (Ac14) and was identified by Associated Professor Dr. Nijisiri Ruangrunsi, College of Public Health Sciences, Chulalongkorn University, Thailand.



### 3.2.4 Preparation of Ac14 ethanolic extract

The leaves of Ac14 was dried at 50°C and pulverized into fine powder. The Ac14 powder was exhaustively extracted with 95% ethanol using soxhlet extraction method. The extract was filtered and evaporated to dryness using rotary evaporator equipped with vacuum pump. The Ac14 extract was stored in well-closed container, protected from light, and kept at -20°C. The yields of Ac14 extract were calculated.

### 3.2.5 Free radical scavenging activities in a cell-free system

#### 3.2.5.1 DPPH free radical scavenging assay

The method of DPPH free radical scavenging assay was slightly modified from Brand-Williams and co-researcher [109]. Five microliters of the various concentration of Ac14 extracts, mangiferin, and positive control (quercetin) was mixed with 195 µl of freshly prepared 80 µM DPPH ethanolic solution. This mixture was store in the dark at room temperature for 90 minutes. The solution was measured the absorbance at 510 nm using microplate reader. The percentage of scavenging activity was calculated by following equation:  $[(A_{\text{blank}} - A_{\text{test}}) / A_{\text{blank}}] \times 100$ , where  $A_{\text{blank}}$  is the absorbance of the DPPH solution without addition of samples,  $A_{\text{test}}$  is the absorbance of the DPPH solution after reacted with the samples. The  $IC_{50}$  values were evaluated from the curve fitting to the above equation.

#### 3.2.5.2 Scavenging of $NO^{\bullet}$

The method of  $NO^{\bullet}$  scavenging assay was slightly modified from Jagetia, G.C method [216]. Various concentrations of Ac14 extracts, mangiferin, and positive control (quercetin) were incubated with 4 mM sodium nitroprusside at room temperature under light for 2.5 hours. After that, Griess reagent was added. The color of this mixture

was developed for 10 minutes. The absorbance of pink solution was measured at 560 nm using microplate reader. The percentage of NO<sup>•</sup> scavenging activity was calculated by the following equation:  $[(A_{\text{blank}} - A_{\text{test}}) / A_{\text{blank}}] \times 100$ , where  $A_{\text{blank}}$  is the absorbance of the reaction mixture without sample addition, and  $A_{\text{test}}$  is the absorbance of the reaction mixture after reacting with the sample.

### 3.2.5.3 Superoxide radical scavenging activity

The generation of superoxide radical ( $O_2^{\bullet-}$ ) was based on non-enzymatic NADH/PMS system with the measurement of  $O_2^{\bullet-}$  quenching via the reduction of nitrotetrazolium blue. The method of superoxide radical scavenging activity was spectrophotometrically measured with minor modification from Fernandes *et al.* [7]. The reaction mixtures comprised of several concentrations of Ac14 extracts, mangiferin, and positive control (quercetin), 553  $\mu\text{M}$  of NADH, 143  $\mu\text{M}$  of NBT, and 9  $\mu\text{M}$  of PMS. The test compounds were dissolved in DMSO while all components were liquefied in 80 mM potassium phosphate buffer pH 7.4. The solution was measured the absorbance at 560 nm using microplate reader. The percentage of  $O_2^{\bullet-}$  scavenging activity was calculated by the following equation:  $([A_{\text{control}} - A_{\text{tests}}] / A_{\text{control}}) \times 100$ . The IC<sub>50</sub> values was evaluated from the curve fitting to the above equation. Each study was performed in triplicate.

### 3.2.5.4 Ferric reducing antioxidant power (FRAP) assay

The method of FRAP assay was slightly modified from Benzie and Strain method [110]. The working FRAP reagent was prepared from 300 mM of acetate buffer (pH 3.6), 10 mM of 2,4,6-tripyridyl-s-triazine (TPTZ) solution and 20 mM of ferric chloride in a 10:1:1 ratio. The 300 mM acetate buffer was composed of 3.1 g of sodium acetate trihydrate ( $C_2H_3NaO_2 \cdot 3H_2O$ ) with 16 ml of glacial acetic acid and adjusted with ultrapure

water to be 1 liter. TPTZ was dissolved in 40 mM hydrochloric acid. Twenty-five microliters of sample were added in a 96-well plate and then 175  $\mu$ l of working FRAP reagent was mixed with sample solution in each well. Next, the solution was incubated at room temperature for 10 minutes, and was observed the absorbance at 595 nm. Ferrous sulfate was used as reference standard to perform the calibration curves. The reducing power capability was expressed in  $\mu$ M ferrous sulfate equivalents in milligrams per dried weight of sample. Each sample was performed in triplicate.

#### 3.2.5.4 Total phenolic contents

The concentration of phenolic compound in Ac14 ethanolic extracts was determined by spectrophotometric procedure with slightly modification from Singleton V.L. protocol [217]. The ethanolic solution of the Ac14 was prepared as a concentration at 1 mg/ml, whereas gallic acid was used as reference standard to perform the calibration curves (concentration varied from 5 – 100  $\mu$ g/ml). The reaction mixture was comprised of 20  $\mu$ l of crude extract or standard solution, 100  $\mu$ l of 10% Folin-Ciocalteu's reagent, which dissolved in water, and 80  $\mu$ l of 7.5% Sodium carbonate solution ( $\text{NaHCO}_3$ ). The mixtures were incubated at room temperature for 1 hour. Next, the absorbance was determined using microplate reader at  $\lambda = 765$  nm. The experiments were done in triplicate. Finally, the content of phenolic compound in extracts was expressed in terms of gallic acid equivalent (mg of GAE per g of extract).

#### 3.2.6 Antidiabetic activity

##### 3.2.6.1 Inhibition of yeast $\alpha$ -glucosinase activity

The inhibition of  $\alpha$ -glucosidase activity was performed with minor modified procedure of Wan *et al.* [218]. The  $\alpha$ -glucosidase enzyme can hydrolysed the synthetic

substrate, p-nitrophenyl- $\alpha$ -D-glucopyranoside (PNPG). The enzyme mechanism results in nitrophenol, which shows the yellow color.

The reaction was done in 96-well plate. Thirty microlitres of 0.5 U/ml of  $\alpha$ -glucosidase enzyme solution was incubated with 30  $\mu$ l of tested solutions (Ac14 extract, mangiferin or acarbose) in DMSO and 0.1 M sodium phosphate buffer (pH 6.9) at 37°C for 15 minutes. Afterwards, the 30  $\mu$ l of substrate (PNPG) was added and incubated at 37°C for 30 minutes. Finally, 80  $\mu$ l of 0.2  $\mu$ M sodium carbonate ( $\text{Na}_2\text{CO}_3$ ) was added for stopped the reaction. The absorbance was measured at 405 nm using microplate reader. All experiments were analysed in triplicate. The percent inhibition was calculated using this formula:

$$\% \text{ inhibition} = [ ( A_{\text{control}} - A_{\text{test}} ) / A_{\text{control}} ] \times 100$$

### 3.2.7 Cytotoxicity activity on cancer cell

#### 3.2.7.1 Cell culture

Human colorectal adenocarcinoma (HT-29), human hepatocellular carcinoma (HepG2) and human breast cancer (MDA-MB-231) were obtained from the American Type Culture Collection (ATCC) and were cultured in complete medium. The complete medium contained 10% (v/v) FBS, 1% (v/v) penicillin-streptomycin and basal media (DMEM).

#### 3.2.7.2 Determination of cytotoxicity activity of Ac14 extract and mangiferin using MTT assay

Three trypsinized cultured cells were seed in 96-well plate at a density of  $1 \times 10^5$  cells/ml of complete medium per well and incubated at 37°C in a humidified atmosphere enriched with 5% (v/v)  $\text{CO}_2$ . After seeding for 24 hours, the cells were

exposed to various concentration of the Ac14 extracts or mangiferin or doxorubicin for 24 hours. The medium was replaced by the MTT solution (0.4 mg/ml) and incubated for 4 hours. After that, the MTT solution was removed and replaced by 100% DMSO. The optical density (OD) was measured at 570 nm using microplate reader.

Three replicates of each experiment were done and the concentrations of compound that induces 50% cell death ( $IC_{50}$ ) in comparison with the control were determined.

### 3.2.8 Cytoprotective effect of mangiferin and Ac14 extract

#### 3.2.8.1 Cell culture

The human umbilical vein endothelial EA.hy926 cell was purchased from American Type Culture Collection (ATCC) (Cat No. CRL-2922). The cells were cultured with seeding density of  $1 \times 10^5$  cells/ml in DMEM media, containing 10% FBS and 1% penicillin-streptomycin, at  $37^\circ\text{C}$  in 5%  $\text{CO}_2$  incubator. The medium was changed every 2-3 days and subcultured every 4-5 days using 0.25% trypsin in PBS. DMSO (final concentration as 0.5%) was used as vehicle control in all experiments of cell system.

#### 3.2.8.2 Determination of the effect of Ac14 extract, mangiferin or $\text{H}_2\text{O}_2$ on cell viability

The cell viability was evaluated using MTT assay. The MTT is reduced by mitochondrial dehydrogenase in viable cells to purple color of formazan crystal, which can be dissolved in DMSO. The intensity of purple solution was measured.

The method was slightly modified from Carmichael *et al.* [219]. Trypsinized sub-confluent cells were seed into 96-well plates at a density of  $1 \times 10^5$  cells/ml and incubated for 24 hours before treatments. Thereupon, the cells were exposed to various concentration of the Ac14 extracts, mangiferin or  $\text{H}_2\text{O}_2$  for 24 hours. The

medium was replaced by the MTT solution (0.4 mg/ml) and incubated for 4 hours. After that, the MTT solution was removed and replaced by 100% DMSO. The optical density (OD) was measured at 570 nm using microplate reader. The percentage of cell viability was calculated by following equation: The percentage of cell survival =  $(OD_{\text{treat}}/OD_{\text{control}}) \times 100$ , Where  $OD_{\text{treat}}$  is the optical density of treated cell, and  $OD_{\text{control}}$  is the optical density of control. The  $IC_{50}$  was determined from percentage of cell survival versus concentration curve.

### 3.2.8.3 Measurement of Ac14 extract, mangiferin or $H_2O_2$ on intracellular ROS

Dichloro-dihydro-fluorescein diacetate (DCFH-DA) was used for determining the generation of intracellular ROS. DCFH-DA can be permeated into the cell and interacted with cytoplasmic esterase to generate dichlorodihydrofluorescein (DCFH). In addition, DCFH is rapidly oxidized to a strongly fluorescent dichlorofluorescein (DCF). Finally, the DCF intensity was obtained from the amount of intracellular ROS including  $H_2O_2$ ,  $OH^{\bullet}$ , and hydroperoxides (ROOH) [220-222].

The accumulation of intracellular ROS was evaluated using DCFH-DA method, which slightly modified from Shirai *et al.* procedure [223]. Trypsinized sub-confluent cells were seed into 96-well plates at a density of  $1 \times 10^5$  cells/ml and incubated for 24 hours before treatments. Thereupon, the cells were exposed to various concentration of the Ac14 extract, mangiferin or  $H_2O_2$  for 24 hours. After that, the cells were washed twice with cold-PBS and incubated with  $5 \mu\text{M}$  of DCFH-DA for 30 minutes. Then, DCFH-DA was removed. The cells were washed with cold-PBS for two times, and incubated with  $250 \mu\text{M}$   $H_2O_2$  for 30 minutes. After that, the cells were washed with cold-PBS for two times. Finally, the absorbance was measured using a fluorescent microplate reader with excitation at 485 nm and emission at 535 nm. The intracellular ROS intensity was calculated by following equation:  $(A_{\text{test}}/A_{\text{control}}) \times 100$ , where  $A_{\text{control}}$

is the absorbance of the untreated cell (control), and  $A_{\text{test}}$  is the absorbance of the cells that pre-incubated with interested substances for 24 hours and followed by incubation of 250  $\mu\text{M}$   $\text{H}_2\text{O}_2$  for 30 minutes.

#### 3.2.8.4 Western blotting analysis

Western blotting analysis is used to determine the specific proteins using acrylamide gel electrophoresis to separate proteins by the size. The proteins on the gel are transferred to PVDF membrane and the specific antibodies are probed.

The trypsinized sub-confluent cells were seeded into 6-well plates at a density of  $1 \times 10^5$  cells/ml and incubated for 24 hours before treatments. The cells were pretreated with Ac14 extract and mangiferin at various concentration in 6-well plates for 24 hours in the absence or presence of  $\text{H}_2\text{O}_2$  for 6 hours. Treated cells were washed with cold-PBS, then collected and centrifuged at 2,400 rpm for 10 minutes. The proteins were extracted using RIPA lysis buffer at  $4^\circ\text{C}$  for 30 minutes. After incubation with lysis buffer, the protein extract was centrifuged at 12,000 rpm for 10 min. The supernatant was collected and protein concentration was measured using Bradford method. The protein extract was mixed with loading buffer and incubated at  $95^\circ\text{C}$  for 5 minutes. Proteins (20  $\mu\text{g}$ ) of each sample was loaded onto 12% sodium dodecyl sulfate polyacrylamide gel electrophoresis (SDS-PAGE) for separated each protein. The gel was transferred onto PVDF membrane. The protein on the membrane was blocked with 5% BSA in TBST buffer at room temperature for 1 hour. Blots were probed with primary antibodies (Cu/Zn-SOD, Bax, Bcl-2, HO-1, and  $\beta$ -actin) at  $4^\circ\text{C}$  for 12 hours. Next, the membrane was washed with TBST buffer, and then blotted with goat polyclonal secondary antibody with horseradish peroxidase at room temperature for 1 hour. The protein bands were detected by chemiluminescence detection reagent and

determined using chemiluminescence gel documentation. The intensities of the bands were computed by ImageJ software.

### 3.2.9 Statistical analysis

All values were presented as mean  $\pm$  SD calculated from at least three independent experiments performed in triplicate. The data was analyzed by one-way analysis of variance (ANOVA). Values of  $p < 0.05$  were determined statistically significant.





### 3.3 DNA Barcoding of selected species in genus *Aquilaria*

#### 3.3.1 Chemicals and reagents

1Kb plus DNA ladder	Vivantis, Malaysia
AccuPrep® Gel Purification Kit	Bioneer, South Korea
Agarose	Invitrogen, USA
dNTPs	Qaigen, Germany
Ethanol	Burdick & Jackson, USA
Lambda DNA- <i>Hind</i> III Digest	New England Biolabs, USA
Liquid nitrogen	
Magnesium chloride (50 mM)	Invitrogen, USA
Primer	Eurofin MWG Operon Inc., USA
Qaigen DNA plant mini kit	Qaigen, Germany
TAE buffer	Invitrogen, USA
<i>Taq</i> DNA polymerase	Invitrogen, USA
Ultrapure water	

จุฬาลงกรณ์มหาวิทยาลัย  
CHULALONGKORN UNIVERSITY

#### 3.3.2 Instruments

Autoclave	HVP-50, Hirayama, USA
Centrifuge	Hettich Lab Technology, Germany
Chemiluminescence document	GE Healthcare, UK
Gel electrophoresis	Bio-Rad, USA
Hot air oven	Binder, Germany
MAFFT software	
MEGA 6.0 software	

PCR machine	Bio-Rad, USA
Water bath	GFL, Germany
UV-Vis spectrophotometer	Spectronic Genesys 5, USA

### 3.3.3 Plant materials

Plant samples were collected from either forest or plantations in Thailand and Singapore. All of the collected plant materials, three samples of *A. crassna*, three samples of *A. malaccensis*, and two samples of *A. subintegra* were listed in table 8. In addition, *Enkleia siamensis* (Thymelaeaceae) were used as outgroup. All plant materials were authenticated by Associate Professor Dr. Nijsiri Ruangrunsi. Plant specimens were deposited at College of Public Health Sciences, Chulalongkorn University.

**Table 8** Plant materials and place of collection

Species	Place of collection	Voucher number
<i>A. crassna</i>	Bangkok, Thailand	AQWT01
	Rayong, Thailand	AQNV02
	Rayong Thailand	AQWT03
<i>A. malaccensis</i>	Pattalung, Thailand	AMNN01
	Tanglin, Singapore	AMWT02
	Tanglin, Singapore	AMWT03
<i>A. subintegra</i>	Trat, Thailand	ASTS01
	Trat, Thailand	ASTS02
<i>Enkleia siamensis</i>	Loei, Thailand	ESKL01

### 3.3.4 Genomic DNA extraction

Fresh or dried leaves of each sample were ground by mortar and pestle under liquid nitrogen to get fine powder. DNA was extracted using DNeasy<sup>®</sup> Plant Mini Kit. The method for extraction was followed the manufacturer's procedure. Total genomic DNA was checked the quality and quantity of DNA on 0.8% agarose gel electrophoresis which stained by SYBR Safe<sup>®</sup> and also visualized under UV light. A 1Kb marker was used as standard molecular size. The genomic DNA was kept at -20<sup>°</sup>C for further PCR experiments.

### 3.3.5 PCR amplification

PCR amplification of each region was performed by 50-100 ng of genomic DNA as a template in 25  $\mu$ l of PCR mixture, which comprised of 1X reaction buffer, 2.5 mM MgCl<sub>2</sub>, 0.2 mM of each dNTPs, 1 U of *Taq* DNA polymerase, and 0.4  $\mu$ M of each primer. Primer for each region are shown in Table 9.

Multiplication of interested DNA region was performed in PCR Thermocycler machine. The PCR cycling program comprises of an initial denaturation step at 95<sup>°</sup>C for 5 minutes to certify the complete separation of DNA strands, followed by strand denaturation at 95<sup>°</sup>C for 30 seconds, primer annealing at optimum temperature in each region primers for 40 seconds, and primer annealing at 72<sup>°</sup>C with suitable time for 30 cycles. Finally, the final extension step at 72<sup>°</sup>C for 10 minutes to ensure that all amplicons are completely extended then held at 4<sup>°</sup>C. PCR products were purified using AccuPrep<sup>®</sup> Gel Purification Kit. The nucleotide sequence was determined using Sanger sequencing technique. The obtained sequences were gathered for the consensus sequences. The sequence alignment was constructed using MUSCLE alignment program. Furthermore, the sequences were submitted to DDBJ nucleotide sequence databases.

**Table 9** Sequence of each primer

Region	Name of primer	Sequence (5' → 3')	Reference
ITS	ITS5_F	GGA AGT AAA AGT CGT AAC AAG G	[224]
	ITS4_R	TCC TCC GCT TAT TGA TAT GC	
<i>matK</i>	3F-KIM f	CGT ACA GTA CTT TTG TGT TTA CGA G	[225]
	1R-KIM r	ACC CAG TCC ATC TGG AAA TCT TGG TTC	
<i>trnH-psbA</i>	psbA3f	GTT ATG CAT GAA CGT AAT GCT C	[226]
	trnHf-05	CGC GCA TGG TGG ATT CAC AAT CC	[227]
<i>rbcL</i>	rbcL-aF	ATG TCA CCA CAA ACA GAG ACT AAA GC	[228]
	rbcL-aR	CTT CTG CTA CAA ATA AGA ATC GAT CTC	[229]
<i>rpoC1</i>	2F	GGC AAA GAG GGA AGA TTT CG	[230]
	4R	CCA TAA GCA TAT CTT GAG TTG G	
<i>ycf1</i>	ycf1bF	TCT CGA CGA AAA TCA GAT TGT TGT GAA T	[205]
	ycf1bR	ATACATGTCAAAGTGATGGAAAA	

### 3.3.6 Data analysis

The DNA sequences in each locus and their combinations were aligned using multiple sequence alignment software; MUSCLE. In addition, the phylogenetic tree was generated using MEGA 7.0 software. The genetic distance was calculated Kimura-2 parameter model. The maximum likelihood analysis was performed using general time reversible model for substitution model and gamma distributed with invariant sites (G+I) pattern for rates among the sites. Furthermore, Bootstrap (1000 replications) method was analyzed to estimate the confidence of the topology of consensus tree.

## CHAPTER IV

### RESULTS

This study was divided into three parts. First of all, the standardization of *A. crassna* leaves was performed according to WHO guidance and also validated the TLC-densitometric method and TLC-image analysis for quantifying the amount of mangiferin in the *A. crassna* leaf extracts. Next, the ethanolic extract of *A. crassna* was determined the biological activities: alpha-glucosidase inhibitory activity, antioxidation activity, cytotoxicity testing and also intracellular antioxidation testing. Finally, the selected plants in genus *Aquilaria* were subjected to determine the sequences in interesting genes for phylogenetic analysis.

#### 4.1 Pharmacognostic specifications of *A. crassna* leaves

##### 4.1.1 Plant materials

The *A. crassna* leaves were collected from several sources and were authenticated by Associate Professor Dr. Nijisiri Ruandrungsi. Fifteen samples were mentioned about the plant location (Table 10).

**Table 10** The samples of *A. crassna* leaves used in this study.

No.	Voucher no.	Locations
Ac01	Ac01-WT0914	Ubol Ratchathani province
Ac02	Ac02-NV1014	Rayong province
Ac03	Ac03-NV1014	Chon Buri province
Ac04	Ac04-WT1014	Phetchabun province
Ac05	Ac05-WT1014	Lampang province
Ac06	Ac06-WT1014	Nakhorn Nayok province
Ac07	Ac07-WT1014	Prachin Buri province
Ac08	Ac08-WT1014	Roi Et province
Ac09	Ac09-AK1014	Chiang Mai province
Ac10	Ac10-NT1014	Nan province
Ac11	Ac11-NT1014	Nan province
Ac12	Ac12-NT1014	Nan province
Ac13	Ac13-NT1014	Nan province
Ac14	Ac14-NT1014	Nan province
Ac15	Ac15-TS1114	Trat province

#### 4.1.2 Macroscopic and microscopic characteristics of *A. crassna* leaves

##### Macroscopic investigation

The morphological evaluation for identification of *A. crassna* was reported. *A. crassna* tree can be grown up to 25-30 m tall. Its bark is brownish grey. Leaves are approximately 7.0-12.0 cm long and 2.5-5.0 cm wide with narrow elliptical or lanceolate shape (Figure 26.A). The color of dried leaf crude drug was green to brownish green. The size was 5.0-10.0 cm long and 1.5-3.5 cm wide. The odor was pleasing scent with slightly sweet taste (Figure 26.B). The macroscopical characters were shown in Figure 26.

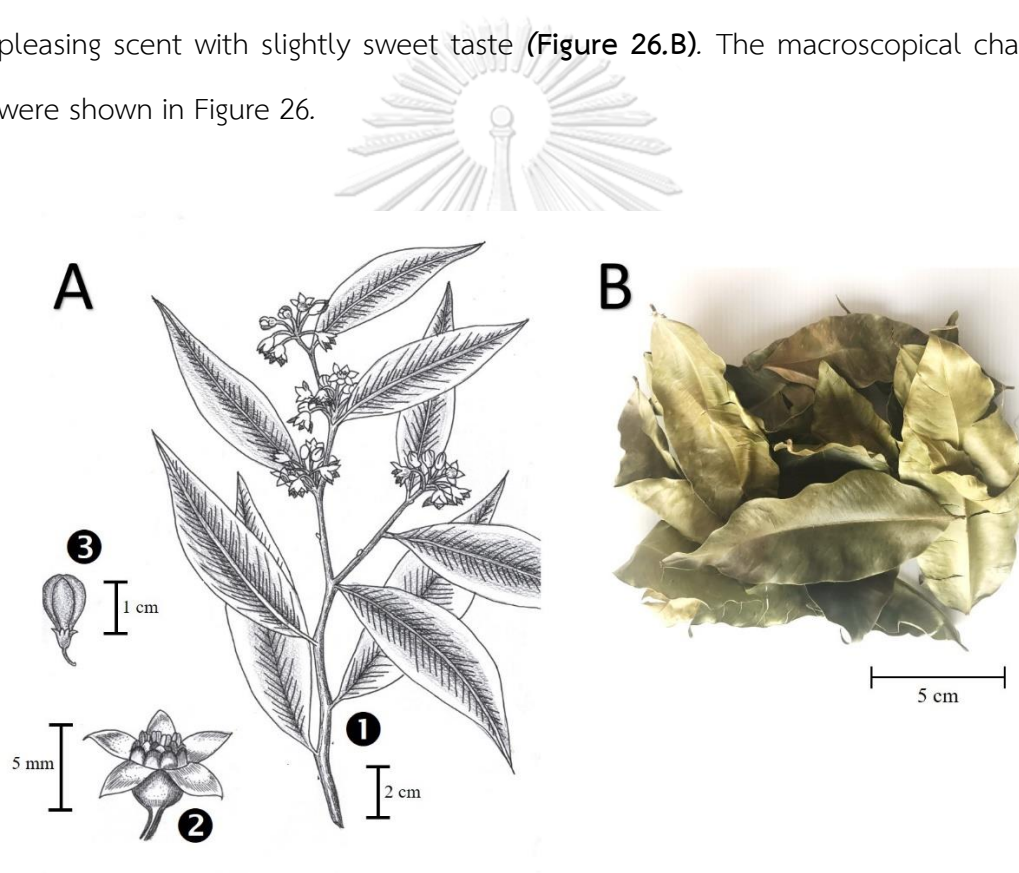


Figure 26 Macroscopic characteristics of *A. crassna*

A) *Aquilaria crassna*; ❶ a part of branch, ❷ flower, ❸ fruit, and B) Crude drug (leaves)

### Microscopic investigation

Microscopic characteristics of *A. crassna* leaves were determined in the transverse section of midrib and lamina, the upper layer of the leaves (upper epidermis), the lower layer of the leaves (lower epidermis), the constant values of leaves, and the powdered drug.

The transverse section through midrib showed group of collenchymas scattered in parenchyma layers underneath the epidermis, collateral vascular bundles. In addition, the transverse section of the lamina displayed the upper epidermis layer, mesophyll layer, group of vascular bundles, and the lower epidermis. The upper epidermis had a single layer of cuticularized rectangular cells. Mesophyll was consisted of 1-2 layers of palisade parenchyma, several layers of spongy parenchyma, and small vascular bundle. Lower epidermis was a single layer of rectangular cell (Figure 27).

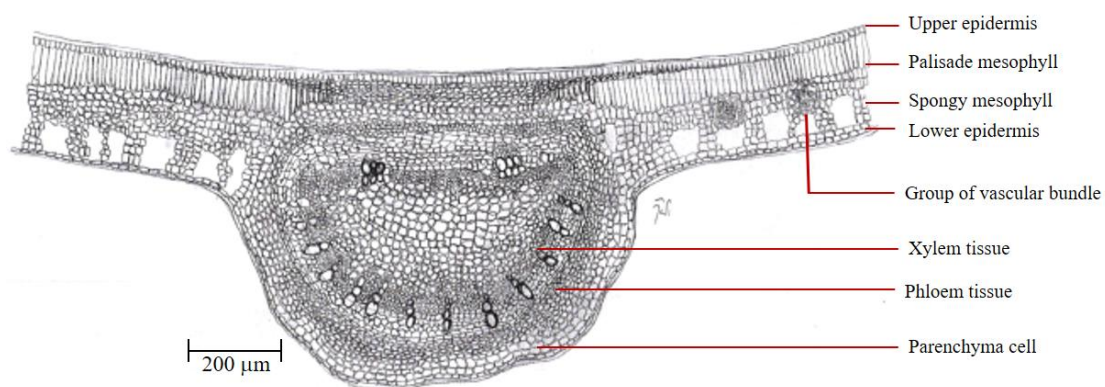


**Figure 27** Transverse section of midrib and lamina of *A. crassna* leaves



The upper epidermal cells were slightly thick-walled polygonal cells (Figure 28.A). The lower epidermal cells were irregular-shape cell in various size and the anomocytic stomata was only found in this layer (Figure 28.B).

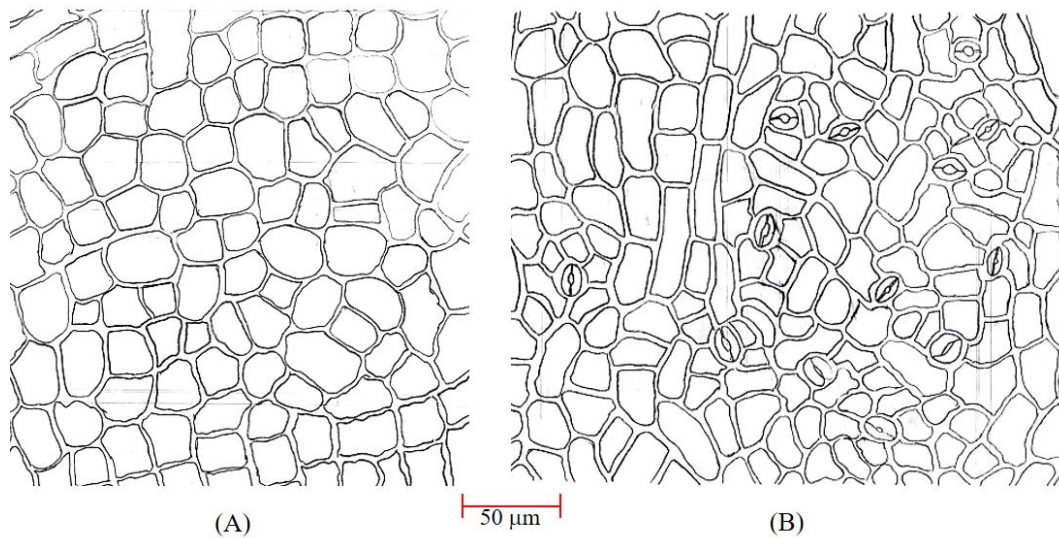


**Figure 28** Microscopic characteristics of the surface views of *A. crassna* lamina.

A) upper epidermis, and B) lower epidermis with anomocytic stomata

The powdered drugs of *A. crassna* are pale green color. The odor is slightly characteristic with pleasing scent. The taste is slightly sweet. The microscopic characteristics of powdered drugs of *A. crassna* (Figure 29) were as follows:

- 1) The fragment of lower epidermis in surface view, showing anomocytic stomata.
- 2) The fragment of upper epidermal cells, which were polygonal in surface views.
- 3) The fragment of the lamina in sectional view, showing the thick, striated cuticle (particularly over the upper epidermis) and two to four rows of palisade cell.
- 4) The fragment of lignified fibrovascular tissues, group of fiber and vessel, reticulate vessel, spiral vessel.

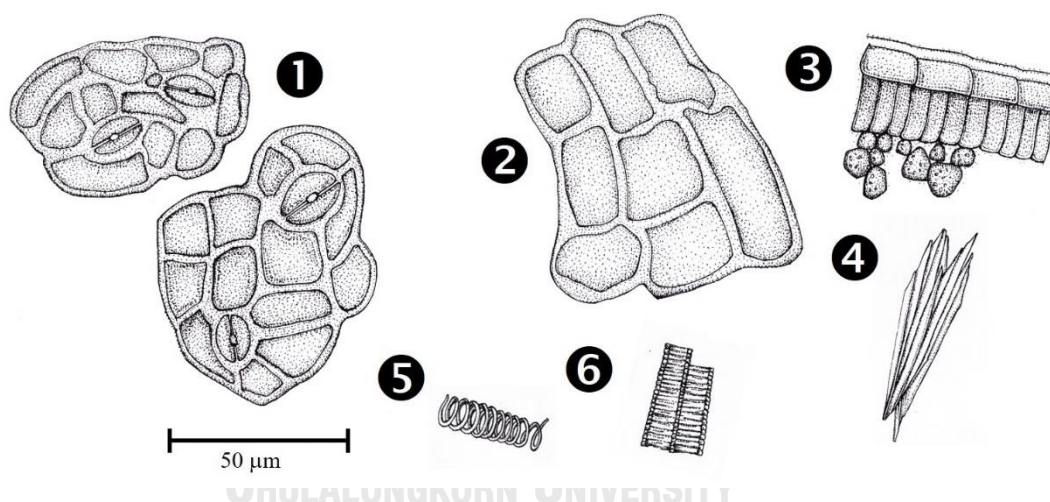


**Figure 29** Microscopic characteristics of powdered *A. crassna*

- 1) lower epidermis in surface view showing anomocytic stomata;
- 2) upper epidermis in surface view;
- 3) part of the lamina in sectional view, showing the upper epidermis, palisade mesophyll and part of spongy mesophyll;
- 4) group of lignified fibers;
- 5) part of spiral vessel;
- 6) part of reticulate vessel

The microscopic leaf constant values of *A. crassna* leaves, which comprised of stomatal number, stomatal index, palisade ratio, and epidermal cell area, were summarized in Table 11.

**Table 11** The microscopic leaf measurement values of *A. crassna* leaves

Parameter	Value (mean $\pm$ SD)*	Min – Max value
Stomatal number	147.60 $\pm$ 13.83 cells/mm <sup>2</sup>	128 – 172 cells/mm <sup>2</sup>
Stomatal index	7.70 $\pm$ 0.38	7.13 – 8.37
Palisade ratio	5.28 $\pm$ 0.49	4.50 – 6.25
Epidermal cell area	814.66 $\pm$ 29.62 $\mu$ m <sup>2</sup>	755.29 – 880.28 $\mu$ m <sup>2</sup>

\* calculated on 90 fields

#### 4.1.3 TLC fingerprinting

The result of one-dimensional TLC fingerprint of ethanolic extract of *A. crassna* leaves were shown in Figure 30. The visualized spot on TLC plate was detected and the R<sub>f</sub> value of each spot was tabulated in Table 12.

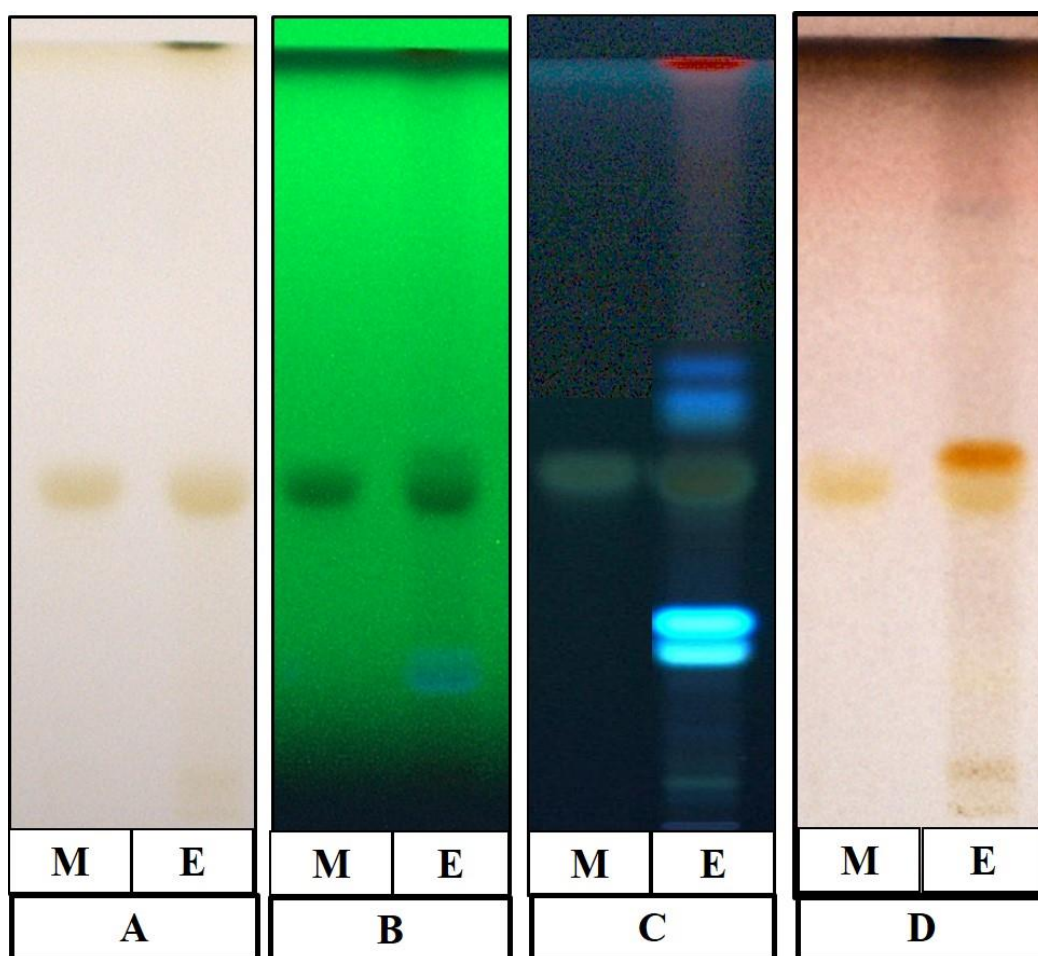


**Figure 30** Thin layer chromatographic fingerprinting of a ethanolic extract of dried *A. crassna* leaves (E) and mangiferin at concentration 0.4 mg/ml (M).

- A) appearance under visible light;
- B) under 254-nm UV light;
- C) under 365-nm UV light, and
- D) detection with anisaldehyde-sulphuric acid and heat

**Table 12**  $R_f$  values of components in the ethanolic extract of *A. crassna* leaves which used ethyl acetate: water: formic acid, 34:6:4 v/v/v respectively as a solvent system

$R_f$	Detecting agents			
	Visible light	UV, 254 nm	UV, 365 nm	Anisaldehyde-sulphuric acid TS
0.05	Brown	-	-	Brown
0.15	-	Blue	-	-
0.18	-	-	Blue	Yellow
0.23	-	-	Blue	-
0.42	Brownish yellow	Quenching	-	Brownish yellow
0.47	-	Quenching	-	Orange red
0.52	-	-	Blue	-
0.62	-	-	Blue	-
0.75	-	-	-	Orange
0.80	-	-	-	Blue purple
0.95	-	-	-	Navy blue
1.00	Green	Quenching	Red	Green

#### 4.1.4 Physico-chemical parameter

The physicochemical constant of *A. crassna* leaf crude drugs were shown in Table 13. Raw data was tabulated in Appendix A.

**Table 13** Physicochemical values (% w/w) of *A. crassna* leaves

Parameter	Content (% by weight)	
	grand mean $\pm$ pooled SD	Min - Max
Loss on drying	8.62 $\pm$ 0.13	7.20 – 10.41
Water content	8.16 $\pm$ 0.14	7.17 – 10.08
Total ash	6.82 $\pm$ 0.09	5.07 – 11.24
Acid-insoluble ash	1.49 $\pm$ 0.03	0.36 – 3.64
Ethanol extractive value	9.07 $\pm$ 0.40	4.57 – 16.19
Water extractive value	16.94 $\pm$ 0.22	10.73 – 22.06

#### 4.1.5 Mangiferin content in ethanolic extract of *A. crassna* leaves

##### 4.1.5.1 Method validation for quantified mangiferin

The method validation for this study was performed following ICH guidance, which comprised specificity, linearity, accuracy, precision, detection limit, quantification limit, and robustness. The results of validated parameters of densitometry method and image analysis method were summarized in Table 14.

**Table 14** The validity parameter of TLC-densitometry and image analysis method

Parameter	TLC-densitometry method	Image analysis method
Specificity		
Peak purity	$r > 0.9950$	-
Peak identity	$r > 0.9995$	-
Linearity Range (ng/spot)	450-1,950	450-1,950
Calibration equation	$y = 8.8423x + 3873.7$	$y = 17.3402x + 1409.2$
Coefficient of determination	$R^2 = 0.9992$	$R^2 = 0.9995$
Accuracy (% Recovery)	99.09-104.97	100.26-102.52
Repeatability (%RSD)	1.52-3.35	0.61-3.48
Intermediate precision (%RSD)	1.26-3.81	2.08-4.03
Limit of detection (ng/spot)	119.11	131.38
Limit of quantitation (ng/spot)	360.93	398.11
Robustness (%RSD)	1.80-2.57	2.39-2.59

#### 4.1.5.1.1 Method validation for TLC-densitometry

### Specificity

Specificity was determined in terms of peak identity and peak purity. The identities of the chromatogram bands of mangiferin in the sample were compared by overlaying the absorption spectra with standard mangiferin (Figure 31). Moreover, peak purity was assessed by comparing the spectra of standard and samples at three different levels; peak start, peak apex and peak end positions. Considerable correlations,  $r$  (start, middle) and  $r$  (middle, end)  $> 0.9950$  were investigated by comparing the spectra of mangiferin standard and corresponding peaks in samples.

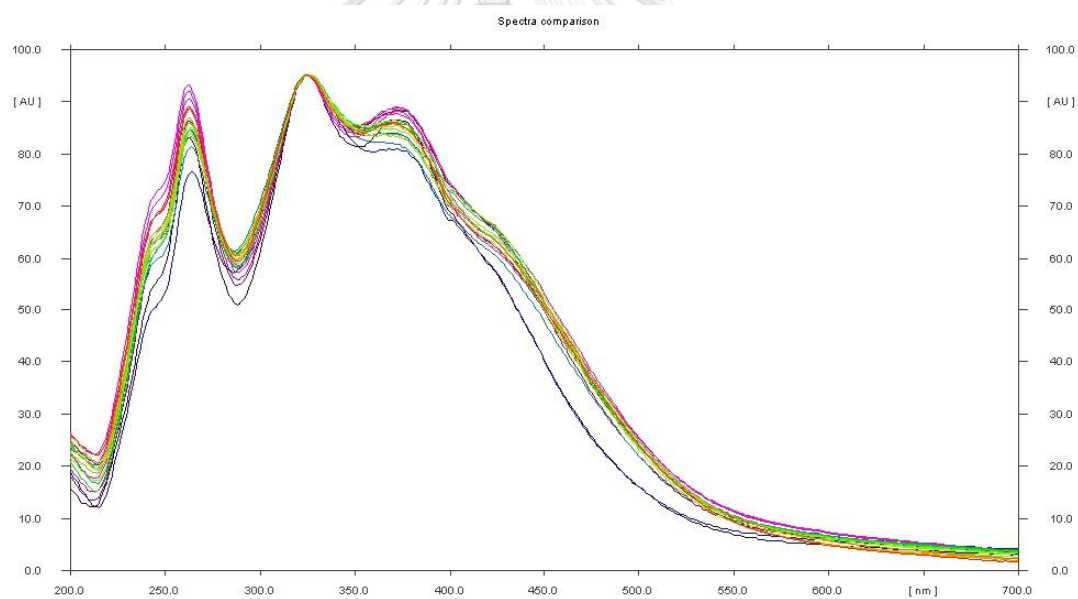


**Figure 31** Absorbance spectra of mangiferin among standard and the *A. crassna* leaf extracts



### Calibration curve

The calibration curve of mangiferin were linear at the range of 450 to 1,950 ng/spot. The equation was  $y = 8.8423x + 3873.7$  and the coefficient of determination ( $R^2$ ) of the curve was 0.9992 (Figure 32).

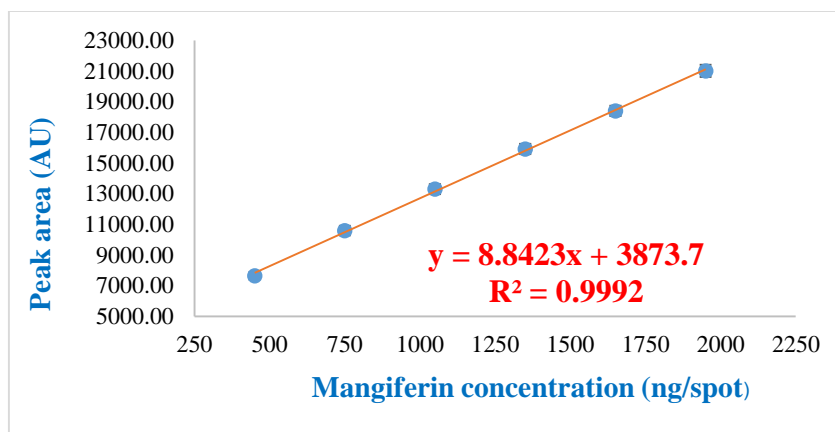


Figure 32 Calibration curve of mangiferin standard by TLC-densitometry

### Accuracy

The accuracy was determined by spiking mangiferin standard (0.15, 0.60, and 1.05  $\mu\text{g}/\text{spot}$ ). The percentage of recovery were judged for accuracy evaluation. The recovery of spiked mangiferin into sample at three different concentrations were between  $99.09 \pm 0.64$  to  $104.97 \pm 0.45\%$  (Table 15).

Table 15 Recovery of mangiferin by TLC-densitometry

Mangiferin added ( $\mu\text{g}/\text{spot}$ )	Mangiferin founded ( $\mu\text{g}/\text{spot}$ )	% recovery
0.00	0.46	-
0.15	0.61	$99.09 \pm 0.64$
0.60	1.06	$104.97 \pm 0.45$
1.05	1.51	$101.67 \pm 2.27$

## Precision

The intra-day precision and inter-day precision were accomplished on sample with different concentrations of mangiferin for three times in the same day and three different days of experiments, respectively. The %RSD was described the precision of the experiments. The %RSD of intra-day precision was ranged from 1.52 – 3.35%, whereas the %RSD of inter-day precision was ranged from 1.26 – 3.81%.

**Table 16** Intra-day and inter-day precision of mangiferin by TLC-densitometry

Intra-day precision		Inter-day precision	
Mangiferin (ng/spot)	%RSD	Mangiferin (ng/spot)	%RSD
0.70	2.81	0.70	3.81
1.20	3.35	1.20	1.53
1.70	1.52	1.70	1.26

## Limit of detection (LOD) and limit of quantitation (LOQ)

LOD and LOQ were estimated based upon the standard deviation of y-intercept of the regression line and the slope of the calibration curve. LOD and LOQ were calculated to be 119.11 ng/spot, and 360.93 ng/spot, respectively.

## Robustness

For robustness evaluation, the relative standard deviation of peak areas was calculated for little changing in ratio of the mobile phase composition. The %RSD of robustness was less than 3% for all tests.

**Table 17** Robustness of mangiferin quantitative analysis by TLC-densitometry method

Mobile phase ratio			Mangiferin peak area (AU)		
EtOAc	water	Formic acid	Mangiferin standard 0.35 mg/ml	Ac02	Ac13
34.0	6.0	4.0	14,304.5	16,356.7	14,082.6
33.9	6.0	4.0	14,176.0	16,010.8	13,912.4
34.1	6.0	4.0	14,138.3	16,057.0	13,932.8
34.0	5.9	4.0	14,904.5	15,430.4	14,575.0
34.0	6.1	4.0	14,480.3	15,663.5	13,905.5
34.0	6.0	3.9	14,400.2	16,213.9	14,535.9
34.0	6.0	4.1	14,270.6	15,277.9	13,921.4
Mean			14,382.1	15,858.6	14,123.6
SD			259.2	407.3	301.4
%RSD			1.80	2.57	2.13

#### 4.1.5.1.1 Method validation for TLC image analysis

##### Calibration curve

The calibration curve of mangiferin were linear at the range of 450 to 1,950 ng/spot. The equation was  $y = 17.3402x + 1409.2$  and the coefficient of determination ( $R^2$ ) of the curve was 0.9995 (Figure 33)

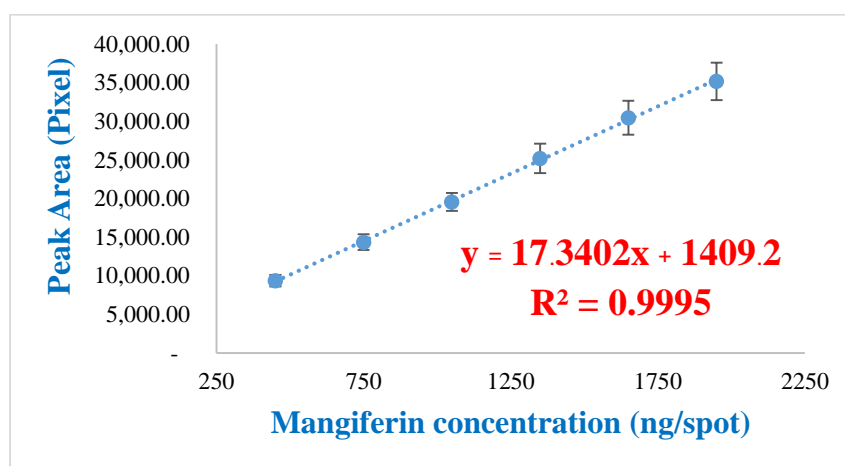


**Figure 33** Calibration curve of mangiferin standard by TLC image analysis method

##### Accuracy

The accuracy was determined by spiking mangiferin standard (0.15, 0.60, and 1.05 ng/spot). The percentage of recovery were judged for accuracy evaluation. The recovery of spiked mangiferin into sample at three different concentrations were between  $100.26 \pm 1.88$  to  $102.52 \pm 1.06\%$  (Table 18).

**Table 18** Recovery of mangiferin by TLC image analysis

Mangiferin added ( $\mu\text{g}/\text{spot}$ )	Mangiferin founded ( $\mu\text{g}/\text{spot}$ )	% recovery
0.00	0.46	-
0.15	0.61	$100.26 \pm 1.88$
0.60	1.06	$100.91 \pm 0.52$
1.05	1.51	$102.52 \pm 1.06$

## Precision

The intra-day precision and inter-day precision were accomplished on sample with different concentrations of mangiferin for three times in the same day and three different days of experiments, respectively. The %RSD was described the precision of the experiments. The %RSD of intra-day precision was ranged from 0.61 – 3.48%, whereas the %RSD of inter-day precision was ranged from 2.08 – 4.03%.

**Table 19** Intra-day precision of mangiferin by TLC image analysis

Intra-day precision		Inter-day precision	
Mangiferin (ng/spot)	%RSD	Mangiferin (ng/spot)	%RSD
0.70	3.48	0.70	4.03
1.20	3.35	1.20	2.38
1.70	0.61	1.70	2.08

## Limit of detection (LOD) and limit of quantitation (LOQ)

LOD and LOQ were estimated based upon the standard deviation of y-intercept of the regression line and the slope of the calibration curve. LOD and LOQ were calculated to be 131.38 ng/spot, and 398.11 ng/spot, respectively.

## Robustness

For robustness evaluation, the relative standard deviation of peak areas was calculated for little changing in ratio of the mobile phase composition. The %RSD of robustness was less than 3% for all tests.

**Table 20** Robustness of mangiferin quantitative analysis by TLC image analysis method

Mobile phase ratio			Mangiferin peak area		
EtOAc	water	Formic acid	Mangiferin standard 0.35 mg/ml	Ac02	Ac13
34.0	6.0	4.0	26,896.620	31,348.355	25,794.887
33.9	6.0	4.0	25,260.078	29,754.251	24,914.132
34.1	6.0	4.0	26,635.054	30,651.224	25,489.904
34.0	5.9	4.0	25,223.421	30,955.729	26,262.395
34.0	6.1	4.0	26,498.071	31,128.204	26,614.695
34.0	6.0	3.9	25,672.169	31,773.813	26,202.997
34.0	6.0	4.1	25,933.361	29,894.268	25,201.385
Mean			26,061.968	30,786.549	25782.914
SD			672.775	743.391	616.061
%RSD			2.59	2.41	2.39

#### 4.1.5.2 Quantitative analysis of mangiferin

The results of extractive yields were tabulated in Table 21. The yield of *A. crassna* leaf ethanolic extract was  $14.53 \pm 2.59$  % of dried weight. The mangiferin content of ethanolic extract was quantified via TLC-densitometry compared with TLC image analysis. The silica GF<sub>254</sub> TLC plate was used as stationary phase, while mobile phase was composed of ethyl acetate: water: formic acid, 34:6:4 v/v/v respectively. Densitogram of *A. crassna* ethanolic extract under UV 254 nm was shown in Figure 34. The R<sub>f</sub> value of mangiferin band was approximately as 0.42-0.48. The densitometric scanning was recorded at  $\lambda = 254$  nm. The amounts of mangiferin in *A. crassna* ethanolic extract which determined using TLC-densitometry and TLC-image analysis were found to be  $1.2992 \pm 0.5980$  and  $1.3036 \pm 0.5874$  % of dried weight, respectively. Furthermore, the mangiferin contents by these two methods were not statistically significant different ( $P > 0.05$ ).

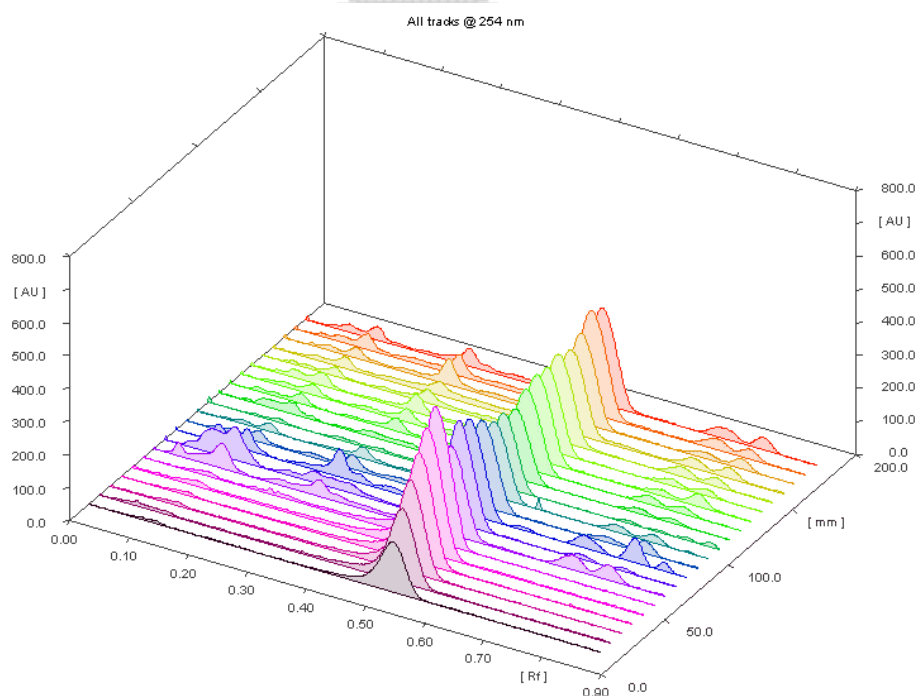


**Figure 34** 3D-TLC densitometric chromatogram of mangiferin standard and the ethanolic extracts of *A. crassna* leaves

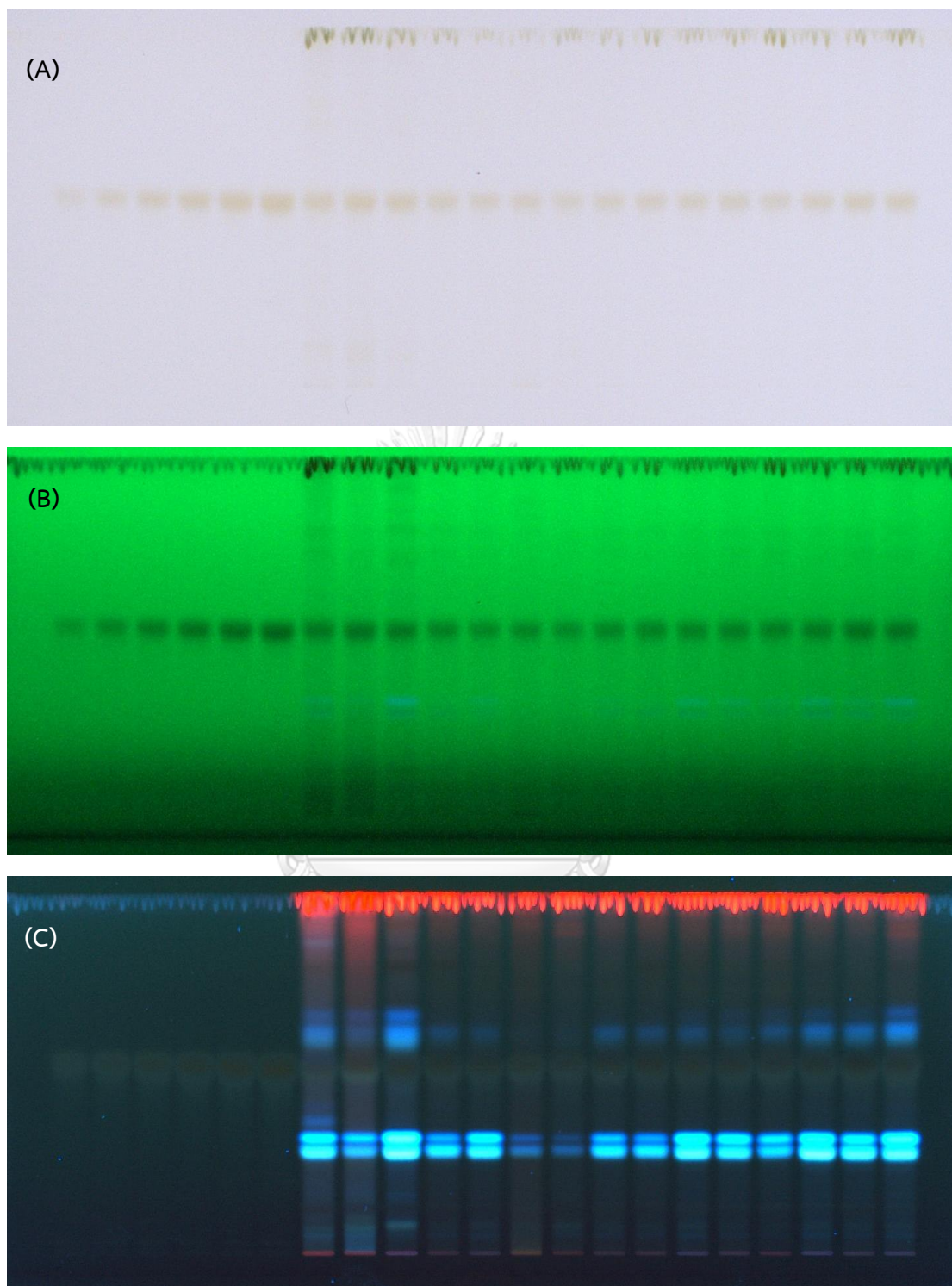


**Figure 35** The developed silica gel-TLC plate by the mobile phase; ethyl acetate: water: acetic acid (34:6:4 v/v/v) visual under visible light (A), UV 254 nm (B), and UV 366 nm; mangiferin standard (tract 1 – 6) and *A. crassna* leaf extracts from 15 different locations (tract 7 – 21)





**Figure 36** The TLC image subtract background from UV 254 nm picture using imageJ software; mangiferin standard (tract 1 – 6) and *A. crassna* leaf extracts from 15 different locations (tract 7 – 21)

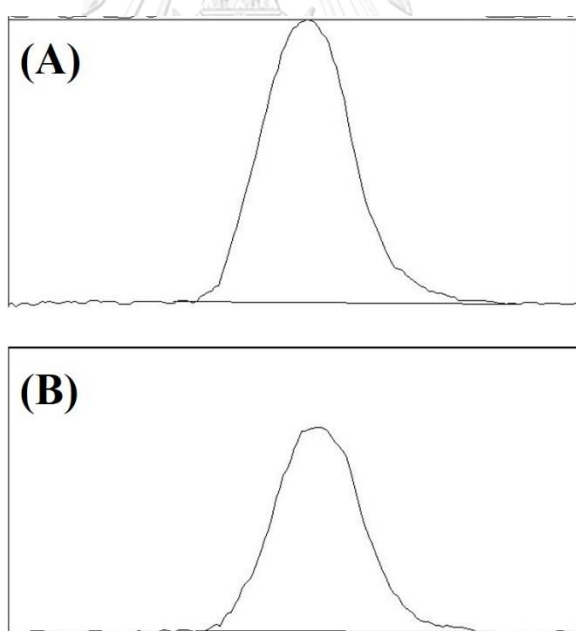


**Figure 37** TLC image analysis chromatogram by imageJ software of mangiferin standard at concentration of 1950 ng/spot (A), and ethanolic extract of sample Ac11 (B)

**Table 21** Extraction yield of *A. crassna* leaves and the amount of mangiferin in ethanolic extract of *A. crassna* leaves by TLC-densitometry and TLC image analysis method

Source	Yields of <i>A. crassna</i> extract (% w/w)	Mangiferin content in <i>A. crassna</i> leaf (g/100g)	
		TLC-densitometric method	TLC image analysis method
Ac01	10.4998	0.3406	0.3406
Ac02	16.6677	0.6612	0.6688
Ac03	14.6031	0.2547	0.2646
Ac04	17.3487	1.8014	1.8293
Ac05	16.4422	1.1867	1.2447
Ac06	14.5807	1.2142	1.2452
Ac07	10.5746	0.7100	0.7320
Ac08	13.1148	1.2754	1.3158
Ac09	20.8008	2.0701	2.0584
Ac10	13.4221	1.1308	1.1512
Ac11	13.5249	1.5694	1.4973
Ac12	14.6087	1.5496	1.5002
Ac13	14.8430	1.7892	1.8208
Ac14	13.3348	2.1662	2.1130
Ac15	13.6461	1.7681	1.7721
Mean ± SD		1.2992 ± 0.5980	1.3036 ± 0.5874

## 4.2 Biological activities of *A. crassna* leaf extract and its metabolite, mangiferin

This study used the ethanolic extract of *A. crassna* leaves from Ac14 and its active metabolites, mangiferin for determining the interesting biological activities. The Ac14 was chosen for determining the biological activities of *A. crassna* leaves because this sample had the highest content of mangiferin when compared to another samples.

### 4.2.1 Alpha-glucosidase inhibitory activity

Ac14 ethanolic extract, mangiferin and acarbose (positive control) exhibited the inhibitory effect of yeast alpha-glucosidase activity in the concentration-response manner (Figure 38). The IC<sub>50</sub> values of Ac14 extract, mangiferin, and acarbose were  $0.184 \pm 0.003$ ,  $0.571 \pm 0.004$ , and  $17.395 \pm 0.019$  mg/ml, respectively.

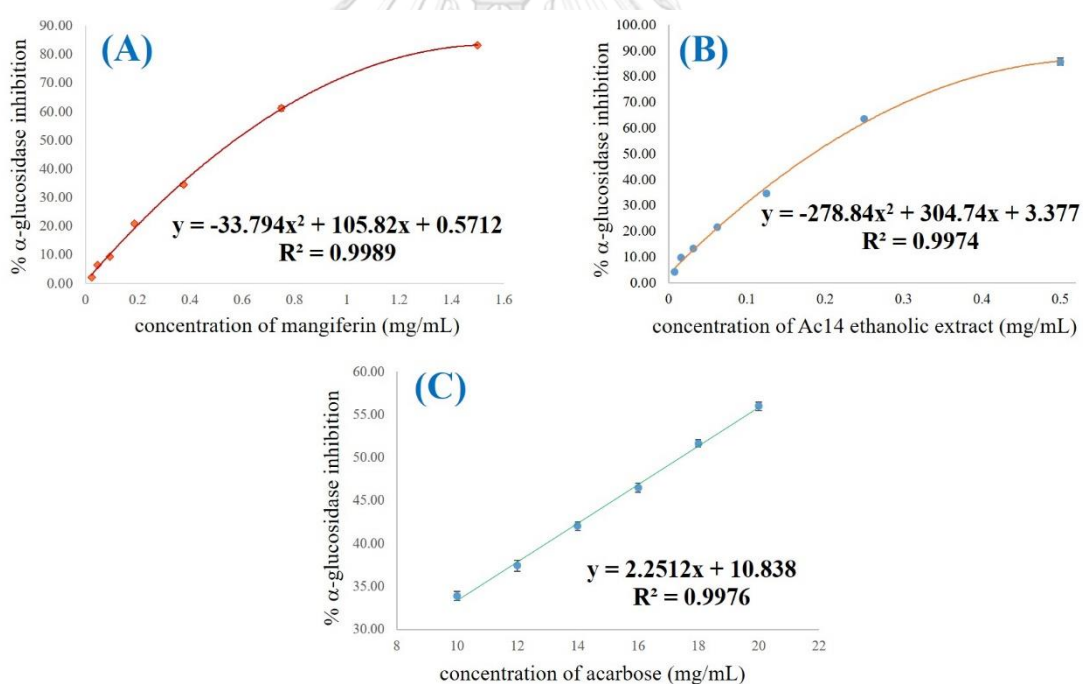


**Figure 38** Dose-response curve of yeast alpha glucosidase inhibitions of mangiferin (A) , Ac14 ethanolic extract (B), and acarbose (C) at various concentrations

## 4.2.2 Antioxidant activities

### 4.2.2.1 DPPH scavenging activity

The DPPH scavenging results of mangiferin and Ac14 ethanolic extract were displayed in Figure 39 as compared with quercetin. From the results,  $IC_{50}$  values of mangiferin, Ac14 extract, and quercetin were calculated from the dose-response curve and found to be  $0.64 \pm 0.01$ ,  $21.54 \pm 0.17$ , and  $3.46 \pm 0.09$   $\mu\text{g/ml}$ , respectively.

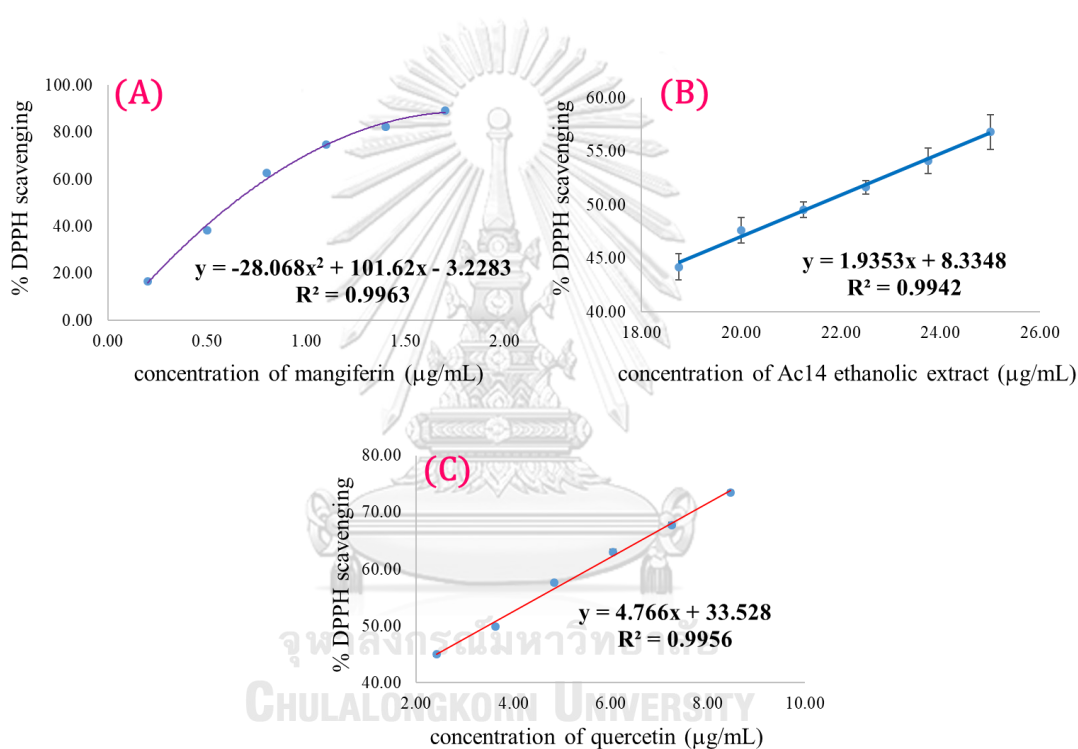


**Figure 39** Dose-response curve of DPPH scavenging activity of mangiferin (A), Ac14 ethanolic extract (B), and quercetin (C) at various concentrations

#### 4.2.2.2 Nitric oxide radical (NO<sup>•</sup>) scavenging activity

The mangiferin and Ac14 ethanolic extract were also displayed a dose-dependent elevation in NO<sup>•</sup> scavenging activity (Figure 40). The percentage inhibition of mangiferin and Ac14 ethanolic extract showed the IC<sub>50</sub> values at 40.55 ± 0.17 and 79.13 ± 0.74 μg/ml, respectively, while the IC<sub>50</sub> value of quercetin was 13.17 ± 0.30 μg/ml.

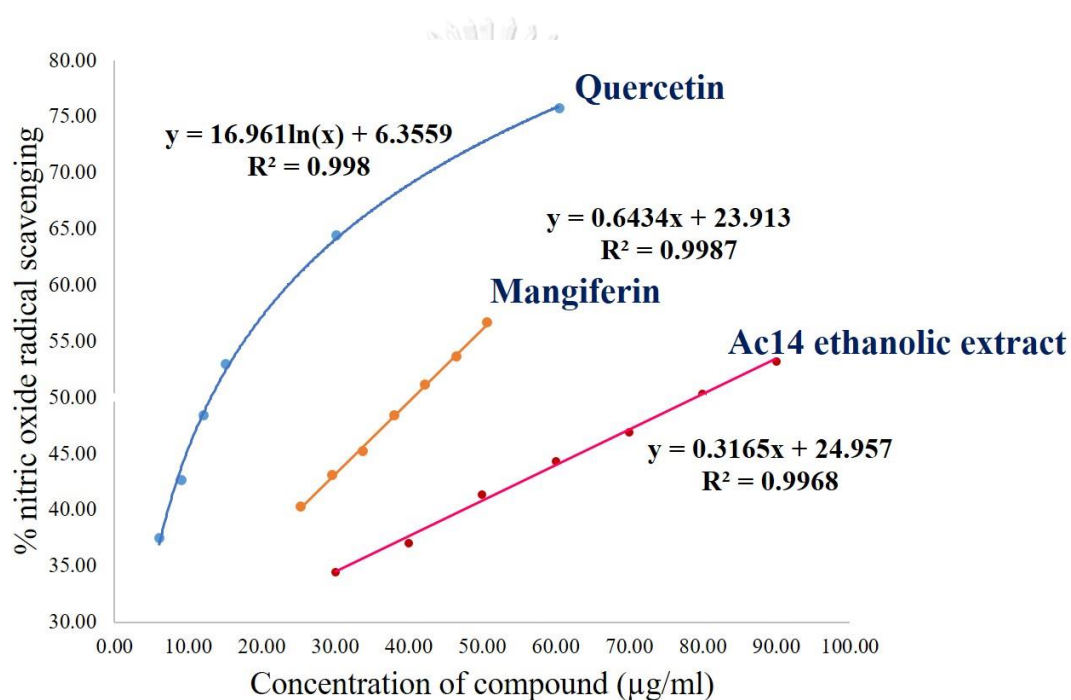


**Figure 40** Dose-response curve of nitric oxide radical scavenging activity of mangiferin, Ac14 ethanolic extract, and quercetin at various concentrations

#### 4.2.2.3 Superoxide radical scavenging activity

The activity of superoxide radical scavenging of mangiferin and Ac14 ethanolic extract was particularly increased with the augmented concentration (Figure 41). According to the results,  $IC_{50}$  values of mangiferin, Ac14 ethanolic extract and quercetin were calculated and found to be  $105.49 \pm 1.28$ ,  $278.12 \pm 4.29$ , and  $16.91 \pm 0.19 \mu\text{g/ml}$ , respectively.

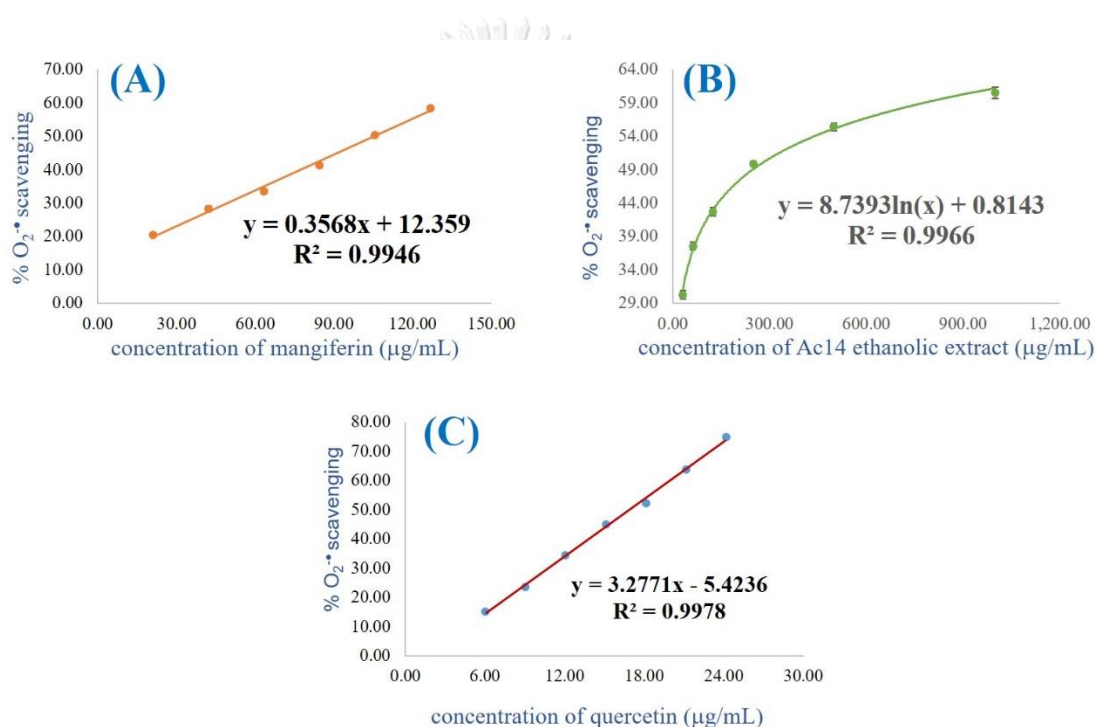


**Figure 41** Dose-response curve of superoxide radical scavenging activity of mangiferin (A), Ac14 ethanolic extract (B), and quercetin (C) at various concentrations

The  $IC_{50}$  which acted as antioxidant activities of Ac14 ethanolic extract; its metabolite, mangiferin, and quercetin (positive control) were summarized in [Table 22](#).

**Table 22** The antioxidant activities of Ac14 ethanolic extract and mangiferin. Quercetin was used as a positive control

<i>In vitro</i> antioxidation assay	$IC_{50}$ ( $\mu\text{g/ml}$ ) *		
	Ac14 extract	Mangiferin	Quercetin
DPPH scavenging	21.54 $\pm$ 0.17	0.64 $\pm$ 0.01	3.46 $\pm$ 0.09
nitric oxide radical scavenging	79.13 $\pm$ 0.74	40.55 $\pm$ 0.17	13.17 $\pm$ 0.30
Superoxide radical scavenging	278.12 $\pm$ 4.29	105.49 $\pm$ 1.28	16.91 $\pm$ 0.19

\* Mean  $\pm$  standard deviation (n = 3)

#### 4.2.2.4 Ferric reducing antioxidant power (FRAP)

The ferric ion reducing antioxidant power of the Ac14 ethanolic extract and mangiferin were evaluated in terms of its capability to reduce TPTZ-Fe<sup>3+</sup> to TPTZ-Fe<sup>2+</sup>. The FRAP values of mangiferin and Ac14 ethanolic extract, which were calculated from ferrous sulfate calibration curve ( $R^2 = 0.9985$ ), were found to be 11.82  $\mu\text{M Fe(II)}/\text{mg}$  and 2.52  $\mu\text{M Fe(II)}/\text{mg}$ , respectively.

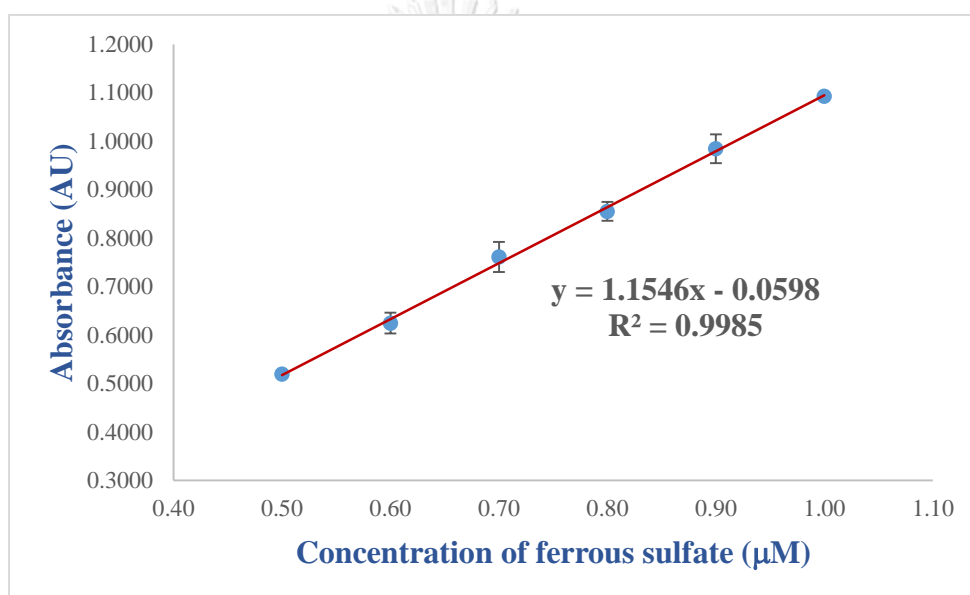


**Figure 42** Standard curve of ferrous sulfate for determining the ferric reducing antioxidant power



#### 4.2.2.5 Total phenolic content (TPC)

The total phenolic content of the Ac14 ethanolic extract, calculated based on the calibration curve of gallic acid ( $R^2 = 0.999$ ), was  $120.18 \pm 0.50$  mg gallic acid equivalents/g (GAE).

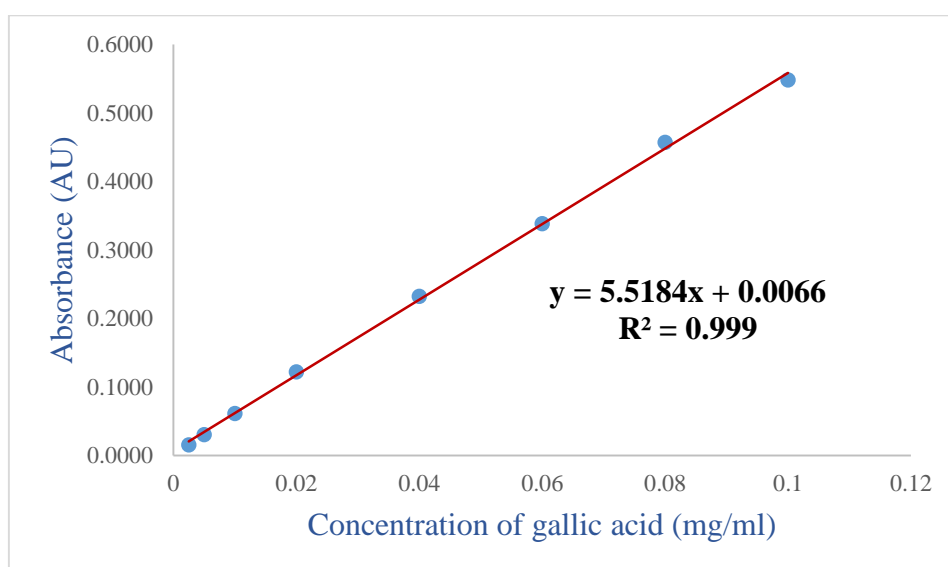


Figure 43 Standard curve of gallic acid for determining the total phenolic content

#### 4.2.3 Cytotoxic activity against cancer cell lines

The cytotoxicities on human cancer cell lines of mangiferin and Ac14 ethanolic extract, as compared to doxorubicin, were demonstrated with concentration-dependent (Figure 44). Ac14 ethanolic extract showed significant toxicity on all tested cancer cells and could be extrapolated to determine the  $IC_{50}$  value. Mangiferin showed cytotoxic potential, but the percentage of cell viability at the highest concentration (100  $\mu\text{g/ml}$ ) was 62.93 % for MDA-231, 67.85 % for HepG2, and 63.52 % for HT-29.  $IC_{50}$  values for cytotoxic activities of Ac14 ethanolic extract, mangiferin, and doxorubicin were tabulated in Table 23.

**Table 23** Cytotoxic activities of Ac14 ethanolic extract, mangiferin, and doxorubicin against cancer cell lines

	$IC_{50}$ ( $\mu\text{g/ml}$ )*		
	MDA-231 (Human breast cancer)	HepG2 (Human hepatocellular carcinoma)	HT-29 (Human colorectal adenocarcinoma)
Ac14 ethanolic extract	33.89 $\pm$ 0.50	53.63 $\pm$ 1.54	51.74 $\pm$ 1.42
Mangiferin	>100	>100	>100
Doxorubicin	0.12 $\pm$ 0.01	2.66 $\pm$ 0.27	0.39 $\pm$ 0.02

\* Mean  $\pm$  standard deviation (n = 3)

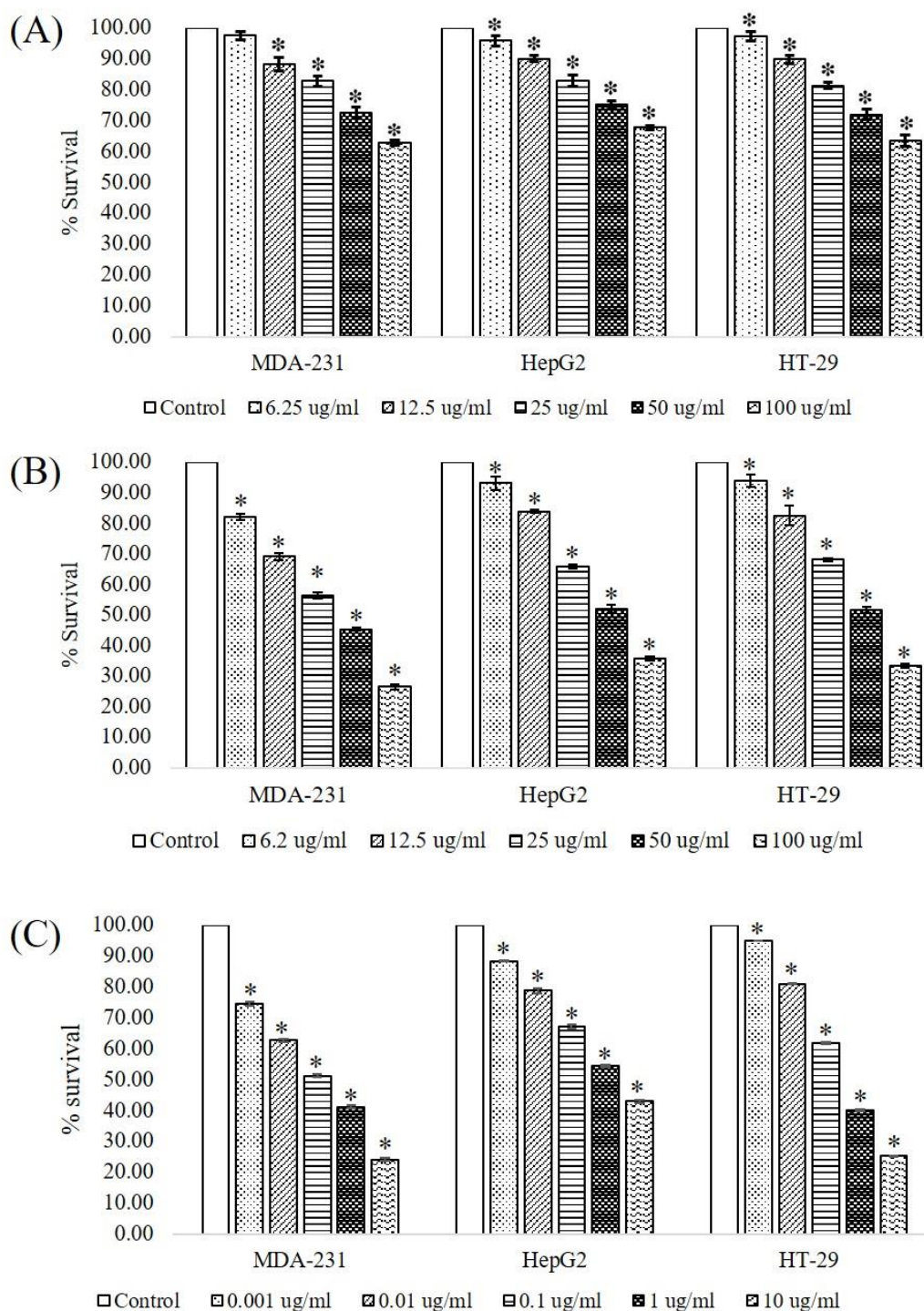


**Figure 44** Cytotoxic activity of mangiferin (A), Ac14 ethanolic extract (B), and doxorubicin (C). Results are expressed as mean  $\pm$  SD, based on at least three independent experiments performed in triplicate.

\*  $P < 0.05$  as compared to vehicle control, Dunnett's test.

#### 4.2.4 Cytotoxic effect on a EA.hy926 cells line and intracellular ROS determination

##### 4.2.4.1 Effect of ethanolic extract of *Aquilaria crassna* leaves and its metabolite, mangiferin on cell viability and intracellular ROS

The ethanolic extract of Ac14 and mangiferin were subjected to determine the cytotoxic effect on EA.hy926 cell by MTT assay. The Ac14 extract decreased the cell viability in a concentration-dependent manner ( $R^2 = 0.9932$ ) with the  $IC_{50}$  value of  $57.39 \pm 4.34 \mu\text{g/ml}$  (Figure 45A). Mangiferin influenced to cell viability in a concentration-dependent manner (Figure 45B), but it did not reach the  $IC_{50}$  value at the highest concentration (200  $\mu\text{g/ml}$ ;  $86.30 \pm 3.29 \%$ ).

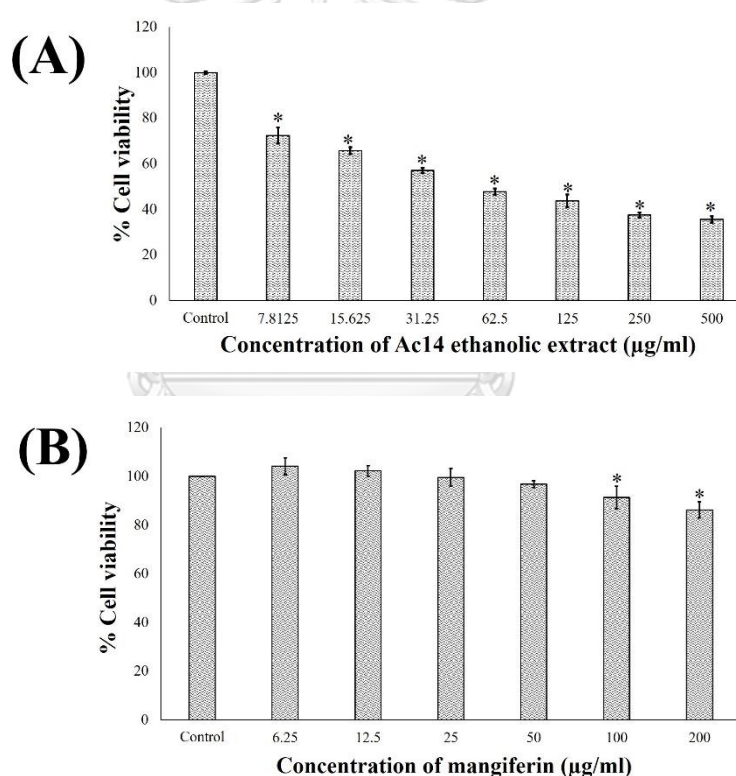


**Figure 45** The viability testing of Ac14 ethanolic extract (A) and mangiferin (B) on EA.hy926 cell. Results are expressed as mean  $\pm$  SD, based on at least three independent experiments performed in triplicate.

\*  $P < 0.05$  as compared to vehicle control, Dunnett's test

The intracellular ROS level was then examined in EA.hy926 cells through DCFH-DA fluorescence dye. The concentration of ethanolic extract of Ac14 at 15.625, 31.25, and 62.5  $\mu\text{g/ml}$  could significantly increase the DCF fluorescence, whereas the concentration at 125, 250, and 500  $\mu\text{g/ml}$  decreased DFC intensity. The ethanolic extract of Ac14 significantly decreased cell viability when increasing the concentration of extract (Figure 46).

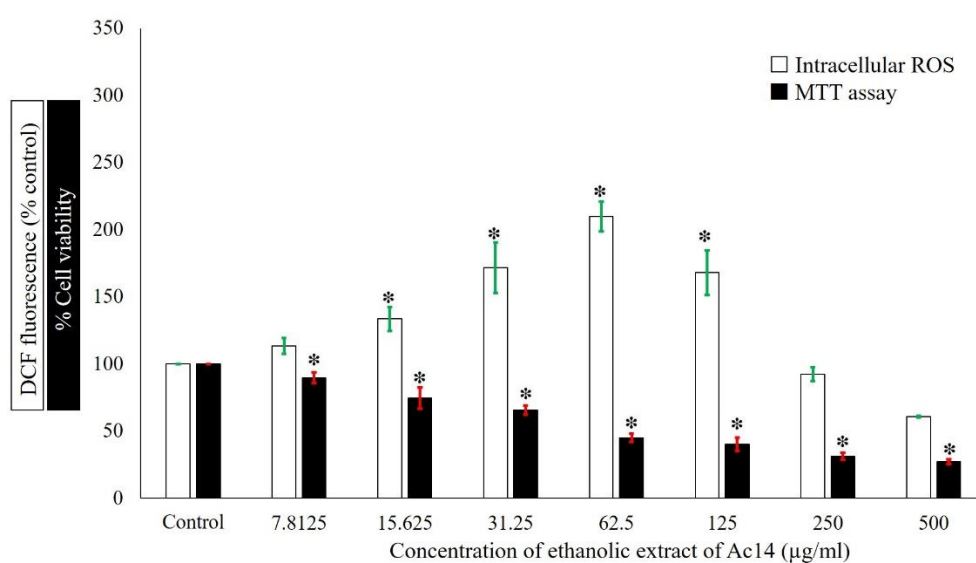


**Figure 46** Effect of ethanolic extract of Ac14 on intracellular ROS generation and cell viability in EA.hy926 cell. Results are expressed as mean  $\pm$  SD, based on at least three independent experiments performed in triplicate.

\*  $P < 0.05$  as compared to vehicle control, Dunnett's test

Mangiferin insignificantly affected to the viability and intracellular ROS level. The intracellular ROS level of the low concentration (3.125 – 50  $\mu\text{g/ml}$ ) did not significantly increase when compared to the control. While the highest concentration (200  $\mu\text{g/ml}$ ) decreased the percentage of intracellular ROS but the viability did not significantly decrease when compared to the control. Interestingly, the lower concentration (3.125 – 50  $\mu\text{g/ml}$ ) could augment the viability.

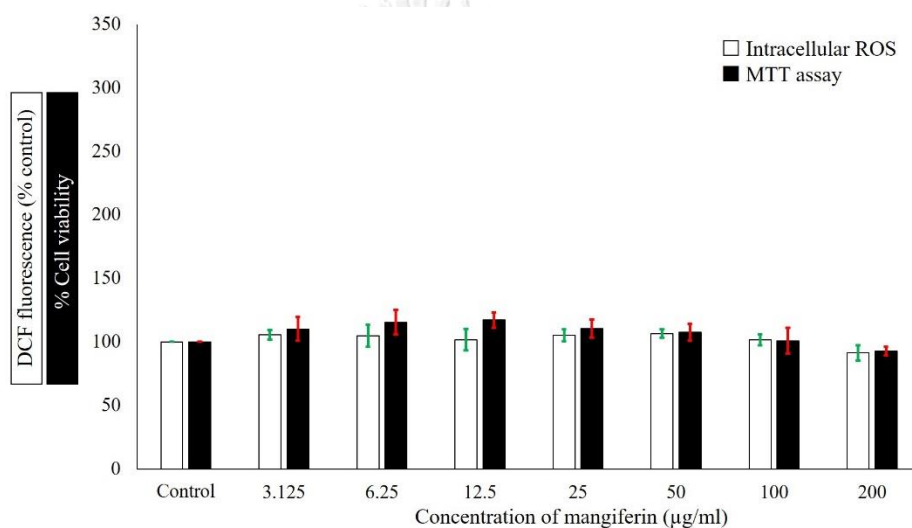


**Figure 47** Effect of mangiferin on intracellular ROS generation and cell viability in EA.hy926 cell. Results are expressed as mean  $\pm$  SD, based on at least three independent experiments performed in triplicate.

\*  $P < 0.05$  as compared to vehicle control, Dunnett's test

#### 4.2.4.2 Effect of H<sub>2</sub>O<sub>2</sub> on cell viability and intracellular ROS

H<sub>2</sub>O<sub>2</sub> is one of the reactive oxygen species that can influence cell death in various cell types. The consequence of H<sub>2</sub>O<sub>2</sub> to induce of EA.hy926 cell injury was ascertained by MTT assay. The results exhibited that H<sub>2</sub>O<sub>2</sub> could diminish the cell viability in dose-response relationship (Figure 48). The IC<sub>50</sub> value after 6-hours incubation of H<sub>2</sub>O<sub>2</sub> was calculated from the dose-response correlation ( $R^2 = 0.9955$ ), and founded to be  $1,319.28 \pm 63.40 \mu\text{M}$ .

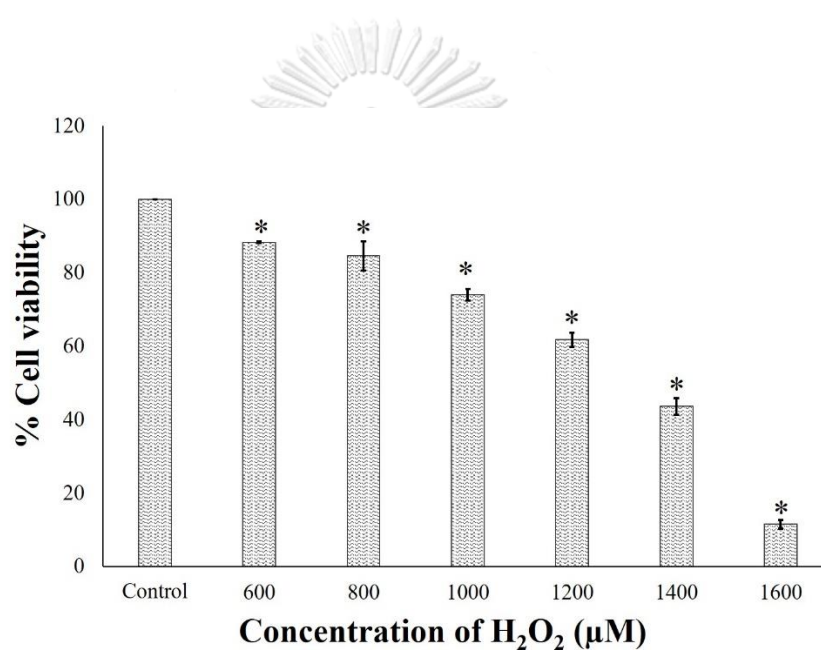


**Figure 48** The viability testing of hydrogen peroxide (H<sub>2</sub>O<sub>2</sub>) on EA.hy926 cell. Results are expressed as mean  $\pm$  SD, based on at least three independent experiments performed in triplicate.

\* P < 0.05 as compared to vehicle control, Dunnett's test

However, hydrogen peroxide has been widely utilized as an inducer of oxidative stress by enlargement of the ROS accumulation which can determine the intensity of DCF using DCFH-DA protocol in cell-based system. The usage of  $H_2O_2$  as ROS inducer should be concern about the rapid decomposition of this substances (3 – 6 hours). Thus, the 0.5 hour performed as the suitable incubation period of  $H_2O_2$  followed as Sapsrithong mentioned [231]. In order to select of proper concentration of  $H_2O_2$  to induce cell injury, the consequence of  $H_2O_2$  on intracellular ROS increasing and the viability of EA.hy926 cell was determined. The result showed that  $H_2O_2$  decreased cell viability, whereas it could increase intracellular ROS level in concentration-dependent manner (Figure 49). Additionally,  $H_2O_2$  at a concentration of 0.25 mM was significantly increased the intracellular ROS and insignificantly effect to viability of EA.hy926 cell when equated to the control. Thus, 0.25 mM of  $H_2O_2$  was chosen for the study of  $H_2O_2$ -induced oxidative stress in Ea.hy926 cells.

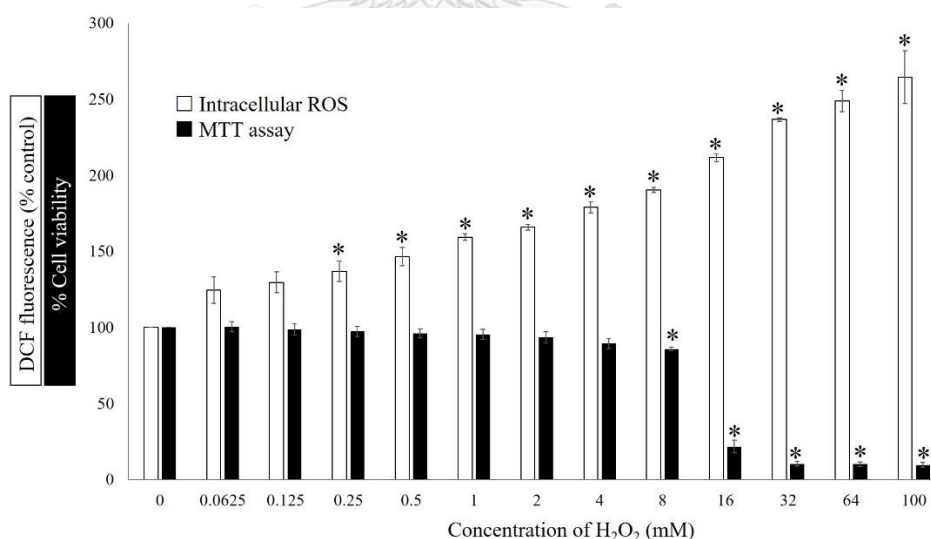


**Figure 49** Effect of  $H_2O_2$  on intracellular ROS generation and cell viability in EA.hy926 cell. Results are expressed as mean  $\pm$  SD, based on at least three independent experiments performed in triplicate.

\*  $P < 0.05$  as compared to vehicle control, Dunnett's test



#### 4.2.4.3 Effect of ethanolic extract of *Aquilaria crassna* leaves and its metabolite, mangiferin on the viability and intracellular ROS of $H_2O_2$ -injured cells

This study performed to test whether mangiferin and *A. crassna* leaf ethanolic extract can be protected the cell from oxidative stress induced by  $H_2O_2$ . The result revealed that viability of cell exposed to 0.25 mM  $H_2O_2$  insignificantly decreased when compared with vehicle control, whereas the viability of the cell pretreated with Ac14 ethanolic extract for 24 h before exposing with 0.25 mM  $H_2O_2$  for 30 min significantly decreased when equate to the vehicle control and cell exposed to 0.25 mM  $H_2O_2$  without pretreated with ethanolic extract (Figure 50).

For intracellular ROS determination, the pretreatment with ethanolic extract of Ac14 and followed by 0.25 mM  $H_2O_2$  for 0.5 h significantly increased the intracellular ROS with concentration-dependent relationship in concentration at 7.8125 – 125  $\mu\text{g/ml}$  when compared to the vehicle control and the  $H_2O_2$ -induced injury. However, the concentration of ethanolic extract of Ac14 at 250  $\mu\text{g/ml}$  and 500  $\mu\text{g/ml}$  declined in intracellular ROS. This consequence was triggered from the combination effect of the toxicity effect of ethanolic extract of Ac14 and the oxidative stress of ROS from  $H_2O_2$  which led to cell death.

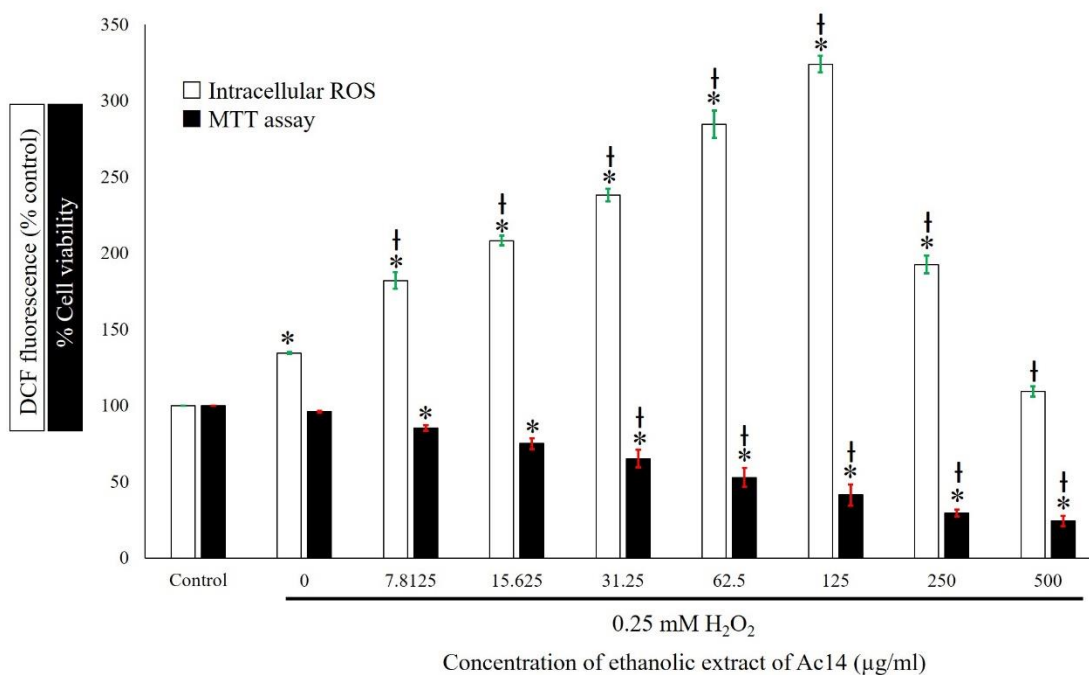


**Figure 50** Effect of ethanolic extract of Ac14 on intracellular ROS generation and cell viability of  $H_2O_2$ -injured EA.hy926 cell. Results are expressed as mean  $\pm$  SD, based on at least three independent experiments performed in triplicate.

\*  $P < 0.05$  as compared to vehicle control, Dunnett's test

†  $P < 0.05$  as compared to 0.25 mM of  $H_2O_2$ , Dunnett's test

The result of mangiferin pretreatment before induced injury with  $H_2O_2$  is interesting. The intensity of DCF with pretreatment before induced injury with  $H_2O_2$  was significantly greater than the vehicle control, but the trend was decreased in a concentration dependent manner. In addition, the intracellular ROS level was significantly diminished when pretreatment with mangiferin at concentration 12.5 – 200  $\mu\text{g/ml}$ . For viability determination, the pretreatment with mangiferin at concentration range from 3.125 to 50  $\mu\text{g/ml}$  and treated with  $H_2O_2$  performed insignificantly effect when compared to the vehicle control. Whereas high concentrations of mangiferin (100 and 200  $\mu\text{g/ml}$ ) decreased the viability with significant difference when compared to vehicle control and the  $H_2O_2$ -induced injury. Thus, this finding implied that the pretreatment with mangiferin in concentration range from 12.5 – 50  $\mu\text{g/ml}$  before injured-cell with 0.25 mM  $H_2O_2$  has a potential in decreasing of the intracellular ROS and can retain the vitality of EA.hy926 cell. In addition, the high concentration of mangiferin (100, 200  $\mu\text{g/ml}$ ) could significantly reduce the intracellular ROS (compared to the treatment with 0.25 mM of  $H_2O_2$ ) with viability above 80%.

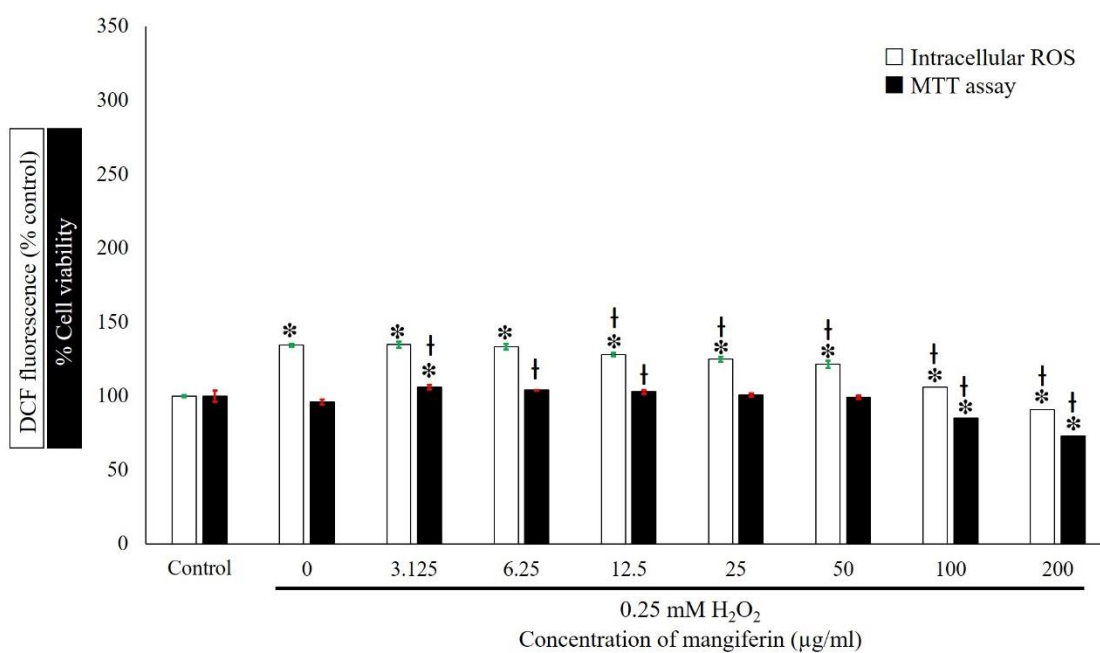


**Figure 51** Effect of mangiferin on intracellular ROS generation and cell viability of  $H_2O_2$ -injured EA.hy926 cell. Results are expressed as mean  $\pm$  SD, based on at least three independent experiments performed in triplicate.

\*  $P < 0.05$  as compared to vehicle control, Dunnett's test

†  $P < 0.05$  as compared to 0.25 mM of  $H_2O_2$ , Dunnett's test

#### 4.2.5 Effect of ethanolic extract of *A. crassna* leaves and its metabolite; mangiferin on protein expression in EA.hy926 cells

##### 4.2.5.1 Effect of ethanolic extract of *A. crassna* leaves and its metabolite; mangiferin on protein expression levels of Cu/Zn-SOD in EA.hy926 cells

To determine whether ethanolic extract of *A. crassna* leaves or mangiferin could manage the expression of Cu/Zn-superoxide dismutase enzyme (SOD-1) in EA.hy926 cell, the Western blot investigation was carried out. The result unveiled that the treatment with only mangiferin could increase the expression of SOD-1 enzyme; whereas, the trend of expression was decreased with dose-dependent relationship. In addition, the treatment with ethanolic extract of Ac14 alone also increased the expression of SOD-1 enzymes in concentration at 25 and 50 µg/ml when compared to the control, but the trend of the SOD-1 expression was decreased in dose-dependent manner. The concentration of ethanolic extract of Ac14 at 100 µg/ml was significantly decreased when compared to the control which might be occurred from cell death (Figure 52).

The H<sub>2</sub>O<sub>2</sub> treatment (at concentration 0.25 mM) for 6 h could downregulate the SOD-1 expression when compared to vehicle control. The pretreatment the cells with mangiferin as well as ethanolic extract of Ac14 prior to 0.25 mM H<sub>2</sub>O<sub>2</sub>-incubated for 6 hours could increase the expression of SOD-1 enzymes when equate to control (Figure 53).

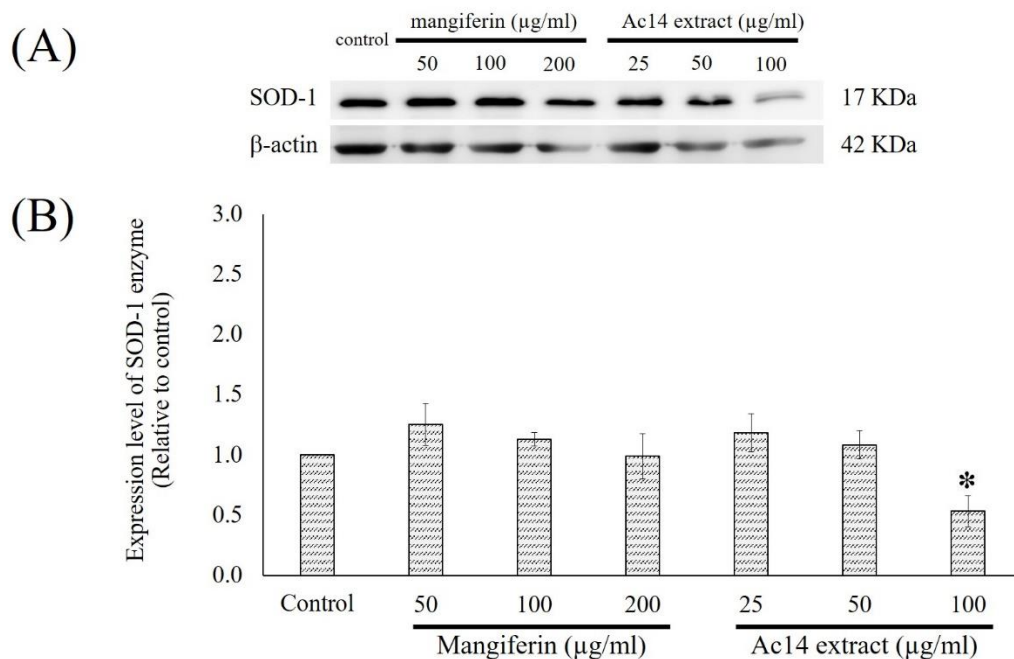


**Figure 52** Effect of mangiferin and ethanolic extract of Ac14 on protein expression of Cu/Zn-SOD in EA.hy926 cell. Cells were incubated with test sample solutions in various concentrations for 24 hours and were investigated by western blot analysis. (A) The protein levels of Cu/Zn-SOD. (B) The intensity of each band was quantitate and AUC of each band were normalized by  $\beta$ -actin band. The protein expression from control group was designated as 1. \* $p < 0.05$  compared to the untreated control. Results were expressed as mean  $\pm$  SD (n = 3).

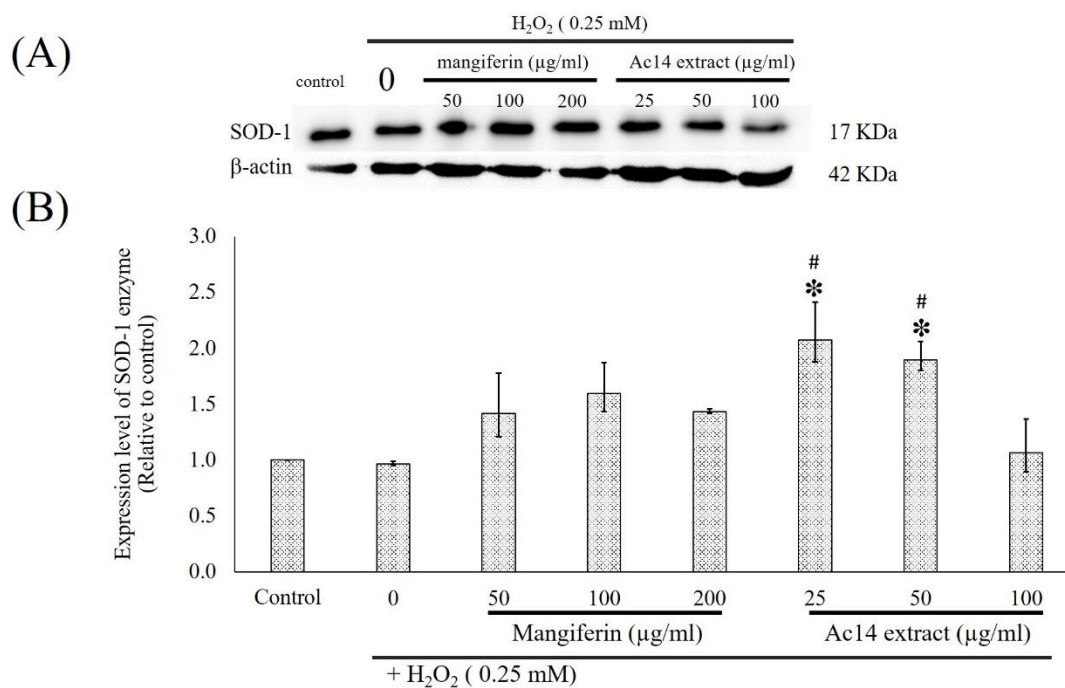


**Figure 53** Effect of mangiferin and ethanolic extract of Ac14 on protein expression of Cu/Zn-SOD in H<sub>2</sub>O<sub>2</sub>-treated EA.hy926 cell. Cells were incubated with test sample solutions in various concentrations for 24 hours followed by 0.25 mM H<sub>2</sub>O<sub>2</sub> for 6 hours and were investigated by western blot analysis. (A) The protein levels of Cu/Zn-SOD. (B) The intensity of each band was quantitate and AUC of each band were normalized by β-actin band. The protein expression from control group was designated as 1. \* p<0.05 compared to the untreated control and # p<0.05 compared to the H<sub>2</sub>O<sub>2</sub>-treated control. Results were expressed as mean ± SD (n = 3).

#### 4.2.5.2 Effect of ethanolic extract of *A. crassna* leaves and its metabolite; mangiferin on protein expression levels of HO-1 in EA.hy926 cells

The expression of HO-1 enzyme when exposed with ethanolic extract of *A. crassna* and mangiferin were determined by Western blot analysis. The results revealed that only mangiferin treatment could insignificantly increase the HO-1 expression, but the trend of expression was decreased in dose-response relationship. The HO-1 expression could be increased when treated with ethanolic extract of Ac14. However, the EA.hy926 cell which treated with ethnolic extract of Ac14 at concentration 100 µg/ml was death with cytotoxic effect of this test compound, so this effect was the cause of decreasing the HO-1 expression level (Figure 54).

The treatment of cell with 0.25 mM of H<sub>2</sub>O<sub>2</sub> could significantly increase the expression of HO-1 when compared to control (Figure 55). The pre-incubation with mangiferin for 24-hour prior H<sub>2</sub>O<sub>2</sub> exposure for 6 hours decreased the expression when compared to the H<sub>2</sub>O<sub>2</sub>-treated control with dose-dependent manner. However, the expression of HO-1 enzyme in pretreated EA.hy926 cell with ethanolic extract of Ac14 before H<sub>2</sub>O<sub>2</sub>-treated for 6 hours significantly augmented when compared to vehicle control and the H<sub>2</sub>O<sub>2</sub>-treated control. This results implied that ethanolic extract of Ac14 boosted endogenous antioxidative HO-1 gene expression to counteract the oxidative damage.



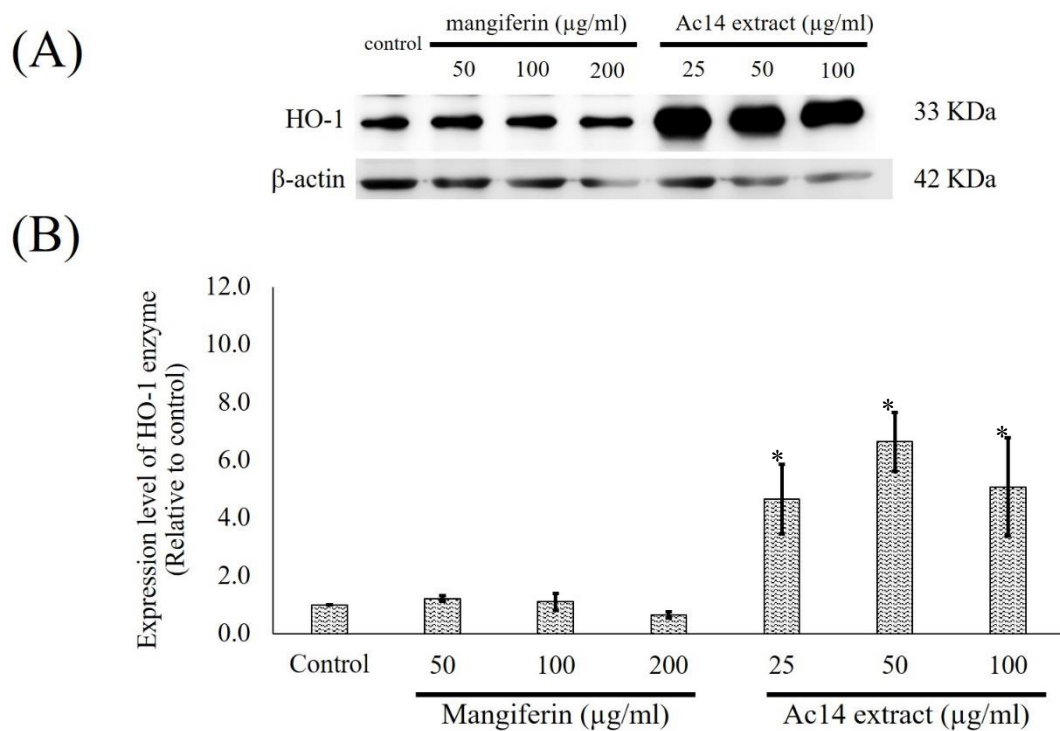


**Figure 54** Effect of mangiferin and ethanolic extract of Ac14 on protein expression of HO-1 in EA.hy926 cell. Cells were incubated with test sample solutions in various concentrations for 24 hours and were investigated by western blot analysis. (A) The protein levels of HO-1. (B) The intensity of each band was quantitate and AUC of each band were normalized by  $\beta$ -actin band. The protein expression from control group was designated as 1. \* $p < 0.05$  compared to the untreated control. Results were expressed as mean  $\pm$  SD (n = 3).

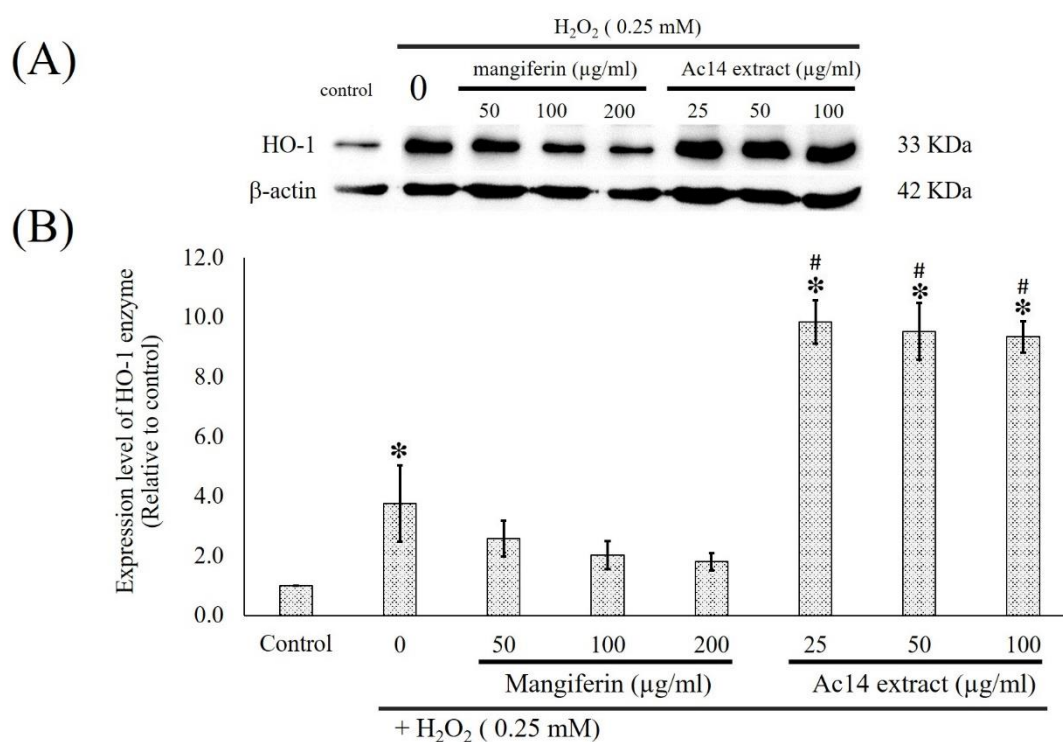


**Figure 55** Effect of mangiferin and ethanolic extract of Ac14 on protein expression of HO-1 in H<sub>2</sub>O<sub>2</sub>-treated EA.hy926 cell. Cells were incubated with test sample solutions in various concentrations for 24 hours followed by 0.25 mM H<sub>2</sub>O<sub>2</sub> for 6 hours and were investigated by western blot analysis. (A) The protein levels of HO-1. (B) The intensity of each band was quantitate and AUC of each band were normalized by  $\beta$ -actin band. The protein expression from control group was designated as 1. \* $p < 0.05$  compared to the untreated control and # $p < 0.05$  compared to the H<sub>2</sub>O<sub>2</sub>-treated control. Results were expressed as mean  $\pm$  SD (n = 3).

#### 4.2.5.3 Effect of ethanolic extract of *A. crassna* leaves and its metabolite; mangiferin on protein expression levels of Bcl-2 and Bax in EA.hy926 cells

The expression of the antiapoptotic factor (Bcl-2) and those of the proapoptotic factor (Bax) were further investigated using Western blotting method. The results found that mangiferin could significantly increase the Bcl-2/Bax ratio when incubated to the EA.hy926 cell, while the response of ratio of Bcl-2/Bax expression of mangiferin was decreased in dose-dependent manner. Interestingly, the Bcl-2 expression of mangiferin-treated cell was up-regulated, while the Bax protein was unchanged from the control. In contrast, all of concentration of the ethanolic extract of Ac14 significantly reduced the expression of Bcl-2 when compared to control, and the intensity of Bax expression were indifferent (Figure 56). Therefore, the expression ratio of Bcl-2/Bax of ethanolic extract of Ac14 were lower than control, and assumed that the ethanolic extract of Ac14 did not have the cytoprotective properties.

The incubation with 0.25 mM H<sub>2</sub>O<sub>2</sub> contributed to the up-regulation in Bax protein which equated to vehicle control. However, the presence of 50, 100 and 200 µg/ml mangiferin displayed cytoprotective activity after treated with 0.25 mM H<sub>2</sub>O<sub>2</sub> by augmenting the Bcl-2 expression and indifferent of Bax expression. Nonetheless, the ethanolic extract of Ac14 decreased the expression of Bcl-2 when compared with the control, and the Bcl-2/Bax ratio was remarkably decreased in a dose-dependent relationship (Figure 57).

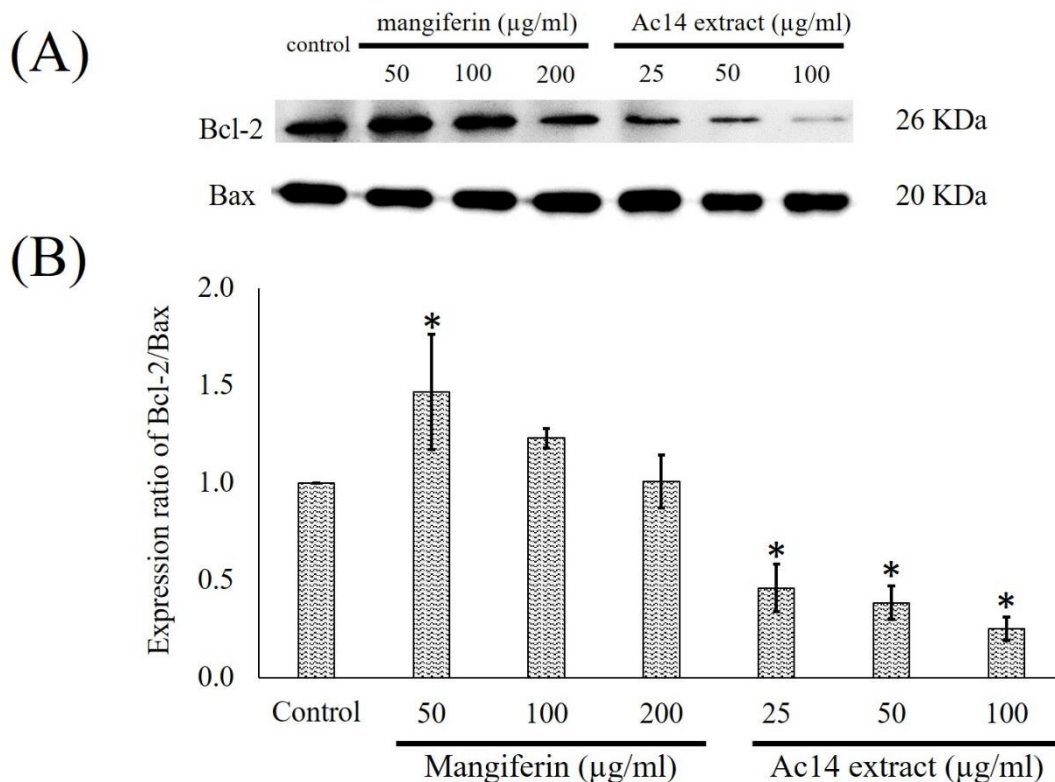


**Figure 56** Effect of mangiferin and ethanolic extract of Ac14 on protein expression of Bcl-2 and Bax in EA.hy926 cell. Cells were incubated with test sample solutions in various concentrations for 24 hours and were investigated by western blot analysis. (A) The protein levels of Bcl-2 and Bax. (B) The ratio of intensity of Bcl-2/Bax ratio was quantitate through AUC of each band. The protein expression from control group was designated as 1. \* $p < 0.05$  compared to the untreated control. Results were expressed as mean  $\pm$  SD (n = 3).

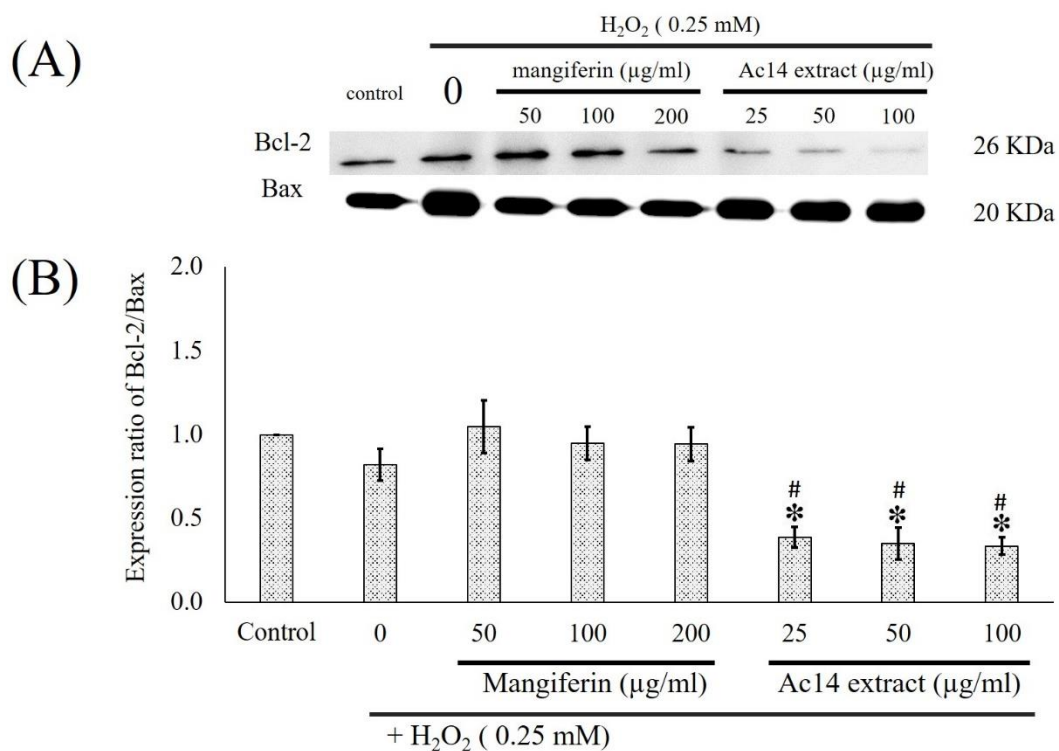


**Figure 57** Effect of mangiferin and ethanolic extract of Ac14 on protein expression of Bcl-2 and Bax in EA.hy926 cell. Cells were incubated with test sample solutions in various concentrations for 24 hours followed by 0.25 mM  $H_2O_2$  for 6 hours and were investigated by western blot analysis. (A) The protein levels of Bcl-2 and Bax. (B) The ratio of intensity of Bcl-2/Bax ratio was quantitate through AUC of each band. The protein expression from control group was designated as 1. \* $p < 0.05$  compared to the untreated control and # $p < 0.05$  compared to the  $H_2O_2$ -treated control. Results were expressed as mean  $\pm$  SD (n = 3).

### 4.3 DNA barcoding of selected species in genus *Aquilaria*

Nowadays, the molecular technique has been extensively used for organism identification. Hollingsworth (2011) was mentioned that the DNA barcoding is the procedure to find one or a few DNA regions which can be discriminated among species and to obtain the genetic information to generate a huge database of creatures. In this research, six interesting loci (ITS regionn, *rbcl* gene, *matK* gene, *trnH-psbA* intergenic spacer, *rpoC1* gene, and *ycf1* gene) were studied for the identification and discrimination of three selected species in the genus *Aquilaria* using DNA barcoding technique.

#### 4.3.1 PCR amplification and DNA sequencing

The six interesting loci were successfully amplified and sequenced for all samples. The PCR products of these six loci were also purified and the sequencing process was done by Sanger sequencing technique. The obtained sequences and accession numbers were shown in Appendix G. The evaluation of the six DNA barcode loci was shown in Table 24 including sequencing length, aligned length, and the percentage of nucleotide variation. The alignment sequences of each locus were demonstrated in Figure 58 – 63 (for ITS regionn, *rbcl* gene, *matK* gene, *trnH-psbA* intergenic spacer, *rpoC1* gene, and *ycf1* gene, respectively). In addition, the estimates of evolutionary divergence between sequences of each locus were tabulated in Table 25 – 30 for ITS region, *rbcl* gene, *matK* gene, *psbA-trnH* intergenic spacer, *rpoC1* gene, and *ycf1* gene, respectively.

**Table 24** Evaluation of the six DNA barcode loci

Parameter assessed Locus	Full/ Partial sequence	Sequence length (bp)	Aligned length (bp)	No. of variable site	% Variation	Log likelihood of tree
ITS region	Partial	682-745	745	20	2.93 %	-1476.87
<i>rbcl</i> gene	Partial	1203	1203	3	0.25 %	-1834.40
<i>matK</i> gene	Partial	812-818	818	5	0.62 %	-1359.39
<i>psbA-trnH intergenic spacer</i>	Partial	441-468	468	1	0.23 %	-787.18
<i>rpoC1</i> gene	Partial	529-531	531	0	0.00 %	-805.16
<i>ycf1</i> gene	Partial	846-850	850	2	0.24 %	-1525.74



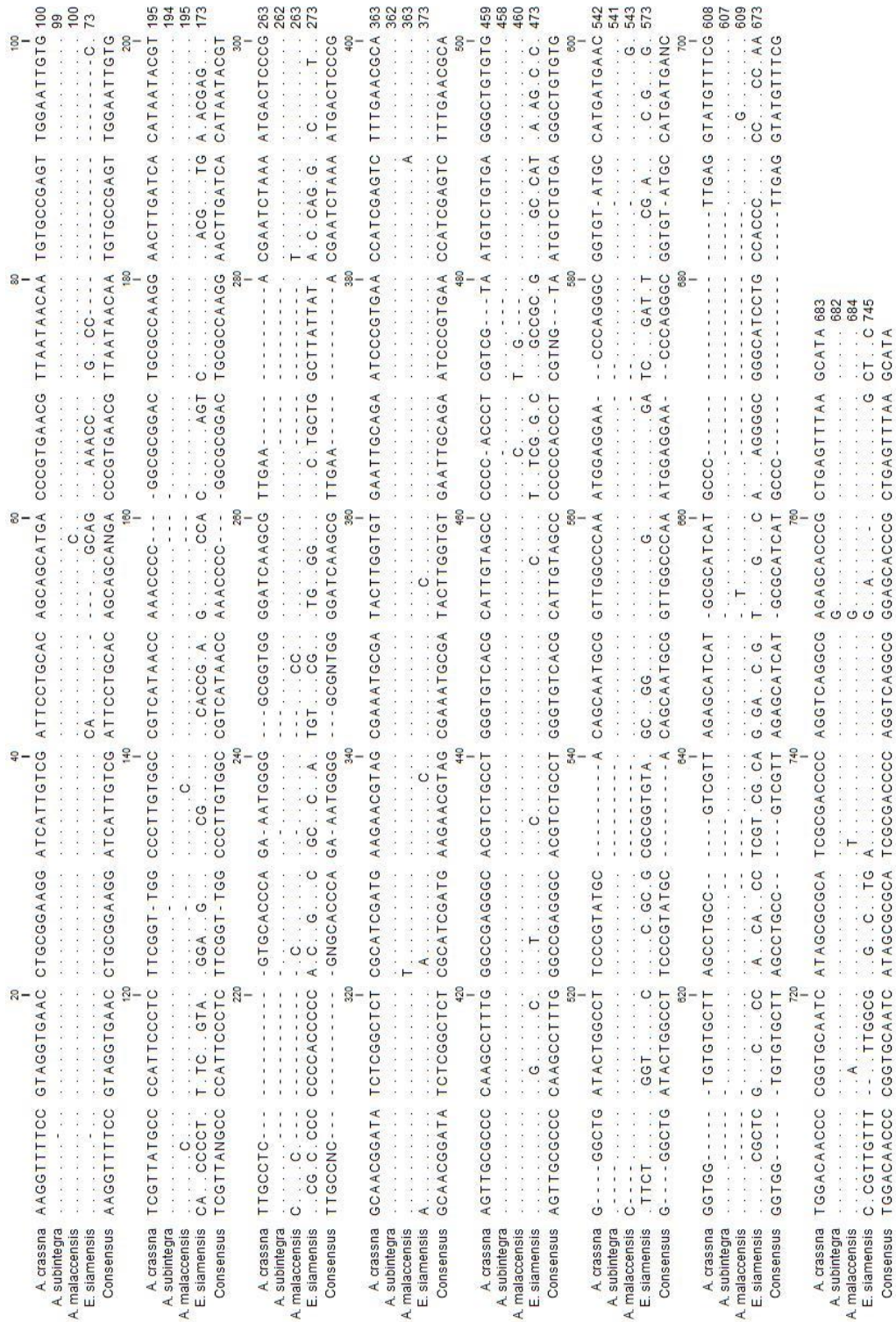


Figure 58 Alignment of partial sequence ITS region of three *Aquilaria* plants and outgroup (*E. siamensis*)



**Table 25** Estimates of evolutionary divergence between sequences of ITS region

	<i>A. crassna</i>	<i>A. malaccensis</i>	<i>A. subintegra</i>	<i>E. siamensis</i>
<i>A. crassna</i>				
<i>A. malaccensis</i>	0.0326			
<i>A. subintegra</i>	0.0016	0.0308		
<i>E. siamensis</i>	3.0483	3.1453	3.0413	

\*The number of base substitutions per site from between sequences were shown.

Analyses were conducted using the Maximum Composite Likelihood model.

**Table 26** Estimates of evolutionary divergence between sequences of *rbcl* gene

	<i>A. crassna</i>	<i>A. malaccensis</i>	<i>A. subintegra</i>	<i>E. siamensis</i>
<i>A. crassna</i>				
<i>A. malaccensis</i>	0.0008			
<i>A. subintegra</i>	0.0017	0.0025		
<i>E. siamensis</i>	0.0211	0.0220	0.0211	

\*The number of base substitutions per site from between sequences were shown.

Analyses were conducted using the Maximum Composite Likelihood model.

A. crassna	GTTGGATTCA	AGGCTGGTGT	TAAAGAGTAT	AAATTGACTT	ATTATACTCC	TGAATATGAA	ACCAAAGATA	CTGATATCTT	GGCAGCATTG	CGAGTAACTC	100
A. subintegra	.....	.....	.....	.....	.....	.....	.....	.....	.....	.....	100
A. malaccensis	.....	A.....	.....	.....	.....	.....	.....	.....	.....	.....	100
E. siamensis	.....	A.....	.....	.....	.....	.....	.....	.....	.....	.....	100
Consensus	GTTGGATTCA	ANGCTGGTGT	TAAAGAGTAT	AAATTGACTT	ATTATACTCC	TGAATATGAA	ACCAAAGATA	CTGATATCTT	GGCAGCATTG	CGAGTAACTC	
A. crassna	CTCAACCTGG	AGTTCGCGCT	GAGGAAGCAG	GGGCTCGGGT	AGCTGCTGAA	TCTTCTACTG	GTACATGGAC	AACTGTGTGG	ACCGACGGGC	TTACCAGCCT	200
A. subintegra	.....	.....	.....	.....	.....	.....	.....	.....	.....	.....	200
A. malaccensis	.....	.....	.....	.....	.....	.....	.....	.....	.....	.....	200
E. siamensis	.....	.....	.....	.....	.....	.....	.....	.....	.....	.....	200
Consensus	CTCAACCTGG	AGTTCGCGCT	GAGGAAGCAG	GGGCTCGGGT	AGCTGCTGAA	TCTTCTACTG	GTACATGGAC	AACTGTGTGG	ACCGACGGGC	TTACCAGCCT	
A. crassna	TGATCGTTAC	AAAGGGCGAT	GCTACCACAT	CGAGCCCGTT	GCTGGGGAAG	AAATCAATA	TATATGTTAT	GTAGCTTACC	CCTTAGACCT	TTTTGAAGAG	300
A. subintegra	.....	.....	.....	.....	.....	.....	.....	.....	.....	.....	300
A. malaccensis	.....	.....	.....	.....	.....	.....	.....	.....	.....	.....	300
E. siamensis	.....	.....	.....	.....	.....	.....	.....	.....	.....	.....	300
Consensus	TGATCGTTAC	AAAGGGCGAT	GCTACCACAT	CGAGCCCGTT	GCTGGGGAAG	AAATCAATA	TATATGTTAT	GTAGCTTACC	CCTTAGACCT	TTTTGAAGAG	
A. crassna	GGTTCTGTTA	CTAACATGTT	TACTTCCATT	GTTGGTAATG	TATTTGGGTT	CAAAGCCCTG	CGCGCTCTAC	GTCTAGAAGA	TCTGCGAATC	CCTACTTCTT	400
A. subintegra	.....	.....	.....	.....	.....	.....	.....	.....	.....	.....	400
A. malaccensis	.....	.....	.....	.....	.....	.....	.....	.....	.....	.....	400
E. siamensis	.....	.....	.....	.....	.....	.....	.....	.....	.....	.....	400
Consensus	GGTTCTGTTA	CTAACATGTT	TACTTCCATT	GTTGGTAATG	TATTTGGGTT	CAAAGCCCTG	CGCGCTCTAC	GTCTAGAAGA	TCTGCGAATC	CCTACTTCTT	
A. crassna	ATATTAANAAC	TTTCCAAGGT	CGGCCTCATG	GCATCCAAGT	TGAAAGAGAT	AAATTGAACA	AGTACGGCCG	TCCCCTATTG	GGATGTAATA	TTAAACCTAA	500
A. subintegra	.....	.....	.....	.....	.....	.....	.....	.....	.....	.....	500
A. malaccensis	.....	.....	.....	.....	.....	.....	.....	.....	.....	.....	500
E. siamensis	.....	.....	.....	.....	.....	.....	.....	.....	.....	.....	500
Consensus	ATATTAANAAC	TTTCCAAGGT	CGGCCTCATG	GCATCCAAGT	TGAAAGAGAT	AAATTGAACA	AGTACGGCCG	TCCCCTATTG	GGATGTAATA	TTAAACCTAA	
A. crassna	ATTGGGGTTA	TCCGCTAAA	ACTACGGTAG	AGCGGTTTAT	GAATGCTTAC	GTGGTGGACT	TGATTTTACC	AAAGATGATG	AGAATGTGAA	CTCCCAACCA	600
A. subintegra	.....	.....	.....	.....	.....	.....	.....	.....	.....	.....	600
A. malaccensis	.....	.....	.....	.....	.....	.....	.....	.....	.....	.....	600
E. siamensis	.....	.....	.....	.....	.....	.....	.....	.....	.....	.....	600
Consensus	ATTGGGGTTA	TCCGCTAAA	ACTACGGTAG	AGCGGTTTAT	GAATGCTTAC	GTGGTGGACT	TGATTTTACC	AAAGATGATG	AGAATGTGAA	CTCCCAACCA	
A. crassna	TTTATGCGTT	GGAGAGACCG	TTTCTTATTT	TGTGCCGAAG	CAATTTATAA	AGCACAGGCT	GAACAGGTTG	AAATCAAAGG	GCATTACTTG	AATGCTACTG	700
A. subintegra	.....	.....	.....	.....	.....	.....	.....	.....	.....	.....	700
A. malaccensis	.....	.....	.....	.....	.....	.....	.....	.....	.....	.....	700
E. siamensis	.....	.....	.....	.....	.....	.....	.....	.....	.....	.....	700
Consensus	TTTATGCGTT	GGAGAGACCG	TTTCTTATTT	TGTGCCGAAG	CAATTTATAA	AGCACAGGCT	GAACAGGTTG	AAATCAAAGG	GCATTACTTG	AATGCTACTG	

Figure 59 Alignment of partial sequence *rbcl* gene of three *Aquilaria* plants and outgroup (*E. siamensis*)

```

A. crassna      CCGGTACATG CGAAGAATG ATCAAAGGG CTGTATTGC CAGAGAATTA GGAGTCCTA TCGTAATGCA TGAATATTTA ACGGGGGGAT TCACGGGCAA 800
A. subintegra  . . . . .
A. malaccensis . . . . .
E. siamensis  . . . . .
Consensus     . . . . .
A. crassna      TACTAGCTTG GCTCATTATT GCCGAGATAA TGGTCTCCTT CTTACATCC ATCGCGCAAT GCACGCAGTT ATTGATAGAC AGAAGAATCA CGGTATGCAC 900
A. subintegra  . . . . .
A. malaccensis . . . . .
E. siamensis  . . . . .
Consensus     . . . . .
A. crassna      TCCCGTGTAC TAGCTAAAGC CTTACGTATG TCTGGTGGAG ATCATATTCA CGCTGGTACA GTAGTAGTA AACTTGAAGG AGAAGAAGAC ATAACTTTGG 1000
A. subintegra  . . . . .
A. malaccensis . . . . .
E. siamensis  . . . . .
Consensus     . . . . .
A. crassna      TCCCGTGTAC TAGCTAAAGC CTTACGTATG TCTGGTGGAG ATCATATTCA CGCTGGTACA GTAGTAGTA AACTTGAAGG AGAAGAAGAC ATAACTTTGG 1100
A. subintegra  . . . . .
A. malaccensis . . . . .
E. siamensis  . . . . .
Consensus     . . . . .
A. crassna      GTTTTGTTGA TTTACTACGT GATGATTTTA TTGAAAAGA TAGAAGCCGT GGTATTTATT TCACTCAAGA TTGGGTCTCT CTACCAGGTG TTATACCCGGT 1100
A. subintegra  . . . . .
A. malaccensis . . . . .
E. siamensis  . . . . .
Consensus     . . . . .
A. crassna      GTTTTGTTGA TTTACTACGT GATGATTTTA TTGAAAAGA TAGAAGCCGT GGTATTTATT TCACTCAAGA TTGGGTCTCT CTACCAGGTG TTATACCCGGT 1200
A. subintegra  . . . . .
A. malaccensis . . . . .
E. siamensis  . . . . .
Consensus     . . . . .
A. crassna      AGCTTCTGGG GGTATTCACG TTTGGCATAT GCCTGCTTTG ACCGAGATCT TTTGGTACTA TGCCGTACTA CAATTTGGTG GAGGAACCTT AGGACACCCCT 1200
A. subintegra  . . . . .
A. malaccensis . . . . .
E. siamensis  . . . . .
Consensus     . . . . .
A. crassna      TGG 1203
A. subintegra  . . . 1203
A. malaccensis . . . 1203
E. siamensis  . . . 1203
Consensus     TGG

```

Figure 59 Alignment of partial sequence rbcL gene of three Aquilaria plants and outgroup (*E. siamensis*) (Cont.)

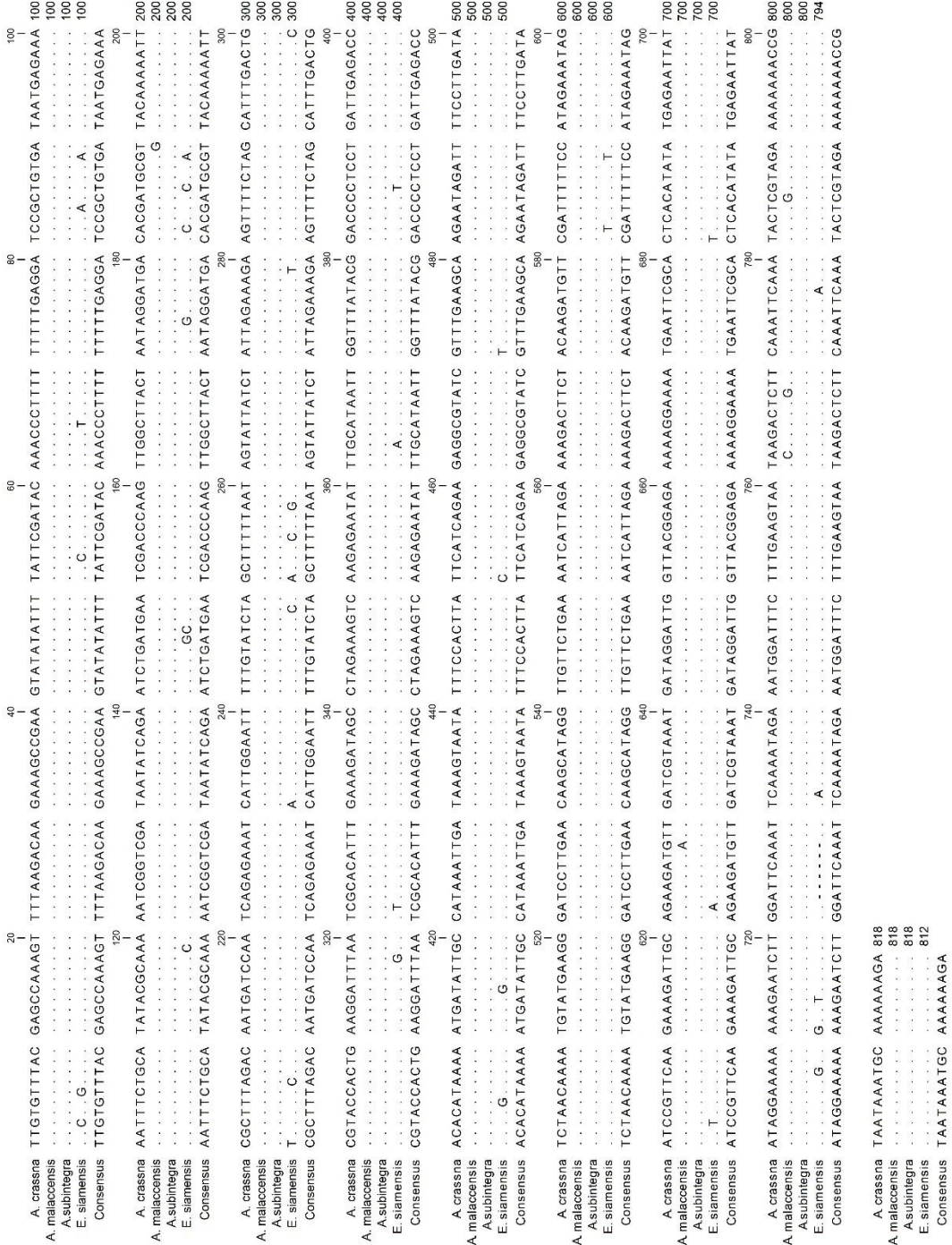


Figure 60 Alignment of partial sequence *matK* gene of three *Aquilaria* plants and outgroup (*E. siamensis*)

**Table 27** Estimates of evolutionary divergence between sequences of *matK* gene

	<i>A. crassna</i>	<i>A. malaccensis</i>	<i>A. subintegra</i>	<i>E. siamensis</i>
<i>A. crassna</i>				
<i>A. malaccensis</i>	0.0062			
<i>A. subintegra</i>	0.0000	0.0062		
<i>E. siamensis</i>	0.0512	0.0580	0.0512	

\*The number of base substitutions per site from between sequences were shown. Analyses were conducted using the Maximum Composite Likelihood model.

**Table 28** Estimates of evolutionary divergence between sequences of *psbA-trnH* intergenic spacer

	<i>A. crassna</i>	<i>A. malaccensis</i>	<i>A. subintegra</i>	<i>E. siamensis</i>
<i>A. crassna</i>				
<i>A. malaccensis</i>	0.0024			
<i>A. subintegra</i>	0.0000	0.0024		
<i>E. siamensis</i>	0.0952	0.0918	0.0952	

\*The number of base substitutions per site from between sequences were shown. Analyses were conducted using the Maximum Composite Likelihood model.

A. crassna	20	40	60	80	100	120	140	160	180	200
A. malaccensis	20	40	60	80	100	120	140	160	180	200
A. subintegra	20	40	60	80	100	120	140	160	180	200
E. siamensis	20	40	60	80	100	120	140	160	180	200
Consensus	20	40	60	80	100	120	140	160	180	200
A. crassna	220	240	260	280	300	320	340	360	380	400
A. malaccensis	220	240	260	280	300	320	340	360	380	400
A. subintegra	220	240	260	280	300	320	340	360	380	400
E. siamensis	220	240	260	280	300	320	340	360	380	400
Consensus	220	240	260	280	300	320	340	360	380	400
A. crassna	320	340	360	380	400	420	440	460	480	500
A. malaccensis	320	340	360	380	400	420	440	460	480	500
A. subintegra	320	340	360	380	400	420	440	460	480	500
E. siamensis	320	340	360	380	400	420	440	460	480	500
Consensus	320	340	360	380	400	420	440	460	480	500

A. crassna GTTATGCATG AACGTAATGC TCATAACTTC CCCCTAGACC TAGCTGCTAT TGAAGCTCCA TCTACAAATG GATAAGACTT TTGCTTTAGT GTATATGATT 100  
 A. malaccensis .....T.....T.....G.....C.....C.....  
 A. subintegra .....T.....T.....G.....C.....C.....  
 E. siamensis .....T.....T.....G.....C.....C.....  
 Consensus GTTATGCATG AACGTAATGC TCATAACTTC CCCCTAGACC TAGCTGCTAT TGAAGCTCCA TCTACAAATG GATAAGACTT TTGCTTTAGT GTATATGATT 100  
 A. crassna TTTTGAAGG AAAAAAAGTA AAGGGGCAAT ACCCAATTC TTGTTTTACC ATTCCAAGA GGATTGGTAT TGCTCCITTA TTTCTTTTAG TAGTCTTTTA 200  
 A. malaccensis .....T.....T.....G.....C.....C.....  
 A. subintegra .....T.....T.....G.....C.....C.....  
 E. siamensis .....T.....T.....G.....C.....C.....  
 Consensus TTTTGAAGG AAAAAAAGTA AAGGGGCAAT ACCCAATTC TTGTTTTACC ATTCCAAGA GGATTGGTAT TGCTCCITTA TTTCTTTTAG TAGTCTTTTA 200  
 A. crassna TTTACTTAGG TTTTTTCTT TACCTTAAC CAACTTTACT ATAACAAAAT AGGAAAAGGT GGTCTTAATG AGTTTGGTTT AGTATCATAC CTT----- 293  
 A. malaccensis .....T.....T.....G.....C.....C.....  
 A. subintegra .....T.....T.....G.....C.....C.....  
 E. siamensis .....T.....T.....G.....C.....C.....  
 Consensus TTTACTTAGG TTTTTTCTT TACCTTAAC CAACTTTACT ATAACAAAAT AGGAAAAGGT GGTCTTAATG AGTTTGGTTT AGTATCATAC CTT----- 293  
 A. crassna ----- AAATTAGTCC TTACCAATCT TTTTGGAAGT TTTTACTGTT TTTTACTGTT TTTTACTGTT TTTTACTGTT TTTTACTGTT TTTTACTGTT TTTTACTGTT 373  
 A. malaccensis .....T.....T.....G.....C.....C.....  
 A. subintegra TACTCATATA TAAATTCAT -----G.....C.....T.....C.....  
 E. siamensis ----- AAATTAGTCC TTACCAATCT TTTTGGAAGT TTTTACTGTT TTTTACTGTT TTTTACTGTT TTTTACTGTT TTTTACTGTT TTTTACTGTT TTTTACTGTT 373  
 Consensus ----- AAATTAGTCC TTACCAATCT TTTTGGAAGT TTTTACTGTT TTTTACTGTT TTTTACTGTT TTTTACTGTT TTTTACTGTT TTTTACTGTT TTTTACTGTT 386  
 A. crassna TCATA----- AAAGTGGAGG GGCGGATGTA GCCAAGTGA TTAAGGCAGT GGATTGTGAA TCCACCATGC GCG 441  
 A. malaccensis .....T.....T.....G.....C.....C.....  
 A. subintegra .....T.....T.....G.....C.....C.....  
 E. siamensis .....T.....T.....G.....C.....C.....  
 Consensus TCATA----- AAAGTGGAGG GGCGGATGTA GCCAAGTGA TTAAGGCAGT GGATTGTGAA TCCACCATGC GCG 441  
 A. crassna ----- AAAGTGGAGG GGCGGATGTA GCCAAGTGA TTAAGGCAGT GGATTGTGAA TCCACCATGC GCG 468  
 A. malaccensis .....T.....T.....G.....C.....C.....  
 A. subintegra .....T.....T.....G.....C.....C.....  
 E. siamensis .....T.....T.....G.....C.....C.....  
 Consensus ----- AAAGTGGAGG GGCGGATGTA GCCAAGTGA TTAAGGCAGT GGATTGTGAA TCCACCATGC GCG 468

**Figure 61** Alignment of partial sequence *psbA-trnH* intergenic spacer of three *Aquilaria* plants and outgroup (*E. siamensis*)

```

      20      40      60      80      100      120      140      160      180      200
A_crassna  GGCAAAG-AG  GGAAGATTTC  GCGAGACTCT  GCGAGACTCT  GCGAGACTCT  GCGAGACTCT  GCGAGACTCT  GCGAGACTCT  GCGAGACTCT
A_malaccensis  . . . . .
A_subintegra  . . . . .
Enkleia_siamensis  . . . . .
Consensus  GGCAAAG-AG  GGAAGATTTC  GCGAGACTCT  GCGAGACTCT  GCGAGACTCT  GCGAGACTCT  GCGAGACTCT  GCGAGACTCT  GCGAGACTCT

      220      240      260      280      300      320      340      360      380      400
A_crassna  TGTTGGTTGC  CTCGGCGAAAT  GGCAATAGAG  CTTTTCCAGA  CATTITGTAAT  TCGTGGTCTA  ATTAGACAAC  ATCTTGCTTC  GAACATAGGA  GTTGCTAAGA
A_malaccensis  . . . . .
A_subintegra  . . . . .
Enkleia_siamensis  . . . . .
Consensus  TGTTGGTTGC  CTCGGCGAAAT  GGCAATAGAG  CTTTTCCAGA  CATTITGTAAT  TCGTGGTCTA  ATTAGACAAC  ATCTTGCTTC  GAACATAGGA  GTTGCTAAGA

      320      340      360      380      400      420      440      460      480      500
A_crassna  GTCAAATTCG  CGAAAAGGGG  CCAATTGTAT  GGCAATAACT  TCAAGAAGTT  ATGCAGGGGC  ATCCTGTATT  GCTGAATAGA  GCGCCTACTC  TGCATAGATT
A_malaccensis  . . . . .
A_subintegra  . . . . .
Enkleia_siamensis  . . . . .
Consensus  GTCAAATTCG  CGAAAAGGGG  CCAATTGTAT  GGCAATAACT  TCAAGAAGTT  ATGCAGGGGC  ATCCTGTATT  GCTGAATAGA  GCGCCTACTC  TGCATAGATT

      380      400      420      440      460      480      500
A_crassna  AGGGATACAG  GCATTCCAAC  CCATTTTAGT  GGAAGGGCGT  GCTATTTGTT  TACACCCATT  TACACCCATT  TACACCCATT  TACACCCATT  TACACCCATT
A_malaccensis  . . . . .
A_subintegra  . . . . .
Enkleia_siamensis  . . . . .
Consensus  AGGGATACAG  GCATTCCAAC  CCATTTTAGT  GGAAGGGCGT  GCTATTTGTT  TACACCCATT  TACACCCATT  TACACCCATT  TACACCCATT  TACACCCATT

      420      440      460      480      500
A_crassna  ATGGCTGTTT  ATGTACCTTT  ATGTTAGAG  GCTCAAGCGG  AGTTTCGTTT  ACTTATGTTT  TCTCATATGA  ATCTCTTGTG  TCCAGGTATT  GGGGATCCTA
A_malaccensis  . . . . .
A_subintegra  . . . . .
Enkleia_siamensis  . . . . .
Consensus  ATGGCTGTTT  ATGTACCTTT  ATGTTAGAG  GCTCAAGCGG  AGTTTCGTTT  ACTTATGTTT  TCTCATATGA  ATCTCTTGTG  TCCAGGTATT  GGGGATCCTA

      520
A_crassna  TTCCGTACC  AACTCAAAGT  -ATGCTTATG  G 529
A_malaccensis  . . . . .
A_subintegra  . . . . .
Enkleia_siamensis  . . . . .
Consensus  TTCCGTACC  AACTCAAAGT  -ATGCTTATG  G

```

Figure 62 Alignment of partial sequence *rhoC1* gene of three *Aquilaria* plants and outgroup (*E. siamensis*)

**Table 29** Estimates of evolutionary divergence between sequences of *rpoC1* gene

	<i>A. crassna</i>	<i>A. malaccensis</i>	<i>A. subintegra</i>	<i>E. siamensis</i>
<i>A. crassna</i>				
<i>A. malaccensis</i>	0.0000			
<i>A. subintegra</i>	0.0000	0.0000		
<i>E. siamensis</i>	0.0251	0.0251	0.0251	

\*The number of base substitutions per site from between sequences were shown. Analyses were conducted using the Maximum Composite Likelihood model.

**Table 30** Estimates of evolutionary divergence between sequences of *ycf1* gene

	<i>A. crassna</i>	<i>A. malaccensis</i>	<i>A. subintegra</i>	<i>E. siamensis</i>
<i>A. crassna</i>				
<i>A. malaccensis</i>	0.0024			
<i>A. subintegra</i>	0.0012	0.0036		
<i>E. siamensis</i>	0.1195	0.1195	0.1210	

\*The number of base substitutions per site from between sequences were shown. Analyses were conducted using the Maximum Composite Likelihood model.



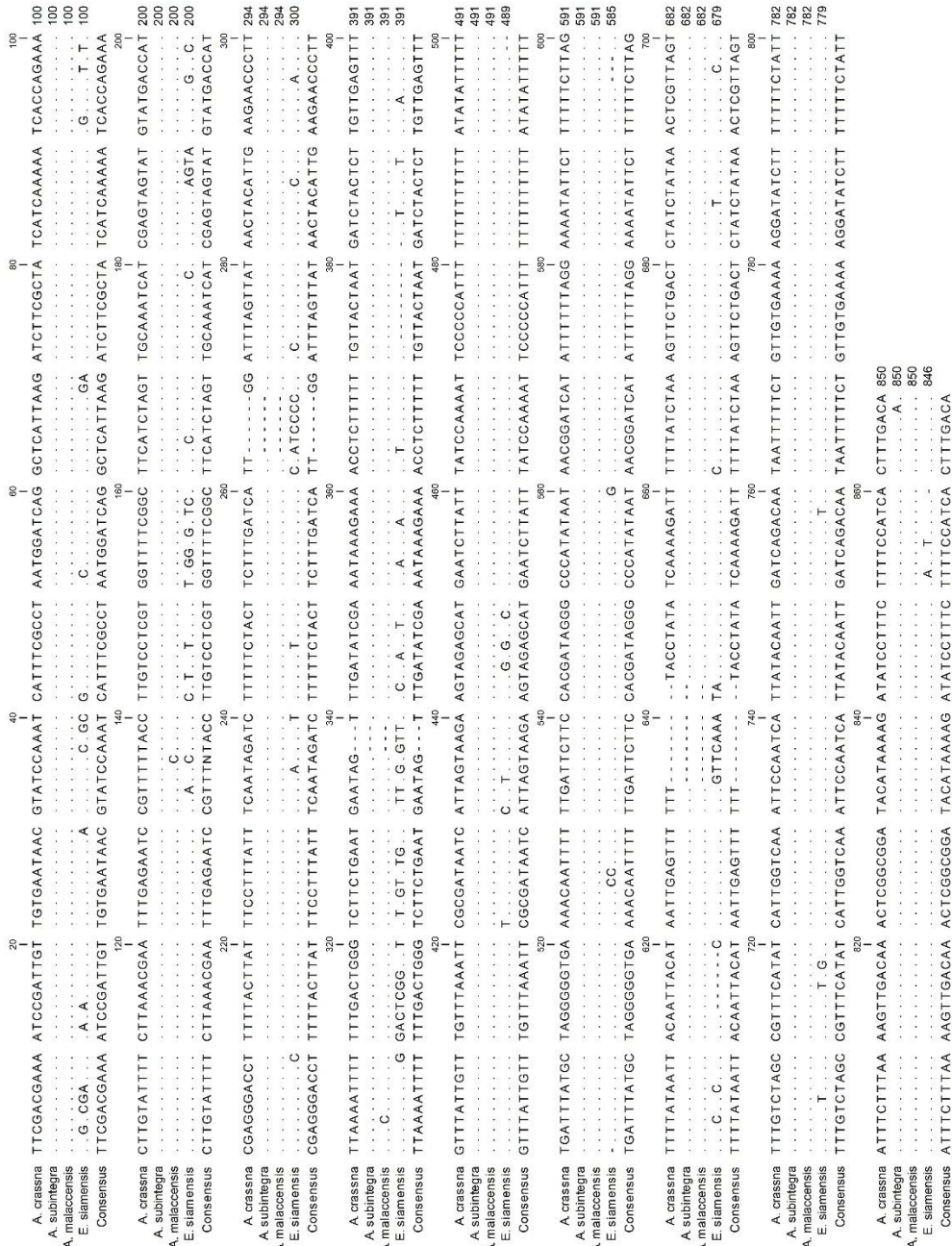


Figure 63 Alignment of partial sequence ycf1 of three Aquilaria plants and outgroup (*E. siamensis*)

#### 4.3.2 Phylogenetic analysis of selected plant in genus *Aquilaria* based on each locus

The phylogenetic relationships among these three *Aquilaria* species and *E. siamensis* (outgroup) were examined in each locus and combination of locus using maximum likelihood method. The log likelihood of the ML tree of each loci was shown in Table 24. In addition, the bootstrap (1,000 replications) statistic-supporting analysis was done to evaluate the confidence of the result topologies of the ML trees found.

##### 4.3.2.1 Phylogenetic tree of ITS region

The maximum likelihood tree based on ITS sequences from these three *Aquilaria* species and *E. siamensis* was displayed in Figure 64 and the highest log likelihood values was found to be -1,476.87. From the dendrogram, *A. crassna* was closely related to *A. subintegra*, while *A. malaccensis* was separated in another branch.

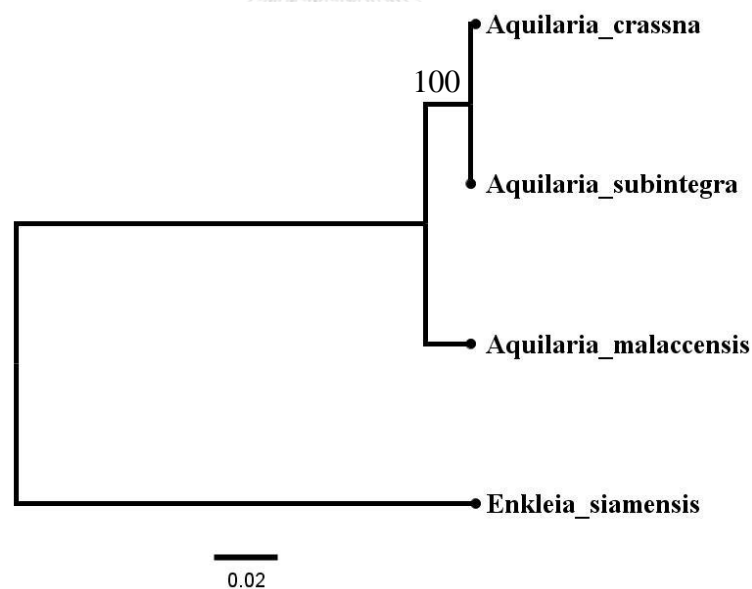


**Figure 64** Molecular phylogenetic analysis by ML method of ITS region

#### 4.3.2.2 Phylogenetic tree of *rbcl* gene

The maximum likelihood tree based on *rbcl* gene partial sequences from these three *Aquilaria* species and *E. siamensis* was displayed in Figure 65 and the highest log likelihood values was found to be -1,834.40. From the dendrogram, *A. crassna* closely related to *A. subintegra*, while *A. malaccensis* was separated in another branch.

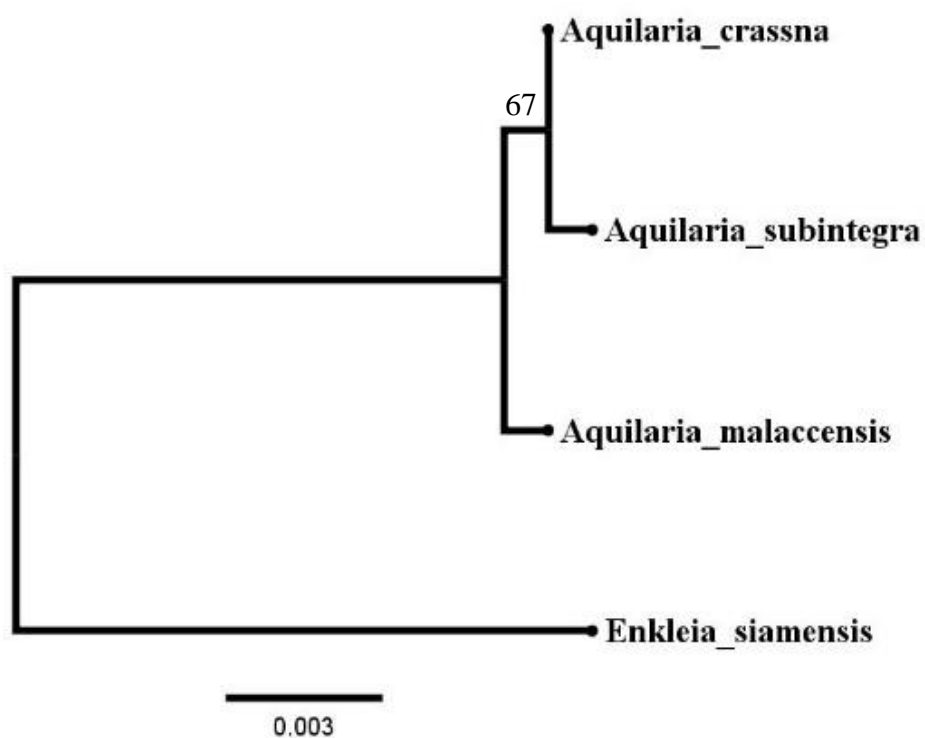


**Figure 65** Molecular phylogenetic analysis by ML method of *rbcl* gene partial sequences

#### 4.3.2.3 Phylogenetic tree of *matK* gene

The maximum likelihood tree based on *matK* gene partial sequences from these three *Aquilaria* species and *E. siamensis* was displayed in Figure 66 and the highest log likelihood values was found to be -1,359.39. From the dendrogram, three *Aquilaria* species were located in the same branch. *A. malaccensis* had longer branch than those two species because of its minor difference in sequence.

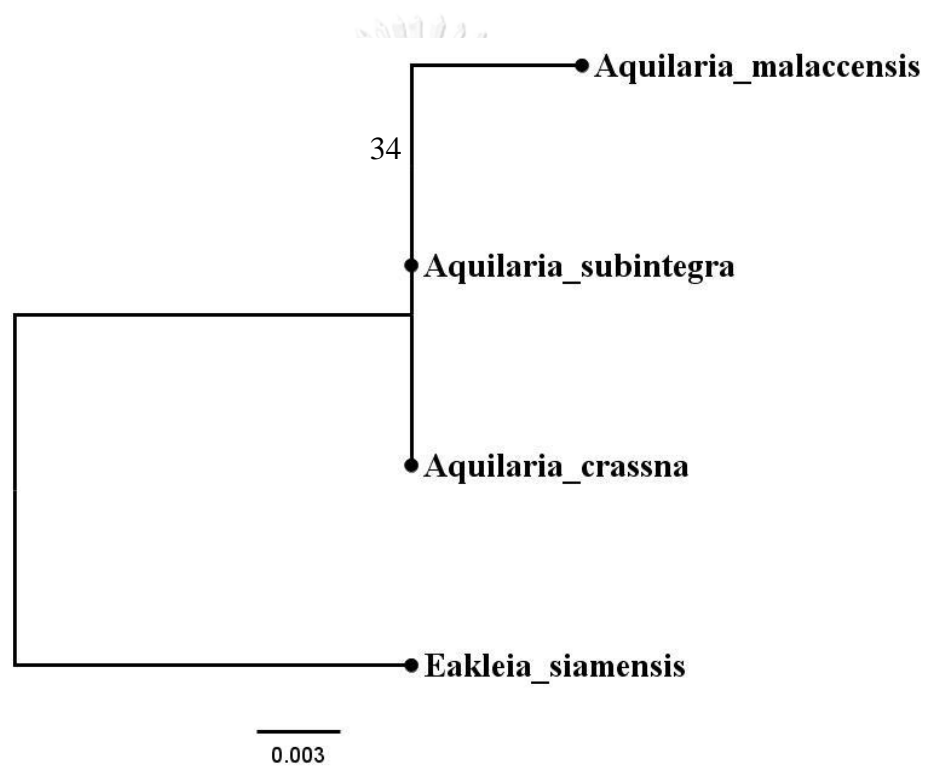


**Figure 66** Molecular phylogenetic analysis by ML method of *matK* gene partial sequences

#### 4.3.2.4 Phylogenetic tree of *psbA-trnH* intergenic spacer

The maximum likelihood tree based on *psbA-trnH* intergenic spacer sequences from these three *Aquilaria* species and *E. siamensis* was displayed in Figure 67 and the highest log likelihood values was found to be -787.18. From the dendrogram, *A. crassna* was closely related to *A. subintegra*, while *A. malaccensis* was separated in another branch.

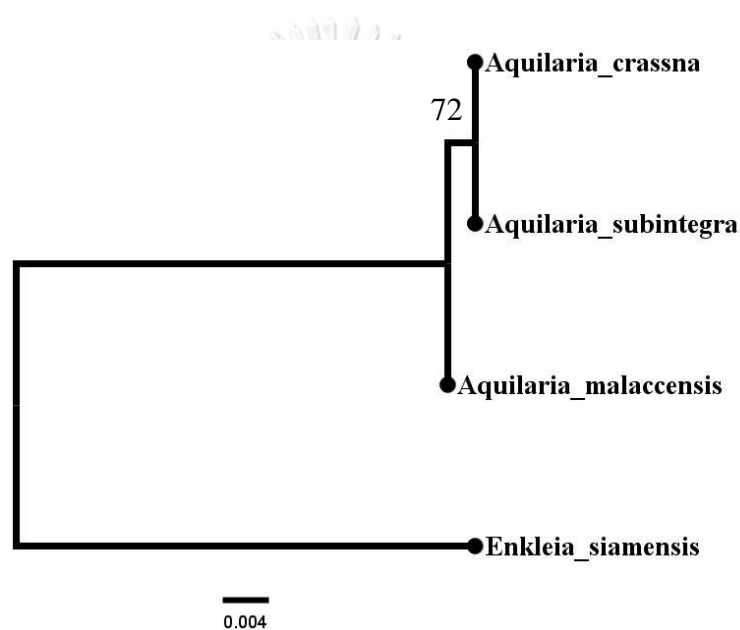


**Figure 67** Molecular phylogenetic analysis by ML method of *psbA-trnH* intergenic spacer sequences

#### 4.3.2.5 Phylogenetic tree of *rpoC1* gene

The maximum likelihood tree based on *rpoC1* gene partial sequences from these three *Aquilaria* species and *E. siamensis* was displayed in Figure 68 and the highest log likelihood values was found to be -805.16. From the dendrogram, three *Aquilaria* species were located in the same branch because its sequences were identical.

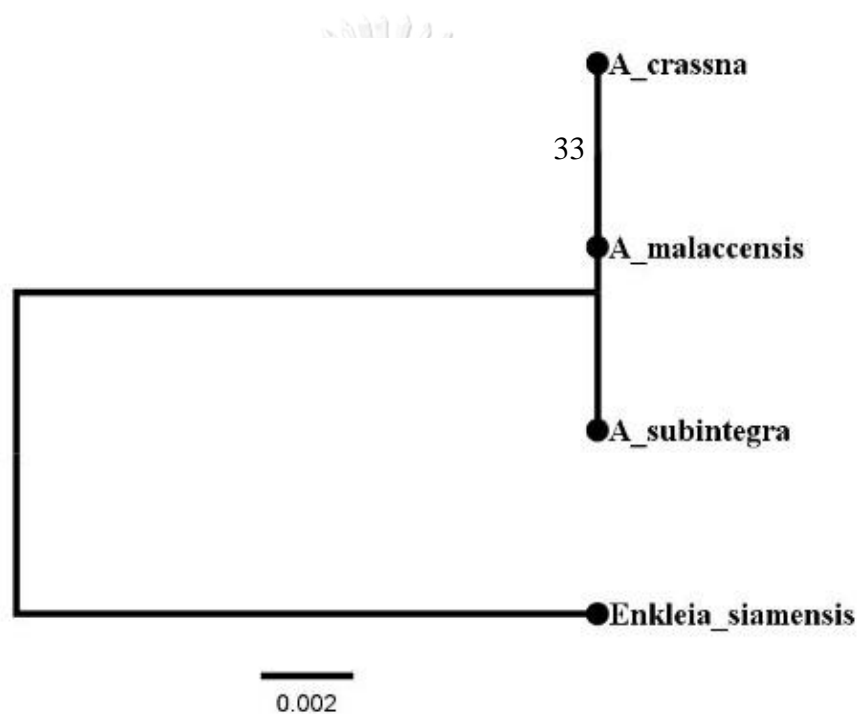


**Figure 68** Molecular phylogenetic analysis by ML method of *rpoC1* gene partial sequences

#### 4.3.2.6 Phylogenetic tree of *ycf1* gene

The maximum likelihood tree based on *ycf1* gene partial sequences from these three *Aquilaria* species and *E. siamensis* was displayed in Figure 69 and the highest log likelihood values was found to be -1,525.74. From the dendrogram, *A. crassna* was closely related to *A. subintegra*, while *A. malaccensis* was separated in another branch.

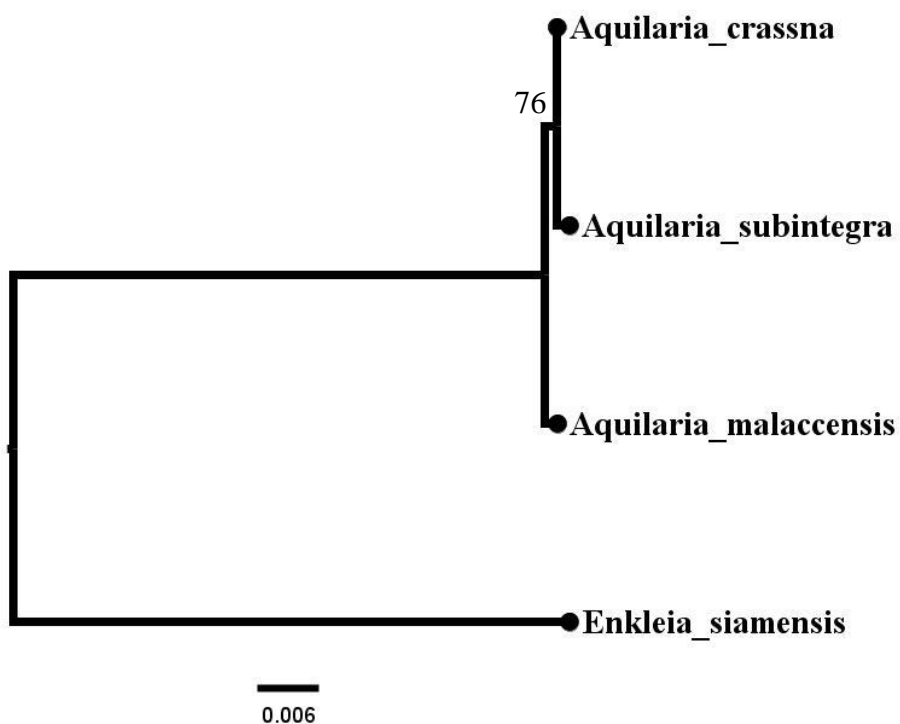
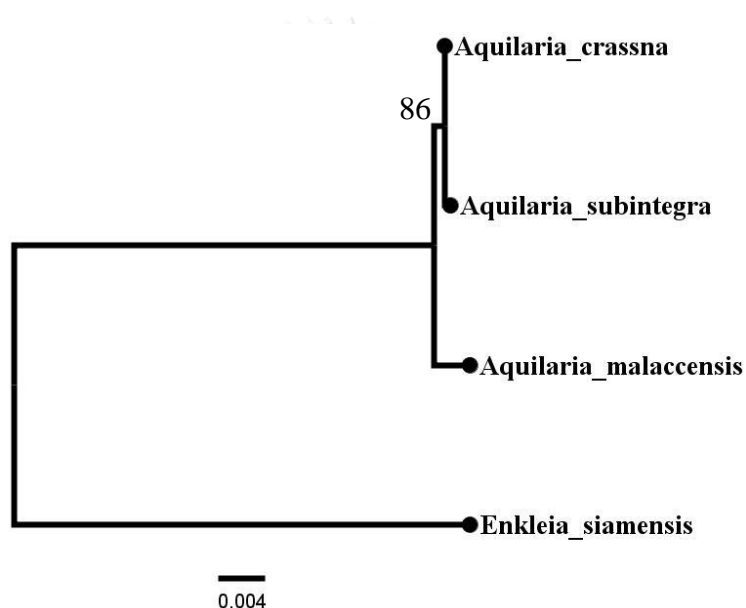


Figure 69 Molecular phylogenetic analysis by ML method of *ycf1* gene partial sequences

#### 4.3.2.6 Phylogenetic tree of combination sequence of chloroplast genome

The maximum likelihood tree based on combination sequence of chloroplast genome; *matK*, *trnH-psbA*, and *ycf1*, from these three *Aquilaria* species and *E. siamensis* was displayed in Figure 70 and the highest log likelihood values was found to be  $-6,319.66$ . From the dendrogram, *A. crassna* was closely related to *A. subintegra*, while *A. malaccensis* was separated in another branch. The genetic distance among these samples were shown in Table 31.



**Figure 70** Molecular phylogenetic analysis by ML method of combination sequence of chloroplast genome

**Table 31** Estimates of evolutionary divergence between combination sequence of chloroplast genome

	<i>A. crassna</i>	<i>A. malaccensis</i>	<i>A. subintegra</i>	<i>E. siamensis</i>
<i>A. crassna</i>				
<i>A. malaccensis</i>	0.0039			
<i>A. subintegra</i>	0.0005	0.0044		
<i>E. siamensis</i>	0.0785	0.0809	0.0791	



## CHAPTER V

### DISCUSSION

Currently, there is an emphasis on the standardization of medicinal plant materials for their therapeutic potentials. The available modern techniques make the identification and evaluation of crude drugs by pharmacognostic studies reliable, accurate and inexpensive. According to WHO, determinations of macroscopic and microscopic characteristics are the first steps towards establishing the identity and the purity of such materials, and these steps should be carried out before any further tests are undertaken.

First of all, this study dealt with the investigation of pharmacognostic specification of *Aquilaria crassna* leaves. Macroscopic characters of *A. crassna* from several sources in this study are slightly differences in length, due to the preparation of these crude drugs in each source, while the microscopic characters are similar. The microscopic characters of *A. crassna* were similar to *A. agallocha* [232], but unicellular trichome was not found in *A. crassna*. The results of these examinations could be beneficial as a basis for correct identification, collection and investigation of the plant. In addition, the constant values of leaf are used as character for identification concerning their constant value in each species. It is interesting to note that the represent data should be used to authenticate the agarwood leaves. These data were the reliable information.

The thin layer chromatographic fingerprinting was performed to identify the individual substances in the mixture and to determine the purity of these substances. The TLC chromatogram showed characteristic fingerprint profiles that could be used as markers for quality evaluation and standardization of crude drug. The  $R_f$  values indicated the position at which the substance was located on chromatogram. The  $R_f$

value is widely recognised as a guide for the identification of medicinal plants. However, it is difficult to obtain exactly reproducible  $R_f$  values as a result of the variety of influences operation during chromatography.

The physicochemical parameters are beneficial for controlling the medicinal plant quality. The investigation of these values is important in ascertaining adulteration or unsuitable management of the herbal drugs. The moisture content was employed to control the water in crude drug. On the other hand, loss on drying controlled the loss in weight (due to water and other volatile materials) of crude drug. The moisture content of the herbal raw materials should be determined and be controlled to make the solution of definite strength. The moisture content of crude drugs should be minimized in order to prevent spoilage due to microbial contamination or decomposition of chemical. The objective of drying of fresh materials was to fix their constituents from the enzymatic or hydrolysis reaction that might alter the chemical composition and to reduce the weight and bulk. The excessive content of water in crude drugs and temperature were the promoter factors of fungal and bacterial growth which caused the spoilage. Therefore, drying should be accomplished as rapidly as possible with good practices.

Total ash analysis is accountable for controlling the purity and quality which indicate the inorganic substances in plant materials after complete incineration. Moreover, acid-insoluble ash defines the acid-insoluble inorganic matters, which can be found in the crude drugs. A high ash value indicates the adulteration, contamination or substitution of plant materials.

The extraction of the crude drug with solvent yields a solution containing many phytochemicals. The water and ethanol extractive values determined the quality and purity of the drug. The determination of ethanol-soluble and water-soluble extractive values were used to control the constituents of crude drugs which inferiority caused

from many factors such as moisture content, temperature, harvesting, drying process, kept duration and storage.

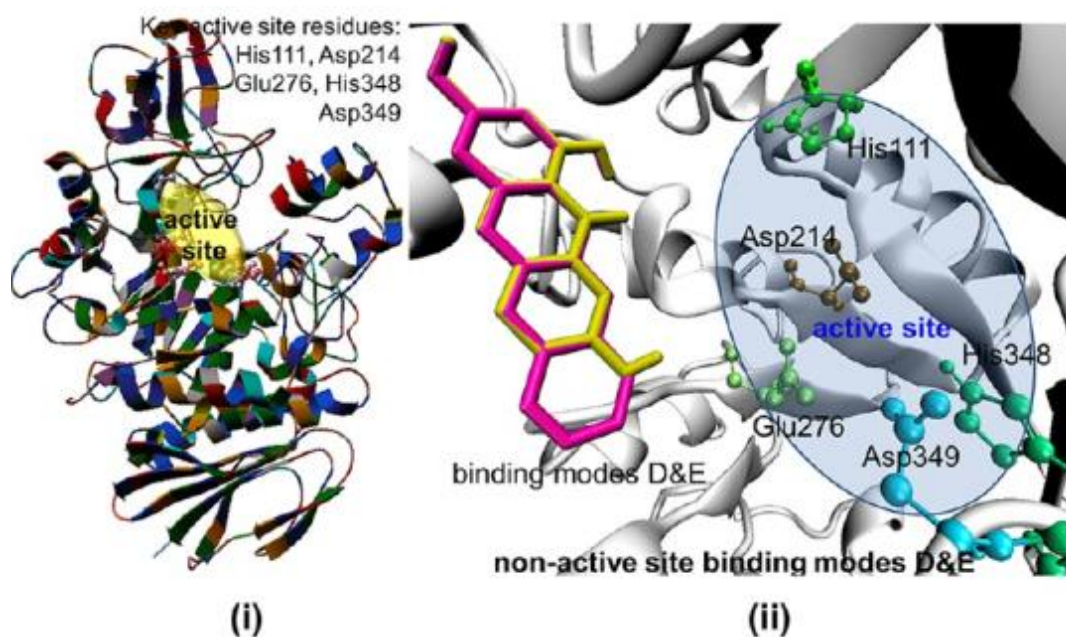
TLC-densitometry is a technique with accuracy and precision for quantitative and qualitative examination in this study. The mangiferin was quantified using the developed TLC-densitometric method. However, the quantitated content were higher than the actual yields (0.0013%) that fractionated by Ray [66]. In addition, the amount of mangiferin of *A. crassna* were closed to *A. sinensis* which performed on HPLC-MS [57]. The difference in mangiferin content may be due to the period of plants, the geographic conditions where the plants are cultivated, the duration of storage, or genetic variations. Moreover, the season of collection and the storage conditions may also lead to fluctuations in the mangiferin content.

Image analysis for quantitation was performed due to its cost effectiveness and simplicity. The image analysis was processed using the TLC chromatogram image, which was then converted from pixel intensity to corresponding peak. The peak area was calculated by ImageJ free software. The quantitative analysis of mangiferin in *A. crassna* leaves using TLC image analysis was developed as well as validated. The amounts of mangiferin in *A. crassna* leaves by these two methods showed no statistically significant difference. The proposed TLC-densitometric and image analysis method were developed and validated for simultaneous quantitative analysis of mangiferin in the ethanolic extracts of *A. crassna* leaves collected from 15 different locations throughout Thailand. Thus, the method could be used for quality control of herbal raw materials as well as extracts.

*A. crassna* has been a part of Ayurvedic, Traditional Chinese Medicine and Traditional Thai Medicine for centuries. The consideration of its side effects, toxicity, and therapeutic levels should determine for therapeutic dose setting. Even though, *A. crassna* leaves tea was claimed by vendor as anticancer and anti-hyperglycemic, but

the scientific experiments are still needed to proof the biological activity and mechanism of action of the herbal product claim.

This study also investigated the effect of Ac14 ethanolic extract and mangiferin on antioxidation activities,  $\alpha$ -glucosidase inhibitory activity, and cytotoxic activity.  $\alpha$ -glucosidase is a membrane-bounded intestinal enzyme that functions as the last step of starch hydrolysis to glucose. From our findings, Ac14 ethanolic extract ( $IC_{50} = 0.5714$  mg/ml) possessed a strong potential as an  $\alpha$ -glucosidase inhibitor to the same degree as other *Aquilaria* species [54, 73]. Moreover, mangiferin ( $IC_{50} = 0.1840$  mg/ml;  $0.4357$  mM) also showed  $\alpha$ -glucosidase inhibitory properties greater than acarbose ( $IC_{50} = 17.3947$  mg/ml;  $26.9432$  mM), which was in accordance with previous reports [18, 54]. In addition, the computational simulation by a molecular docking technique revealed that 1,3-dihydroxybenzoxanthone compound concurrently binded to the non-competitive site of yeast  $\alpha$ -glucosidase (Figure 71) [233]. Therefore, this compound might exhibit a significant synergistic inhibition of glucosidase enzyme.



**Figure 71** The nonactive site binding nodes in  $\alpha$ -glucosidase.

(i) the active site of  $\alpha$ -glucosidase. (ii) the relative position of binding sites, and the active site. 1,3,7-trihydroxyxanthone and 1,3-dihydroxybenzoxanthone are highlighted in yellow and red, respectively [228]

As it is known, some degenerative disorders result from oxidative stress in human cells. The *in vitro* antioxidation assay is signified by the ability to scavenge the free radicals. In this study, Ac14 ethanolic extract ( $IC_{50} = 21.54 \pm 0.17 \mu\text{g/ml}$ ) and mangiferin ( $IC_{50} = 0.64 \pm 0.01$ ) could scavenge the DPPH radical with  $IC_{50}$  values similar to previous reports [5, 64, 66].  $\text{NO}^\cdot$ , an unstable reactive nitrogen species, can be quantitatively determined using Griess reagent, while  $\text{O}_2^{\cdot-}$  is the initiator of various toxic reactive oxygen species which attack the biomolecules, leading to undesirable alterations [234]. This study implied that Ac14 ethanolic extract and mangiferin had the potential as a natural antioxidant by prohibiting RNS and ROS, which might be due to its phenolic properties. Phenolic compounds are comprehended to possess the high anion scavenging capability [235].

The FRAP assay as well as the determination of total phenolic content were the techniques used for evaluation the antioxidation capacity of the testing sample. The capacity of Ac14 ethanolic extract on the FRAP assay and total phenolic content differed from prior research studies because of the extraction procedure, as well as the geographical location of plantation [46]. In addition, the concentration of ethanol and the solid-to-solvent ratio of *A. crassna* leaf extraction had a significant effect on total phenolic content and scavenging activities, whereas, the extraction time had an insignificant effect [73].

MTT assay is a precise and uncomplicated method that provides beneficial information on the anticancer, antiproliferative and cytotoxic determination. This method quantifies the metabolic action of viable cells through the mitochondrial enzyme converting soluble yellow tetrazolium salt to dark blue water-insoluble formazan crystal [118]. The cytotoxic activity of *A. crassna* leaf extract has not been previously investigated, whereas the other parts; oil and stem bark, have been proved as having anticancer activity [236]. From these findings, mangiferin showed a significant cytotoxic effect to MDA-231, HepG2, and HT-29 cells, but  $IC_{50}$  were greater than 100  $\mu\text{g/ml}$ . The previous research mentioned that the 300  $\mu\text{M}$  (126.70  $\mu\text{g/ml}$ ) of mangiferin could inhibit the proliferation of breast cancer cells at a rate of 50% [237]. Therefore, *A. crassna* leaves might be used as an indigenous source for anti-proliferative of colorectal cancer, hepatic cancer and breast cancer but it is still necessary to examine the *in vivo* biological activity in a further study in order to explore the possible use of this plant to treat illness.

Oxidative stress has been identified as a critical pathological process involving the evaluation of atherosclerosis and other cardiovascular diseases. Generally, under the normal conditions, endothelial cells preserve an exquisite equilibrium in the vasculature between the vasodilators and vasoconstrictors by promoting effects of

antioxidation and pro-oxidation and also anti-inflammation and pro-inflammation [238, 239]. Here, the endothelial EA.hy926 cells line was utilized as a model to discuss the *in vitro* anti-oxidation and anti-apoptotic properties of ethanolic extract of *A. crassna* and its metabolite, mangiferin. The EA.hy926 cell line was originated by the merging of human umbilical vein endothelial cells (HUVECs) with the human lung carcinoma cell line A549 [240]. The main factor of cardiovascular disease pathogenesis is induced by the ROS which generated in the endothelium [241]. Evidence suggested that the ROS signal encouraged activities of endothelial cells and influenced cell injury and apoptosis via antioxidant-induced protein and carbohydrate modification, lipid peroxidation, and DNA strand nicks [242]. Administration of H<sub>2</sub>O<sub>2</sub> as a suitable model to deliver and augment intracellular ROS production leads to cellular oxidative stress and persuades cell death [243]. Secondary active metabolites from medicinal plants which have potentially potent antioxidant capability had been utilized to reduce oxidative stress-induced injury [244-246]. Results indicated that intracellular ROS in EA.hy926 cell under H<sub>2</sub>O<sub>2</sub>-treated oxidative stress was significantly decreased by mangiferin in dose-dependent manner. This suggested that the protective effect of mangiferin might be concerned with the suppression of intracellular ROS production. Unfortunately, the ethanolic extract of *A. crassna* significantly augmented the intracellular ROS production. This could lead an imbalance in oxidative stress and anti-oxidation defense; thus, the cells were damaged by excessive oxidative stress and possible apoptosis [247, 248].

Superoxide dismutase (SOD) is a vital antioxidation enzyme that can defend the oxidative stress-induced injury in endothelial cells [249]. The reaction mechanism of SOD acts to remove superoxide by considerably expediting its conversion to hydrogen peroxide which is then eliminated by glutathione peroxidase (GPx) and catalase to water [231, 250].

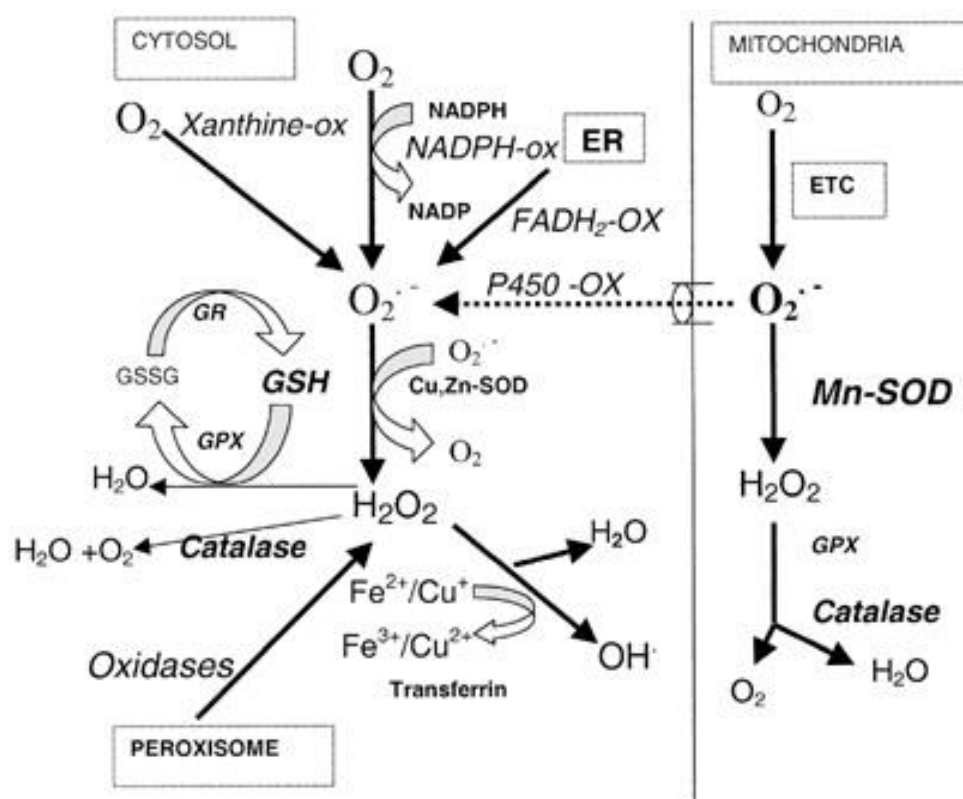


**Figure 72** The generation of ROS and endogenous antioxidant mechanism [94]

In Western blotting analysis, mangiferin increase the expression of SOD-1 when compared to the vehicle control and H<sub>2</sub>O<sub>2</sub>-treated control; however, the trend of expression level was decline in dose-dependent manner. Thus, our results demonstrated the cytoprotective ability of mangiferin. This may be ascribed to quenching of the ROS generated in the cells owing to oxidative stress induced by H<sub>2</sub>O<sub>2</sub>. In addition, various reports mentioned that mangiferin showed the cytoprotective effects against chemical-induced toxicity, such as cyclophosphamide in myocardial tissue and mercury in HepG2 cells [251, 252].

The heme oxygenase system is a regulator of endothelial cell integrity and oxidative stress [253, 254]. Evidences suggested that HO-1 is powerfully induced by oxidative stress and its substrate heme. The capability of HO-1 proposes a



compensating system to oxidative stress injury [255]. A previous study founded that the expression of HO-1 in human HL60 myeloid leukemia cells was enhanced by mangiferin [256], while this study determined that mangiferin induced the expression of HO-1 protein in EA.hy926 cells. In addition, other research indicated that mangiferin also activated Nrf2 signaling and upregulated NQO1 expression in detoxification pathway [257]. Mangiferin may, therefore, provide some advantage through the activation of HO-1 protein in cellular detoxification mechanism. Nevertheless, the trend of HO-1 expression level was decreasee in dose-dependent manner. Reduction of HO-1 expression level when increasing the amount of mangiferin might associate with the result of intracellular ROS. This implies that mangiferin potentially decrease the cellular oxidative stress and induce decline in HO-1 expression levels.

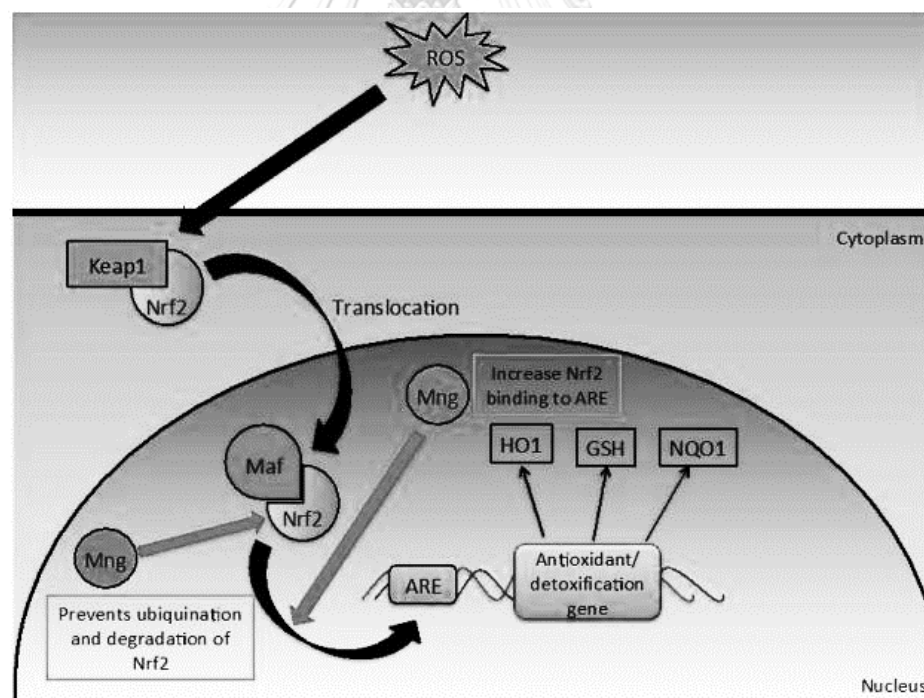


**Figure 73** The effect of mangiferin on Nrf2/ARE detoxification pathway [19]

To probe the mechanism of mangiferin protecting EA.hy926 cells from H<sub>2</sub>O<sub>2</sub>-induced apoptosis, the expression of apoptosis-related proteins; Bcl-2 and Bax, was investigated. The Bcl-2 protein family, a significant regulator of apoptotic mechanism, comprised of anti-apoptotic proteins such as Bcl-2, Bcl-XL, and Bfl-1, and pro-apoptotic proteins such as Bax, Bak, Bid and Bad [258]. The steadiness of pro-apoptotic Bax and anti-apoptotic Bcl-2 is understood to be crucial in cell death or survival determination [259]. This study demonstrated that pretreatment with mangiferin increased the Bcl-2 expression with dose-dependent manner, while the Bax expression was reduced compared to the H<sub>2</sub>O<sub>2</sub>-treated control. This result concurred with Kavitha who concluded that mangiferin could prevent 1-methyl-4-phenyl-1,2,3,6-tetrahydropyridine-induced apoptosis in mouse model [260]. Conversely, Pan *et al.* discovered that mangiferin down-regulated the mRNA and protein expression levels of Bcl-2, and up-regulated Bax in CNE2 nasopharyngeal carcinoma cells [261]. As a results, mangiferin led to augmented apoptosis. In addition, the Bcl-2/Bax ratio play a vital role in determining whether cells undergo apoptosis [262]. This ratio controls the release of cytochrome C from mitochondria to cytosol, associated with the caspase cascade activation [263]. The caspase-3 plays a key role in apoptosis process. Here, Western blotting analysis showed that mangiferin was able to arouse the expression of Bcl-2 protein, but constrain the expression of Bax protein which increased the Bcl-2/Bax ratio. Thus, mangiferin protects EA.hy926 against H<sub>2</sub>O<sub>2</sub>, probably *via* regulation of mitochondria apoptotic mechanism.

Lastly, *Aquilaria* is a genus of endangered flowering plants which are a part from Thymelaeaceae family. Currently, the environmental source of agarwood typically impacts consumer preference. This is mostly suggestive of the species maturing in specific areas and, as a result, the expected quality of agarwood resin. Since merchants and potential buyers think agarwood is derived from a distinctive

*Aquilaria* species and has characteristic fragrance with therapeutic features, the market prices are settled accordingly. As an example, the pleasantness of agarwood from *A. crassna* when burnt is favored for certain ceremonies [264], while those living in the Middle East tend to prefer essential oils taken from *A. malaccensis* due to its robust smell compared to other species [265]. Thus, a vital act for ensuring quality for a client is the validation step. Also typically employed for plant validation together with chemical profile assessments are morphological examinations and cytological determinations [27, 266]. Then again, CITES has been proposed for improvement of the *Aquilaria* species classification process, which is primarily based on floral and fruit attributes compared to other methods and relies on a fast and precise detection system [267].

The molecular techniques are utilized productively to support the morphological information for the authentication process [268]. DNA barcoding is an approved molecular technique which uses a short region as a barcoding region for species discrimination [34, 269]. DNA barcoding is recognized as a powerful technique for species discrimination in plants, and also enables experts to resolve the relationships among taxa, forensic identification, and species authentication of endangered species and medicinal plant materials [43, 270].

The CBOL Plant Working Group recommended *rbcL* and *matK* gene as a plant barcode to identifying plants at species-level [271]. In this study, the results from the phylogenetic tree reconstruction of the *rbcL* gene among *Aquilaria* species found that *A. malaccensis* was separated from those two species but the genetic distances were insignificantly different. Thus, the *rbcL* gene barcode was unsuitable for species identification because of its low discrimination power. While the genetic distance of the *matK* gene sequences in *A. crassna* and *A. subintegra*, which was calculated based on a sequences comparison, could explain why these two species were so closely

related (D value = 0.000). However, *A. malaccensis* displayed a slight difference from those two species (D value = 0.002). These two recommended barcoding regions were unsuitable for use as *Aquilaria* species identification. In addition, this implication conformed to Jiao *et al.*'s conclusion [272], which noted that the *rbcL* and *matK* sequence data among *A. sinensis* and close species was unsuitable for cladogram reconstruction as well as species identification.

The non-coding *psbA-trnH* spacer region was also endorsed as a global land plant barcode that could be utilized for discrimination at species-level [273]. Our results revealed that the genetic distance of intergenic spacer of *psbA-trnH* was similar to the result from *matK* gene, but the phylogenetic tree characteristic was different due to the percentage variable regions. In addition, the positions of the variable site and their percentages were critical for phylogenetic tree reconstruction [274]. So, our results implied that *psbA-trnH* intergenic spacer was unsuitable for *Aquilaria* species identification owing to its low discrimination power.

In addition, Chase *et al.* (2007) suggested that the combination of two plastid barcoding regions among the *matK* gene, non-coding region of *psbA-trnH*, *rpoB*, and the *rpoC* gene were suitable for land plants [275]. It was mentioned that the *rpoC1* gene sequences could be utilized for the determination of universality and/or sequence quality [271]. In our work, all *Aquilaria* sequences were also identical in each one of the nucleotides. The *rpoC1* region was unsuitable for species authentication because of its non-existent discrimination power; however, it could be used as a quality control marker from a high percentage of successfully amplified and sequenced properties.

Recently, the *ycf1* gene has been proposed as an effective barcoding marker because this gene was conserved but showed high amount of variables in angiosperm [276]. This gene could potentially be used for phylogenetic determination in various

plants, such as pines [277], orchids [203]. In ML tree analysis, each of the species was separated into branches with a high bootstrap value. This gene was an interesting cpDNA barcoding region in *Aquilaria* species discrimination due to the variable regions, but the genetic distances among *Aquilaria* species were too low. So, only the cpDNA barcode region was inappropriate to use for identifying *Aquilaria* plants which is in agreement with the previous findings [278]. The combination of three barcoding regions; *matK*, *psbA-trnH* intergenic spacer, and *ycf1*, determined the genetic relationship using ML tree, but it exhibited low genetic distances. Thus, the only one loci or combination loci of *matK*, *trnH-psbA*, and *ycf1* region can be classified into only two groups; *A. malaccensis* and a group of both *A. crassna* and *A. subintegra*.

The nuclear DNA not only performs as a barcoding loci, but it is also used for molecular systematic investigation in species-level identification [36]. The internal transcribed spacer (ITS) region among the nuclear ribosomal cistron is recommended as probable barcoding in plants, fungi, and bacteria [279, 280]. In our work, there were some variable sites which could be utilized in the specification of different species which were able to distinctly separate *A. malaccensis* apart from those two species. The genetic distance from *A. crassna* and *A. subintegra* sequences, in comparison, was too low, but some variable sites could be used for distinguishing at species-level. Thus, the ITS region was an optimum tool for resolving the *Aquilaria* species-level discrimination according to previous reports [272, 281]. Nevertheless, there were some concerns about using ITS as a barcoding region because ITS region could quickly evolve and require neighboring locus (5.8S) for the determination of the sequence comparative relation [36]. However, each barcoding locus could be suitable for genus discrimination (among *Aquilaria* and *Enkleia*) in Thymelaeaceae family because there was a high genetic distance and the branch of *Enkleia* in each tree was isolated from the group of *Aquilaria*.

## CHAPTER VI

### CONCLUSION

The results obtained from this study will play a significant role in setting standards for this medicinal plant. This study provides useful information for the identification of *A. crassna* leaves and will help those who handle this plant to maintain its quality. Thus, the standards and the barcoding loci sequences presented in this study will help minimize the adulteration of *A. crassna* samples and will be of great use for researchers in selecting correct herbal specimens. The establishment of the *Aquilaria* species DNA barcoding database is beneficial to the application of the authentication step of traditional medicine uses, thus, it also increases the medical practitioners' overall confidence in terms of therapeutic outcomes and safety profiles. The results of this investigation may be useful in the preparation of a monograph for this plant. In addition, this present study projected the scientific efficacy evaluation including *in vitro* antioxidant, anti-diabetic, cytotoxicity activities, and the cytoprotective properties of *A. crassna* leaves and mangiferin.



## REFERENCES

1. คณะกรรมการพัฒนาระบบยาแห่งชาติ, บัญชียาหลักแห่งชาติ พ.ศ. 2560. Vol. 134 ตอนพิเศษ 119 ง 2560: ราชกิจจานุเบกษา.
2. Department of medical sciences, Ministry of Public Health, *Thai Herbal Pharmacopoeia 2016*. 2016, Bangkok: The agricultural co-operative federation of Thailand, Ltd.
3. ZY., S., *Modern research on Chinese herbal medicine*. 1997, Beijing, China: Peking medical college and Peking union medical college associated press.
4. Pranakhon, R., Pannangpetch, P., and Aromdee, C., *Antihyperglycemic activity of agarwood leaf extracts in STZ-induced diabetic rats and glucose uptake enhancement activity in rat adipocytes*. Songklanakarin Journal of Sciences and Technology, 2011. **33**(4): p. 405-410.
5. Sattayasai, J., et al., *Antipyretic, analgesic and anti-oxidative activities of Aquilaria crassna leaves extract in rodents*. J Ayurveda Integr Med, 2012. **3**(4): p. 175-9.
6. Huda, A., et al., *Antioxidant activity of Aquilaria malaccensis (thymelaeaceae) leaves*. Pharmacognosy Research, 2009. **1**(5): p. 270-273.
7. Kakino, M., et al., *Agarwood induced laxative effects via acetylcholine receptors on loperamide-induced constipation in mice*. Biosci Biotechnol Biochem, 2010. **74**(8): p. 1550-5.
8. Kakino, M., et al., *Agarwood (Aquilaria crassna) extracts decrease high-protein high-fat diet-induced intestinal putrefaction toxins in mice*. Pharmaceutical analysis acta, 2012. **3**: p. 152.
9. Ray, G., Leelamanit W, Sithisarn P, Jiratchariyakul W., *Antioxidative Compounds from Aquilaria crassna Leaf*. Mahidol J Pharm Sci, 2014. **41**(4): p. 54-58.
10. Anila, L. and Vijayalakshmi, N.R., *Flavonoids from Emblica officinalis and Mangifera indica-effectiveness for dyslipidemia*. J Ethnopharmacol, 2002. **79**(1): p. 81-7.
11. Djemgou, P.C., et al., *C-Glucoside xanthone from the stem bark extract of Bersama engleriana*. Pharmacognosy Res, 2010. **2**(4): p. 229-32.
12. Gururaja, G.M., et al., *Cholesterol esterase inhibitory activity of bioactives from leaves of Mangifera indica L*. Pharmacognosy Res, 2014. **7**(4): p. 355-62.
13. Nag G., et al., *Antioxidant, anti-acetylcholinesterase and anti-glycosidase properties of three species of Swertia, their xanthenes and amarogentin: A comparative study*. Pharmacognosy journal, 2015. **7**(2): p. 117-123.
14. Ichiki, H., et al., *New antidiabetic compounds, mangiferin and its glucoside*. Biol Pharm Bull, 1998. **21**(12): p. 1389-90.

15. Muruganandan, S., et al., *Effect of mangiferin on hyperglycemia and atherogenicity in streptozotocin diabetic rats*. Journal of ethnopharmacology, 2005. **97**(3): p. 497-501.
16. Dineshkumar, B., Mitra, A., and Manjunatha, M., *Studies on the anti-diabetic and hypolipidemic potentials of mangiferin (xanthone glucoside) in streptozotocin-induced type 1 and type 2 diabetic model rats*. International Journal of Advances in Pharmaceutical Sciences, 2010. **1**(1): p. 75-85.
17. Kumar, B.D., et al., *Effect of Mangiferin and Mahanimbine on Glucose Utilization in 3T3-L1 cells*. Pharmacogn Mag, 2013. **9**(33): p. 72-5.
18. Ganogpichayagrai, A., Palanuvej, C., and Ruangrunsi, N., *Antidiabetic and anticancer activities of Mangifera indica cv. Okrong leaves*. J Adv Pharm Technol Res, 2017. **8**(1): p. 19-24.
19. Gold-Smith, F., Fernandez, A., and Bishop, K., *Mangiferin and Cancer: Mechanisms of Action*. Nutrients, 2016. **8**(7).
20. Luczkiewicz, P., et al., *Mangiferin: A promising therapeutic agent for rheumatoid arthritis treatment*. Med Hypotheses, 2014. **83**(5): p. 570-4.
21. Sato, T., et al., *Mechanism of antioxidant action of pueraria glycoside (PG)-1 (an isoflavonoid) and mangiferin (a xanthonoid)*. Chem Pharm Bull (Tokyo), 1992. **40**(3): p. 721-4.
22. Vyas, A., et al., *Perspectives on medicinal properties of mangiferin*. Mini Rev Med Chem, 2012. **12**(5): p. 412-25.
23. Telang, M., et al., *Therapeutic and cosmetic applications of mangiferin: a patent review*. Expert Opin Ther Pat, 2013. **23**(12): p. 1561-80.
24. Leiro, J., et al., *Expression profiles of genes involved in the mouse nuclear factor-kappa B signal transduction pathway are modulated by mangiferin*. Int Immunopharmacol, 2004. **4**(6): p. 763-78.
25. P.K., M., *Quality Control of Herbal Drugs*. 2002, New Delhi, India: Business Horizons.
26. Singh, M.P. and Sharma, C.S., *Pharmacognostical evaluation of Terminalia chebula fruits on different market samples*. International journal of ChemTech Research, 2010. **2**: p. 57-61.
27. Thitikornpong, W., Phadungcharoen, T., and Sukrong, S., *Pharmacognostic evaluations of Lagerstroemia speciosa leaves*. Journal of Medicinal Plants Research, 2011. **5**(8): p. 1330-1337.
28. Pferschy-Wenzig, E.M. and Bauer, R., *The relevance of pharmacognosy in pharmacological research on herbal medicinal products*. Epilepsy & Behavior, 2015. **52**: p. 344-362.



29. Mishra, P., *et al.*, *DNA barcoding: an efficient tool to overcome authentication challenges in the herbal market*. *Plant Biotechnology Journal*, 2016. **14**(1): p. 8-21.
30. Parveen, I., *et al.*, *DNA Barcoding for the Identification of Botanicals in Herbal Medicine and Dietary Supplements: Strengths and Limitations*. *Planta Med*, 2016. **82**(14): p. 1225-35.
31. Pawar, R.S., *et al.*, *Assessment of the Authenticity of Herbal Dietary Supplements: Comparison of Chemical and DNA Barcoding Methods*. *Planta Med*, 2017. **83**(11): p. 921-936.
32. Ying, L., *et al.*, *DNA markers in the authentication of Traditional Chinese Medicine*. *Journal of Medicinal Plants Research*, 2014. **8**(2): p. 121-127.
33. Ganie, S.H., *et al.*, *Authentication of medicinal plants by DNA markers*. *Plant Gene*, 2015. **4**: p. 83-99.
34. Hebert, P.D.N., *et al.*, *Biological identifications through DNA barcodes*. *Proceedings of the Royal Society B-Biological Sciences*, 2003. **270**(1512): p. 313-321.
35. Che, J., *et al.*, *Universal COI primers for DNA barcoding amphibians*. *Mol Ecol Resour*, 2012. **12**(2): p. 247-58.
36. Kress, W.J., *et al.*, *Use of DNA barcodes to identify flowering plants*. *Proceedings of the National Academy of Sciences of the United States of America*, 2005. **102**(23): p. 8369-8374.
37. Kress, W.J. and Erickson, D.L., *A two-locus global DNA barcode for land plants: the coding *rbcl* gene complements the non-coding *trnH-psbA* spacer region*. *Plos One*, 2007. **2**(6): p. e508.
38. Hollingsworth, P.M., *et al.*, *A DNA barcode for land plants*. *Proceedings of the National Academy of Sciences of the United States of America*, 2009. **106**(31): p. 12794-12797.
39. Yao, H., *et al.*, *Use of ITS2 region as the universal DNA barcode for plants and animals*. *Plos One*, 2010. **5**(10).
40. Hollingsworth, P.M., Graham, S.W., and Little, D.P., *Choosing and using a plant DNA barcode*. *Plos One*, 2011. **6**(5): p. e19254.
41. Li, D.Z., *et al.*, *Comparative analysis of a large dataset indicates that internal transcribed spacer (ITS) should be incorporated into the core barcode for seed plants*. *Proceedings of the National Academy of Sciences of the United States of America*, 2011. **108**(49): p. 19641-19646.
42. Techen, N., *et al.*, *The use of polymerase chain reaction (PCR) for the identification of Ephedra DNA in dietary supplements*. *Planta Medica*, 2006. **72**(3): p. 241-247.

43. Li, X.W., *et al.*, *Plant DNA barcoding: from gene to genome*. Biological Reviews, 2015. **90**(1): p. 157-166.
44. The Plant List. *Aquilaria* - *The Plant List* 2013 July 19, 2017; Available from: <http://www.theplantlist.org/1.1/browse/A/Thymelaeaceae/Aquilaria/>.
45. Peterson, B., *Thymelaeaceae*, in *Flora of Thailand Volume 6 Part 3*, T. Santisuk and K. Larsen, Editors. 1997, Diamond printing Co., Ltd.: Bangkok. p. 226-232.
46. Kamonwannasit, S., *et al.*, *Antibacterial activity of Aquilaria crassna leaf extract against Staphylococcus epidermidis by disruption of cell wall*. Annals of Clinical Microbiology and Antimicrobials, 2013. **12**.
47. Khalil, A.S., *et al.*, *Characterization of methanolic extracts of agarwood leaves* Journal of Applied and Industrial Sciences, 2013. **1**(3): p. 78-88.
48. Nik Noor Asma Nik Wil, *et al.*, *In vitro antioxidant activity and phytochemical screening of Aquilaria malaccensis leaf extracts*. Journal of Chemical & Pharmaceutical Research, 2014. **6**(12): p. 688-693.
49. Dash, M., Patra, J.K., and Panda, P.P., *Phytochemical and antimicrobial screening of extracts of Aquilaria agallocha Roxb*. African Journal of Biotechnology, 2008. **7**(20): p. 3531-3534.
50. Huda, A.W.N., *et al.*, *Antioxidant activity of Aquilaria malaccensis (thymelaeaceae) leaves*. Pharmacognosy Research, 2009. **1**(5): p. 270-273.
51. Nie, C., *et al.*, *Studies on chemical constituents of leaves of Aquilaria sinensis*. Zhongguo Zhong Yao Za Zhi, 2009. **34**: p. 858-860.
52. Wang, H.G., *et al.*, *Antitumor constituents from the leaves of Aquilaria sinensis (Lour.) Gilg*. Chemistry and industry of forest products, 2008. **28**: p. 1-5.
53. Kang, Y.F., *et al.*, *Secondary Metabolites from the Leaves of Aquilaria sinensis*. Chemistry of Natural Compounds, 2014. **50**(6): p. 1110-1112.
54. Feng, J., Yang, X.W., and Wang, R.F., *Bio-assay guided isolation and identification of alpha-glucosidase inhibitors from the leaves of Aquilaria sinensis*. Phytochemistry, 2011. **72**(2-3): p. 242-247.
55. Li, C.T., *et al.*, *Secondary metabolites from the leaves of Aquilaria agallocha*. Journal of advances in chemistry, 2015. **11**(3): p. 3552-3556.
56. Qi, J., *et al.*, *Flavonoid and a rare benzophenone glycoside from the leaves of Aquilaria sinensis*. Chem Pharm Bull (Tokyo), 2009. **57**(2): p. 134-7.
57. Yu, Q., *et al.*, *Qualitative and quantitative analysis of phenolic compounds in the leaves of Aquilaria sinensis using liquid chromatography-mass spectrometry*. Phytochemical analysis, 2013. **24**(4): p. 349-356.

58. Xia, F., *et al.*, *Further chemical investigation of leaves of Aquilaria sinensis*. Zhongguo Zhong Yao Za Zhi, 2013. **38**: p. 3299–3303.
59. Hara, H., *et al.*, *Laxative effect of agarwood leaves and its mechanism*. Bioscience Biotechnology and Biochemistry, 2008. **72**(2): p. 335-345.
60. Ito, T., *et al.*, *Identification of phenolic compounds in Aquilaria crassna leaves via liquid chromatography-electrospray ionization mass spectroscopy*. Food science and technology research, 2012. **18**(2): p. 259-262.
61. Kakino, M., *et al.*, *Agarwood Induced Laxative Effects via Acetylcholine Receptors on Loperamide-Induced Constipation in Mice*. Bioscience Biotechnology and Biochemistry, 2010. **74**(8): p. 1550-1555.
62. Ito, T., *et al.*, *Quantification of polyphenols and pharmacological analysis of water and ethanol-based extracts of cultivated agarwood leaves*. Journal of nutritional science and vitaminology, 2012. **58**(2): p. 136-142.
63. Pranakhon, R., Aromdee, C., and Pannangpetch, P., *Effects of iriflophenone 3-C--glucoside on fasting blood glucose level and glucose uptake*. Pharmacognosy Magazine, 2015. **11**(41): p. 82-89.
64. Tay, P.Y., *et al.*, *Assessment of extraction parameters on antioxidant capacity, polyphenol content, epigallocatechin gallate (EGCG), epicatechin gallate (ECG) and iriflophenone 3-C-beta-glucoside of agarwood (Aquilaria crassna) young leaves*. Molecules, 2014. **19**(8): p. 12304-12319.
65. Sun, J., *et al.*, *Five new benzophenone glycosides from the leaves of Aquilaria sinensis (Lour.) Gilg*. Chinese Chemical Letters, 2014. **25**(12): p. 1573-1576.
66. Ray, G., *et al.*, *Antioxidative compounds from aquilaria crassna leaf*. Mahidol university journal of pharmaceutical sciences, 2014. **41**(4): p. 54-58.
67. Qi, J., *et al.*, *Flavonoid and a rare benzophenone glycoside from the leaves of Aquilaria sinensis*. Chemical and pharmaceutical bulletin, 2009. **57**(2): p. 134-137.
68. Lu, J.J., *et al.*, *Antioxidant activity and structure–activity relationship of the flavones from the leaves of Aquilaria sinensis*. Chinese journal of natural medicines, 2008. **6**(6): p. 456-460.
69. Feng, J. and Yang, X., *Constituents from the leaves of Aquilaria sinensis*. Zhongguo Zhong Yao Za Zhi, 2012. **37**(2): p. 230-234.
70. Yang, X.B., *et al.*, *Aquisiflavoside, a new nitric oxide production inhibitor from the leaves of Aquilaria sinensis*. Journal of asian natural products research, 2012. **14**(9): p. 867-872.
71. Feng, J. and Yang, X., *Liposolubility constituents from leaves of Aquilaria sinensis*. Zhongguo Zhong Yao Za Zhi 2011. **36**: p. 2092-2095.

72. Khalil, A.S., *et al.*, *Characterization of methanolic extracts of agarwood leaves*. Journal of applied and industrial sciences, 2013. **1**(3): p. 78-88.
73. Zulkiflie, N.L., *et al.* *Antidiabetic activities of Malaysian agarwood (Aquilaria spp.) leaves extract*. in *National Conference On Industry-Acamedia Initiative in Biotechnology (CIA:BIOTECH 2013)*. 2013. Pahang, Malaysia.
74. Jiang, S. and Tu, P., *Effects of 95% ethanol extract of Aquilaria sinensis leaves on hyperglycemia in diabetic db/db mice*. Journal of chinese pharmaceutical sciences, 2011. **20**: p. 609-614.
75. Zhou, M.H., *et al.*, *Antinociceptive and anti-inflammatory activities of Aquilaria sinensis (Lour.) Gilg. leaves extract*. Journal of Ethnopharmacology, 2008. **117**(2): p. 345-350.
76. Hashim, Y.Z.H.Y., Ismail, N.I., and Abbas, P., *Analysis of chemical compounds of agarwood oil from different species by gas chromatography mass spectrometry (GCMS)*. International islamic university malaysia engineering journal, 2014. **15**: p. 55-60.
77. Bahrani, H., *et al.*, *Isolation and Characterisation of Acetylcholinesterase Inhibitors from Aquilaria subintegra for the Treatment of Alzheimer's Disease (AD)*. Current Alzheimer Research, 2014. **11**(2): p. 206-214.
78. Vakati, K., *et al.*, *Evaluation of hepatoprotective activity of ethanolic extract of Aquilaria agallocha leaves (EEAA) against CCl4 induced hepatic damage in rat*. Scholars Journal of Applied Medical Sciences, 2013. **1**(1): p. 9-12.
79. Kakino, M., *et al.*, *Laxative effects of agarwood on low-fiber diet-induced constipation in rats*. BMC Complementary and Alternative Medicine, 2010. **10**.
80. Information, N.C.f.B. *Pubchem Compound Database; CID=5281647, Mangiferin*. 2005 [cited 2017 July 19 ]; Available from: <http://pubchem.ncbi.nlm.nih.gov/compound/5281647>.
81. Matkowski, A., *et al.*, *Mangiferin - a bioactive xanthonoid, not only from mango and not just antioxidant*. Mini-reviews in medicinal chemistry, 2013. **13**(3): p. 439-455.
82. Sekar, M., *Molecules of interest – Mangiferin – A review*. Annual Research & Review in Biology, 2015. **5**(4): p. 307-320.
83. Zhang, B.P., Fang, J., and Chen, Y., *Antioxidant effect of mangiferin and its potential to be a cancer chemoprevention agent*. Letters in Drug Design & Discovery, 2013. **10**(3): p. 239-244.
84. Benard, O. and Chi, Y.L., *Medicinal properties of mangiferin, structural features, derivative synthesis, pharmacokinetics and biological activities*. Mini-Reviews in Medicinal Chemistry, 2015. **15**(7): p. 582-594.

85. Jyotshna, Khare, P., and Shanker, K., *Mangiferin: A review of sources and interventions for biological activities*. Biofactors, 2016. **42**(5): p. 504-514.
86. Lauricella, M., et al., *Multifaceted Health Benefits of Mangifera indica L. (Mango): The Inestimable Value of Orchards Recently Planted in Sicilian Rural Areas*. Nutrients, 2017. **9**(5).
87. Organization, W.H., *Quality control methods for herbal materials*. 2011, Geneva: World Health Organization.
88. Joshi, D.D., *Herbal Drugs and Fingerprints*. TLC: Herbal Drugs and Fingerprints. 2012, India: Springer.
89. Sherma, J., *Thin layer chromatographic*. 2005, New York: Marcel Dekker.
90. Stroka, J., Spangenberg, B., and Anklam, E., *New approaches in TLC-densitometry*. Journal of Liquid Chromatography & Related Technologies, 2002. **25**(10-11): p. 1497-1513.
91. CAMAG. *CAMAG TLC SCANNER 4*. 2017 [cited 2017 July 21, 2017]; Available from: [http://www.camag.com/en/tlc\\_hptlc/products/evaluation\\_documentation\\_tlc-ms\\_bioluminenscence/tlc\\_scanner\\_4.cfm](http://www.camag.com/en/tlc_hptlc/products/evaluation_documentation_tlc-ms_bioluminenscence/tlc_scanner_4.cfm).
92. Ferreira, T. and Rasband, W. *ImageJ User Guide*. 2012; IJ 1.46r:[Available from: <https://imagej.nih.gov/ij/docs/guide/user-guide.pdf>].
93. Martindale, J.L. and Holbrook, N.J., *Cellular response to oxidative stress: Signaling for suicide and survival*. Journal of Cellular Physiology, 2002. **192**(1): p. 1-15.
94. Willcox, J.K., Ash, S.L., and Catignani, G.L., *Antioxidants and prevention of chronic disease*. Critical Reviews in Food Science and Nutrition, 2004. **44**(4): p. 275-295.
95. Serafini, M., *Back to the origin of the 'antioxidant' hypothesis: the lost role of the antioxidant network in disease prevention*. Journal of Food and Agriculture, 2006. **86**(13): p. 1989-1991.
96. Nordberg, J. and Arner, E.S., *Reactive oxygen species, antioxidants, and the mammalian thioredoxin system*. Free Radic Biol Med, 2001. **31**(11): p. 1287-312.
97. Droge, W., *Free radicals in the physiological control of cell function*. Physiological Reviews, 2002. **82**(1): p. 47-95.
98. Lu, J. and Holmgren, A., *The thioredoxin antioxidant system*. Free Radical Biology and Medicine, 2014. **66**: p. 75-87.
99. Cai, H. and Harrison, D.G., *Endothelial dysfunction in cardiovascular diseases - The role of oxidant stress*. Circulation Research, 2000. **87**(10): p. 840-844.
100. Sarma, A.D., Mallick, A.R., and Ghosh, A.K., *Free radicals and their role in different clinical conditions: an overview*. International Journal of Pharma Sciences and Research, 2010. **1**(3): p. 185-192.

101. Cepinskas, G., Rui, T., and Kvietys, P.R., *Interaction between reactive oxygen metabolites and nitric oxide in oxidant tolerance*. Free Radical Biology and Medicine, 2002. **33**(4): p. 433-440.
102. Loscalzo, J., *Nitric oxide insufficiency, platelet activation, and arterial thrombosis*. Circulation Research, 2001. **88**(8): p. 756-762.
103. Achike, F.I. and Kwan, C.Y., *Nitric oxide, human diseases and the herbal products that affect the nitric oxide signalling pathway*. Clinical and Experimental Pharmacology and Physiology, 2003. **30**(9): p. 605-615.
104. Gobbel, G.T., Chan, T.Y.Y., and Chan, P.H., *Nitric oxide- and superoxide-mediated toxicity in cerebral endothelial cells*. Journal of Pharmacology and Experimental Therapeutics, 1997. **282**(3): p. 1600-1607.
105. Beckman, J.S., et al., *Apparent hydroxyl radical production by peroxynitrite: implications for endothelial injury from nitric oxide and superoxide*. Proc Natl Acad Sci U S A, 1990. **87**(4): p. 1620-4.
106. Wink, D.A. and Mitchell, J.B., *Chemical biology of nitric oxide: Insights into regulatory, cytotoxic, and cytoprotective mechanisms of nitric oxide*. Free Radical Biology and Medicine, 1998. **25**(4-5): p. 434-456.
107. Pisoschi, A.M. and Negulescu, G.P., *Methods for Total Antioxidant Activity Determination: A Review*. Biochemistry & Analytical Biochemistry, 2011. **1**: p. 106.
108. Alam, M.N., Bristi, N.J., and Rafiquzzaman, M., *Review on in vivo and in vitro methods evaluation of antioxidant activity*. Saudi Pharmaceutical Journal, 2013. **21**(2): p. 143-152.
109. Brandwilliams, W., Cuvelier, M.E., and Berset, C., *Use of a Free-Radical Method to Evaluate Antioxidant Activity*. Food Science and Technology-Lebensmittel-Wissenschaft & Technologie, 1995. **28**(1): p. 25-30.
110. Benzie, I.F.F. and Strain, J.J., *The ferric reducing ability of plasma (FRAP) as a measure of "antioxidant power": The FRAP assay*. Analytical Biochemistry, 1996. **239**(1): p. 70-76.
111. Tarpey, M.M., Wink, D.A., and Grisham, M.B., *Methods for detection of reactive metabolites of oxygen and nitrogen: in vitro and in vivo considerations*. American Journal of Physiology-Regulatory Integrative and Comparative Physiology, 2004. **286**(3): p. R431-R444.
112. Everette, J.D., et al., *Thorough Study of Reactivity of Various Compound Classes toward the Folin-Ciocalteu Reagent*. Journal of Agricultural and Food Chemistry, 2010. **58**(14): p. 8139-8144.

113. Blainski, A., Lopes, G.C., and de Mello, J.C.P., *Application and Analysis of the Folin Ciocalteu Method for the Determination of the Total Phenolic Content from Limonium Brasiliense L.* *Molecules*, 2013. **18**(6): p. 6852-6864.
114. Organization, W.H. *WHO | Diabetes mellitus*. 2017; Available from: <http://www.who.int/mediacentre/factsheets/fs138/en/>.
115. Kimura, T. *Development of Mulberry Leaf Extract for Suppressing Postprandial Blood Glucose Elevation, Hypoglycemia - Causes and Occurrences*. 2011; Available from: <https://www.intechopen.com/books/hypoglycemia-causes-and-occurrences/development-of-mulberry-leaf-extract-for-suppressing-postprandial-blood-glucose-elevation>.
116. Bode, B., *Incorporating postprandial and fasting plasma glucose into clinical management strategies*. *Insulin*, 2008. **3**(1): p. 17-27.
117. Patil, P., et al., *Food protein-derived bioactive peptides in management of type 2 diabetes*. *Eur J Nutr*, 2015. **54**(6): p. 863-80.
118. Mosmann, T., *Rapid colorimetric assay for cellular growth and survival: application to proliferation and cytotoxicity assays*. *J Immunol Methods*, 1983. **65**(1-2): p. 55-63.
119. Denizot, F. and Lang, R., *Rapid colorimetric assay for cell growth and survival. Modifications to the tetrazolium dye procedure giving improved sensitivity and reliability*. *J Immunol Methods*, 1986. **89**(2): p. 271-7.
120. Stoddart, M.J., *Cell Viability Assays: Introduction*, in *Mammalian Cell Viability. Methods in Molecular Biology (Methods and Protocols)*, M. Stoddart, Editor. 2011, Humana Press: New York.
121. Sylvester, P.W., *Optimization of the tetrazolium dye (MTT) colorimetric assay for cellular growth and viability*. *Methods Mol Biol*, 2011. **716**: p. 157-68.
122. Patravale, V., Dandekar, P., and R., J., *Nanotoxicology: evaluating toxicity potential of drug-nanoparticles*. *Nanoparticulate Drug Delivery*, 2012: p. 123-155.
123. Chen, J.W., et al., *Propofol protects against hydrogen peroxide-induced oxidative stress and cell dysfunction in human umbilical vein endothelial cells*. *Molecular and Cellular Biochemistry*, 2010. **339**(1-2): p. 43-54.
124. Gong, G.H., et al., *Rutin inhibits hydrogen peroxide-induced apoptosis through regulating reactive oxygen species mediated mitochondrial dysfunction pathway in human umbilical vein endothelial cells*. *European Journal of Pharmacology*, 2010. **628**(1-3): p. 27-35.
125. Qian, J.C., et al., *Ophiopogonin D prevents H<sub>2</sub>O<sub>2</sub>-induced injury in primary human umbilical vein endothelial cells*. *Journal of Ethnopharmacology*, 2010. **128**(2): p. 438-445.

126. Kuo, W.W., et al., *Crude extracts of Solanum lyratum protect endothelial cells against oxidized low-density lipoprotein-induced injury by direct antioxidant action*. Journal of Vascular Surgery, 2009. **50**(4): p. 849-860.
127. Edgell, C.J., McDonald, C.C., and Graham, J.B., *Permanent cell line expressing human factor VIII-related antigen established by hybridization*. Proc Natl Acad Sci U S A, 1983. **80**(12): p. 3734-7.
128. Li, J.K., et al., *Protective effects of farrerol against hydrogen-peroxide-induced apoptosis in human endothelium-derived EA.hy926 cells*. Canadian Journal of Physiology and Pharmacology, 2013. **91**(9): p. 733-740.
129. Xie, F.S., et al., *Vaccarin attenuates the human EA.hy926 endothelial cell oxidative stress injury through inhibition of Notch signaling*. International Journal of Molecular Medicine, 2015. **35**(1): p. 135-142.
130. Wang, B.X., et al., *7, 8-Dihydroxyflavone Protects an Endothelial Cell Line from H<sub>2</sub>O<sub>2</sub> Damage*. Plos One, 2015. **10**(8).
131. Hou, Y.Z., et al., *Protective effect of Ligusticum chuanxiong and Angelica sinensis on endothelial cell damage induced by hydrogen peroxide*. Life Sciences, 2004. **75**(14): p. 1775-1786.
132. Liu, H.T., et al., *Chitosan oligosaccharides attenuate hydrogen peroxide-induced stress injury in human umbilical vein endothelial cells*. Pharmacological Research, 2009. **59**(3): p. 167-175.
133. Rajendran, P., et al., *Antioxidants and human diseases*. Clin Chim Acta, 2014. **436**: p. 332-47.
134. Elakkad, A.M., et al., *T-786C variation in the promoter sequence of human eNOS gene markedly influences its expression level*. Drug Discoveries and Therapeutics, 2017. **11**(4): p. 193-197.
135. Seto, S.W., et al., *Sailuotong Prevents Hydrogen Peroxide (H<sub>2</sub>O<sub>2</sub>)-Induced Injury in EA.hy926 Cells*. International Journal of Molecular Sciences, 2017. **18**(1).
136. Le, G.Y., Essackjee, H.C., and Ballard, H.J., *Intracellular adenosine formation and release by freshly-isolated vascular endothelial cells from rat skeletal muscle: effects of hypoxia and/or acidosis*. Biochem Biophys Res Commun, 2014. **450**(1): p. 93-8.
137. Fukai, T. and Ushio-Fukai, M., *Superoxide Dismutases: Role in Redox Signaling, Vascular Function, and Diseases*. Antioxidants & Redox Signaling, 2011. **15**(6): p. 1583-1606.
138. Chang, L.Y., et al., *Molecular immunocytochemistry of the CuZn superoxide dismutase in rat hepatocytes*. J Cell Biol, 1988. **107**(6 Pt 1): p. 2169-79.



139. Crapo, J., et al., *Copper,zinc superoxide dismutase is primarily a cytosolic protein in human cells*. Proceedings of the National Academy of Sciences of United States of America, 1992. **89**(21): p. 10405-9.
140. Levanon, D., et al., *Architecture and anatomy of the chromosomal locus in human chromosome 21 encoding the Cu/Zn superoxide dismutase*. EMBO Journal, 1985. **4**(1): p. 77-84.
141. McCord, J.M. and Fridovich, I., *Superoxide dismutase. An enzymic function for erythrocuprein (hemocuprein)*. J Biol Chem, 1969. **244**(22): p. 6049-55.
142. Rigo, A., et al., *The binding of copper ions to copper-free bovine superoxide dismutase. Properties of the protein recombined with increasing amounts of copper ions*. Biochem J, 1977. **161**(1): p. 31-5.
143. Abdureyim, S., et al., *Anti-inflammatory, immunomodulatory, and heme oxygenase-1 inhibitory activities of ravan napas, a formulation of uighur traditional medicine, in a rat model of allergic asthma*. Evid Based Complement Alternat Med, 2011. **2011**.
144. Liu, A.D., et al., *Ischemic Preconditioning Protects Against Liver Ischemia/Reperfusion Injury via Heme Oxygenase-1-Mediated Autophagy*. Critical Care Medicine, 2014. **42**(12): p. E762-E771.
145. McDaid, J., et al., *Heme oxygenase-1 modulates the allo-immune response by promoting activation-induced cell death of T cells*. FASEB J, 2005. **19**(3): p. 458-60.
146. Zhu, X., et al., *Heme oxygenase-1 system and gastrointestinal inflammation: a short review*. World J Gastroenterol, 2011. **17**(38): p. 4283-8.
147. Li, Y., et al., *A review of melatonin in hepatic ischemia/reperfusion injury and clinical liver disease*. Ann Med, 2014. **46**(7): p. 503-11.
148. Maines, M.D., *The heme oxygenase system: a regulator of second messenger gases*. Annu Rev Pharmacol Toxicol, 1997. **37**: p. 517-54.
149. Ozawa, E., et al., *Ferritin/alanine aminotransferase ratio as a possible marker for predicting the prognosis of acute liver injury*. Journal of Gastroenterology and Hepatology, 2011. **26**(8): p. 1326-1332.
150. Vile, G.F., et al., *Heme oxygenase 1 mediates an adaptive response to oxidative stress in human skin fibroblasts*. Proc Natl Acad Sci U S A, 1994. **91**(7): p. 2607-10.
151. Balla, G., et al., *Ferritin: a cytoprotective antioxidant strategem of endothelium*. J Biol Chem, 1992. **267**(25): p. 18148-53.
152. Soares, M.P., et al., *Expression of heme oxygenase-1 can determine cardiac xenograft survival*. Nature Medicine, 1998. **4**(9): p. 1073-1077.

153. Brouard, S., *et al.*, Carbon monoxide generated by heme oxygenase 1 suppresses endothelial cell apoptosis. *J Exp Med*, 2000. **192**(7): p. 1015-26.
154. Gozzelino, R., Jeney, V., and Soares, M.P., *Mechanisms of cell protection by heme oxygenase-1*. *Annu Rev Pharmacol Toxicol*, 2010. **50**: p. 323-54.
155. Elmore, S., *Apoptosis: a review of programmed cell death*. *Toxicol Pathol*, 2007. **35**(4): p. 495-516.
156. Abou-Ghali, M. and Stiban, J., *Regulation of ceramide channel formation and disassembly: Insights on the initiation of apoptosis*. *Saudi J Biol Sci*, 2015. **22**(6): p. 760-72.
157. Hsu, H., Xiong, J., and Goeddel, D.V., *The TNF receptor 1-associated protein TRADD signals cell death and NF-kappa B activation*. *Cell*, 1995. **81**(4): p. 495-504.
158. Kischkel, F.C., *et al.*, *Cytotoxicity-dependent APO-1 (Fas/CD95)-associated proteins form a death-inducing signaling complex (DISC) with the receptor*. *EMBO J*, 1995. **14**(22): p. 5579-88.
159. Chicheportiche, Y., *et al.*, *TWEAK, a new secreted ligand in the tumor necrosis factor family that weakly induces apoptosis*. *Journal of Biological Chemistry*, 1997. **272**(51): p. 32401-32410.
160. Ashkenazi, A. and Dixit, V.M., *Death receptors: signaling and modulation*. *Science*, 1998. **281**(5381): p. 1305-8.
161. Hitoshi, Y., *et al.*, *Toso, a cell surface, specific regulator of Fas-induced apoptosis in T cells*. *Immunity*, 1998. **8**(4): p. 461-71.
162. Kataoka, T., *et al.*, *FLIP prevents apoptosis induced by death receptors but not by perforin/granzyme B, chemotherapeutic drugs, and gamma irradiation*. *Journal of Immunology*, 1998. **161**(8): p. 3936-42.
163. Peter, M.E. and Krammer, P.H., *Mechanisms of CD95 (APO-1/Fas)-mediated apoptosis*. *Curr Opin Immunol*, 1998. **10**(5): p. 545-51.
164. Chinnaiyan, A.M., *The apoptosome: heart and soul of the cell death machine*. *Neoplasia*, 1999. **1**(1): p. 5-15.
165. Scaffidi, C., *et al.*, *The role of c-FLIP in modulation of CD95-induced apoptosis*. *J Biol Chem*, 1999. **274**(3): p. 1541-8.
166. Susin, S.A., *et al.*, *Two distinct pathways leading to nuclear apoptosis*. *J Exp Med*, 2000. **192**(4): p. 571-80.
167. Schimmer, A.D., *Inhibitor of apoptosis proteins: Translating basic knowledge into clinical practice*. *Cancer Research*, 2004. **64**(20): p. 7183-7190.

168. Ekert, P.G. and Vaux, D.L., *The mitochondrial death squad: hardened killers or innocent bystanders?* *Curr Opin Cell Biol*, 2005. **17**(6): p. 626-30.
169. Yang, E., et al., *Bad, a heterodimeric partner for Bcl-XL and Bcl-2, displaces Bax and promotes cell death.* *Cell*, 1995. **80**(2): p. 285-91.
170. Oda, E., et al., *Noxa, a BH3-only member of the Bcl-2 family and candidate mediator of p53-induced apoptosis.* *Science*, 2000. **288**(5468): p. 1053-8.
171. Cory, S. and Adams, J.M., *The BCL2 family: Regulators of the cellular life-or-death switch.* *Nature Reviews Cancer*, 2002. **2**(9): p. 647-656.
172. Liu, F.T., Newland, A.C., and Jia, L., *Bax conformational change is a crucial step for PUMA-mediated apoptosis in human leukemia.* *Biochemical and Biophysical Research Communications*, 2003. **310**(3): p. 956-962.
173. Hebert, P.D.N., et al., *Ten species in one: DNA barcoding reveals cryptic species in the neotropical skipper butterfly *Astrartes fulgerator*.* *Proceedings of the National Academy of Sciences of the United States of America*, 2004. **101**(41): p. 14812-14817.
174. Stewart, C.N., *Monitoring the presence and expression of transgenes in living plants.* *Trends in Plant Science*, 2005. **10**(8): p. 390-396.
175. Yoon, C.K., *Forensic-Science - Botanical Witness for the Prosecution.* *Science*, 1993. **260**(5110): p. 894-895.
176. Coyle, H.M., et al., *Forensic botany: Using plant evidence to aid in forensic death investigation.* *Croatian Medical Journal*, 2005. **46**(4): p. 606-612.
177. Mildenhall, D.C., *Hypericum pollen determines the presence of burglars at the scene of a crime: An example of forensic palynology.* *Forensic Science International*, 2006. **163**(3): p. 231-235.
178. Galimberti, A., et al., *DNA barcoding as a new tool for food traceability.* *Food Research International*, 2013. **50**(1): p. 55-63.
179. Huxley-Jones, E., et al., *Use of DNA barcoding to reveal species composition of convenience seafood.* *Conservation Biology*, 2012. **26**(2): p. 367-371.
180. Newmaster, S.G., et al., *Testing candidate plant barcode regions in the Myristicaceae.* *Molecular Ecology Resources*, 2008. **8**(3): p. 480-490.
181. Froeschke, G. and von der Heyden, S., *A Review of Molecular Approaches for Investigating Patterns of Coevolution in Marine Host-Parasite Relationships.* *Advances in Parasitology*, Vol 84, 2014. **84**: p. 209-252.
182. Hillis, D. and Davis, S., *Ribosomal DNA: intraspecific polymorphism, concerted evolution, and phylogeny reconstruction.* *Systematic Zoology*, 1988. **37**(1): p. 63-66.

183. Hillis, D.M. and Dixon, M.T., *Ribosomal DNA: molecular evolution and phylogenetic inference*. Q Rev Biol, 1991. **66**(4): p. 411-53.
184. Sahin, F.P., *et al.*, *DNA authentication of Plantago herb based on nucleotide sequences of 18S-28S rRNA internal transcribed Spacer region*. Biological & Pharmaceutical Bulletin, 2007. **30**(7): p. 1265-1270.
185. Zhang, Y.B., *et al.*, *Molecular authentication of Chinese herbal materials*. Journal of Food and Drug Analysis, 2007. **15**(1): p. 1-9.
186. Sukrong, S., *et al.*, *Molecular analysis of the genus Mitragyna existing in Thailand based on rDNA ITS sequences and its application to identify a narcotic species: Mitragyna speciosa*. Biological & Pharmaceutical Bulletin, 2007. **30**(7): p. 1284-1288.
187. Johnson, L.A. and Soltis, D.E., *Phylogenetic Inference in Saxifragaceae Sensu-Stricto and Gilia (Polemoniaceae) Using Matk Sequences*. Annals of the Missouri Botanical Garden, 1995. **82**(2): p. 149-175.
188. Johnson, L.A. and Soltis, D.E., *Matk DNA-Sequences and Phylogenetic Reconstruction in Saxifragaceae S-Str.* Systematic Botany, 1994. **19**(1): p. 143-156.
189. Hilu, K.W. and Liang, H.P., *The matK gene: Sequence variation and application in plant systematics*. American Journal of Botany, 1997. **84**(6): p. 830-839.
190. Neuhaus, H. and Link, G., *The chloroplast trNALys(UUU) gene from mustard (Sinapis alba) contains a class II intron potentially coding for a maturase-related polypeptide*. Current Genetics, 1987. **11**(4): p. 251-7.
191. Wolfe, K.H., Morden, C.W., and Palmer, J.D., *Function and evolution of a minimal plastid genome from a nonphotosynthetic parasitic plant*. Proc Natl Acad Sci U S A, 1992. **89**(22): p. 10648-52.
192. Xiang, Q., Soltis, D., and Soltis, P., *Phylogenetic relationships of Cornaceae and close relatives inferred from matK and rbcL sequences*. Am J Bot, 1998. **85**(2): p. 285.
193. Wakasugi, T., *et al.*, *Updated gene map of tobacco chloroplast DNA*. Plant Molecular Biology Reporter, 1998. **16**(3): p. 231-241.
194. Carelse, O., Chetsanga, C.J., and Mubumbila, M.V., *Identification of a trnH (Gug) gene and of several pseudogenes downstream of psbA gene in the common bean chloroplast genome*. Plant Science, 1994. **98**(1): p. 47-52.
195. Rubinoff, D., Cameron, S., and Will, K., *Are plant DNA barcodes a search for the Holy Grail?* Trends Ecol Evol, 2006. **21**(1): p. 1-2.
196. Vongsak, B., *et al.*, *Sequencing analysis of the medicinal plant Stemona tuberosa and five related species existing in Thailand based on trnH-psbA chloroplast DNA*. Planta Medica, 2008. **74**(14): p. 1764-1766.

197. Sijben-Muller, G., et al., *Spinach plastid genes coding for initiation factor IF-1, ribosomal protein S11 and RNA polymerase alpha-subunit*. Nucleic Acids Research, 1986. **14**(2): p. 1029-44.
198. Ohme, M., et al., *A tobacco chloroplast DNA sequence possibly coding for a polypeptide similar to E. coli RNA polymerase beta-subunit*. FEBS Lett, 1986. **200**(1): p. 87-90.
199. Ohyama, K., et al., *Chloroplast gene organization deduced from complete sequence of liverwort Marchantia polymorpha chloroplast DNA*. Nature 1986. **322**: p. 572-574.
200. Watson, J. and Surzycki, S., *Both the chloroplast and nuclear genomes of Chlamydomonas reinhardi share homology with Escherichia coli genes for transcriptional and translational components*. Current Genetics, 1983. **7**(3): p. 201-210.
201. Lerbs, S., Brautigam, E., and Parthier, B., *Polypeptides of DNA-dependent RNA polymerase of spinach chloroplasts: characterization by antibody-linked polymerase assay and determination of sites of synthesis*. EMBO J, 1985. **4**(7): p. 1661-6.
202. Kikuchi, S., et al., *Uncovering the protein translocon at the chloroplast inner envelope membrane*. Science, 2013. **339**(6119): p. 571-574.
203. Neubig, K.M., et al., *Phylogenetic utility of ycf1 in orchids: a plastid gene more variable than matK*. Plant Systematics and Evolution, 2009. **277**(1-2): p. 75-84.
204. Drew, B.T. and Sytsma, K.J., *The South American radiation of Lepechinia (Lamiaceae): phylogenetics, divergence times and evolution of dioecy*. Botanical Journal of the Linnean Society, 2013. **171**(1): p. 171-190.
205. Dong, W.P., et al., *ycf1, the most promising plastid DNA barcode of land plants*. Scientific Reports, 2015. **5**.
206. Mullis, K., Ferré, F., and Gibbs, R., *The Polymerase chain reaction*. 1994, Boston: Birkhäuser.
207. Maxam, A.M. and Gilbert, W., *A new method for sequencing DNA*. 1977. Biotechnology, 1992. **24**: p. 99-103.
208. Sanger, F., Nicklen, S., and Coulson, A.R., *DNA sequencing with chain-terminating inhibitors*. Proc Natl Acad Sci U S A, 1977. **74**(12): p. 5463-7.
209. Corpet, F., *Multiple sequence alignment with hierarchical clustering*. Nucleic Acids Res, 1988. **16**(22): p. 10881-90.
210. Do, C.B. and Katoh, K., *Protein multiple sequence alignment*. Methods Mol Biol, 2008. **484**: p. 379-413.
211. Nei, M. and Kumar, S., *Molecular evolution and phylogenetics*. 2000, New York: Oxford University Press.

212. Huelsenbeck, J.P. and Crandall, K.A., *Phylogeny estimation and hypothesis testing using maximum likelihood*. Annual Review of Ecology and Systematics, 1997. **28**: p. 437-466.
213. Yang, Z.H. and Rannala, B., *Bayesian phylogenetic inference using DNA sequences: A Markov Chain Monte Carlo method*. Molecular Biology and Evolution, 1997. **14**(7): p. 717-724.
214. Hill, T., et al., *Genetic algorithm for large-scale maximum parsimony phylogenetic analysis of proteins*. Biochimica Et Biophysica Acta-General Subjects, 2005. **1725**(1): p. 19-29.
215. Efron, B. and Tibshirani, R., *Bootstrap methods for standard errors, confidence intervals, and other measures of statistical accuracy*. Statistical Science, 1986. **1**(1): p. 54-75.
216. Jagetia, G.C., et al., *The evaluation of nitric oxide scavenging activity of certain herbal formulations in vitro: A preliminary study*. Phytotherapy Research, 2004. **18**(7): p. 561-565.
217. Singleton, V.L., Orthofer, R., and Lamuela-Raventos, R.M., *Analysis of total phenols and other oxidation substrates and antioxidants by means of Folin-Ciocalteu reagent*. Oxidants and Antioxidants, Pt A, 1999. **299**: p. 152-178.
218. Wan, L.S., et al., *Xanthone glycoside constituents of Swertia kouitchensis with alpha-glucosidase inhibitory activity*. Journal of Natural Products, 2013. **76**(7): p. 1248-1253.
219. Carmichael, J., et al., *Evaluation of a tetrazolium-based semiautomated colorimetric assay: assessment of radiosensitivity*. Cancer Res, 1987. **47**(4): p. 943-6.
220. Wang, H. and Joseph, J.A., *Quantifying cellular oxidative stress by dichlorofluorescein assay using microplate reader*. Free Radical Biology and Medicine, 1999. **27**(5-6): p. 612-616.
221. Girard-Lalancette, K., Pichette, A., and Legault, J., *Sensitive cell-based assay using DCFH oxidation for the determination of pro- and antioxidant properties of compounds and mixtures: Analysis of fruit and vegetable juices*. Food Chemistry, 2009. **115**(2): p. 720-726.
222. Eruslanov, E. and Kusmartsev, S., *Identification of ROS using oxidized DCFDA and flow-cytometry*. Methods in Molecular Biology, 2010. **594**: p. 57-72.
223. Shirai, M., et al., *Effect of quercetin and its conjugated metabolite on the hydrogen peroxide-induced intracellular production of reactive oxygen species in mouse fibroblasts*. Bioscience Biotechnology and Biochemistry, 2002. **66**(5): p. 1015-1021.
224. White, T.J., et al., *Amplification and Direct Sequencing of Fungal Ribosomal RNA genes for Phylogenetics*, in *PCR Protocols A Guide to Methods and Applications*, M.A. Innis, et al., Editors. 1990, Academic Press, Inc.: New York. p. 315-322.

225. Lee, H.-L., et al. *Development of plant DNA barcoding markers from the variable noncoding regions of chloroplast genome*. in *Abstract presented at the Second International Barcode of Life Conference*. 2007. Academia Sinica, Taipei, Taiwan.
226. Sang, T., Crawford, D.J., and Stuessy, T.F., *Chloroplast DNA phylogeny, reticulate evolution, and biogeography of Paeonia (Paeoniaceae)*. *American Journal of Botany*, 1997. **84**(8): p. 1120-1136.
227. Tate, J.A. and Simpson, B.B., *Paraphyly of Tarasa (Malvaceae) and diverse origins of the polyploid species*. *Systematic Botany*, 2003. **28**(4): p. 723-737.
228. Levin, R.A., et al., *Family-level relationships of Onagraceae based on chloroplast *rbcl* and *ndhF* data*. *American Journal of Botany*, 2003. **90**(1): p. 107-115.
229. Kress, W.J., et al., *Plant DNA barcodes and a community phylogeny of a tropical forest dynamics plot in Panama*. *Proceedings of the National Academy of Sciences of the United States of America*, 2009. **106**(44): p. 18621-18626.
230. Sass, C., et al., *DNA Barcoding in the Cycadales: Testing the Potential of Proposed Barcoding Markers for Species Identification of Cycads*. *Plos One*, 2007. **2**(11).
231. Sapsrithong, T., et al., *Cissus quadrangularis ethanol extract upregulates superoxide dismutase, glutathione peroxidase and endothelial nitric oxide synthase expression in hydrogen peroxide-injured human ECV304 cells*. *J Ethnopharmacol*, 2012. **143**(2): p. 664-72.
232. TANG, W.P., CHEN, Shu Si, *Study on anatomical structure of leaf of Aquilaria agallocha*. *Guihaia*, 2005. **25**(3): p. 4.
233. Liu, Y., et al., *Binding Mechanism and Synergetic Effects of Xanthone Derivatives as Noncompetitive alpha-Glucosidase Inhibitors: A Theoretical and Experimental Study*. *Journal of Physical Chemistry B*, 2013. **117**(43): p. 13464-13471.
234. Valko, M., et al., *Role of oxygen radicals in DNA damage and cancer incidence*. *Molecular and Cellular Biochemistry*, 2004. **266**(1-2): p. 37-56.
235. Robak, J. and Gryglewski, R.J., *Flavonoids are scavengers of superoxide anions*. *Biochem Pharmacol*, 1988. **37**(5): p. 837-41.
236. Dahham, S.S., et al., *The Anticancer, Antioxidant and Antimicrobial Properties of the Sesquiterpene beta-Caryophyllene from the Essential Oil of Aquilaria crassna*. *Molecules*, 2015. **20**(7): p. 11808-11829.
237. Li, H.Z., et al., *Mangiferin exerts antitumor activity in breast cancer cells by regulating matrix metalloproteinases, epithelial to mesenchymal transition, and beta-catenin signaling pathway*. *Toxicology and Applied Pharmacology*, 2013. **272**(1): p. 180-190.

238. Higashi, Y., *et al.*, *Endothelial Function and Oxidative Stress in Cardiovascular Diseases*. Circulation Journal, 2009. **73**(3): p. 411-418.
239. Vanhoutte, P.M., *Endothelial dysfunction and atherosclerosis*. European Heart Journal, 1997. **18**: p. E19-E29.
240. Bouis, D., *et al.*, *Endothelium in vitro: a review of human vascular endothelial cell lines for blood vessel-related research*. Angiogenesis, 2001. **4**(2): p. 91-102.
241. Li, J.M. and Shah, A.M., *Endothelial cell superoxide generation: regulation and relevance for cardiovascular pathophysiology*. American Journal of Physiology-Regulatory Integrative and Comparative Physiology, 2004. **287**(5): p. R1014-R1030.
242. Lum, H. and Roebuck, K.A., *Oxidant stress and endothelial cell dysfunction*. American Journal of Physiology-Cell Physiology, 2001. **280**(4): p. C719-C741.
243. Hou, X.L., *et al.*, *Dihydromyricetin protects endothelial cells from hydrogen peroxide-induced oxidative stress damage by regulating mitochondrial pathways*. Life Sciences, 2015. **130**: p. 38-46.
244. Diaz, M.N., *et al.*, *Mechanisms of disease - Antioxidants and atherosclerotic heart disease*. New England Journal of Medicine, 1997. **337**(6): p. 408-416.
245. Maron, D.J., *Flavonoids for reduction of atherosclerotic risk*. Curr Atheroscler Rep, 2004. **6**(1): p. 73-8.
246. Siekmeier, R., Steffen, C., and Maerz, W., *Role of oxidants and antioxidants in atherosclerosis: Results of in vitro and in vivo investigations*. Journal of Cardiovascular Pharmacology and Therapeutics, 2007. **12**(4): p. 265-282.
247. Jia, Y.N., *et al.*, *Total flavonoids from Rosa Laevigata Michx fruit attenuates hydrogen peroxide induced injury in human umbilical vein endothelial cells*. Food and Chemical Toxicology, 2012. **50**(9): p. 3133-3141.
248. Verma, S., *et al.*, *A self-fulfilling prophecy: C-reactive protein attenuates nitric oxide production and inhibits angiogenesis*. Circulation, 2002. **106**(8): p. 913-9.
249. Lefer, D.J. and Granger, D.N., *Oxidative stress and cardiac disease*. American Journal of Medicine, 2000. **109**(4): p. 315-323.
250. D'Souza, V., *et al.*, *Increased oxidative stress from early pregnancy in women who develop preeclampsia*. Clinical and Experimental Hypertension, 2016. **38**(2): p. 225-232.
251. Agarwala, S., *et al.*, *Mangiferin, a dietary xanthone protects against mercury-induced toxicity in HepG2 cells*. Environmental Toxicology, 2012. **27**(2): p. 117-127.
252. Bhatt, L., Sebastian, B., and Joshi, V., *Mangiferin protects rat myocardial tissue against cyclophosphamide induced cardiotoxicity*. Journal of Ayurveda and Integrative Medicine, 2017. **8**(2): p. 62-67.



253. Abraham, N.G., et al., *Heme oxygenase-1 attenuates glucose-mediated cell growth arrest and apoptosis in human microvessel endothelial cells*. *Circulation Research*, 2003. **93**(6): p. 507-514.
254. Hayashi, S., et al., *Induction of heme oxygenase-1 suppresses venular leukocyte adhesion elicited by oxidative stress role of bilirubin generated by the enzyme*. *Circulation Research*, 1999. **85**(8): p. 663-671.
255. Turkseven, S., et al., *Antioxidant mechanism of heme oxygenase-1 involves an increase in superoxide dismutase and catalase in experimental diabetes*. *American Journal of Physiology-Heart and Circulatory Physiology*, 2005. **289**(2): p. H701-H707.
256. Zhao, J., et al., *Mangiferin increases Nrf2 protein stability by inhibiting its ubiquitination and degradation in human HL60 myeloid leukemia cells*. *International Journal of Molecular Medicine*, 2014. **33**(5): p. 1348-1354.
257. Zhang, B.P., et al., *Mangiferin activates the Nrf2-ARE pathway and reduces etoposide-induced DNA damage in human umbilical cord mononuclear blood cells*. *Pharmaceutical Biology*, 2015. **53**(4): p. 503-511.
258. Zhong, Z.G., et al., *Progallin A isolated from the acetic ether part of the leaves of *Phyllanthus emblica* L. induces apoptosis of human hepatocellular carcinoma BEL-7404 cells by up-regulation of Bax expression and down-regulation of Bcl-2 expression*. *J Ethnopharmacol*, 2011. **133**(2): p. 765-72.
259. Wang, W., et al., *Tanshinone IIA attenuates neuronal damage and the impairment of long-term potentiation induced by hydrogen peroxide*. *J Ethnopharmacol*, 2011. **134**(1): p. 147-55.
260. Kavitha, M., et al., *Mangiferin attenuates MPTP induced dopaminergic neurodegeneration and improves motor impairment, redox balance and Bcl-2/Bax expression in experimental Parkinson's disease mice*. *Chem Biol Interact*, 2013. **206**(2): p. 239-47.
261. Pan, L.L., et al., *Mangiferin Induces Apoptosis by Regulating Bcl-2 and Bax Expression in the CNE2 Nasopharyngeal Carcinoma Cell Line*. *Asian Pacific Journal of Cancer Prevention*, 2014. **15**(17): p. 7065-7068.
262. Gupta, S., Afaq, F., and Mukhtar, H., *Involvement of nuclear factor-kappa B, Bax and Bcl-2 in induction of cell cycle arrest and apoptosis by apigenin in human prostate carcinoma cells*. *Oncogene*, 2002. **21**(23): p. 3727-38.
263. Kang, M.H. and Reynolds, C.P., *Bcl-2 Inhibitors: Targeting Mitochondrial Apoptotic Pathways in Cancer Therapy*. *Clinical Cancer Research*, 2009. **15**(4): p. 1126-1132.

264. Compton, J. and Ishihara, A., *The use and trade of agarwood in japan*, in *TRAFFIC Southeast Asia and TRAFFIC East Asia-Japan*. 2010. p. 1-21.
265. Antonopoulou, M., *et al.*, *The Trade and Use of Agarwood (Oudh) in the United Arab Emirates 2010*: Selangor.
266. Suwanchaikasem, P., Phadungcharoen, T., and Sukrong, S., *Authentication of the Thai medicinal plants sharing the same common name 'Rang Chuet': Thunbergia laurifolia, Crotalaria spectabilis, and Curcuma aff. amada by combined techniques of TLC, PCR-RFLP fingerprints, and antioxidant activities*. *Scienceasia*, 2013. **39**(2): p. 124-133.
267. Barden, A., *et al.*, *Heart of the matter : agarwood use and trade and CITES implementation for Aquilaria malaccensis 2000*: Cambridge. p. 1-51.
268. Mookamul, P., *et al.*, *Species identification and sex determination of the genus Nepenthes (Nepenthaceae)*. *Pak J Biol Sci*, 2007. **10**(4): p. 561-7.
269. Hebert, P.D.N. and Gregory, T.R., *The promise of DNA barcoding for taxonomy*. *Systematic Biology*, 2005. **54**(5): p. 852-859.
270. Techen, N., *et al.*, *DNA barcoding of medicinal plant material for identification*. *Current Opinion in Biotechnology*, 2014. **25**: p. 103-110.
271. Hollingsworth, P.M., *et al.*, *A DNA barcode for land plants*. *Proceedings of the National Academy of Sciences of the United States of America*, 2009. **106**(31): p. 12794-12797.
272. Jiao, L.C., *et al.*, *DNA barcoding for identification of the endangered species Aquilaria sinensis: comparison of data from heated or aged wood samples*. *Holzforschung*, 2014. **68**(4): p. 487-494.
273. Kress, W.J. and Erickson, D.L., *A Two-Locus Global DNA Barcode for Land Plants: The Coding rbcL Gene Complements the Non-Coding trnH-psbA Spacer Region*. *Plos One*, 2007. **2**(6).
274. Grievink, L.S., *et al.*, *Phylogenetic Tree Reconstruction Accuracy and Model Fit when Proportions of Variable Sites Change across the Tree*. *Systematic Biology*, 2010. **59**(3): p. 288-297.
275. Chase, M.W., *et al.*, *A proposal for a standardised protocol to barcode all land plants*. *Taxon*, 2007. **56**(2): p. 295-299.
276. Dong, W.P., *et al.*, *Highly Variable Chloroplast Markers for Evaluating Plant Phylogeny at Low Taxonomic Levels and for DNA Barcoding*. *Plos One*, 2012. **7**(4).
277. Gernandt, D.S., *et al.*, *Phylogenetic Relationships of Pinus Subsection Ponderosae Inferred from Rapidly Evolving cpDNA Regions*. *Systematic Botany*, 2009. **34**(3): p. 481-491.

278. Chen, S.L., *et al.*, *A renaissance in herbal medicine identification: From morphology to DNA*. *Biotechnology Advances*, 2014. **32**(7): p. 1237-1244.
279. Alvarez, I. and Wendel, J.F., *Ribosomal ITS sequences and plant phylogenetic inference*. *Molecular Phylogenetics and Evolution*, 2003. **29**(3): p. 417-434.
280. Stoeckle, M., *Taxonomy, DNA, and the bar code of life*. *Bioscience*, 2003. **53**(9): p. 796-797.
281. Lee, S.Y., *et al.*, *DNA Barcoding of the Endangered Aquilaria (Thymelaeaceae) and Its Application in Species Authentication of Agarwood Products Traded in the Market*. *Plos One*, 2016. **11**(4).





APPENDICES

จุฬาลงกรณ์มหาวิทยาลัย  
**CHULALONGKORN UNIVERSITY**

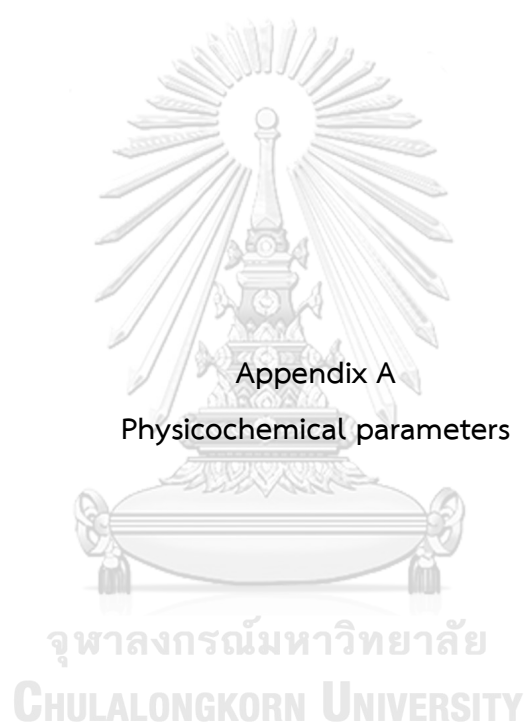


**Table 32** Physicochemical values of *A. crassna* leaves from 15 different sources

Sources	No.	% by weight					
		Loss on drying	Water content	Total ash	Acid-insoluble ash	Ethanol extractive value	Water extractive value
Ac01	1	10.074	10.247	5.239	0.659	4.836	16.505
	2	10.343	9.997	5.214	0.635	4.569	16.870
	3	10.408	9.997	5.072	0.624	5.278	16.842
Ac02	1	8.350	7.998	7.271	1.453	5.568	14.619
	2	8.145	7.747	7.541	1.502	5.588	14.191
	3	8.434	7.998	7.454	1.459	6.519	14.330
Ac03	1	8.991	8.749	6.917	1.519	8.097	16.892
	2	9.030	8.500	6.963	1.463	7.358	16.445
	3	9.258	8.499	6.740	1.474	7.578	16.856
Ac04	1	9.776	8.497	6.107	1.554	12.458	20.244
	2	9.836	8.498	6.199	1.603	10.930	20.157
	3	9.956	8.249	6.049	1.708	10.720	19.688
Ac05	1	8.209	7.999	6.414	1.525	12.004	20.105
	2	8.585	7.999	6.436	1.469	10.455	19.694
	3	8.304	8.248	6.425	1.539	11.629	19.334
Ac06	1	7.664	6.999	8.643	2.648	9.555	21.668
	2	7.539	7.250	8.834	2.750	9.319	22.057
	3	7.576	7.249	8.790	2.649	9.156	22.022
Ac07	1	9.402	9.248	5.753	0.855	5.835	17.063
	2	9.434	8.998	5.839	0.830	5.329	17.398
	3	9.122	9.248	5.760	0.809	5.310	17.167
Ac08	1	9.727	8.247	5.648	0.934	6.648	14.868
	2	10.106	7.997	5.420	0.984	6.126	14.449
	3	9.742	8.247	5.543	0.980	6.419	14.603
Ac09	1	8.714	8.249	6.634	0.860	16.192	10.971
	2	8.465	7.998	6.571	0.820	15.810	11.014
	3	8.500	8.247	6.626	0.810	15.857	10.728

**Table 32** Physiocochemical values of *A. crassna* leaves from 15 different sources (Cont.)

Sources	No.	% by weight					
		Loss on drying	Water content	Total ash	Acid-insoluble ash	Ethanol extractive value	Water extractive value
Ac10	1	8.571	7.997	6.442	1.344	9.232	15.109
	2	8.362	8.247	6.528	1.350	9.603	15.088
	3	8.464	8.248	6.346	1.304	9.177	14.949
Ac11	1	8.160	7.750	7.136	1.893	9.556	17.096
	2	8.173	7.998	7.209	1.828	9.458	17.038
	3	8.029	7.750	7.185	1.877	9.538	17.143
Ac12	1	7.305	6.998	11.243	3.613	9.538	15.373
	2	7.201	7.331	10.958	3.638	9.639	15.476
	3	7.361	7.331	11.074	3.618	9.486	15.696
Ac13	1	8.158	7.749	6.750	1.958	10.692	21.578
	2	8.203	8.000	6.708	1.939	10.744	21.058
	3	8.205	7.997	6.915	1.920	10.560	21.117
Ac14	1	8.013	7.750	6.224	1.159	10.056	17.719
	2	8.021	7.749	6.303	1.144	10.028	17.686
	3	8.001	7.998	6.198	1.169	10.057	17.820
Ac15	1	8.124	7.748	5.939	0.370	8.596	15.119
	2	8.010	7.664	5.913	0.360	8.515	15.031
	3	8.071	7.665	5.777	0.365	8.406	15.544

Appendix B  
Alpha-glucosidase inhibitory activities



จุฬาลงกรณ์มหาวิทยาลัย  
**CHULALONGKORN UNIVERSITY**



**Table 33** The percentage of yeast alpha-glucosidase inhibition of Ac14 extract

Concentration ( $\mu\text{g/ml}$ )	Percentage of inhibition
7.8125	4.28 $\pm$ 0.51
15.625	9.87 $\pm$ 0.91
31.25	13.34 $\pm$ 2.29
62.5	21.50 $\pm$ 1.50
125	3.60 $\pm$ 1.77
250	63.65 $\pm$ 1.61
500	85.81 $\pm$ 3.95

\* Each value represented the mean  $\pm$  SD of three experiments. Each experiment was performed triplicate.

**Table 34** The percentage of yeast alpha-glucosidase inhibition of mangiferin

Concentration ( $\mu\text{g/ml}$ )	Percentage of inhibition
23.4375	2.06 $\pm$ 1.00
46.875	6.44 $\pm$ 0.66
93.75	9.42 $\pm$ 0.85
187.5	20.81 $\pm$ 1.53
375	34.50 $\pm$ 1.58
750	61.11 $\pm$ 2.46
1500	83.26 $\pm$ 1.53

\* Each value represented the mean  $\pm$  SD of three experiments. Each experiment was performed triplicate.

**Table 35** The percentage of yeast alpha-glucosidase inhibition of acarbose

Concentration (mg/ml)	Percentage of inhibition
10.00	33.93 ± 1.56
12.00	37.45 ± 1.91
14.00	42.03 ± 1.57
16.00	46.53 ± 1.65
18.00	51.68 ± 1.20
20.00	56.01 ± 1.48

\* Each value represented the mean ± SD of three experiments. Each experiment was performed triplicate.





**Table 36** The percentage of DPPH scavenging activity of Ac14 extract

Concentration ( $\mu\text{g/ml}$ )	Percentage of scavenging activity
2.42	44.22 $\pm$ 1.20
3.63	47.62 $\pm$ 1.20
4.84	49.55 $\pm$ 0.74
6.04	51.65 $\pm$ 0.64
7.25	54.14 $\pm$ 1.19
8.46	56.82 $\pm$ 1.62

**Table 37** The percentage of DPPH scavenging activity of mangiferin

Concentration ( $\mu\text{g/ml}$ )	Percentage of scavenging activity
0.20	16.53 $\pm$ 0.98
0.50	38.39 $\pm$ 2.94
0.80	62.60 $\pm$ 1.17
1.10	74.62 $\pm$ 1.61
1.40	82.42 $\pm$ 2.67
1.70	89.12 $\pm$ 1.37

**Table 38** The percentage of DPPH scavenging activity of quercetin

Concentration ( $\mu\text{g/ml}$ )	Percentage of scavenging activity
2.42	44.98 $\pm$ 0.92
3.63	49.89 $\pm$ 0.81
4.84	57.59 $\pm$ 0.84
6.04	63.01 $\pm$ 1.30
7.25	67.79 $\pm$ 1.37
8.46	73.48 $\pm$ 0.93

**Note:** Each value represented the mean  $\pm$  SD of three experiments. Each experiment was performed triplicate.

**Table 39** The percentage of NO<sup>•</sup> scavenging activity of Ac14 extract

Concentration (µg/ml)	Percentage of scavenging activity
30	34.42 ± 0.37
40	37.05 ± 0.69
50	41.35 ± 0.79
60	44.33 ± 0.51
70	46.90 ± 1.06
80	50.35 ± 0.76
90	53.23 ± 0.96

**Table 40** The percentage of NO<sup>•</sup> scavenging activity of mangiferin

Concentration (µg/ml)	Percentage of scavenging activity
25.34	40.32 ± 0.74
29.56	43.10 ± 0.77
33.79	45.23 ± 0.68
38.01	48.44 ± 0.78
42.23	51.17 ± 0.58
46.46	53.63 ± 0.27
50.68	56.68 ± 1.07

**Table 41** The percentage of NO<sup>•</sup> scavenging activity of quercetin

Concentration (µg/ml)	Percentage of scavenging activity
6.04	37.52 ± 0.38
9.07	42.66 ± 0.71
12.09	48.40 ± 0.65
15.11	52.97 ± 0.65
30.22	64.44 ± 0.91

Note: Each value represented the mean ± SD of three experiments. Each experiment was performed triplicate.

**Table 42** The percentage of  $O_2^{\bullet-}$  scavenging activity of Ac14 extract

Concentration ( $\mu\text{g/ml}$ )	Percentage of scavenging
31.25	$30.22 \pm 1.92$
62.5	$37.57 \pm 1.88$
125	$42.68 \pm 1.80$
250	$49.89 \pm 1.16$
500	$55.40 \pm 1.78$
1000	$60.48 \pm 2.50$

**Table 43** The percentage of  $O_2^{\bullet-}$  scavenging activity of mangiferin

Concentration ( $\mu\text{g/ml}$ )	Percentage of scavenging
21.12	$20.52 \pm 1.41$
42.23	$28.25 \pm 2.27$
63.35	$33.48 \pm 2.09$
84.47	$41.38 \pm 0.98$
105.59	$50.34 \pm 1.34$
126.70	$58.43 \pm 1.05$

**Table 44** The percentage of  $O_2^{\bullet-}$  scavenging activity of quercetin

Concentration ( $\mu\text{g/ml}$ )	Percentage of scavenging
6.04	$15.01 \pm 1.62$
9.07	$23.59 \pm 1.05$
12.09	$34.41 \pm 1.57$
15.11	$45.01 \pm 1.49$
18.13	$52.15 \pm 1.17$
21.16	$63.79 \pm 1.40$
24.18	$74.74 \pm 2.08$

Note: Each value represented the mean  $\pm$  SD of three experiments. Each experiment was performed triplicate.



**Table 45** Cytotoxic activity of Ac14 extract against MDA-231 cell line

Concentration ( $\mu\text{g/ml}$ )	% Viability
6.25	82.09 $\pm$ 0.92
12.5	69.10 $\pm$ 1.18
25	56.41 $\pm$ 1.02
50	45.37 $\pm$ 0.41
100	26.57 $\pm$ 0.81

**Table 46** Cytotoxic activity of mangiferin against MDA-231 cell line

Concentration ( $\mu\text{g/ml}$ )	% Viability
6.25	97.58 $\pm$ 1.30
12.5	88.42 $\pm$ 2.20
25	82.82 $\pm$ 1.63
50	72.67 $\pm$ 1.90
100	62.93 $\pm$ 0.78

**Table 47** Cytotoxic activity of doxorubicin against MDA-231 cell line

Concentration ( $\mu\text{g/ml}$ )	% Viability
0.001	74.59 $\pm$ 1.06
0.01	62.79 $\pm$ 1.04
0.1	51.26 $\pm$ 0.83
1	41.23 $\pm$ 0.75
10	24.15 $\pm$ 1.00

Note: Each value represented the mean  $\pm$  SD of three experiments. Each experiment was performed triplicate.



**Table 48** Cytotoxic activity of Ac14 extract against HepG2 cell line

Concentration ( $\mu\text{g/ml}$ )	% Viability
6.25	93.12 $\pm$ 2.15
12.5	83.93 $\pm$ 0.48
25	65.87 $\pm$ 0.81
50	51.99 $\pm$ 1.35
100	35.76 $\pm$ 0.68

**Table 49** Cytotoxic activity of mangiferin against HepG2 cell line

Concentration ( $\mu\text{g/ml}$ )	% Viability
6.25	95.86 $\pm$ 2.15
12.5	90.08 $\pm$ 0.48
25	82.96 $\pm$ 0.81
50	75.34 $\pm$ 1.35
100	67.85 $\pm$ 0.68

**Table 50** Cytotoxic activity of doxorubicin against HepG2 cell line

Concentration ( $\mu\text{g/ml}$ )	% Viability
6.25	88.48 $\pm$ 0.51
12.5	78.86 $\pm$ 1.81
25	67.17 $\pm$ 1.12
50	54.44 $\pm$ 0.49
100	43.06 $\pm$ 0.94

**Note:** Each value represented the mean  $\pm$  SD of three experiments. Each experiment was performed triplicate.

**Table 51** Cytotoxic activity of Ac14 extract against HT-29 cell line

Concentration ( $\mu\text{g/ml}$ )	% Viability
6.25	94.00 $\pm$ 2.02
12.5	82.50 $\pm$ 3.22
25	68.16 $\pm$ 0.46
50	51.74 $\pm$ 1.02
100	33.34 $\pm$ 0.76

**Table 52** Cytotoxic activity of mangiferin against HT-29 cell line

Concentration ( $\mu\text{g/ml}$ )	% Viability
6.25	97.30 $\pm$ 1.47
12.5	89.87 $\pm$ 1.24
25	81.42 $\pm$ 1.09
50	72.05 $\pm$ 1.56
100	63.52 $\pm$ 1.99

**Table 53** Cytotoxic activity of doxorubicin against HT-29 cell line

Concentration ( $\mu\text{g/ml}$ )	% Viability
6.25	95.01 $\pm$ 0.23
12.5	81.05 $\pm$ 0.52
25	61.97 $\pm$ 0.73
50	40.10 $\pm$ 0.76
100	25.30 $\pm$ 0.30

Note: Each value represented the mean  $\pm$  SD of three experiments. Each experiment was performed triplicate.



**Table 54** The percentage of cell viability of Ac14 extract at various concentrations for 24 h measured by MTT assay.

Concentration ( $\mu\text{g/ml}$ )	% Viability
Control	100.00 $\pm$ 0.00
7.8125	89.80 $\pm$ 2.38
15.625	74.68 $\pm$ 4.55
31.25	65.80 $\pm$ 1.94
62.5	45.02 $\pm$ 1.79
125	40.40 $\pm$ 2.94
250	31.37 $\pm$ 1.47
500	27.30 $\pm$ 1.08

Each value represented the mean  $\pm$  SD of three experiments. Each experiment was performed triplicate.

**Table 55** The percentage of DCF fluorescence of Ac14 extract at various concentrations for 24 h measured by DCFH-DA assay.

Concentration ( $\mu\text{g/ml}$ )	% DCF fluorescence
Control	100.00 $\pm$ 0.00
7.8125	113.52 $\pm$ 3.41
15.625	133.62 $\pm$ 5.11
31.25	171.76 $\pm$ 10.84
62.5	209.87 $\pm$ 6.50
125	168.08 $\pm$ 9.64
250	92.46 $\pm$ 2.97
500	60.91 $\pm$ 0.39

Each value represented the mean  $\pm$  SD of three experiments. Each experiment was performed triplicate.

**Table 56** The percentage of cell viability of mangiferin at various concentrations for 24 h measured by MTT assay.

Concentration ( $\mu\text{g/ml}$ )	% viability
Control	100.00 $\pm$ 0.00
3.125	110.21 $\pm$ 5.45
6.25	115.45 $\pm$ 5.67
12.5	117.16 $\pm$ 3.53
25	110.50 $\pm$ 4.11
50	107.61 $\pm$ 3.77
100	100.90 $\pm$ 5.84
200	92.79 $\pm$ 1.93

Each value represented the mean  $\pm$  SD of three experiments. Each experiment was performed triplicate.

**Table 57** The percentage of DCF fluorescence of mangiferin at various concentrations for 24 h measured by DCFH-DA assay.

Concentration ( $\mu\text{g/ml}$ )	% DCF fluorescence
Control	100.00 $\pm$ 0.00
3.125	105.68 $\pm$ 2.24
6.25	104.88 $\pm$ 5.07
12.5	101.65 $\pm$ 4.91
25	105.21 $\pm$ 2.78
50	106.55 $\pm$ 1.85
100	101.60 $\pm$ 2.47
200	91.39 $\pm$ 3.48

Each value represented the mean  $\pm$  SD of three experiments. Each experiment was performed triplicate.

**Table 58** The percentage of cell viability of H<sub>2</sub>O<sub>2</sub> at various concentrations for 0.5 h measured by MTT assay.

Concentration (mM)	% viability
Control	100.00 ± 0.00
0.0625	100.37 ± 3.39
0.125	98.93 ± 3.66
0.25	97.45 ± 3.42
0.5	96.16 ± 3.06
1	95.51 ± 3.42
2	93.40 ± 3.67
4	89.45 ± 3.18
8	85.85 ± 1.20
16	21.77 ± 4.10
32	10.42 ± 1.45
64	10.26 ± 1.49
100	9.64 ± 1.53

Each value represented the mean ± SD of three experiments. Each experiment was performed triplicate.

**Table 59** The percentage of DCF fluorescence of H<sub>2</sub>O<sub>2</sub> at various concentrations for 0.5 h measured by DCFH-DA assay.

Concentration (mM)	% DCF fluorescence
Control	100.00 ± 0.00
0.0625	124.58 ± 8.59
0.125	129.57 ± 6.84
0.25	136.89 ± 6.82
0.5	146.55 ± 6.00
1	159.33 ± 2.15
2	165.83 ± 1.75
4	178.97 ± 3.69
8	190.38 ± 1.58
16	211.62 ± 2.53
32	236.66 ± 1.21
64	248.67 ± 6.95
100	264.42 ± 17.44

Each value represented the mean ± SD of three experiments. Each experiment was performed triplicate.

**Table 60** The percentage of cell viability of pretreatment with Ac14 extract for 24 h prior to 0.25 mM H<sub>2</sub>O<sub>2</sub> for 0.5 h measured by MTT assay.

Concentration (µg/ml)	% viability
Control	100.00 ± 0.00
0.00	96.06 ± 0.59
7.8125	85.18 ± 1.89
15.625	75.00 ± 3.66
31.25	65.13 ± 5.86
62.5	52.81 ± 6.02
125	41.33 ± 6.85
250	29.34 ± 2.23
500	24.19 ± 3.24

Each value represented the mean ± SD of three experiments. Each experiment was performed triplicate.

**Table 61** The percentage of DCF fluorescence of pretreatment with Ac14 extract for 24 h prior to 0.25 mM H<sub>2</sub>O<sub>2</sub> for 0.5 h by DCFH-DA assay.

Concentration (µg/ml)	% DCF fluorescence
Control	100.00 ± 0.00
0.00	134.36 ± 0.56
7.8125	182.03 ± 5.28
15.625	208.26 ± 3.22
31.25	238.11 ± 4.11
62.5	284.43 ± 8.99
125	323.85 ± 5.45
250	192.44 ± 5.72
500	109.17 ± 3.35

Each value represented the mean ± SD of three experiments. Each experiment was performed triplicate.



**Table 62** The percentage of cell viability of pretreatment with mangiferin for 24 h prior to 0.25 mM H<sub>2</sub>O<sub>2</sub> for 0.5 h measured by MTT assay.

Concentration (µg/ml)	% viability
Control	100.00 ± 0.00
0.00	96.06 ± 0.59
3.125	105.93 ± 3.78
6.25	104.01 ± 1.75
12.5	102.81 ± 1.44
25	100.81 ± 0.29
50	99.26 ± 1.25
100	85.22 ± 1.20
200	73.01 ± 1.17

Each value represented the mean ± SD of three experiments. Each experiment was performed triplicate.

**Table 63** The percentage of DCF fluorescence of pretreatment with mangiferin for 24 h prior to 0.25 mM H<sub>2</sub>O<sub>2</sub> for 0.5 h measured by DCFH-DA assay.

Concentration (µg/ml)	% DCF fluorescence
Control	100.00 ± 0.00
0.00	134.36 ± 0.56
3.125	134.83 ± 0.87
6.25	133.37 ± 0.97
12.5	127.98 ± 2.02
25	124.86 ± 1.95
50	121.42 ± 1.04
100	106.02 ± 1.82
200	90.99 ± 2.46

Each value represented the mean ± SD of three experiments. Each experiment was performed triplicate.



Appendix F

Protein expression SOD-1, HO-1, Bcl-2, Bax, and  $\beta$ -actin on EA.hy926 cell

จุฬาลงกรณ์มหาวิทยาลัย  
CHULALONGKORN UNIVERSITY

**Table 64** The relative ratio of Ac14 extract on the protein expressions of SOD-1, HO-1, and Bcl-2/Bax ratio in EA.hy926 cells normalized by  $\beta$ -actin and quantitated by Western blot analysis

Concentration ( $\mu\text{g/ml}$ )	SOD-1	HO-1	Bcl-2/Bax ratio
Control	1.00 $\pm$ 0.00	1.00 $\pm$ 0.00	1.00 $\pm$ 0.00
25	1.18 $\pm$ 0.16	4.66 $\pm$ 1.21	0.46 $\pm$ 0.12
50	1.08 $\pm$ 0.12	6.64 $\pm$ 1.02	0.39 $\pm$ 0.09
100	0.53 $\pm$ 0.13	5.08 $\pm$ 1.70	0.25 $\pm$ 0.06

Each value represented the mean  $\pm$  SD of three experiments. Each experiment was performed triplicate.

**Table 65** The relative ratio of Ac14 extract on the protein expressions of SOD-1, HO-1 in  $\text{H}_2\text{O}_2$ -treated EA.hy926 cells normalized by  $\beta$ -actin and quantitated by Western blot analysis

Concentration ( $\mu\text{g/ml}$ )	SOD-1	HO-1	Bcl-2/Bax ratio
Control	1.00 $\pm$ 0.00	1.00 $\pm$ 0.00	1.00 $\pm$ 0.00
0	0.96 $\pm$ 0.02	3.76 $\pm$ 1.28	0.82 $\pm$ 0.10
25	2.07 $\pm$ 0.34	9.85 $\pm$ 0.72	0.39 $\pm$ 0.06
50	1.90 $\pm$ 0.17	9.54 $\pm$ 0.95	0.35 $\pm$ 0.09
100	1.07 $\pm$ 0.30	9.35 $\pm$ 0.52	0.33 $\pm$ 0.05

Each value represented the mean  $\pm$  SD of three experiments. Each experiment was performed triplicate.

**Table 66** The relative ratio of mangiferin on the protein expressions of SOD-1, HO-1, and Bcl-2/Bax ratio in EA.hy926 cells normalized by  $\beta$ -actin and quantitated by Western blot analysis

Concentration ( $\mu\text{g/ml}$ )	SOD-1	HO-1	Bcl-2/Bax ratio
Control	1.00 $\pm$ 0.00	1.00 $\pm$ 0.00	1.00 $\pm$ 0.00
50	1.26 $\pm$ 0.17	1.22 $\pm$ 0.09	1.47 $\pm$ 0.29
100	1.13 $\pm$ 0.06	1.11 $\pm$ 0.28	1.23 $\pm$ 0.05
200	0.99 $\pm$ 0.19	0.65 $\pm$ 0.11	1.01 $\pm$ 0.14

Each value represented the mean  $\pm$  SD of three experiments. Each experiment was performed triplicate.

**Table 67** The relative ratio of mangiferin on the protein expressions of SOD-1, HO-1 in  $\text{H}_2\text{O}_2$ -treated EA.hy926 cells normalized by  $\beta$ -actin and quantitated by Western blot analysis

Concentration ( $\mu\text{g/ml}$ )	SOD-1	HO-1	Bcl-2/Bax ratio
Control	1.00 $\pm$ 0.00	1.00 $\pm$ 0.00	1.00 $\pm$ 0.00
0	0.96 $\pm$ 0.02	3.76 $\pm$ 1.28	0.82 $\pm$ 0.10
50	1.42 $\pm$ 0.36	2.59 $\pm$ 0.60	1.05 $\pm$ 0.16
100	1.60 $\pm$ 0.28	2.04 $\pm$ 0.47	0.95 $\pm$ 0.10
200	1.43 $\pm$ 0.02	1.81 $\pm$ 0.30	0.94 $\pm$ 0.10

Each value represented the mean  $\pm$  SD of three experiments. Each experiment was performed triplicate.



Appendix G

The accession number of submitted DNA sequences of *Aquilaria* species and outgroup (*E.siamensis*) of six barcoding locus

จุฬาลงกรณ์มหาวิทยาลัย  
CHULALONGKORN UNIVERSITY

**Table 68** Plant materials and their respective accession numbers

Species	Geographical location	Voucher No.	Accession number					
			ITS	matK	rbcl	rpoC1	psbA-trnH intergenic spacer	ycf1
<i>A. crassna</i> Pierre ex Lecomte	Bangkok, Thailand	AQWT01	LC384009	LC383997	LC383710	LC383849	LC384006	LC384001
	Rayong, Thailand	AQWT02						
	Nan, Thailand	AQVT03						
<i>A. malaccensis</i> Lam.	Pattalung, Thailand	AMNN01	LC384010	LC383998	LC383712	LC383850	LC384005	LC384002
	Tanglin, Singapore	AMWT02						
	Tanglin, Singapore	AMWT03						
<i>A. subintegra</i> Ding Hou	Trat, Thailand	ASTS01	LC384011	LC383999	LC383711	LC383851	LC384007	LC384003
	Trat, Thailand	ASTS02						
<i>Enkleia siamensis</i> (Kurz) Nerviing	Loei, Thailand	ESKL01	LC384012	LC384000	LC383713	LC383852	LC384008	LC384004

## VITA

Mr. Woratouch Thitikornpong was born on July 21, 1985 in Bangkok, Thailand. He received his Bachelor's degree of Science (Second Honors) in Pharmacy from the Faculty of Pharmaceutical Sciences, Chulalongkorn University, Thailand in 2008, and got Master's degree of Sciences (Pharmacognosy) from the Faculty of Pharmaceutical Sciences, Chulalongkorn University, Thailand in 2010. He attended to study Doctor of Philosophy in Public Health Sciences (Traditional Thai and alternative medicines), Chulalongkorn University, Thailand. During the study, he received the 100th Anniversary Chulalongkorn University Fund for Doctoral Scholarships and the 90th Anniversary of Chulalongkorn University, Rachadapiseksomphot Endowment Fund from Graduate School.

### Publications

Thitikornpong W, Ongpipattanakul B, Palanuvej C, Ruangrunsi N. Pharmacognostic specification and mangiferin content of *Aquilaria crassna* leaves. *Pharmacognosy journal*. 2018;10(2):293-298.

Thitikornpong W, Palanuvej C, Ruangrunsi N. In vitro antidiabetic, antioxidation and cytotoxicity activities of ethanolic extract of *Aquilaria crassna* leaves and its active compound; mangiferin. (submitted to *Indian Journal of Traditional Knowledge*)

Thitikornpong W, Palanuvej C, Ruangrunsi N. DNA barcoding for authentication of the endangered plants in genus *Aquilaria*. (submitted to *Thai Journal of Pharmaceutical Sciences*)

### Honor

Outstanding award in oral presentation in The JSPS-NRCT Follow-Up Seminar 2017 and 33rd International Annual Meeting in Pharmaceutical Sciences (JSPS-NRCT 2017 and IAMPS33), March 2-3, 2017.